

Neutron activation characterization of the chemical elements in preparation for nuclear reactor decommissioning

AS Maodi

 [orcid.org/ 0000-0002-4588-8598](https://orcid.org/0000-0002-4588-8598)

Dissertation accepted in partial fulfilment of the requirements for
the degree *Master of Sciences in Engineering Sciences with
Nuclear Engineering* at the North West University

Supervisor: Prof DE Serfontein

Co-Supervisor: Mr TJ van Rooyen

Graduation: July 2020

Student number: 25905570

PREFACE

Firstly, I would like to thank the LORD God for his grace in my life.

To my study-leader Prof Dawid Serfontein who was my lecturer for Nuclear Engineering, I would like to thank you for your encouragement and support throughout my study journey. Your work ethic and leadership are so inspiring. I will forever be grateful for the opportunity that you awarded me as a lecture and study leader.

To my co-study leader and mentor, Mr Johann van Rooyen. We thank God for you. I would like to thank you for your expertise, assistance, guidance, and patience throughout the process of writing this piece of work. Without your help, this dissertation would not have been possible. I will forever be grateful for your assistance, guidance, encouragement and more than anything, the training, and skills you transferred to me and other students wholeheartedly without holding back. Necsa and the Nuclear industry as a whole are blessed to have a gem like you.

To Necsa — the South African Nuclear Energy Corporation — thank you for granting me the opportunity of a lifetime. You paid my fees and granted me generous study leave to attend classes; I will forever be grateful for that.

To LandisGyr I am grateful for the study-leave you granted me to be able to meet with my co-study leader for progression on this writeup.

To my parents Daniel and Sinah, thank you for the love and support in everything I do, I love you.

To my son Lethabo, you inspire me to raise the bar, I am proud to be your mother, I love you.

To my partner, thank you for your unwavering love, support, and understanding, I love you.

To my ex-colleagues from Necsa for encouraging me to pick up where I left off, many thanks for the love, support, and inspiration.

ABSTRACT

At nuclear reactor facilities, intense neutron radiation fields are encountered inside and around reactor vessels. Engineering materials exposed to the neutron field absorb neutrons in nuclear reactions, and radioisotopes are produced in this way. This process is termed *neutron activation*. Neutron activation produces radionuclides in irradiated materials, i.e. the irradiated materials become radioactive. Some neutron activation reactions are of commercial interest, e.g. the production of the radionuclide Ir-192 from irradiated Ir-191. Most radionuclides produced by neutron activation, are undesired, long-lived radioisotopes and will place a radioactive waste burden on the licensed facility, adding to total operational costs and inflating future liabilities. After irradiation by the neutron field ends, long-lived radionuclides will remain present in irradiated materials and will present radiological and radioactive waste-disposal problems such as e.g. (1) a radiation field will be present around the activated material and will expose workers to doses of ionising radiation, and (2) some activated material may not pass clearance level criteria set by e.g. the IAEA and will therefore have to be disposed of as radioactive waste, at a significant cost.

An inquiry into the systematics of neutron activation, using radiation transport and materials activation codes, was designed and successfully concluded. The systematic study showed that neutron activation will, specifically under high neutron fluence-rate conditions, depend in a profoundly non-linear way on the fluence-rate. For this reason, it is incorrect to attempt to perform a neutron activation calculation at a chosen reference integral fluence-rate ϕ_{ref} and then attempt to scale activities and dose-rates linearly for other fluence-rates. There are no “shortcuts” i.e. every neutron activation problem is unique and must, therefore, be modelled individually.

Using a representative neutron spectrum calculated for a typical light water reactor (LWR), a total of 81 chemical elements were irradiated and cooled down under specific scenarios that represent important decommissioning and operational scenarios. For selected important scenarios, the elements were ranked in terms of the unshielded dose-rate at 1 m from a point-source with a reference mass of 1 g of each irradiated chemical element. These tables clearly show which elements are high-activators, intermediate activators and low-activators, for different irradiation scenarios. This information may be used to select low-activation materials for new reactor facilities, and for components that must be replaced in existing nuclear facilities. The tabulated results can serve to guide decommissioning engineers, project managers,

radiation protection specialists and neutron radiography teams. Neutron radiography teams can use the information to e.g. pre-empt which radiographed components will be highly radioactive, and which will remain radioactive for a long time, after exposure to neutrons, based on known material compositions. Decommissioning engineers can use the information to e.g. pre-empt that steels with the same neutron irradiation history as aluminium-alloys, will have a significantly higher burden of long-lived radionuclides.

A comprehensive literature study on the nature and importance of the formation of long-lived radionuclides by neutron activation, for nuclear reactor decommissioning, was undertaken and presented. From the literature-study emerged a list of high-activator elements as well as problematic, long-lived radioisotopes formed by neutron activation. A total of approximately 1700 calculations with the activation code FISPACT-II 3.00 were performed, in order to describe the systematics of neutron activation in realistic irradiation-and-cooldown scenarios, focusing on reactor decommissioning. The full set of systematic FISPACT-II calculations served to verify and validate the list of high-activation materials and problematic long-lived radionuclides gathered from the literature survey.

A comprehensive set of graphs are presented to show how induced activities and photon dose-rate fields will evolve over the first 50 years after the end of irradiation, for chemical elements used in important engineering materials such as low-alloys steels, stainless steel-alloys, nickel-alloys, ordinary concrete, magnetite concrete and hematite concrete. The durations of these irradiations range from 1 hour to 60 years.

A notable result was that, for a decommissioning scenario, titanium-alloys are significantly more benign neutron activators compared to steel-alloys. Problematic elements that are high-activators in practically all irradiation scenarios are europium (Eu), cobalt (Co), caesium (Cs), silver (Ag) and niobium (Nb). The testing of raw materials used in concrete close to a nuclear reactor must be designed to minimise the amount of the above high-activators in the concrete. Al-alloys and steel-alloys used in intense neutron fields must also be tested to minimise the high-activators. Benign elements that are low-activators in practically all irradiation scenarios are aluminium (Al), Silicon (Si), magnesium (Mg) and titanium (Ti). Where practical and possible, aluminium-alloys and titanium-alloys must, therefore, be preferred in areas where significant neutron fluence-rates are expected.

TABLE OF CONTENTS

PREFACE.....	II
ABSTRACT.....	III
TABLE OF CONTENTS	V
LIST OF FIGURES.....	XIV
LIST OF TABLES.....	XX
ABBREVIATIONS AND SPECIAL NOMENCLATURE	XXV
1 INTRODUCTION.....	1
1.1 Background and Rationale.....	1
1.1.1 Neutron Activation.....	1
1.1.2 Clearance Levels: IAEA.....	1
1.1.3 Clearance Levels: Canadian Nuclear Safety Commission (CNSC) 2018.....	3
1.1.4 Clearance Levels: Nuclear Industry Safety Directors Forum (NISDF, 2017)	4
1.1.5 Materials Affected by Neutron Activation at Necsa, South Africa	7
1.1.6 Reactor Decommissioning: The Need for Knowledge about the Systematics of the Neutron Activation of Elements in Engineering Materials	8
1.2 Research Problem, Research Purpose and Research Objectives	9
1.3 Research Hypothesis	10
2 RESEARCH METHODOLOGY.....	11
2.1 Outline of the Research Methodology	11
2.2 Identities of the Main Chemical Elements Encountered in Engineering Structures in Nuclear Power Plants.....	12

2.3	The Magnitude of Neutron Fluence-Rates in and Around the SAFARI-1 Reactor and its Peripheral Irradiation Facilities	13
2.4	Concise Symbolic Nomenclature for Irradiation-and-Cooldown Scenarios.....	16
2.5	Decommissioning Scenario: Time-Dependence and Intensity of Neutron Fluence-Rate Field.....	17
2.6	Fuel-Assembly Irradiation Scenario: Time-Dependence and Intensity of Neutron Fluence-Rate Field	19
2.7	Neutron Radiography (NRAD) Scenario: Time-Dependence and Intensity of Neutron Fluence-Rate Field	20
2.8	Scenario-Analysis Methodology.....	21
2.9	Research Questions to be Investigated	21
2.9.1	RQ1: Linearity or Non-Linearity?.....	21
2.9.2	RQ2: Ranking of Elements for Irradiation Cases DECO_60a_6a_φ.....	21
2.9.3	RQ3: Ranking of Elements for Irradiation Case DECO_1a_6a_1E14.....	22
2.9.4	RQ4: Ranking of Elements for Irradiation Case NRAD_1h_30d_1E9 as well as for Case NRAD_1d_30d_1E9.....	22
2.9.5	RQ5: Graphs of Activities and Dose-Rates for Cases DECO_60a_50a_φ.....	22
2.9.6	RQ6: Graphs of Activities and Dose-Rates for Cases DECO_1a_50a_1E14 and DECO_1a_50a_1E15.....	22
2.9.7	RQ7: Graphs of Activities and Dose-Rates for Case NRAD_1h_1000d_1E9 and Case NRAD_1d_1000d_1E9.....	23
2.9.8	RQ8: Completeness Issue	23
2.10	Constraints and Limitations of the Investigation.....	23
3	LITERATURE REVIEW	25

3.1	Introduction: Neutron Activation Calculations for Decommissioning of Nuclear Reactors	25
3.2	Physics of Neutron Activation.....	26
3.3	The IAEA’s Recommended Methodology for Calculations Related to Reactor Decommissioning — Transport Models and Activation Models	26
3.4	Decommissioning Options	28
3.5	Important Radionuclides Produced by Neutron Activation at Nuclear Reactor Facilities; Elements that Produce Long-Lived, Problematic Radionuclides	28
3.5.1	IAEA Publications Dealing with Neutron Activation and Decommissioning	29
3.5.2	The Induced Neutron-Activation Source Term in Nuclear Facilities (IAEA, 2019)....	29
3.5.3	Radiological Characterisation of the Radionuclide Inventory of the Decommissioning Radioactive Waste at a TRIGA Mark II Research Reactor	31
3.5.4	Trace Elements in Reactor Steels: Implications for Decommissioning — Niobium (Nb) and Nitrogen (N)	33
3.5.5	The UK is Advised to Dissociate from Euratom’s European Basic Safety Standards Directive (BSSD 2013/59/Euratom) to Keep Decommissioning Affordable.....	34
3.5.6	An In-Depth Look at Long-Lived Neutron Activation Products in Reactor Materials	34
3.5.7	A Significant Number of MTRs to be Decommissioned or Upgraded in the Near Future	37
3.5.8	Activation Calculations — Overview of Codes and Nuclear Data	37
3.5.9	Trace-Elements are Often Most Problematic	38
3.5.10	Monte-Carlo Aided Design of Neutron Shielding Concretes.....	38
3.5.11	Four Studies on the Neutron Activation of Engineering Materials — Experimental and Computational	38

3.5.12 Activation calculation for the dismantling and decommissioning of a light water reactor using MCNP with ADVANTG and ORIGEN-S	39
3.5.13 Activation of the Concrete Bio-Shield	39
3.5.14 Activation Neutronics for Swiss Nuclear Power Plants (NPPs).....	40
3.5.15 A Decade of Japanese Studies on Low-Activation Concrete	41
3.5.16 Three Key Concepts: (1) Activation-Hazardous Elements, (2) Activation-Hazardous Trace Elements and (3) Radioactivity-Hazardous Nuclides	44
3.5.17 The Need for a Systematic Approach to Neutron Activation at NPPs	45
3.5.18 “Novel Tools for Estimation of Activation Dose” — MCNP, ATTILA, FISPACT-II and ORIGEN	45
3.5.19 Case-Study: Decommissioning of a VVR-S Research Reactor	46
3.5.20 Preliminary Evaluation of Decommissioning Wastes for Nuclear Power Reactors in South Korea.....	46
3.5.21 The radionuclide Ca-41 in nuclear reactor concrete	47
3.5.22 Decontamination and Dismantling of Radioactive Concrete Structures.....	47
3.5.23 Decommissioning Planning for an Austrian MTR	49
3.5.24 Reactor Decommissioning Experience in the UK	50
3.5.25 Implementation of the Decommissioning of Two Research Reactors in France	50
3.5.26 Decommissioning Experience in Pakistan	51
3.5.27 A Good Practice Guide for Radiological Sentencing	51
3.5.28 Decommissioning Plan for the Trojan PWR	51
3.5.29 Clearance Levels for the Recycling of Metallic Scrap.....	52
3.6 Summary and Conclusions: Literature Survey.....	54

4	CALCULATION MODELS: NEUTRON ACTIVATION.....	59
4.1	First Step in a Neutron Activation Calculation: Evaluating of the Neutron Spectrum	59
4.2	The Radiation Transport Code MCNP6.2 and the Calculation Model of the SAFARI-1 Reactor used to Calculate the Neutron Fluence-Rate....	64
4.3	The Activation Code FISPACT-II.....	64
4.4	Details of FISPACT Calculations	66
5	RESULTS	67
5.1	Research Question RQ₁: Neutron Activation: A Non-Linear Function of Neutron Fluence-Rate ϕ	67
5.1.1	Case-Study to Demonstrate the Non-Linearity of Neutron Activation as a Function of the Fluence-Rate ϕ	67
5.1.2	Reason for the non-linearity of neutron activation as a function of ϕ , especially at higher fluence-rates ϕ	82
5.1.3	Burnup of Target-Isotopes in Irradiated Materials	83
5.1.4	Non-linearity in the Neutron Activation of Iron (Fe; $Z = 26$)	88
5.1.5	Non-linearity in the Neutron Activation of Manganese (Mn; $Z = 25$).....	91
5.1.6	Non-linearity of the neutron activation of Chromium (Cr; $Z = 24$).....	93
5.1.7	Non-linearity in the Neutron Activation of Vanadium (V; $Z = 23$).....	96
5.1.8	Non-linearity in the Neutron Activation of Titanium (Ti; $Z = 22$).....	96
5.1.9	Conclusions: Non-linearity of Neutron Activation.....	96
5.2	Research Question RQ₂: Ranking of the Elements in a Decommissioning Irradiation Scenario	97
5.2.1	Ranking of the Elements According to the Dose-Rates from the Irradiation-and-Cooldown Scenario <u>DECO_60yr_6yr_1E14</u>	97

5.2.2 Ranking of the Elements According to the Dose-Rates from the Irradiation-and-Cooldown Scenario <u>DECO_60yr_6yr_1E13</u>	100
5.2.3 Ranking of the Elements According to the Dose-Rates from the Irradiation-and-Cooldown Scenario <u>DECO_60yr_6yr_1E12</u>	103
5.2.4 Ranking of the Elements According to the Dose-Rates from the Irradiation-and-Cooldown Scenario <u>DECO_60yr_6yr_1E11</u>	105
5.2.5 Ranking of the Elements According to the Dose-Rates from the Irradiation-and-Cooldown Scenario <u>DECO_60yr_6yr_1E10</u>	108
5.2.6 Ranking of the Elements According to the Dose-Rates from the Irradiation-and-Cooldown Scenario <u>DECO_60yr_6yr_1E9</u>	108
5.2.7 Ranking of the Elements According to the Dose-Rates from the Irradiation-and-Cooldown Scenario <u>DECO_60yr_6yr_1E8</u>	108
5.2.8 Ranking of the Elements According to the Dose-Rates from the Irradiation-and-Cooldown Scenario <u>DECO_60yr_6yr_1E7</u>	109
5.3 Research Question RQ3: Ranking of the Elements in a Fuel-Assembly (FA) End-Adapter Exposure Scenario <u>DECO_1yr_6yr_1E14</u>.....	109
5.4 Research Question RQ4: Ranking of the Elements in a Neutron Radiography (NRAD) Exposure Scenario.....	113
5.4.1 Ranking of the elements in a Neutron Radiography (NRAD) Exposure Scenario <u>NRAD_1h_30d_1E9</u>	113
5.4.2 Radiological Ranking of the Elements in a Neutron Radiography (NRAD) Exposure Scenario <u>NRAD_1d_30d_1E9</u>	116
5.5 Research Question RQ5: Graphing Activities and Dose-Rates of selected elements used in engineering materials, for decommissioning scenarios <u>DECO_60yr_50yr_φ</u>.....	119
5.5.1 Plots of Activity and Dose-Rates for Scenario <u>DECO_60yr_50yr_1E14</u>	119

5.5.2	Plots of Activity and Dose-Rates for Scenario <u>DECO_60yr_50yr_1E13</u>	121
5.5.3	Plots of Activity and Dose-Rates for Scenario <u>DECO_60yr_50yr_1E12</u>	124
5.5.4	Plots of Activity and Dose-Rates for Scenario <u>DECO_60yr_50yr_1E11</u>	127
5.5.5	Plots of Activity and Dose-Rates for Scenario <u>DECO_60yr_50yr_1E10</u>	129
5.5.6	Plots of Activity and Dose-Rates for Scenario <u>DECO_60yr_50yr_1E9</u>	131
5.5.7	Plots of Activity and Dose-Rates for Scenario <u>DECO_60yr_50yr_1E8</u>	133
5.5.8	Plots of Activities and Dose-Rates for Scenario <u>DECO_60yr_50yr_1E7</u>	135
5.6	Research Question RQ6: Plots of Activities and Dose-Rates for Scenarios <u>DECO_1yr_50yr_1E15</u> and <u>DECO_1yr_50yr_1E14</u> for the Fuel- Assembly End-Adaptors	135
5.6.1	Plots of Activities and Dose-Rates for Scenario <u>DECO_1yr_50yr_1E15</u> for MTR Fuel- Assemblies	135
5.6.2	Plots of Activities and Dose-Rates for Scenario <u>DECO_1yr_50yr_1E14</u> for MTR Fuel- Assemblies	139
5.7	Research Question RQ7: Plots of Activities and Dose-Rates for Neutron Radiography Irradiation Scenarios	142
5.7.1	Plots of Activities and Dose-Rates for the NRAD irradiation scenario <u>NRAD_1h_1000d_1E9</u>	142
5.7.2	Plots of Activities and Dose-Rates for the NRAD irradiation scenario <u>NRAD_1d_30d_1E9</u>	145
5.8	Research Question RQ8: Completeness of the Lists of High-Activator Chemical Elements and Problematic Activation Radionuclides.....	147
5.8.1	Defining the Completeness Issue.....	147
5.8.2	Addition #1: Ba as a Parent of Cs-137.....	147
5.8.3	{Nuclide, Activity}-matrices or NA-matrices for Discrete Irradiation Scenarios	148

5.8.4	Activation Matrices for Selected Elements Under Irradiation Scenario <u>DECO_60yr_6yr_1E14</u>	148
5.8.5	A Shorter Route to Answer Research Question RQ8 — the Completeness Issue	159
5.9	Revisiting Research Question RQ1: Linearity or Non-Linearity	167
5.9.1	The Design of a Computational Experiment to Probe the Linearity Issue	167
5.9.2	Linear and Non-Linear Neutron Activation Behaviour of Titanium (Ti)	167
5.9.3	Linear and Non-Linear Neutron Activation Behaviour of Chromium (Cr).....	169
5.9.4	Linear and Non-Linear Neutron Activation Behaviour of Manganese (Mn).....	171
5.9.5	Linear and Non-Linear Neutron Activation Behaviour of Iron (Fe)	173
5.9.6	Linear and Non-Linear Neutron Activation Behaviour of Cobalt (Co).....	175
5.9.7	Linear and Non-Linear Neutron Activation Behaviour of Nickel (Ni).....	175
5.9.8	Linear and Non-Linear Neutron Activation Behaviour of Copper (Cu).....	176
5.9.9	Linear and Non-Linear Neutron Activation Behaviour of Silver (Ag).....	177
5.9.10	Linear and Non-Linear Neutron Activation Behaviour of Caesium (Cs)	177
5.9.11	Linear and Non-Linear Neutron Activation Behaviour of Europium (Eu)	179
5.9.12	Clusters of Technologically Important and Abundant Elements that “Chain-Breed” Towards a Long-Lived Radionuclide of an Element to their RHS in the Periodic Table (PT) 179	
5.9.13	Conclusions about the Non-Linearity of Neutron Activation	181
5.10	Proposed Terminology (Addition by the Co-Supervisor, TJvR)	181
6	SUMMARY AND CONCLUSIONS.....	183
6.1	General Summary	183
6.2	Major Summary and Conclusion (SC) Points	184
6.3	Research Hypothesis Proven.....	186

6.4	Novel Contributions to the Field of Neutron Activation.....	187
6.5	Proposed Follow-Up Investigation(s).....	188
6.6	Proposed Publication of a Monograph	189
ANNEXURE A:	TECHNICAL DETAILS OF FISPACT-II	
	CALCULATIONS.....	190
	Discussion of a Representative FISPACT-II Calculation Model.....	190
BIBLIOGRAPHY.....		- 206 -

LIST OF FIGURES

Figure 1: Relative abundance of the chemical elements in the earth's upper continental crust as a function of the atomic number Z	13
Figure 2: Diagram of the top-view of the core and core-box of the SAFARI-1 MTR at Necsa	14
Figure 3: Schematic top-view of the Neutron Radiography Facility at the SAFARI-1 reactor, Necsa	15
Figure 4: The IAEA's summary of the steps required in decommissioning work involving neutron-activated systems, structures and components (SSCs)	27
Figure 5: Two Al-rods in water-pool just outside the core of the SAFARI-1 reactor	59
Figure 6: Neutron spectrum in the irradiated Al-rods in the water pool close to the SAFARI-1 reactor.....	60
Figure 7: Calculated neutron spectra in 6 structures in and around the SAFARI-1 reactor core.....	62
Figure 8: Mathematical form of the "ideal neutron spectrum", coded in MathCAD 14	63
Figure 9: Mass-% of the stable isotopes of Fe before and after prolonged exposure to intense irradiation by neutrons — the isotopic composition of the element Fe is markedly perturbed by the exposure to neutrons	88
Figure 10: Activities produced by the neutron irradiation of selected elements for an irradiation scenario <u>DECO_60yr_50yr_1E14</u>	120
Figure 11: Dose-rates produced by the neutron irradiation of selected elements, for scenario <u>DECO_60yr_50yr_1E14</u>	121

Figure 12: Activities produced by the neutron irradiation of selected elements, for scenario <u>DECO_60yr_50yr_1E13</u>	122
Figure 13: Dose-rates produced by the neutron irradiation of selected elements, for scenario <u>DECO_60yr_50yr_1E13</u>	123
Figure 14: Activities produced by the neutron irradiation of selected elements, for scenario <u>DECO_60yr_50yr_1E12</u>	125
Figure 15: Dose-rates produced by the neutron irradiation of selected elements, under scenario <u>DECO_60yr_50yr_1E12</u>	126
Figure 16: Activities produced by the neutron irradiation of selected elements, for scenario <u>DECO_60yr_50yr_1E11</u>	127
Figure 17: Dose-rates produced by the neutron irradiation of selected elements, for scenario <u>DECO_60yr_50yr_1E11</u>	128
Figure 18: Activities produced by the neutron irradiation of selected elements, for scenario <u>DECO_60yr_50yr_1E10</u>	129
Figure 19: Dose-rates produced by the neutron irradiation of selected elements, for scenario <u>DECO_60yr_50yr_1E10</u>	130
Figure 20: Activities produced by the neutron irradiation of selected elements, for scenario <u>DECO_60yr_50yr_1E9</u>	131
Figure 21: Dose-rates produced by the neutron irradiation of selected elements, for scenario <u>DECO_60yr_50yr_1E9</u>	132
Figure 22: Activities produced by the neutron irradiation of selected elements, for scenario <u>DECO_60yr_50yr_1E8</u>	133
Figure 23: Dose-rates produced by the neutron irradiation of selected elements, for scenario <u>DECO_60yr_50yr_1E8</u>	134

Figure 24: Activities produced by the neutron irradiation of selected elements, for highly exposed Al-alloy in an MTR fuel-assembly that is exposed under irradiation scenario <u>DECO_1yr_50yr_1E15</u>	136
Figure 25: Dose-rates produced by the neutron irradiation of selected elements, for a fuel-assembly end-adaptor irradiation scenario <u>DECO_1yr_50yr_1E15</u>	138
Figure 26: Activities produced by the neutron irradiation of selected elements, for a fuel-assembly end-adaptor irradiation scenario <u>DECO_1yr_50yr_1E14</u>	139
Figure 27: Dose-rates produced by the neutron irradiation of selected elements, for a fuel-assembly end-adaptor irradiation scenario <u>DECO_1yr_50yr_1E14</u>	141
Figure 28: Activities produced by the neutron irradiation of selected elements, for a neutron radiography (NRAD) irradiation scenario <u>NRAD_1h_30d_1E9</u>	143
Figure 29: Dose-rates produced by the neutron irradiation of selected elements, for a neutron radiography irradiation scenario <u>NRAD_1h_30d_1E9</u>	144
Figure 30: Activities produced by the neutron irradiation of selected elements, for a neutron radiography (NRAD) irradiation scenario <u>NRAD_1d_30d_1E9</u>	145
Figure 31: Dose-rates produced by the neutron irradiation of selected elements, for a neutron radiography irradiation scenario <u>NRAD_1d_30d_1E9</u>	146
Figure 32: Mathcad-14 implementation of Eq. (7) (page 154) — calculation of the cooling time required to meet regulatory clearance levels	155
Figure 33: Ratio of activities A(t) induced in Ti by neutron activation at $\phi = 1E10 \text{ cm}^{-2} \text{ s}^{-1}$ and at $\phi = 1E9 \text{ cm}^{-2} \text{ s}^{-1}$ i.e. in the low fluence-rate domain; a ratio of 10 indicates linear behaviour	168

- Figure 34: Ratio of activities $A(t)$ induced in Ti by neutron activation at $\phi = 1E14 \text{ cm}^{-2} \text{ s}^{-1}$ and at $\phi = 1E13 \text{ cm}^{-2} \text{ s}^{-1}$ i.e. in the medium-high fluence-rate domain; a ratio of 10 indicates linear behaviour168
- Figure 35: Ratio of activities $A(t)$ induced in Ti by neutron activation at $\phi = 1E15 \text{ cm}^{-2} \text{ s}^{-1}$ and at $\phi = 1E14 \text{ cm}^{-2} \text{ s}^{-1}$ i.e. in the high fluence-rate domain.....169
- Figure 36: Ratio of activities $A(t)$ induced in Cr by neutron activation at $\phi = 1E10 \text{ cm}^{-2} \text{ s}^{-1}$ and at $\phi = 1E9 \text{ cm}^{-2} \text{ s}^{-1}$ i.e. in the low fluence-rate domain; a ratio of 10 indicates linear behaviour170
- Figure 37: Ratio of activities $A(t)$ induced in Cr by neutron activation at $\phi = 1E14 \text{ cm}^{-2} \text{ s}^{-1}$ and at $\phi = 1E13 \text{ cm}^{-2} \text{ s}^{-1}$ i.e. in the medium-high fluence-rate domain; a ratio of 10 indicates linear behaviour170
- Figure 38: Ratio of activities $A(t)$ induced in Cr by neutron activation at $\phi = 1E15 \text{ cm}^{-2} \text{ s}^{-1}$ and at $\phi = 1E14 \text{ cm}^{-2} \text{ s}^{-1}$ i.e. in the high fluence-rate domain.....171
- Figure 39: Ratio of activities $A(t)$ induced in Mn by neutron activation at $\phi = 1E13 \text{ cm}^{-2} \text{ s}^{-1}$ and at $\phi = 1E12 \text{ cm}^{-2} \text{ s}^{-1}$ i.e. in the intermediate fluence-rate domain; a ratio of 10 indicates linear behaviour172
- Figure 40: Ratio of activities $A(t)$ induced in Mn by neutron activation at $\phi = 1E14 \text{ cm}^{-2} \text{ s}^{-1}$ and at $\phi = 1E13 \text{ cm}^{-2} \text{ s}^{-1}$ i.e. in the medium-high fluence-rate domain; a ratio of 10 indicates linear behaviour172
- Figure 41: Ratio of activities $A(t)$ induced in Mn by neutron activation at $\phi = 1E15 \text{ cm}^{-2} \text{ s}^{-1}$ and at $\phi = 1E14 \text{ cm}^{-2} \text{ s}^{-1}$ i.e. in the high neutron fluence-rate domain173
- Figure 42: Ratio of activities $A(t)$ induced in Fe by neutron activation at $\phi = 1E14 \text{ cm}^{-2} \text{ s}^{-1}$ and at $\phi = 1E13 \text{ cm}^{-2} \text{ s}^{-1}$ i.e. in the medium-high fluence-rate domain; a ratio of 10 indicates linear behaviour174
- Figure 43: Ratio of activities $A(t)$ induced in Fe by neutron activation at $\phi = 1E15 \text{ cm}^{-2} \text{ s}^{-1}$ and at $\phi = 1E14 \text{ cm}^{-2} \text{ s}^{-1}$ i.e. in the high neutron

	fluence-rate domain; a ratio of 10 indicates linear activation behaviour.....	174
Figure 44:	Ratio of activities $A(t)$ induced in Co by neutron activation at $\phi = 1E15 \text{ cm}^{-2} \text{ s}^{-1}$ and at $\phi = 1E14 \text{ cm}^{-2} \text{ s}^{-1}$ i.e. in the high neutron fluence-rate domain; a ratio of 10 indicates linear activation behaviour.....	175
Figure 45:	Ratio of activities $A(t)$ induced in Ni by neutron activation at $\phi = 1E15 \text{ cm}^{-2} \text{ s}^{-1}$ and at $\phi = 1E14 \text{ cm}^{-2} \text{ s}^{-1}$ i.e. in the high neutron fluence-rate domain; a ratio of 10 indicates linear behaviour	176
Figure 46:	Ratio of activities $A(t)$ induced in Cu by neutron activation at $\phi = 1E15 \text{ cm}^{-2} \text{ s}^{-1}$ and at $\phi = 1E14 \text{ cm}^{-2} \text{ s}^{-1}$ i.e. in the high neutron fluence-rate domain; a ratio of 10 indicates linear activation behaviour.....	176
Figure 47:	Ratio of activities $A(t)$ induced in Ag by neutron activation at $\phi = 1E15 \text{ cm}^{-2} \text{ s}^{-1}$ and at $\phi = 1E14 \text{ cm}^{-2} \text{ s}^{-1}$ i.e. in the high neutron fluence-rate domain; a ratio of 10 indicates linear behaviour	177
Figure 48:	Ratio of activities $A(t)$ induced in the element caesium (Cs) by neutron activation at $\phi = 1E14 \text{ cm}^{-2} \text{ s}^{-1}$ and at $\phi = 1E13 \text{ cm}^{-2} \text{ s}^{-1}$ i.e. in the medium-high fluence-rate domain; a ratio of 10 indicates linear behaviour.....	178
Figure 49:	Ratio of activities $A(t)$ induced in Cs by neutron activation at $\phi = 1E15 \text{ cm}^{-2} \text{ s}^{-1}$ and at $\phi = 1E14 \text{ cm}^{-2} \text{ s}^{-1}$ i.e. in the high neutron fluence-rate domain	178
Figure 50:	Ratio of activities $A(t)$ induced in the element europium (Eu) by neutron activation at $\phi = 1E14 \text{ cm}^{-2} \text{ s}^{-1}$ and at $\phi = 1E13 \text{ cm}^{-2} \text{ s}^{-1}$ i.e. in the medium-high fluence-rate domain; a ratio of 10 indicates linear behaviour.....	179
Figure 51:	The Periodic Table of the Elements (Holden et al., 2018).....	180

Figure 52: Reaction cross-section for the neutron activation reaction $\text{Co-59} + \text{n} \rightarrow \text{Co-60}$204

LIST OF TABLES

Table 1: Unconditional clearance levels for radionuclides, according to (IAEA, 1996)	2
Table 2: Clearance levels and clearance and exemption classifications of important radionuclides, as set by the Canadian Nuclear Safety Commission (CNSC, 2018).....	3
Table 3: Surface clearance levels for selected radionuclides, for the re-use of metallic items	4
Table 4: Irradiation-and-cooldown scenario $\boxed{\text{DECO}_{60a_{6a}} 1E14}$	16
Table 5: Irradiation-and-cooldown scenario $\boxed{\text{DECO}_{T_{\text{irrad}} T_{\text{cool}} \phi}}$	16
Table 6: Irradiation-and-cooldown scenario $\boxed{\text{NRAD}_{T_{\text{irrad}} T_{\text{cool}} \phi}}$	17
Table 7: Radionuclides that will typically be produced during the neutron-induced activation process in nuclear fission reactor facilities (IAEA, 2019) 30	
Table 8: Major activation radionuclides in decommissioning waste at a TRIGA Mark II research reactor, reported by (Ackermann, 2017)	31
Table 9: Radionuclides that are significantly present in reactor concrete subjected to neutron irradiation (NEA, 2011)	48
Table 10: Clearance levels for metal scrap recycling (Lentijo, 2002)	53
Table 11: Summary of long-lived activation-radionuclides and the materials in which they are produced, during the operation of a nuclear power plant (NPP).....	55
Table 12: Specification of an “All-Element” Material that Contains 100 g of Every Chemical Element Found in Nature	67

Table 13: Activities at $\phi = 1\text{E}14 \text{ cm}^{-2} \text{ s}^{-1}$ compared to activities at $\phi = 1\text{E}13 \text{ cm}^{-2} \text{ s}^{-1}$, for the activation of an all-element target material in the high fluence-rate domain	70
Table 14: Activities at $\phi = 1\text{E}9 \text{ cm}^{-2} \text{ s}^{-1}$ compared to activities at $\phi = 1\text{E}8 \text{ cm}^{-2} \text{ s}^{-1}$ for the activation of an all-element target material in the low neutron fluence-rate domain	75
Table 15: Mass-depletion and mass-augmentation in a hypothetical material that initially contains all terrestrial elements, and is irradiated under scenario <u>DECO_60yr_1E14</u>	83
Table 16: Typical change in the isotopic composition of Fe undergoing intense neutron irradiation in scenario <u>DECO_60yr_6yr_1E14</u>	86
Table 17: Activities of induced radionuclides for the irradiation of a 100 g sample of Fe at two integral neutron fluence-rates that differ by a factor 10 in magnitude, namely $\phi_{lo} = 1\text{E}13 \text{ cm}^{-2} \text{ s}^{-1}$ and $\phi_{hi} = 1\text{E}14 \text{ cm}^{-2} \text{ s}^{-1}$.	89
Table 18: Summary by FISPACT-II of the pathways for the formation of selected radionuclides in a Fe sample irradiated at a high neutron fluence-rate	90
Table 19: Pathway summary for the formation of the radionuclide Co-60 from the irradiation of a sample that initially contained 100% pure Fe, by an intense field of LWR neutrons	91
Table 20: Activities of induced radionuclides for the irradiation of a 0.1 kg sample of Mn at two neutron fluence-rates that differ by a factor 10 in magnitude.....	92
Table 21: Activities of induced radionuclides for the irradiation of a 0.1 kg sample of the element Cr at two neutron fluence-rates that differ by a factor 10 in magnitude	94
Table 22: Radiological ranking of the elements for an irradiation scenario <u>DECO_60yr_6yr_1E14</u>	97

Table 23: Radiological ranking of the elements for an irradiation scenario DECO_60yr_6yr_1E13	100
Table 24: Radiological ranking of the elements for irradiation scenario DECO_60yr_6yr_1E12	103
Table 25: Radiological ranking of the elements for the irradiation scenario DECO_60yr_6yr_1E11	105
Table 26: Radiological ranking of the elements in a fuel-assembly end-adaptor irradiation scenario DECO_1yr_6yr_1E14	109
Table 27: FISPACT input specification for Al-6082	112
Table 28: Radiological ranking of the elements in the irradiation scenario NRAD_1h_30d_1E9	113
Table 29: Radiological ranking of the elements in an NRAD irradiation scenario NRAD_1d_30d_1E9	116
Table 30: Activation matrix for the element Mg, under irradiation scenario DECO_60yr_6yr_1E14	148
Table 31: Activation matrix for the element Al, under irradiation scenario DECO_60yr_6yr_1E14	149
Table 32: Activation matrix for the element Si, under irradiation scenario DECO_60yr_6yr_1E14	150
Table 33: Activation matrix for the element Ca, under irradiation scenario DECO_60yr_6yr_1E14	151
Table 34: Activation matrix for the element Ti, under irradiation scenario DECO_60yr_6yr_1E14	152
Table 35: Activation matrix for the element vanadium (V), under irradiation scenario DECO_60yr_6yr_1E14	153

Table 36: Activation matrix for the element chromium (Cr), under irradiation scenario DECO_60yr_6yr_1E14	155
Table 37: Activation matrix for the element manganese (Mn), under irradiation scenario DECO_60yr_6yr_1E14	156
Table 38: Activation matrix for the element iron (Fe), under irradiation scenario DECO_60yr_6yr_1E14	157
Table 39: Activation matrix for the element cobalt (Co), under irradiation scenario DECO_60yr_6yr_1E14	157
Table 40: Activation matrix for the element Nickel (Ni), under irradiation scenario DECO_60yr_6yr_1E14	158
Table 41: FISPACT-II material input for the calculational experiment designed to identify problematic long-lived radionuclides produced at LWR facilities.....	159
Table 42: Identification of problematic, long-lived radionuclides produced at LWR plants.....	161
Table 43: Radionuclides found to exceed clearance limits in a DECO_60yr_6yr_1E10 irradiation-cooling scenario.....	163
Table 44: Final, verified list of radionuclides of highest concern, at times 6 years or longer after reactor shutdown, from the viewpoint of ease-of-clearance of long-term irradiated engineering materials	166
Table 45: Seven irradiation scenarios used to investigate whether neutron activation behaves linearly	167
Table 46: Non-linearity in the activation of the element zirconium (Zr)	180
Table 47: The NIST's calculated results for the neutron activation of 100 grams of ^{nat}Cr in neutron fluence-rates of $\phi_{lo} = 1\text{E}8 \text{ cm}^{-2} \text{ s}^{-1}$ and $\phi_{hi} = 1\text{E}15 \text{ cm}^{-2} \text{ s}^{-1}$, for $T_{irr} = 1 \text{ yr}$ and $T_{cool} = 1 \text{ yr}$, compared with	

calculations using FISPACT-II models developed in this work, for
identical exposures.....187

ABBREVIATIONS AND SPECIAL NOMENCLATURE

α	α -particle
ACE	“A Compact ENDF” cross-section files, used by the MCNP code
ALARA	As Low As Reasonably Achievable, i.e. the need to optimize radiation protection as far as possible, to lower worker and public exposure to ionising radiation doses as far as possible below regulatory dose-limits
ATTILA	A radiation transport code based on a numerical solver that deterministically solves the Linear Boltzmann Transport Equation, without the use of empirical corrections ¹
BSSD	Basic Safety Standards Directive (by Euratom)
BWR	Boiling Water Reactor
CA	Criticality Accident
CL	Clearance Level
CNR	Center for Neutron Research (at the NIST, USA)
CNSC	Canadian Nuclear Safety Commission
d	Deuteron, i.e. a 2_1H nucleus
DR	Dose-Rate
DIPR	Dedicated Isotope Production Reactor
EA	End-Adaptors of MTR fuel-assemblies

¹ Note by co-supervisor TJvR: A major bottleneck in using MCNP is the creation of Constructive Surface Geometry (CSG) surface-cards and cell-cards, which can be extremely time-consuming to both build and verify. Attila4MC provides CAD integration with MCNP, allowing 3D solid models to be imported into Attila4MC, meshed, then exported in a format readable by the unstructured mesh capabilities in MCNP.

ENDF/B	Evaluated Nuclear Data File, type B
EU	European Union
FA	Fuel-Assembly
FISPACT	A materials activation code, developed by the UKAEA
FR	Fluence-Rate
γ	Ionising photon also referred to as a γ -photon or γ -ray
HEU	High Enrichment Uranium
HEU ₉₀	High Enrichment Uranium with enrichment grade 90 % U-235 by mass
HEU ₄₅	High Enrichment Uranium with enrichment grade 45 % U-235 by mass
HFR	High-Flux Reactor
IAEA	International Atomic Energy Agency
ICRP	International Commission on Radiological Protection
ICRU	International Commission on Radiation Units and Measurements
ID	Inner Diameter
IP	Ionising Photon (this is used in place of the typical but imprecise term used in the nuclear industry — “ γ -ray”)
LANL	Los Alamos National Laboratories
LEU	Low Enrichment Uranium
LEU ₂₀	Low Enrichment Uranium with enrichment grade 19.75 % U-235 by mass
LHS	Left Hand Side
LODE	(systems of) Linear Ordinary Differential Equations
LWR	Light Water Reactor

MCNP	Monte Carlo N-Particle code
MTR	Materials Testing Reactor, nowadays rather called Research Reactor
n	Neutron
$(n, 2n)$	(neutron, 2-neutron) nuclear reaction
(n, α)	(neutron, alpha-particle) nuclear reaction
(n, d)	(neutron, deuteron) nuclear reaction
(n, γ)	(neutron, photon) nuclear reaction
(n, p)	(neutron, proton) nuclear reaction
(n, np)	(neutron, neutron + proton) nuclear reaction
(n, t)	(neutron, tritium) nuclear reaction
NA	Neutron Activation
$\{N, A\}$	$\{Nuclide, Activity\}$ -matrix, i.e. a 2-column matrix where the elements of the first column contain the identity of a radionuclide and the second column the corresponding activities of these nuclides
NAP	Neutron Activation Product
NBDR	Natural Background Dose-Rate, i.e. a dose-rate of circa 0.1 $\mu\text{Sv/h}$.
NCRP	National Council on Radiation Protection and Measurements, USA
NEA	Nuclear Energy Agency
Necsa	The South African Nuclear Energy Corporation SOC Ltd
NFR	Neutron Fluence-Rate
NFRs	Neutron Fluence-Rates
NIST	National Institute of Standards and Technology (USA)

NNR	National Nuclear Regulator
NPP	Nuclear Power Plant
NRAD	Neutron Radiography (facility)
NS	Neutron Spectrum
OECD	Organisation for Economic Co-operation and Development
ORIGEN	Oak Ridge Isotope GENERation—a neutron activation and inventory code within the SCALE system developed at ORNL
ORNL	Oak Ridge National Laboratories, USA
PDR	Photon Dose-Rate (also called the Gamma Dose-Rate)
PFN	Prompt Fission Neutron
PT	Periodic Table (of the chemical elements)
PWR	Pressurized Water Reactor
RCS	Reactor Coolant System
RHS	Right Hand Side
RP	Radiation Protection
RPV	Reactor Pressure Vessel
RPVH	Reactor Pressure Vessel Head
RQ	Research Question
RR	Research Reactor
SAFARI-1	A 20 MW _t MTR at Necca, Pelindaba, South Africa
SHEQ	Safety, Health, Environment and Quality
SS	Stainless-Steel

SS-304	Stainless-Steel 304
SS-304L	Stainless-Steel 304L (low-carbon; better suited for welding)
SS-316	Stainless-Steel 316
SS-316L	Stainless-Steel 316L (low-carbon; better suited for welding)
SSC	Structures, Systems and Components
t	Triton, i.e. a 3_1H nucleus
TALYS	A Nuclear Model Code System for the Analysis and Prediction of Nuclear Reactions and the Generation of Nuclear Data
TENDL	TALYS-based Evaluated Nuclear Data Library; TENDL is a nuclear data library which provides the output of the TALYS nuclear model code system for direct use in both basic physics and applications. The 10th version is TENDL-2019 (December 2019), which is based on both default and adjusted TALYS calculations and nuclear data from other sources
T_{cool}	Cooling time (i.e. decay time)
T_{irr}	Irradiation time
TJvR	T. Johann van Rooyen (co-supervisor for this dissertation)
TP	Target Plate
UK	United Kingdom
UKAEA	UK Atomic Energy Agency
USA	United States of America
V&V	Verification and Validation
WAC	Waste Acceptance Criteria
XS	Cross-section

1 INTRODUCTION

1.1 Background and Rationale

1.1.1 Neutron Activation

At nuclear reactor facilities, significant neutron radiation fields are encountered inside and around the reactor vessel. Engineering materials exposed to the neutron field, as well as radionuclide production targets undergoing neutron irradiation, absorb neutrons in nuclear reactions, and radioisotopes are produced in this way. This process is termed *neutron activation*. Neutron activation produces radionuclides in irradiated materials, i.e. irradiated materials will become radioactive because radioisotopes are produced inside the materials undergoing irradiation by neutrons. Some neutron activation reactions are commercially beneficial, e.g. the production of Ir-192 from irradiated Ir-191. Other radionuclides produced by neutron activation, are undesired and may place a radioactive waste burden on the licensed facility, adding to total operational costs. After irradiation by the neutron field ends, radionuclides will remain present in irradiated materials and will present radiological and radioactive waste-disposal problems such as e.g.

- A radiation field will be present around the activated material and will expose workers to doses of ionising radiation.
- Some activated material may not pass clearance level criteria set by e.g. the IAEA and will therefore have to be disposed of as radioactive waste, at a significant cost.

1.1.2 Clearance Levels: IAEA

The IAEA sets distinct *clearance levels* for different classes of radioisotopes, based on model-based radiation exposure calculations and radiological risk-assessment criteria. Table 1 is a summary of information in (IAEA, 1996), showing the clearance levels of 5 categories of radionuclides. The clearance level of a radionuclide is the activity per unit mass or per unit surface area, at which the material may be released into e.g. the public domain.

Table 1: Unconditional clearance levels for radionuclides, according to (IAEA, 1996)

Clearance Category	Clearance Level — Lower Limit	Clearance Level — Upper Limit	Radionuclides	Half-Life
1	0.1 Bq/g	1.0 Bq/g	Na-22	2.6018 a
			Co-60	5.2712 a
			Na-24	14.957 h
			Mn-54	312.2 d
			Zn-65	243.93 d
			Nb-94	20,400 a
			Ag-110m	249.95 d
			Sb-124	60.2 d
			Cs-134	2.0652 a
			Cs-137	30.08 a
			Eu-152	13.517 a
			Pb-210	22.2 a
2	1 Bq/g	10 Bq/g	Co-58	70.86 d
			Fe-59	44.495 d
			Sr-90	28.79 a
			Ru-106	371.8 d
			In-111	2.8063 d
			I-131	8.0252 d
			Ir-192	73.83 d
			Au- 198	2.6941 d
3	10 Bq/g	100 Bq/g	Cr-51	27.701 d
			Co-57	271.7 d
			Tc-99m	6.02 h
			I-123	13.2235 h
			I-125	59.407 d
			I-129	1.57000E7 a
			Ce-144	284.91 d
			Tl-201	3.0442 d
4	100 Bq/g	1000 Bq/g	C-14	5700 a
			P-32	14.268 d
			Cl-36	3.0129994E5 a
			Fe-55	2.744 a
			Sr-89	50.563 d
			Y-90	2.6666667 d
			Tc-99	2.111E5 a
			Cd-109	1.2638189 a
5	1000 Bq/g	10 000 Bq/g	H-3	12.32 a
			S-35	87.37 d
			Ca-45	162.61 d
			Ni-63	101.2 a
			Pm-147	2.6234 a

In Table 1 the 5 Clearance Categories of (IAEA, 1996) have been colour-coded to guide the eye.

From Table 1 it is seen that e.g. the radionuclides Na-22, Mn-54, Co-60, Zn-65, Nb-94, Ag-110m, Cs-134, Eu-152 and Pb-201 are most problematic, if formed in materials, because the clearance levels for these radionuclides are highly restrictive; the presence of these radionuclides at levels above a level as low as 0.1 Bq/g, can prevent the unconditional clearance of such materials. If e.g. the activity per unit mass of Co-60 or Eu-152 in concrete of a reactor building that is decommissioned, exceeds 0.1 Bq/g by more than a factor of, e.g. 2, all this concrete will have to be broken up and drummed in standard 200-litre waste drums, and sent to a national waste-disposal facility, at great cost. From Table 1 it is also seen that other radionuclides, particularly H-3, Ca-45 and Ni-63, enjoy much more lenient clearance levels than the “most problematic radioisotope” category.

1.1.3 Clearance Levels: Canadian Nuclear Safety Commission (CNSC) 2018

The Canadian Nuclear Safety Commission sets forth (CNSC, 2018) information, including clearance level and clearance and exemption classification, for a reasonably comprehensive list of radionuclides encountered in the nuclear reactor industry. These are summarised in Table 2. Class A refers to the most hazardous, most-restricted radionuclides while Class C refers to the least hazardous, least restricted nuclides. The primary reason for including Table 2, is that the other reference guides ((NISDF, 2017), (IAEA, 1996) and (IAEA, 2004)) omit the radioisotope Ba-133, whereas (CNSC, 2018) does categorise and list it.

Table 2: Clearance levels and clearance and exemption classifications of important radionuclides, as set by the Canadian Nuclear Safety Commission (CNSC, 2018)

Radionuclide	Clearance and Exemption Classification	CNSC Clearance Level (Bq/g)
Na-22	Class A	1.0E1
Co-60	Class A	1.0E1
Cs-137	Class A	1.0E1
Ba-133	Class B	1.0E2
H-3	Class C	1.0E6

Radionuclide	Clearance and Exemption Classification	CNSC Clearance Level (Bq/g)
C-14	Class C	1.0E4
Cr-51	Class C	1.0E3
Fe-55	Class C	1.0E4

In Table 2, the CNSC's three Clearance and Exemption Classification Classes have been colour-coded to guide the eye.

1.1.4 Clearance Levels: Nuclear Industry Safety Directors Forum (NISDF, 2017)

In a publication, *The UK Nuclear Industry Guide To: Clearance and Radiological Sentencing: Principles, Process and Practices* (NISDF, 2017), surface-activity clearance levels for an exhaustive list of radionuclides, are listed in the unit Bq/cm²; values for selected radionuclides are listed in Table 3, which is a sorted and colour-coded representation of the information in Table F.1 on page 181 of (NISDF, 2017).

Table 3: Surface clearance levels for selected radionuclides, for the re-use of metallic items

Radionuclide	Z	A	Surface clearance levels for re-use of metallic items (Bq/cm ²)
Pb-210	82	210	0.660
Co-60	27	60	1.00
Na-22	11	22	1.10
Ag-108m	47	108	1.30
Ag-110m	47	110	1.30
Nb-94	41	94	1.40
Bi-207	83	207	1.40
Cs-134	55	134	1.60
Eu-154	63	154	1.80
Eu-152	63	152	2.00
Co-56	27	56	2.10
Sc-46	21	46	3.40
Zr-95	40	95	3.60
Mn-54	25	54	3.70
Cs-137	55	137	3.70
I-129	53	129	4.00

Radionuclide	Z	A	Surface clearance levels for re-use of metallic items (Bq/cm²)
Ta-182	73	182	4.20
Sb-124	51	124	5.10
Sb-125	51	125	5.20
Zn-65	30	65	6.30
Tb-160	65	160	7.30
Co-58	27	58	8.00
Os-185	76	185	8.70
Ir-192	77	192	9.20
Se-75	34	75	14.0
Ru-106	44	106	14.0
Cl-36	17	36	15.0
Sr-90	38	90	15.0
Sr-85	38	85	16.0
Sn-113	50	113	18.0
Co-57	27	57	30.0
Ce-139	58	139	30.0
Gd-153	64	153	31.0
Te-123m	52	123	37.0
Eu-155	63	155	41.0
Ce-144	58	144	68.0
Cd-109	48	109	91.0
I-125	53	125	130
W-181	74	181	140
Tc-97	43	97	150
Mo-93	42	93	170
Cs-135	55	135	220
Zr-93	40	93	290
Te-127m	52	127	300
Tl-204	81	204	310
Tc-97m	43	97	560
Tc-99	43	99	570
Tm-170	69	170	660
C-14	6	14	770
Y-91	39	91	810
Nb-93m	41	93	1000
Pm-147	61	147	1000
As-73	33	73	1100
Ca-45	20	45	1200
Fe-55	26	55	1500
S-35	16	35	1800
W-185	74	185	2000
Ni-63	28	63	3000

Radionuclide	Z	A	Surface clearance levels for re-use of metallic items (Bq/cm ²)
Sm-151	62	151	3200
Tm-171	69	171	3200
Ni-59	28	59	7100
Mn-53	25	53	1.50E+04
H-3	1	3	2.50E+04

To guide the eye, the 5 distinct hazard-classes of radionuclides set by (NISDF, 2017) have been colour-coded in Table 3.

In Table 3 the nuclides Na-22, Co-60, Zn-65, Ag-108m, Ag-110m, Nb-94, Cs-134, Eu-154, Eu-152, Mn-54 and Zn-65 are — as in Table 1 — found amongst the group having the lowest clearance levels, i.e. these are the *most* dangerous group of radionuclides. Note that Table 3 adds Ag-108m to the “most problematic nuclides” list; this isotope is absent in Table 1. As in Table 1, the radio-isotopes Fe-55, Ni-63 and H-3 belong to the *least* problematic categories of radionuclides having the highest i.e. most liberal/lenient clearance levels.

When materials are tested to determine either the activity per unit mass or per unit surface area, a decision is made whether the material may be cleared unconditionally, whether it must be stored for an additional period of time to allow unconditional clearance levels to be met, or whether it must be disposed of as radioactive waste at a disposal facility. Because this process is analogous to the operation of a court of law pronouncing judgement, it is termed “radiological sentencing” (NISDF, 2017).

The surface clearance-level information in Table 3, as taken from (NISDF, 2017) is exceptionally valuable because the clearance levels are directly and quantitatively derived from dosimetry models, with minimal rounding-off of numerical results, taking into account the following exposure scenarios and pathways:

1. Skin dose from the re-use of cleared equipment
2. Dose from inadvertent ingestion incurred during the reuse of equipment
3. External gamma dose incurred during the reuse of cleared equipment
4. Inhalation dose incurred during normal use of cleared equipment
5. Inhalation dose incurred during cleaning/sanding of cleared equipment

6. Inhalation dose incurred during repair/scrapping of cleared equipment.

Clearance level information published by other regulatory and advisory agencies typically suffers from excessive rounding-off of numerical values — see e.g. the objections raised by (Public Health England, 2018) as presented in §3.5.5 on page 34. The information in Table 3 does not suffer from severe rounding-off and coarse category-binning. The clearance levels for a wide range of radionuclides are derived from dosimetry models and are specified individually to 3 significant digits. (In contrast, the (IAEA, 1996) presents clearance levels in wide category-bins, as is evident in Table 1 on page 2.)

1.1.5 Materials Affected by Neutron Activation at Necsa, South Africa

At Necsa, Pelindaba, South Africa, the SAFARI-1 research reactor² has been in operation since 1965. Since circa 1998, this reactor is chiefly operated as a Dedicated Isotope Production Reactor (DIPR). Since 1995, SAFARI-1 runs at a nominal power of 20 MW. This means that approximately $1.5E18$ neutrons are released from nuclear fission events, every second. Neutron fluence-rates³ inside the reactor core generally ranges between $2E14 \text{ cm}^{-2} \text{ s}^{-1}$ and $5E14 \text{ cm}^{-2} \text{ s}^{-1}$ (SAFARI-1, 2005). Neutron fluence-rates in the aluminium core-box that surrounds the core can be as high as approximately $1.5E14 \text{ cm}^{-2} \text{ s}^{-1}$ (Van Rooyen, 2016) The fuel-assemblies are supported by the core grid-plate where the average neutron fluence-rate is circa $5E13 \text{ cm}^{-2} \text{ s}^{-1}$ (Van Rooyen, 2019). In the water pool around the reactor, neutron fluence-rates can reach

² An older term for a research reactor is a Materials Testing Reactor (MTR). The neutron fluence-rates attainable in a research reactor is typically a factor 10 to 20 times higher than the fluence-rates that will be encountered in a power reactor, and in the 1950s — when power reactor technology was still under development — different materials were irradiated for e.g. 3 years in an MTR to ascertain how they would perform over 40 years of exposure to neutrons in a power reactor. Today, these compact, low-temperature nuclear reactors are more typically used as DIPRs — Dedicated Isotope Production Reactors, and these complexes often also host a neutron radiography facility, which does not compete with the commercial radionuclide production programme.

³ Note by co-supervisor TJvR: Both the ICRP and ICRU specify that the correct term is *fluence-rate* and not “flux”; the latter is considered a “slang” term peculiar to the US nuclear engineering community – see (ICRP, 2010), (ICRU, 2011) and (ICRU and ICRP, 2017). For this reason, only the terms *fluence* and *fluence-rate* will be used in this work. Further, the American “slang” term “decay” will only seldomly be used; the preferred, proper physics term is (radioactive) *transition* — see the article *On Being Understood: Clarity and Jargon in Radiation Protection* by (Strom and Watson, 2002).

$5E13 \text{ cm}^{-2} \text{ s}^{-1}$ (Van Rooyen, 2015) while the fluence-rate in adjacent facilities such as the Neutron Radiography (NRAD) facility, can be as high as $1E9 \text{ cm}^{-2} \text{ s}^{-1}$ in specimens irradiated by the direct neutron beam (Van Rooyen, 2016b). Engineering materials that are exposed to intense neutron irradiation, such as the Al-alloy grid-plate, the core-box around the core, the Be and Al and Pb elements in the core, the balance of the core vessel structure, as well as practically all structural materials in the water-pool closer than circa 150 cm from the outer surface of the reactor core-box, may undergo significant neutron activation. Neutron beams entering the NRAD facility will activate the materials of the shielded irradiation chamber, as well as samples that are investigated via e.g. neutron tomography.

1.1.6 Reactor Decommissioning: The Need for Knowledge about the Systematics of the Neutron Activation of Elements in Engineering Materials

Operating licenses state that sites where nuclear reactors operate, must be returned to “greenfield status” after *decommissioning* — see e.g. the Youtube video⁴ (*Decommissioning a Nuclear Reactor*, 2013) on reactor decommissioning, referenced in the Bibliography. Greenfield status (also known as “unrestricted re-use”) is an endpoint wherein a parcel of land that had been in industrial use is, in principle, restored to the conditions existing before the construction of the plant. All power plants — coal, gas, and nuclear — have a finite life beyond which it is no longer economical to operate them. At this point they must be decommissioned; that is, they must be dismantled, and their components disposed of either by sale or scrapping or by being sent to a special repository for hazardous material. In some cases, the buildings that housed the plant may be put to other uses. However, in many cases, contamination is unacceptable so that the buildings must be demolished. The land on which the plant was built may also have been polluted with hazardous material, and in this case, other remedial measures like removal and replacement of the top-soil or clay-capping may be required to render the site safe in perpetuity (IAEA, 2002).

Many journal publications and conference proceedings such as e.g. (Kinno et al., 2011), (Alhajali et al., 2009), (Alhajali et al., 2016), (Bingham, 1965), (Evans et al., 1984), (Klein et al., 2001), (Klein and Moers, 2000), (Žagar and Ravnik, 2002) as well as (Žagar et al., 2004), mention that the presence of, especially, the elements Co (cobalt) and Eu (europium) in concrete

⁴ Refer to the References on page # for the full reference.

deployed in neutron radiation fields, lead to expensive radioactive waste-disposal problems, caused by neutron activation, when a nuclear reactor is decommissioned.

Knowledge of the “systematics” of the neutron activation of all the important chemical elements found in the biosphere, which may be present in engineering materials that will be exposed to significant fluence-rates of neutrons, must be developed for several reasons. When, e.g., a new reactor facility is built, knowledge of the systematics of neutron activation can guide engineers to select engineering materials that will minimise long-term neutron activation problems. When a rig is designed to be deployed close to a reactor, such knowledge of the systematics of neutron activation can also guide engineers to select “benign” materials that will minimize the future radioactive waste burden — a significant future liability.

During the design phase⁵, knowledge of the systematics of NA can guide engineers to specify materials, and to test raw materials, to guard against the incorporation of e.g. Co and Eu into “nuclear concrete”, i.e. concrete deployed in significantly intense neutron radiation fields. Likewise, such knowledge will be able to guide designers to select low-activation metal alloys. Examples of questions that will have to be answered by design engineers are: Which alloy will activate less: Al-6082 or SS-304L? Which concrete will activate less: Hematite concrete or ordinary concrete? Can commercially available Borax ($\text{Na}_2[\text{B}_4\text{O}_5(\text{OH})_4] \cdot 8\text{H}_2\text{O}$) be used to add the neutron-absorber boron to a neutron shield, or should the more expensive special compound B_4C be used; if so, why? In which chemical form should boron be added to a large underfloor water-tank at a particle accelerator facility, where it must serve as a neutron trap and a radiation shield —sodium-containing Borax or ammonium pentaborate?

1.2 Research Problem, Research Purpose and Research Objectives

The research problem to be solved is to use calculational methods to develop a systematic understanding and description of the “systematics” of the non-linear irradiation fluence-rate dependence of the radiological behaviour of every important chemical element, when the element is irradiated by a neutron field having a characteristic, standard LWR neutron spectrum,

⁵ Nuclear safety regulators such as the NNR forbid “design as you build”, i.e. structures, systems and components (SSCs) where radiation and nuclear safety are at stake, must be pre-designed and the design approved by the regulator, before building commences.

at a given fluence-rate, over operationally relevant irradiation and cooling times. Irradiation scenarios important to reactor decommissioning will be investigated, i.e. the theme of this dissertation is the *quantification of the systematics of the neutron activation characterisation of the chemical elements, in support of the decommissioning of nuclear reactors.*

1.3 Research Hypothesis

The research hypothesis at the foundation of this work can be formulated as follows: In nature, there exists a finite number (approximately 290) of stable or nearly stable isotopes, which are encountered in less than approximately 100 chemical elements. Every engineering material e.g. steel-alloys, aluminium-alloys, nickel-alloys and titanium-alloys will contain a subset of the chemical elements found in the Periodic Table (PT). To know how a given engineering material will respond, via neutron activation, with exposure to a neutron radiation field, one can perform *calculational experiments* using computer software *codes* and *nuclear data*, to quantify the individual neutron-activation “fingerprint” of each individual chemical element. In an engineering material composed of many chemical elements, the aggregated effect of the exposure of the ensemble of chemical elements to a given, fixed neutron exposure scenario, will be the superposition of the neutron activation “fingerprints” of individual chemical elements — for the identical neutron exposure scenario. With this methodology, it will be possible to individually investigate every chemical element via calculational experiments and then to sort or order the elements from *high-activator* to *low-activator* as well as into subsets such as e.g. (1) *highly problematic activators*, (2) *somewhat problematic activators* and (3) *benign, low-activators* for different practical, decommissioning-related irradiation-and-cooldown scenarios. These sorted lists of the elements can guide engineers in selecting low-activation construction materials for new reactor facilities and guide decommissioning planners to know which irradiated materials will be highly problematic, less problematic and non-problematic.

2 RESEARCH METHODOLOGY

2.1 Outline of the Research Methodology

The *research methodology* involves planning and conducting in the order of 1600+ *calculational experiments*. These calculational experiments are at the foundation of the following detailed research methodology:

1. Use the radiation transport code MCNP6.2 (LANL, 2018a) to calculate a single, representative, typical LWR neutron spectrum in 709 neutron energy groups — the neutron-energy multigroup structure that is required by the activation code FISPACT-II 3.0 (Sublet et al., 2015) to enable the use of modern ENDF format nuclear data such as TENDL-2017. This neutron spectrum will be characteristic and representative of the neutron field inside and around any thermal-spectrum LWR.
2. Use the activation code FISPACT-II 3.0 to calculate the total activity of all radionuclides formed in a reference mass of each element in the Periodic Table, except Tc and Pm, which are practically absent in nature and are therefore not encountered in engineering materials such as metal alloys and concretes.
3. Use the activation code FISPACT-II 3.0 to quantify the photon dose-rate (PDR) at a reference distance (1 m) from a reference mass (1 g) of an unshielded point source of every element in the Periodic Table. As before, the elements Tc and Pm are not considered.
4. Identify several elements that are of high interest for deployment in engineering structures such as steel-alloys, aluminium-alloys and bio-shield concretes. Use the activation code FISPACT-II 3.0 to calculate (1) the time-dependence of the dose-rate at the reference distance of 1 m from a reference mass of 1 g of irradiated elemental material, and (2) the time-dependence of the total activity in a reference mass of 100 g of irradiated elemental material. (The mass of 100 g was selected because the code FISPACT-II gives masses in grams, which can then be directly interpreted as a mass-%.)
5. Calculate “characteristic activation matrixes” for selected elements, irradiated under the above decommissioning scenario, i.e. 60 years of irradiation by a selected constant neutron fluence-rate with the LWR energy-spectrum $\phi(E)$, followed by 6 years of cooldown at a zero neutron fluence-rate.

Calculational models have been developed to serve as “calculational experiments” designed to probe and systematise the radiological behaviour of chemical elements, when such an element is irradiated by a neutron field having a characteristic, standard LWR neutron spectrum, at a given fluence-rate, in (1) a decommissioning scenario, (2) 1-year long irradiation of structural parts of fuel-assemblies, and (3) neutron radiography scenarios, i.e. short-term exposures.

2.2 Identities of the Main Chemical Elements Encountered in Engineering Structures in Nuclear Power Plants

Figure 1 shows the abundance of the chemical elements in the earth’s upper continental crust⁶. For practical reasons, construction materials must make use of relatively abundant minerals and metals.

⁶ Source: https://en.wikipedia.org/wiki/Abundance_of_elements_in_Earth%27s_crust

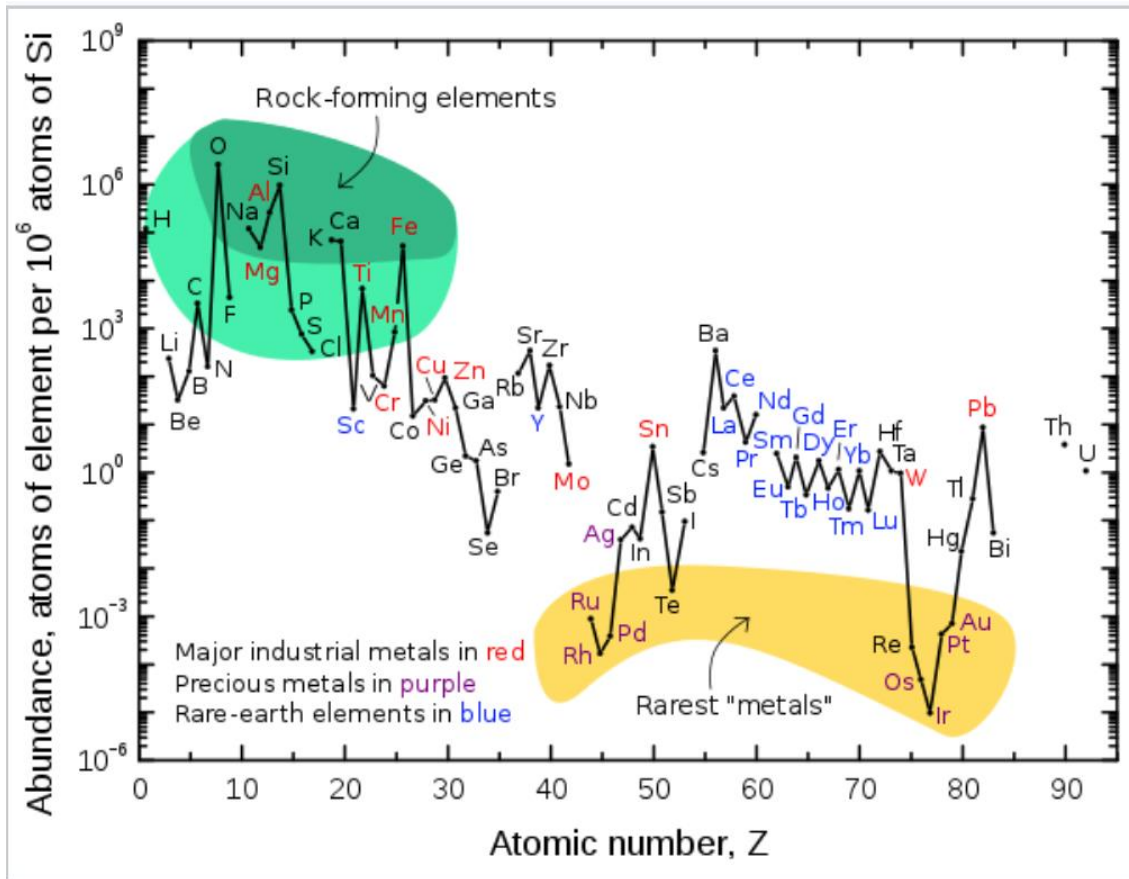


Figure 1: Relative abundance of the chemical elements in the earth's upper continental crust as a function of the atomic number Z

The construction material concrete is mainly composed of O, Si, Al and Ca, all of which are available in abundance in the earth's crustal material. Steel-alloys use mainly Fe along with Mn and Cr, all of which are in good abundance. Aluminium-alloys contain mainly Al, Mg and Si and varying quantities of Mn, Cu and Zn, all of which are relatively abundant and therefore readily available.

In steel-alloys, the trace metals Co and Nb are always present, but with a large quantitative variance. In concretes, variable fractions of trace-elements such as Co, Cs and Eu will be present. The trace-element Ag may also be encountered in engineering structures.

2.3 The Magnitude of Neutron Fluence-Rates in and Around the SAFARI-1 Reactor and its Peripheral Irradiation Facilities

The aim of this section is to quantify the range of neutron fluence-rates that will prevail in and around the SAFARI-1 reactor during full-power operation.

Figure 2 is a diagram of the top-view of the core and core-box of the SAFARI-1 MTR at Necsa, drawn by the SAFARI-1 Drawing Office.

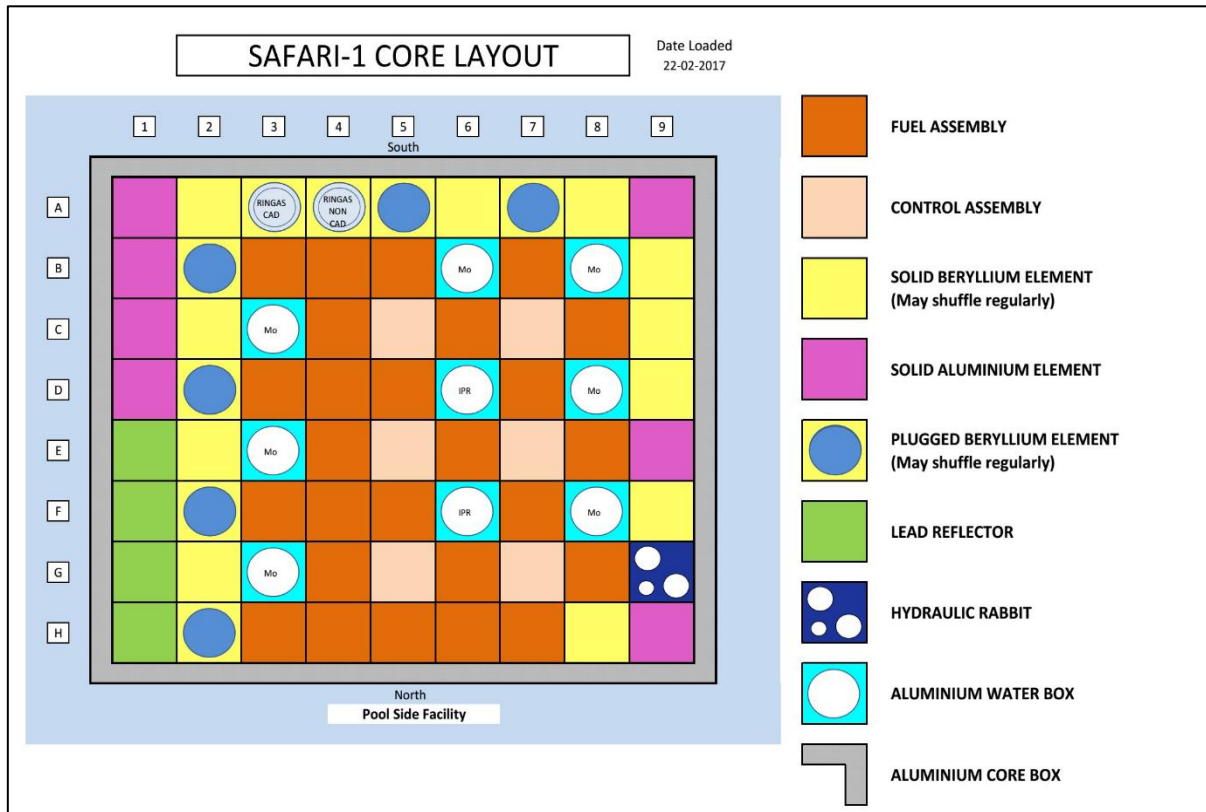


Figure 2: Diagram of the top-view of the core and core-box of the SAFARI-1 MTR at Necsa

The following components seen in Figure 2 will receive neutron fluence-rates above circa $3.0E14 \text{ cm}^{-2} \text{ s}^{-1}$ for a duration of less than 1 year:

- Fuel-assemblies
- Control-assemblies and their fuel-followers.

The following important components seen in Figure 2 will receive neutron fluence-rates between approximately $\phi \approx 0.5 \times 10^{14}$ and $1.5 \times 10^{14} \text{ cm}^{-2} \text{ s}^{-1}$ over the entire ± 60 yr operating lifetime of the reactor:

- Core-Box (CB)
- Be-reflector elements (BER)
- Lead elements (seen on the lower LHS)
- Grid-Plate (GP).

Neutron fluence-rates (NFRs) exiting beam-lines or entering the Large Irradiation Facility will be in the order of $\phi \approx 1.0 \times 10^9 \text{ cm}^{-2} \text{ s}^{-1}$ while NFRs in exposed components in the water pool around the reactor tank will depend on the distance from the core; fluence-rates in these regions will generally be well below $\phi = 1.0 \times 10^{13} \text{ cm}^{-2} \text{ s}^{-1}$.

Figure 3 presents a top view of the Neutron Radiography (NRAD) facility at the SAFARI-1 reactor⁷.

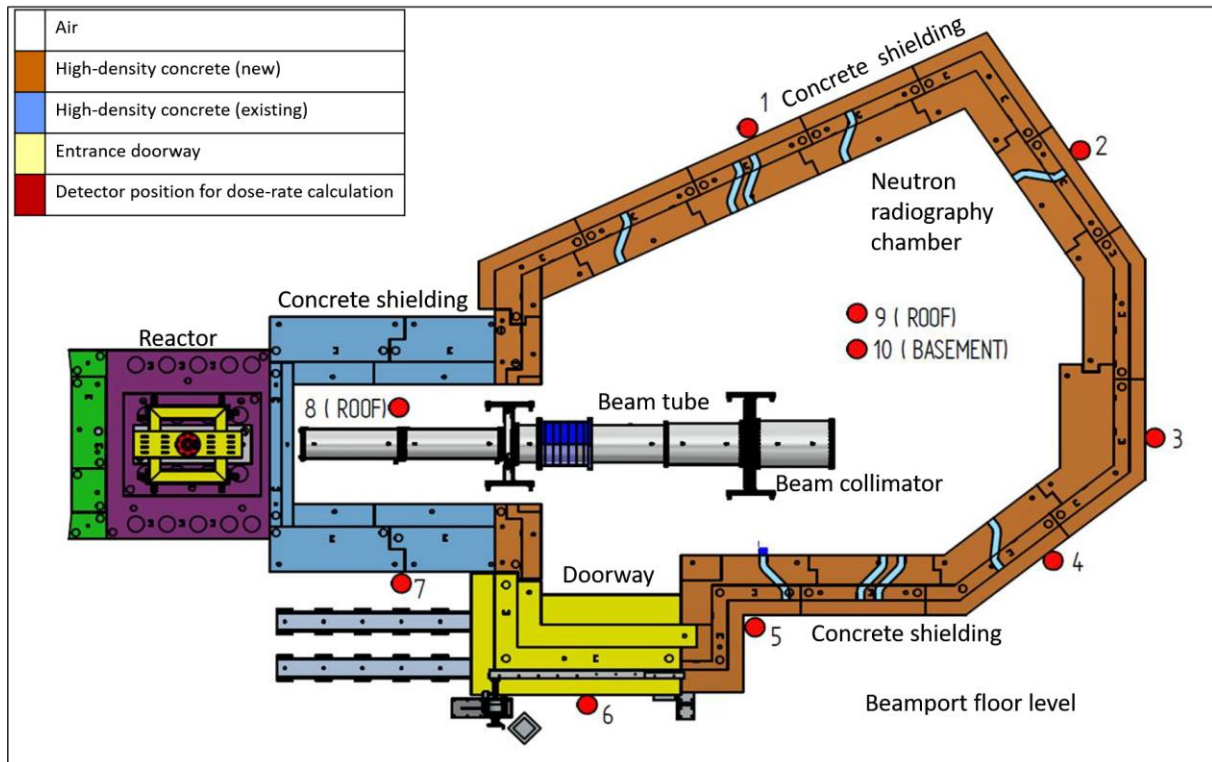


Figure 3: Schematic top-view of the Neutron Radiography Facility at the SAFARI-1 reactor, Necsca

In Figure 3 the neutron-beam enters from the LHS and hits the thick part of the high-Fe concrete shielding wall on the RHS (i.e. on the inside wall opposite to detector position 3 which is depicted by a small red circle). The maximum neutron fluence-rate in the primary NRAD beam is $\phi \approx 1.0 \times 10^9 \text{ cm}^{-2} \text{ s}^{-1}$ and the maximum beam-size is a circular beam with a radius of 24.7 cm — refer to (Grünauer, 2005) and (Van Rooyen, 2016b). All neutron fluence-rates in

⁷ This is a Necsca engineering drawing by the SAFARI-1 Drawing Office.

NRAD facility structures will, therefore, be capped below the above ceiling-value of $\phi \approx 1.0 \times 10^9 \text{ cm}^{-2} \text{ s}^{-1}$.

As a general rule, it can be said that materials that are exposed to NFRs of magnitude

$$\phi > 5.0 \times 10^{14} \text{ cm}^{-2} \text{ s}^{-1}$$

cannot be deployed in a nuclear reactor for more than circa 1 year. In an MTR, such high NFRs are encountered in fuel-assemblies. In the SAFARI-1 MTR, fuel-assemblies are never deployed for more than a maximum of approximately 310 days.

Components exposed to sustained maximum NFRs of magnitude

$$\phi < 2.0 \times 10^{14} \text{ cm}^{-2} \text{ s}^{-1}$$

can be deployed for the full 60 yr service life of the reactor, provided that that (1) they are manufactured from suitable materials such as e.g. 6000-series Al-alloys and (2) are regularly mechanically assessed by means of e.g. ultrasonic testing, to ensure fitness for continued service.

2.4 Concise Symbolic Nomenclature for Irradiation-and-Cooldown Scenarios

A symbolic notation was developed to present a concise, clear and informative definition of decommissioning-related (“DECO”) irradiation-and-cooldown scenarios. The meaning of the descriptor **DECO_60a_6a_1E14** is defined in Table 4.

Table 4: Irradiation-and-cooldown scenario **DECO_60a_6a_1E14**

Decommissioning Scenario DECO_60a_6a_1E14		
ϕ_n	=	$10^{14} \text{ cm}^{-2} \text{ s}^{-1}$
T_{irrad}	=	60 yr
T_{cool}	=	6 yr

The general symbolic specification for a decommissioning irradiation-and-cooldown scenario is **DECO_T_{irrad}_T_{cool}_φ** which should be read as specified in Table 5.

Table 5: Irradiation-and-cooldown scenario **DECO_T_{irrad}_T_{cool}_φ**

Decommissioning Scenario DECO_T_{irrad}_T_{cool}_φ	
---	--

Neutron fluence-rate	=	$\phi \text{ (cm}^{-2} \text{ s}^{-1}\text{)}$
Irradiation time	=	T_{irrad}
Cooling time	=	T_{cool}

The nomenclature $\boxed{\text{NRAD_}T_{irrad}_T_{cool}_\phi}$ signifies the irradiation of specimens in the neutron radiography (NRAD) facility, usually at $\phi \leq 10^9 \text{ cm}^{-2} \text{ s}^{-1}$, usually for durations $T_{irrad} \leq 1 \text{ d}$ and also for relatively short cooling periods such as cooling times below e.g. 100 days. The meaning of the symbolic notation $\boxed{\text{NRAD_}T_{irrad}_T_{cool}_\phi}$ is specified in Table 6.

Table 6: Irradiation-and-cooldown scenario $\boxed{\text{NRAD_}T_{irrad}_T_{cool}_\phi}$

Decommissioning Scenario $\boxed{\text{NRAD_}T_{irrad}_T_{cool}_\phi}$		
Neutron fluence-rate	=	$\phi \text{ (cm}^{-2} \text{ s}^{-1}\text{)}$
Irradiation time	=	T_{irrad}
Cooling time	=	T_{cool}

2.5 Decommissioning Scenario: Time-Dependence and Intensity of Neutron Fluence-Rate Field

By the term *decommissioning scenario*, we usually indicate an exposure of a material structure or component to an averaged neutron fluence-rate for 60 years, followed by a 6-year cooling period that will allow short-lived radionuclides to transition to negligible levels. The reasoning behind the above time-line is that (1) most nuclear reactors are nowadays operated for approximately 60 years, and (2) many nuclear reactor facilities opt to allow 5 to 10 years of “cooling” for the most activated structures such as reactor pressure vessels (RPVs), RPV heads, core-vessels (also known as core-boxes), grid-plates and control-rod drive-mechanisms (CRDMs), before completing the decommissioning and returning the site to the mandatory green-field status. The benefit of waiting 5 to 10 years, is a substantial reduction in worker exposure to ionising radiation — an exposure that involves a risk of radiation-related cancer — see e.g. (Van Rooyen, 2006), (Preston et al., 2003), (Leuraud et al., 2015) and (Kodama et al., 2012).

Let the variables ϕ denote fluence-rate, E energy and t time. Then the decommissioning scenario function $\phi_{deco}(E, t)$, with irradiation time and cooling time defined as **DECO_60a_6a_φ**, can be expressed as Eq. (1):

$$\phi_{deco}(E, t) = \begin{cases} \phi(E) & \forall \quad 0 \leq t \leq 60 \text{ yr} \\ 0 & \forall \quad t \geq 60 \text{ yr}. \end{cases} \quad (1)$$

The *decommissioning* irradiation-and-cooldown scenario (“deco”) of Eq. (1), involves 60 years of irradiation at a given neutron fluence-rate, followed by 6 years of cooling. The generic case **DECO_60a_6a_φ** will be investigated for the following discrete selection of real-world neutron integral fluence-rates ϕ :

- **DECO_60a_6a_1E14**: $\phi = 1E14 \text{ cm}^{-2} \text{ s}^{-1}$ — this is representative of irradiation of the Al-alloy of the reactor core-box, beryllium reflector elements, Pb-elements in the reflector region and the grid-plate.
- **DECO_60a_6a_1E13**: $\phi = 1E13 \text{ cm}^{-2} \text{ s}^{-1}$ — this is representative of the irradiation of structures just outside the core boundaries and just below the grid-plate.
- **DECO_60a_6a_1E12**: $\phi = 1E12 \text{ cm}^{-2} \text{ s}^{-1}$ — this is representative of the irradiation of structures such as the neutron beamline internals close to the core, and structures in the water-pool situated at roughly 20 cm to 30 cm from the core boundary.
- **DECO_60a_6a_1E11**: $\phi = 1E11 \text{ cm}^{-2} \text{ s}^{-1}$ — this is representative of the irradiation of structures such as the neutron beamline internals further from the core, and structures in the water-pool situated at roughly 30 cm to 40 cm from the core boundary.
- **DECO_60a_6a_1E10**: $\phi = 1E10 \text{ cm}^{-2} \text{ s}^{-1}$ — this is representative of the irradiation of structures such as the neutron beamline internals still further from the core, and structures in the water-pool situated at roughly 40 cm to 60 cm from the core boundary.
- **DECO_60a_6a_1E09**: $\phi = 1E09 \text{ cm}^{-2} \text{ s}^{-1}$ — this is representative of the long-term irradiation of shielding inside the NRAD facility that is directly struck by the neutron radiography beam.
- **DECO_60a_6a_1E08**: $\phi = 1E08 \text{ cm}^{-2} \text{ s}^{-1}$ — this is representative of the long-term irradiation of the shielding of the NRAD facility that is directly struck by the neutron-radiography beam when e.g. a less intense beam is used.

- **DECO_60a_6a_1E07**: $\phi = 1E07 \text{ cm}^{-2} \text{ s}^{-1}$ — this is representative of the long-term irradiation of the shielding inside the NRAD facility, for deeper/adjacent shielding strata.

2.6 Fuel-Assembly Irradiation Scenario: Time-Dependence and Intensity of Neutron Fluence-Rate Field

Another scenario that will be considered is the irradiation of structural parts of fuel-assemblies. In the SAFARI-1 reactor, fuel-assemblies are deployed for a maximum of 12 fuel cycles, i.e. for a total time of approximately $12 \times 25 \text{ days} \approx 300 \text{ days}$. This time duration will be, conservatively, approximated as 1 year. The neutron fluence-rate in the maximum fluence regions of the fuel-plate cladding can reach peak values approaching $\phi \approx 1E15 \text{ cm}^{-2} \text{ s}^{-1}$. Note that no structure inside the SAFARI-1 MTR will be irradiated at such an extremely high neutron fluence-rate for more than 1 year because material-failure will become very likely should irradiation times exceed 1 year. The end-adapters (which can also be called “nozzles”) of the fuel-assemblies will “see” neutron fluence-rates of circa $\phi \approx 1E14 \text{ cm}^{-2} \text{ s}^{-1}$, also for a maximum of 300 days, which will be approximated as 1 year. These two irradiation scenarios for non-fuel materials inside fuel-assemblies (FAs) are defined in Eq. (2) and Eq. (3):

$$\phi_{FA_{Clad_{Peak}}}(E, t) = \begin{cases} \phi = 1E15 \text{ cm}^{-2} \text{ s}^{-1} & \forall \quad 0 \leq t \leq 1 \text{ yr} \\ 0 & \forall \quad t \geq 1 \text{ yr} \end{cases} \quad (2)$$

and

$$\phi_{FA_{EA}}(E, t) = \begin{cases} \phi = 1E14 \text{ cm}^{-2} \text{ s}^{-1} & \forall \quad 0 \leq t \leq 1 \text{ yr} \\ 0 & \forall \quad t \geq 1 \text{ yr}. \end{cases} \quad (3)$$

Limited or no attention will be focused on scenario $\phi_{FA_{Clad_{Peak}}}(E, t)$, because the combined activity of all activation-products in the fuel-cladding is completely overwhelmed by that of the fission products formed inside the “meat” region of the fuel plates (T. J. Van Rooyen, 2017).

In contrast, the sawn-off FA end-adapters (EAs) contain no fission products and only activation products and will be investigated and reported, under the title **DECO_1a_6a_1E14**, which signifies 1 year of irradiation at $\phi = 1E14 \text{ cm}^{-2} \text{ s}^{-1}$ followed by 6 years of cooling.

2.7 Neutron Radiography (NRAD) Scenario: Time-Dependence and Intensity of Neutron Fluence-Rate Field

A limited number of additional irradiation scenarios will also be investigated, in order to be able to provide neutron activation related answers to groups that utilize neutron beams produced by an MTR, as well as to radiation protection staff. The NRAD (Neutron Radiography) research team typically irradiates samples — which are usually either industrial or paleontological in nature — at maximum neutron beam intensities of $\phi = 1E9 \text{ cm}^{-2} \text{ s}^{-1}$ for e.g. 1 to 18 hours, in neutron tomography. To be able to answer the NRAD group's questions about material activation, the two neutron radiography/tomography scenarios of Eq. (4) and Eq. (5) will, therefore, be investigated, on an element-by-element basis:

$$\phi_{NRAD_{short}}(E, t) = \begin{cases} \phi = 1E9 \text{ cm}^{-2} \text{ s}^{-1} & \forall \quad 0 \leq t \leq 1 \text{ hr} \\ 0 & \forall \quad t \geq 1 \text{ hr}. \end{cases} \quad (4)$$

as well as

$$\phi_{NRAD_{long}}(E, t) = \begin{cases} \phi = 1E9 \text{ cm}^{-2} \text{ s}^{-1} & \forall \quad 0 \leq t \leq 1 \text{ day} \\ 0 & \forall \quad t \geq 1 \text{ day}. \end{cases} \quad (5)$$

For the neutron irradiations in the NRAD facility, cooling times in the order of hours and days are important, because staff has to enter the facility to remove samples from the irradiation position, and place them on “cooling” racks for later removal, once dose-rates are acceptably low, in accordance with Necs SHEQ Instructions — see e.g. (Van Niekerk, 2010) as well as (Van der Merwe, 2017).

The ranking of the elements of the periodic table for the neutron radiography/tomography irradiation-and-cooldown scenario of Eq. (4) will be reported as **NRAD_1h_30d_1E9** i.e. 1 hour of exposure followed by 30 days of cooling.

The ranking of the elements of the periodic table for the neutron radiography/tomography irradiation-and-cooling scenario of Eq. (5) will be denoted as **NRAD_1d_30d_1E9**, i.e. 1 day of exposure followed by 30 days of cooling.

2.8 Scenario-Analysis Methodology

The above scenario-analysis methodology was designed to uncover clear, systematic knowledge about which elements are “benign” and which are “problematic” in under real-life neutron irradiation scenarios where the neutrons have an LWR energy-spectrum (as in Figure 6 on page 60). Development of the systematics of neutron-activation will have a range of benefits, such as e.g. the ability to guide engineers to select low-activation alloys, low-activation concrete, and to be able to pre-emptively know which materials will pose radiation hazards at decommissioning time. Such knowledge can be used to lower the exposure of workers to ionising radiation from activated structures during the decommissioning phase.

2.9 Research Questions to be Investigated

The following *research questions* (“RQ”) will be investigated and answered, using the methodology outlined above:

2.9.1 RQ₁: Linearity or Non-Linearity?

Is neutron activation for a given and fixed {material; irradiation time; cooling time; neutron spectrum $\phi(E)$ } set of conditions, a linear function of the integral neutron fluence-rate ϕ , or not? If not, is there a sub-domain of linearity, and when does linearity of neutron activation break down? If activities and dose-rates for e.g. DECO_7d_6a_1E14 is 10 times higher than for DECO_7d_6a_1E13, then neutron activation can be said to behave linearly. If, however, activities and dose-rates do not scale linearly with the intensity ϕ of the neutron fluence-rate, then neutron activation is a non-linear process.

2.9.2 RQ₂: Ranking of Elements for Irradiation Cases DECO_60a_6a_φ

For the Decommissioning Scenario defined in § 2.5 on page 17, calculate the ranking order of all irradiated elements in terms of the dose-rate at a distance of 1 m from a reference mass of 1 g of each irradiated chemical element, at $T_{cool} = 6$ yr, for all integral fluence-rates ϕ that are investigated.

2.9.3 RQ_3 : Ranking of Elements for Irradiation Case DECO_1a_6a_1E14

For the fuel-assembly (FA) end-adapter (“nozzle”) exposure scenario defined in § 2.6 on page 19, calculate the radiological ranking order of all irradiated chemical elements in terms of the dose-rate at a distance of 1 m from a reference mass of 1 g, for each irradiated chemical element, for $T_{irrad} = 1$ yr and at $T_{cool} = 6$ yr, for the integral fluence-rate $\phi = 10^{14}$ cm⁻² s⁻¹ — realistic irradiation conditions for FA end-adapters.

2.9.4 RQ_4 : Ranking of Elements for Irradiation Case NRAD_1h_30d_1E9 as well as for Case NRAD_1d_30d_1E9

For the Neutron Radiography Scenario defined in § 2.7 on page 19, calculate the ranking order of all irradiated elements in terms of the photon dose-rate at a distance of 1 m from a reference mass of 1 g of each irradiated chemical element, at $T_{cool} = 30$ days, for an integral fluence-rate of $\phi = 10^9$ cm⁻² s⁻¹.

2.9.5 RQ_5 : Graphs of Activities and Dose-Rates for Cases DECO_60a_50a_φ

Graphically display the (1) total induced activity in irradiated samples, and (2) the photon dose-rate at 1 m from a 1 g irradiated sample, for all integral fluence-rates under investigation, for a standardised selection of important elements present in engineering materials such as concretes, steel-alloys and Al-alloys, as a function of cooling time, from $T_{cool} = 0$ to $T_{cool} = 50$ yr.

2.9.6 RQ_6 : Graphs of Activities and Dose-Rates for Cases DECO_1a_50a_1E14 and DECO_1a_50a_1E15

For the Fuel-Assembly End-Adapter Scenario ($\phi = 1.0E14$ cm⁻² s⁻¹), graph the (1) total induced activity in irradiated samples, and (2) the photon dose-rate at 1 m from a 1 g irradiated sample, for the standardised selection of important elements, as a function of cooling time, from $T_{cool} = 0$ to $T_{cool} = 50$ yr. Repeat for the maximum fluence-rate that may prevail in the FA cladding, namely $\phi = 1.0E15$ cm⁻² s⁻¹.

2.9.7 *RQ*₇: Graphs of Activities and Dose-Rates for Case **NRAD_1h_1000d_1E9** and Case **NRAD_1d_1000d_1E9**

For the Neutron Radiography scenario ($\phi = 10^9 \text{ cm}^{-2} \text{ s}^{-1}$), which considers two discrete irradiation times of either 1 hour or 1 day, graphically display the (1) total induced activity in samples, and (2) photon dose-rate at 1 m from an irradiated sample with a mass of 1 g, for a selection of important elements, as a function of cooling time, from $T_{\text{cool}} = 0$ to $T_{\text{cool}} = 1000$ days, using a logarithmic time-axis, to highlight dose-rates that will prevail in the first hours and days after irradiation.

2.9.8 *RQ*₈: Completeness Issue

The literature survey will identify a list of (1) the most problematic high-activator chemical elements, along with a list of (2) the most problematic radionuclides formed by neutron activation.

The exhaustive set of FISPACT-II neutron-activation calculations — for every element in the periodic table, at many integral fluence-rates and many irradiation scenarios — must be used to test whether the above two lists are indeed complete and without “gaps”. In other words, have any “highly problematic radionuclides” been identified in FISPACT-II calculations, that are omitted from the literature about neutron activation issues at nuclear reactor facilities? This research question will be referred to as the “completeness issue” and will be restricted to circa 72 elements that are commonly or possibly encountered in engineering materials.

2.10 Constraints and Limitations of the Investigation

The scope of this investigation is bounded as follows:

- Only chemical elements found in engineering materials and the biosphere will be investigated; esoteric target-elements such as Tc and Pm as well as the noble gases Ne, Kr, Xe and Rn will be neglected.
- Fissioning elements such as Th, U and Pu will not be investigated as they are not considered to be structural engineering materials. Other radioactive elements such as radium (Ra) will also be ignored.

- Only neutron activation, and not nuclear fission, is considered. In other words, the focus is solely on neutron activation products and not on fission-products.
- It will be assumed that all elements initially contain the typical, average natural abundance of isotopes found on the earth's crust and the biosphere (as specified in e.g. (Meija et al., 2016)), i.e. no isotopically enriched or isotopically depleted target-materials will be considered.
- Only a single, representative neutron energy-spectrum from an LWR will be considered, i.e. the neutron spectrum is well moderated by, especially, the neutron scatterer ^1H , which is abundant in light water, i.e. H_2O . This *standard LWR neutron spectrum* $\phi_{LWR}(E)$ is shown in Figure 6 on page 60.

3 LITERATURE REVIEW

3.1 Introduction: Neutron Activation Calculations for Decommissioning of Nuclear Reactors

Many nuclear reactor facilities that were constructed in the 1960s and 1970s are approaching the decommissioning phase of their lifetimes — their initial design lifetimes were typically 40 years, which have usually been extended to approximately 60 years. Globally, 447 nuclear reactors are in operation as of January 2020. Of those, nearly 70 % are older than 30 years (25 % are older than 40 years). Around 200 commercial reactors are earmarked for shutdown before 2040 (Lurchak, 2020). Amongst these is the SAFARI-1 reactor at Necsa, Pelindaba, South Africa.

Nuclear regulators require that a formal *Decommissioning Plan* be developed and submitted for regulatory approval, when a nuclear reactor facility has to be decommissioned. In South Africa, the NNR has e.g. developed Regulatory Document RD-0026, Decommissioning of Nuclear Facilities (NNR, 2008). RD-0026 states that the operator of the reactor must develop a Decommissioning Strategy as well as a Decommissioning Plan which must both be submitted for regulatory approval.

To develop a decommissioning strategy and a decommissioning plan, an accurate estimate of the radioactive inventory of a facility (the so-called “source term”) is required. The “source term” entails the identity, time-dependent activity and emission characteristics of radionuclides, along with their spatial distribution in structures, systems and components (SSCs) that needs to be processed, treated or removed in order to meet the regulatory requirements for releasing the facility from regulatory control. When spent nuclear fuel is removed, the largest percentage of the source term for nuclear fission reactor is represented by neutron activation products — neutrons released in fission events are slowed down via scattering and subsequently cause nuclear reactions that produce radionuclides.

After the source term has been determined, dose-rate calculations (often called shielding calculations) are performed in support of measures to assess and control exposures to ionising radiation during the decommissioning work. The general rule is that nuclear safety regulators require the bulk of these dose-rate and dose-budgeting calculations to be completed *before* decommissioning work is allowed to begin — regulators have a severe dislike of any *modus*

operandi that reeks of design-while-you-build or plan-while-you-demolish; Nuclear Safety regulators want designs and plans to be finalised before construction or decommissioning begins. The information from such calculations and technical reports are also needed for safety assessments by national radioactive waste-disposal institutes, who need to make certain that their WAC (Waste Acceptance Criteria) are met.

3.2 Physics of Neutron Activation

Activation by neutrons is the result of nuclear reactions. A neutron can interact with an atomic nucleus in several ways, and in most cases, these reactions lead to the production of a radioactive nucleus. If a neutron has high energy (in the MeV range), the reactions that most often occur are the types that result in the emission of charged particles. Examples include (n, p) , (n, α) , (n, d) and (n, t) reactions (here p signifies a proton, α an alpha-particle, d a deuteron and t tritium). In most cases, the result of these reactions is an altered nucleus, with atomic numbers Z and mass numbers A different from those of the target nucleus. In the case of many nuclear reactions, the resultant nucleus is left in an excited state. The neutron absorption cross-sections associated with these reactions strongly depend on the energy of the incident neutron.

After being slowed down by the scattering processes (e.g. thermalization), the energy of a neutron becomes very low — it enters the eV range or the sub-eV range. In this energy range, the most important category of nuclear reaction is (n, γ) -reactions, also known as *radiative capture* reactions. All (n, γ) -reactions are exothermic i.e. exo-ergic, i.e. there are no threshold energies for the neutron energy. The cross-sections of (n, γ) -reactions with slow neutrons are usually orders of magnitude higher than those for nuclear reactions with higher energy neutrons. Given that an LWR is designed to effectively thermalize neutrons, it follows that radionuclides produced by (n, γ) -reactions will usually be the dominant neutron activation products encountered at such facilities.

3.3 The IAEA's Recommended Methodology for Calculations Related to Reactor Decommissioning — Transport Models and Activation Models

The IAEA (IAEA, 1988), (IAEA, 1998), (IAEA, 2002), (IAEA, 2005), (IAEA, 2006) and (IAEA, 2019), summarises the general methodology that must be followed for reactor

decommissioning related activation inventory and dose-rate calculations and related activities, as shown in Figure 4 (taken from (IAEA, 2019)).

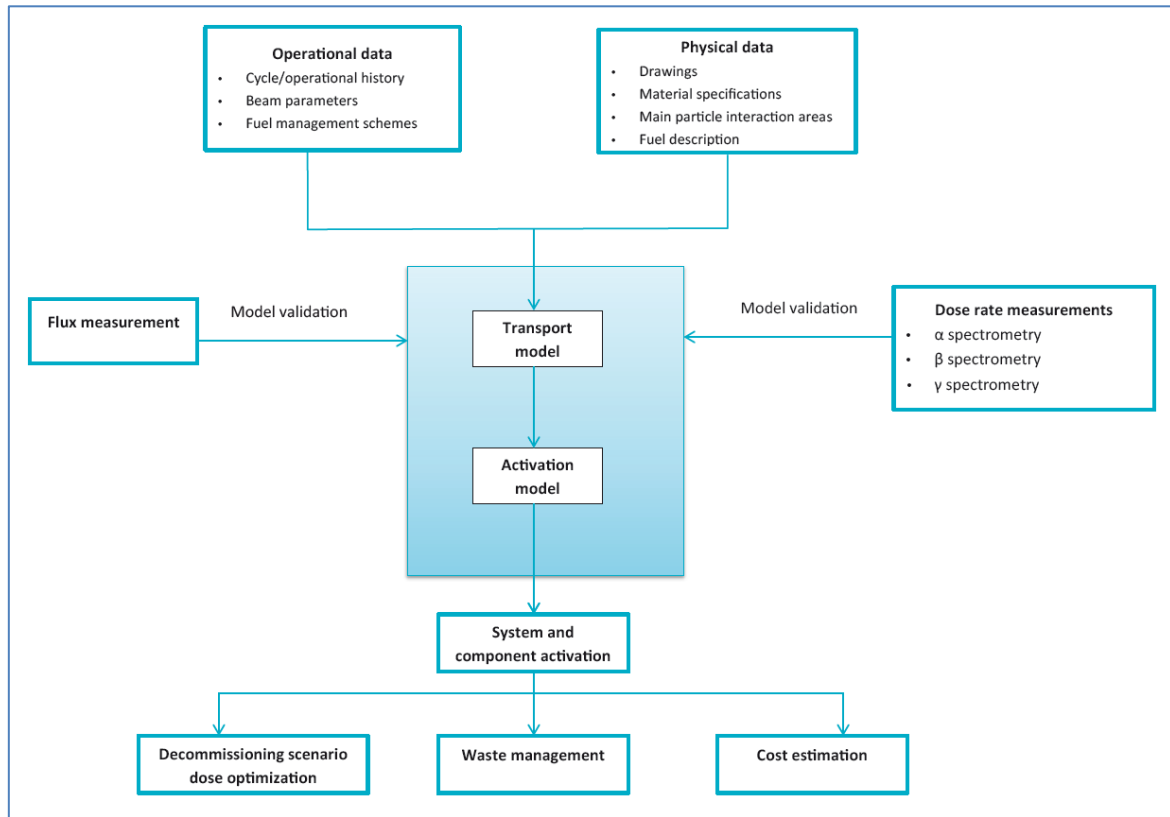


Figure 4: The IAEA’s summary of the steps required in decommissioning work involving neutron-activated systems, structures and components (SSCs)

Note the concepts “Transport model” and “Activation model” in Figure 4. In neutron activation calculations, the purpose of the *transport model* is to have a calculation model of e.g. the nuclear reactor and all the adjacent materials that will be subject to a neutron fluence-rate in excess of, say, $1\text{E}4\text{ cm}^{-2}\text{ s}^{-1}$, where neutron activation can elevate dose-rates well above the natural background level. The transport model is typically a calculation model for a Monte Carlo code such as MCNP6 (the preferred radiation transport code in the USA) or TRIPOLI (a radiation transport code preferred by AREVA). The transport model yields, as a main computed result, a representative neutron spectrum function $\phi_n(E)$ in each irradiated structure. A calculation model that incorporates the source of neutrons, the irradiated structure as well as the immediate environment that will have a quantitative impact on the neutron spectrum function $\phi_n(E)$ in the irradiated structure, is set up and run in e.g. the code MCNP6.2 (LANL, 2018a). A (1) multigroup representation of the neutron spectrum function $\phi_n(E)$, as well as (2) the total i.e. energy-integrated neutron fluence-rate, i.e.

$$\phi = \int \phi_n(E) dE$$

are now ported to a calculation model developed for an activation code such as FISPACT-II 3.0 (Sublet et al., 2015). The results of the material-activation calculations can now be used as input for follow-on dose-rate calculations that will, typically, use transport codes such as MCNP, to construct safety-cases for submission to nuclear regulators and for planning decommissioning activities. Areas of planning that rely on activation calculations include decommissioning scenario selection, waste-disposal planning and dose optimisation (also called ALARA planning).

3.4 Decommissioning Options

In a lecture on Decommissioning, (Kaliatka, 2016) the author states that the main decommissioning options (strategies) are:

1. **Immediate Dismantling:** The dismantling and decontamination activities begin within a few months or years; this decommissioning option is also known as *Early Site Release*.
2. **Deferred Dismantling:** Postponement of the final release of regulatory controls (usually for a period of 5 to 60 years). Deferred Dismantling involves placing the facility into long-term storage, also called *Safe Storage* or *Safe Enclosure*. Prior to Safe Enclosure, spent fuel assemblies are removed, systems are drained, loose radioactive waste is removed and areas are secured. Deferred dismantling allows for the substantial decay of radionuclides with half-lives below approximately 1 to 5 years.
3. **Entombment:** Placing the facility into a condition with most of the radioactive material remaining on-site, without an attempt to remove it completely. This option had to be followed at Chernobyl — it was the only viable methodology.

3.5 Important Radionuclides Produced by Neutron Activation at Nuclear Reactor Facilities; Elements that Produce Long-Lived, Problematic Radionuclides

In this section, problematic chemical elements that activate to produce significant activities of problematic radionuclides, as reported by different authorities and investigators, are listed. Where necessary, omissions and imperfections in published literature are pointed out and corrected.

3.5.1 IAEA Publications Dealing with Neutron Activation and Decommissioning

A comprehensive IAEA publication (IAEA, 1998) deals with the *radiological characterisation of shut-down nuclear reactors for decommissioning purposes*. From page 17 to 24, the major activation radionuclides are treated individually; these nuclides are: H-3, C-14, Na-22, Cl-36, Ca-41, Mn-54, Fe-55, Ni-59, Ni-63, Co-60, Zn-65, Mo-93, Zr-93, Nb-94, Ag-108m, Ag-110m, Sb-125, Ba-133, Cs-134, Eu-152, Eu-154, Eu-155 and Ho-166m.

(IAEA, 2002) mentions the identities of the noteworthy, long-lived activation products in nuclear facilities as Co-60, Ni-63, Ba-133, Eu-152 and Eu-154. As less noteworthy or less prevalent, they list H-3, Be-10, C-14, Ni-59, Nb-94 and Sb-125.

(IAEA, 2007) deals with the *Characterisation and Testing of Materials for Nuclear Reactors* and stresses the need to (1) use low-activation construction materials and (2) test raw materials for problematic neutron-activating trace-elements such as Co and Eu.

(IAEA, 2019) deals in detail with *methodologies for assessing the induced activation source term for use in decommissioning applications*. The neutron transport codes MCNP, TRIPOLI, FLUKA and GEANT are introduced and discussed, as are the activation codes FISPACT-II and ORIGEN. Verification and validation are also placed under the investigative spotlight.

3.5.2 The Induced Neutron-Activation Source Term in Nuclear Facilities (IAEA, 2019)

In this subsection, information from (IAEA, 2019) is discussed in deeper detail. The IAEA lists the radionuclides that will typically be produced during the neutron-induced activation process in nuclear fission reactor facilities; these nuclides are listed in Table 7 (IAEA, 2019).

Table 7: Radionuclides that will typically be produced during the neutron-induced activation process in nuclear fission reactor facilities (IAEA, 2019)

Material	Radionuclide	T _{1/2}	Material	Radionuclide	T _{1/2}
Stainless steel	¹⁴ C	5 730 y	Carbon steel	⁵¹ Cr	27.7 d
	⁵¹ Cr	27.7 d		⁵⁴ Mn	312.2 d
	⁵⁴ Mn	312.2 d		⁵⁵ Fe	2.73 y
	⁵⁵ Fe	2.73 y		⁵⁹ Fe	45.1 d
	⁵⁹ Fe	45.1 d		⁵⁸ Co	70.88 d
	⁵⁸ Co	70.88 d		⁶⁰ Co	5.271 y
	⁶⁰ Co	5.271 y		⁵⁹ Ni	76 000 y
	⁵⁹ Ni	76 000 y		⁶³ Ni	100 y
	⁶³ Ni	100 y		⁹³ Mo	3 500 y
	^{108M} Ag	418 y		⁹⁴ Nb	24 000 y
			⁹⁹ Tc	213 000 y	
Concrete	³ H	12.33 y	Graphite	³ H	12.33 y
	¹⁵² Eu	13.5 y		¹⁴ C	5 730 y
	¹⁵⁴ Eu	8.59 y		³⁶ Cl	301 000 y
	⁵⁵ Fe	2.73 y		⁴⁶ Sc	83.81 d
	⁵⁹ Fe	45.1 d		⁵⁴ Mn	312.2 d
	⁵⁴ Mn	312.2 d		⁵⁹ Fe	45.1 d
	⁶⁰ Co	5.271 y		⁶⁰ Co	5.271 y
	⁴¹ Ca	102 000 y		¹²⁴ Sb	60.2 d
	⁴⁵ Ca	162.7 d		¹³¹ Ba	11.8 d
	¹³⁴ Cs	2.064 8 y		¹³³ Ba	10.51 y
	¹⁸² Ta	114.4 d		¹⁵² Eu	13.5 y
	⁶⁵ Zn	243.8 d		¹⁵⁴ Eu	8.59 y
	⁹⁵ Zr	64.02 d			

Of the nuclides in Table 7, the following belong to the group having very restrictive clearance levels, as listed in Table 1 (page 2) and Table 3 (page 4): Mn-54, Co-60, Zn-65, Nb-94, Ag-108m, Sb-124, Cs-134 and Eu- 152.

Some radionuclides that are in Table 1 and Table 3, but are absent from the IAEA's list in Table 7, are Ag-110m and Cs-137. The omission of Ag-110m is an oversight because 48.16 % of Ag is Ag-109 (Holden et al., 2018), which readily activates to Ag-110m, which has a half-life of circa 250 days (Audi et al., 2017). The absence of Cs-137 in Table 7 is discussed below.

3.5.3 Radiological Characterisation of the Radionuclide Inventory of the Decommissioning Radioactive Waste at a TRIGA Mark II Research Reactor

(Ackermann, 2017) performed a radiological characterisation of the radionuclide inventory of the decommissioning radioactive waste of the FiR 1 TRIGA Mark II research reactor located at Espoo in Finland. She determined an activity inventory of all the important activated components and structures, via calculations, measurements and the literature. The transport code MCNP was used to calculate neutron spectra, and the activation calculations were performed with the code ORIGEN-S in SCALE 6.1. Gamma-spectrometry was used to identify and quantify activation radionuclides in irradiated structures. She summarises the major activation radionuclides found in the decommissioning waste, which includes the aluminium reactor vessel and nearby concrete shielding; her list is shown in Table 8 and includes the nuclear reactions responsible for the presence of the detected radionuclides.

Table 8: Major activation radionuclides in decommissioning waste at a TRIGA Mark II research reactor, reported by (Ackermann, 2017)

Activation Product	Half-life [67]	Formation Mechanism	Emission Type	Method of Measurement
^3H	12.32 y	Neutron capture in the neutron moderator, and in the concrete biological shield ($^6\text{Li}(n,\alpha)^3\text{H}$, $^2\text{H}(n,\gamma)^3\text{H}$ and $^3\text{He}(n,p)^3\text{H}$)	Pure β emitter No γ emission	Discussed in section 2.4.3.
^{14}C	5700 y	$^{14}\text{N}(n,p)^{14}\text{C}$, $^{13}\text{C}(n,\gamma)^{14}\text{C}$ and $^{17}\text{O}(n,\alpha)^{14}\text{C}$, and through indirect reactions	Pure β emitter	LSC; similar to ^3H
^{22}Na	2.602 y	$^{23}\text{Na}(n,2n)^{22}\text{Na}$ and $^{23}\text{Na}(\gamma,n)^{22}\text{Na}$	β^+ and γ emission	γ spectrometry
^{36}Cl	3.01×10^5 y	$^{35}\text{Cl}(n,\gamma)^{36}\text{Cl}$ and $^{39}\text{K}(n,\alpha)^{36}\text{Cl}$, and indirectly through ^{34}S	β^- emission or EC with weak X-ray emission	γ spectrometry
^{39}Ar	269 y	$^{39}\text{K}(n,p)^{39}\text{Ar}$ and $^{38}\text{Ar}(n,\gamma)^{39}\text{Ar}$	β^- emission	Proportional β^- counting or LSC
^{41}Ca	1.02×10^5 y	$^{40}\text{Ca}(n,\gamma)^{41}\text{Ca}$	EC with weak X-ray emission	Chemical separation and LSC
^{54}Mn	312.2 d	$^{54}\text{Fe}(n,p)^{54}\text{Mn}$	EC with 835 keV γ emission	γ spectrometry
^{55}Fe	2.744 y	$^{54}\text{Fe}(n,\gamma)^{55}\text{Fe}$	EC with weak X-ray emission	Chemical separation and X-ray spectrometry - hard to measure and can be correlated to ^{60}Co
^{59}Ni	7.6×10^4 y	$^{58}\text{Ni}(n,\gamma)^{59}\text{Ni}$	EC with continuous bremsstrahlung spectrum	Hard to measure and can be correlated to ^{60}Co ; can be measured by the X-ray spectrometry of ^{60}Co
^{63}Ni	101.2 y	$^{62}\text{Ni}(n,\gamma)^{63}\text{Ni}$	β^- emission	Hard to measure and can be correlated to ^{60}Co ; measured by chemical separation followed by LSC
^{60}Co	5.274 y	$^{59}\text{Co}(n,\gamma)^{60}\text{Co}$	β^- emission followed by emission of 2 major γ rays (1.17 and 1.33 MeV)	γ spectroscopy

⁶⁵ Zn	243.9 d	⁶⁴ Zn(n, γ) ⁶⁵ Zn	EC and β^+ emission	γ spectrometry
⁹³ Mo	4.0×10 ³ y	⁹² Mo(n, γ) ⁹³ Mo	EC	Detection of characteristic X-rays using an intrinsic Ge diode
⁹³ Zr	1.61×10 ⁶ y	⁹² Zr(n, γ) ⁹³ Zr	β^- emission, with low energy γ emission of daughter	Chemical separation and β counting
⁹⁴ Nb	2.03×10 ⁴ y	⁹³ Nb(n, γ) ⁹⁴ Nb	β^- emission followed by γ cascade	γ spectrometry
^{108m} Ag	438 y	¹⁰⁷ Ag(n, γ) ^{108m} Ag	EC with weak X-ray emission, followed by β^- emission	γ spectroscopy
^{110m} Ag	249.8 d	¹⁰⁹ Ag(n, γ) ^{110m} Ag	β^- emission, followed by β^- emission of the daughter	γ spectroscopy
¹²⁵ Sb	2.759 y	¹²⁴ Sb(n, γ) ¹²⁵ Sb	β^- emission, followed by β^- and γ emission of the daughter	γ spectroscopy
¹³³ Ba	10.55 y	¹³² Ba(n, γ) ¹³³ Ba	EC and γ emission	γ spectroscopy
¹³⁴ Cs	2.065 y	¹³³ Cs(n, γ) ¹³⁴ Cs	β^- emission or EC	γ spectroscopy
^{152,154,155} Eu	13.52 y 8.601 y 4.753 y	Neutron capture in ¹⁵¹ Eu and ¹⁵³ Eu, or by chain absorptions in Sm.	¹⁵² Eu decays by β^- emission, followed by α emission ^{154,155} Eu decays β^- emission	γ spectroscopy or β counting
^{166m} Ho	1.20×10 ³ y	¹⁶⁵ Ho(n, γ) ^{166m} Ho	β^- emission	Chemical separation and γ spectroscopy

Of the nuclides in Table 8, the following belong to the group having very restrictive clearance levels, as listed in Table 1 (page 2) and Table 3 (page 4): Na-22, Co-60, Mn-54, Zn-65, Nb-94, Ag-108m, Ag-110m, Sb-125, Cs-134 and Eu- 152.

Two nuclides that are present in Table 1 and Table 3, but are absent from Ackerman's list, are Na-24 and Cs-137. The nuclide Na-24 is not problematic because its half-life is shorter than 15 hours; Cs-137 cannot readily be activated from natural Cs, which may be present in engineering materials as an unwanted trace element, because the mass-number of the single stable Cs isotope, Cs-133, is far below 137. In other words, any trace of Cs-133 will readily activate to Cs-134 (by absorbing a single neutron), but the successive neutron-absorption "ladder" to Cs-137 involve 4 successive neutron capture reactions so that Cs-137 is generally not an important activation product. On page 56, however, we show that Cs-137 can be readily formed when the element barium (Ba) is irradiated by reactor neutrons.

Table 8 (Ackermann, 2017) contains the nuclear reactions responsible for producing the problem-nuclides. The neutron irradiation of the following target-elements will produce the listed nuclides: Na, Cl, K, Ca, Fe, Co, Ni, Zn, Mo, Nb, Ag, Ba, Cs, Eu and Ho. The use of several of these elements are unavoidable — at a PWR and BWR, e.g. the reactor pressure vessel (RPV) can only be manufactured from steel (Fe) and reactor internals will invariably contain thousands of kilograms of stainless steels, which all contain Fe and Ni. Practically all types of concrete will contain at least 4 % Ca. Sometimes it turns out that SS-304 will not

suffice in a specific application, and that SS-316 must be specified; the latter contains between 2.5 % and 3 % Mo, which will activate to Mo-93, Nb-94 and Tc-99. The elements that can be minimised, are the high-activator *trace* elements such as Co, Nb, Ag, Ba, Cs, Eu and Ho, which are usually not required to be present in metal alloys or bio-shield concrete, but merely “slip in” as impurities.

3.5.4 Trace Elements in Reactor Steels: Implications for Decommissioning — Niobium (Nb) and Nitrogen (N)

In an article *Trace elements in reactor steels: implications for decommissioning* (Stephens Jr and Pohl, 1978), the authors emphasize the dominant role of the element niobium (Nb) in the activation of steel-alloys. They state,

Trace elements in stainless steel have been systematically examined to produce long-lived radioisotopes through neutron activation in reactors. Niobium-94 has been identified as the most important impurity. It is a long-lived ($T_{half} = 20,000$ yr) gamma-ray emitter (0.7 MeV and 0.87 MeV), which is produced by the neutron capture reaction ${}_{41}^{93}\text{Nb}(n,\gamma){}_{41}^{94}\text{Nb}$. Through X-ray fluorescence, Nb concentrations of 160 ± 20 ppm have been found in type-304 stainless steel (SS-304), which agrees with earlier published values. At this concentration, the gamma radiation dose-rate inside the pressure vessel of a nuclear reactor would remain close to [10 mSv/hr] for thousands of years after the ${}^{60}\text{Co}$ activity has decayed. This could be important for the delayed dismantling option considered for reactors.

(In the above quotation, dose-rate units were changed from the original rem/h to the SI units mSv/h.)

(Stephens Jr and Pohl, 1978) also state that nitrogen as an impurity in steel-alloys will result in the formation of up to 1000 Ci of C-14 over the lifetime of a PWR. The nuclear reaction that forms C-14 from N-14, is ${}_{7}^{14}\text{N}(n,p){}_{6}^{14}\text{C}$. Although C-14 is only a β^{-1} -emitter, its long half-life of 5700 yr, coupled to the crucial role of carbon in the biosphere, may lead nuclear safety regulators to regulate a very strict and expensive method for the safe disposal of radioactive nuclear reactor components that contain high activities of the radionuclide C-14.

3.5.5 The UK is Advised to Dissociate from Euratom’s European Basic Safety Standards Directive (BSSD 2013/59/Euratom) to Keep Decommissioning Affordable

(Public Health England, 2018) reports that the European Union has published regulations — the European Basic Safety Standards Directive (BSSD) (2013/59/Euratom) — that lower the activity-concentration for unconditional release for the radionuclide C-14 from 10 Bq/g to 1 Bq/g. These lowered limits will greatly impact the decommissioning of nuclear facilities. The Euratom BSSD limit for the isotope Cs-137 was also lowered from 1 Bq/g to 0.1 Bq/g. The UK Public Health body investigated the calculational methodology followed by Euratom and discovered that the reason for the lowered release standard for Cs-137 is not scientific in nature, but the result of numerical round-off errors in calculations. The lowered EU release standards for C-14 are found to be based on a very cautious drinking-water scenario; applying a more realistic scenario results in a release-limit value that is an order of magnitude higher, namely the previous limiting value of 10 Bq/g. The conclusion (Public Health England, 2018) is that the UK has good reason to dissociate themselves from the lowered 2013 Euratom BSSD release-limits values for C-14 and Cs-137, and should rather stick to the demonstrably more sensible pre-2013 clearance criteria for these two radioisotopes.

3.5.6 An In-Depth Look at Long-Lived Neutron Activation Products in Reactor Materials

(Evans et al., 1984) presents an in-depth look at long-lived activation products in reactor materials. Samples of stainless steels, vessel steel, concrete and concrete ingredients were analysed for up to 52 elements in order to develop a database for activatable major, minor and trace elements. An evaluation was made for the nuclear reactions that could produce long-lived neutron activation products. Selected samples of activated steel and concrete were subjected to a limited radiochemical analysis programme intended to serve as verification of the calculation models and code. Reasonably good agreement between calculated and measured results was obtained. The authors (Evans et al., 1984) point out that measured levels of the long-lived radionuclide ^{94}Nb in activated stainless steel was notably high. This radionuclide is of interest and concern, because Nb-94 has a long half-life ($2.03004\text{E}4$ yr), and emits two rather intense medium-energy gamma-photons at $E_{\gamma} = 0.8711$ MeV and $E_{\gamma} = 0.7026$ MeV. The combination of a long half-life with the emission of intense ionising photons at energies above 0.5 MeV, is quite rare and this combination makes ^{94}Nb a dangerous, long-lived and problematic radionuclide, with a low clearance limit.

The only stable isotope of Nb is Nb-93, which activates to Nb-94 via a neutron capture reaction. Niobium is used to manufacture high-strength carbon steels, boron steels and stainless steels. We can now formulate a preliminary conclusion namely that niobium-steels should not be used in reactor facilities in areas where neutron fluence-rates $\phi_n \geq 10^6 \text{ cm}^{-2} \text{ s}^{-1}$ may be encountered.

(Evans et al., 1984) investigated activation of reactor pressure vessels (low carbon steel), vessel cladding (usually SS-304L) and stainless-steel internals (usually SS-304L), as well as the bio-shield (which is composed of concrete and steel). Material samples were analysed for up to 52 elements. Materials such as metal alloys showed little variation in the major elements, but a wide variability of up to a factor of 10 in trace-element concentrations, notably cobalt and niobium — the direct precursors to the highly problematic radionuclides Co-60 and Nb-94. The authors note that Nb was the most problematic trace element observed in stainless steel-alloys. (Evans et al., 1984) report a wide range of compositional variation in concrete samples, reflecting the geological differences in the quarry sites used to obtain the aggregate. The rebar (i.e. reinforcing steel bars/rods) used in concrete structures were found to add significant amounts of Fe, Co and Nb to the bio-shield. The authors report that 52 radionuclides with half-lives higher than 5 years were considered in their investigation. Most of these long-lived radioisotopes are formed by (n, γ) -reactions, with the notable exceptions of Mn-54, C-14 and H-3, which are produced in (n, p) , (n, α) and (n, t) nuclear reactions. Photonuclear reactions, i.e. (γ, n) -reactions, were found to be negligible. The authors found that the most highly activated metallic component in a PWR is the core shroud (usually SS-304), followed by the reactor pressure vessel (RPV). Only a handful of long-lived radionuclides consistently dominated the activation inventory. They report that Co-60 was found to dominate the total activity from 5 years to about 20 years, while it dominated the photon dose-rate to 100 years. After 100 years, Nb-94 becomes dominant. The nickel isotopes Ni-59 and Ni-63 dominates the activity after 20 years, but contribute very little to the dose-rate, because they emit no γ -radiation but are “soft β ”-emitters. In concrete, the activity is initially dominated by H-3 and, after circa 300 years, by Ca-41. Both H-3 and Ca-41 do not produce external dose-rates, but are only hazardous if ingested or inhaled. The photon dose-rate from the bio-shield (i.e. concrete with inner rebar) was dominated by Eu-152 and Co-60.

(Evans *et al.*, 1984: 10) quotes a study by Woolam, dated 1978, calling it “perhaps the most complete combined experimental and theoretical analysis of activation products”. Several samples of activated mild steel and concrete were subjected to radiochemical analyses (steel)

and gamma-spectrometry (concrete). Woolam's results indicated that, on a 10-year time scale, the dismantling dose, i.e. the decommissioning dose, would be dominated in mild steel by Co-60, but in concrete by Eu-152. On a 100-year time scale, Woolam reported, Ag-108m and Nb-94 would dominate in steel, whereas Eu-152 remains the dominant dose-producing isotope in concrete. From the perspective of the disposal of debris, however, Ni-63 dominates on a timescale from 10 to 100 years, while Ni-59 dominates after 1000 years or more. Up to 10 to 20 years, Eu-152 dominates the restriction on the disposal of concrete, while on a timescale of 100 years and more, Ca-41 dominates. In Woolam's analyses, the following radionuclides were reported as significant activation products that impact on either (1) permission to dispose of debris, or (2) worker-dose: H-3, C-14, Cl-36, Ca-41, Fe-55, Co-60, Ni-59, Ni-63, Nb-94, Ag-108m, Sm-151, Eu-152 and Eu-154.

(Evans *et al.*, 1984: 11) quotes a study, dating from 1982, by Bergeman and co-workers at the decommissioned Gudremmingen NPP in Germany, in which radiochemical analyses were carried out for a wide variety of irradiated concrete and steel samples. In addition to Woolam's list, the following additional radionuclides were identified as significant: Mn-54 and Cs-134. The study quantified the total activation product activity present in the RPV and internals, as 1.4E6 Ci at an elapsed time of 6 years after the final shutdown. The analysts also found that (Evans *et al.*, 1984: 11) the concrete bio-shield close to the reactor, only exceeds clearance levels up to a depth of circa 110 cm into the concrete. At depths in excess of 110 cm into the concrete, the total activity per unit mass was found to be below 4 Bq/g.

(Evans *et al.*, 1984: 12) reports on a study by Smith, Konzek and Kennedy in the USA, dated 1978. The same radionuclides listed above were encountered, with the notable addition of Mo-93 and Tc-99, both of which are related to the presence of initial Mo in the steel or concrete.

In their own radio-analytical, gamma-spectrometric and calculational investigations, (Evans *et al.*, 1984: 12) confirmed the above list of radionuclides of concern, and added Ba-133 as an additional nuclide of potential concern, but only if barites (barium sulphate) shielding concrete is used. A final addition to the list is the neutron-driven formation of Be-10 in the beryllium-reflectors of MTRs. The radionuclide Be-10 is formed when Be-9 captures a neutron; Be-10 has a very long half-life of 1.51E6 years and emits no ionising photons, but only low to medium energy β -electrons. A factor that keeps the formation-rate of Be-10 from Be-9 low, is the low cross-section of approximately 10 millibarns (mb) for the nuclear reaction ${}^9_4\text{Be} (n, \gamma) {}^{10}_4\text{Be}$.

3.5.7 A Significant Number of MTRs to be Decommissioned or Upgraded in the Near Future

(Meier et al., 2017) states that, in 2016, there were 241 operating research reactors in the world. More than 70 % of them were (in 2016) above 30 years in age and in excess of 50 % were above 40 years old. For these reasons, a significant number of MTRs will have to enter decommissioned or receive upgrades and life extensions. The authors state,

Decommissioning, life extension and upgrading involve manipulating and removing equipment and components located close to the reactor core which has suffered material activation. These activated materials could induce dose-rate exposures for workers or electronics tools, mostly via gamma emission decay. In nuclear reactors, material activation is mainly produced by neutron capture.

Neutron capture rates are a function of neutron interaction cross-section σ and neutron flux ϕ in each component. Neutron capture reactions produce radioactive isotopes during reactor operation which then transition during shutdown periods. Therefore, the authors conclude, “the reactor operation history has to be considered to calculate the dose-rate around the component at the removal/handling time.” They calculated neutron fluence-rates in a comprehensive list of structures, and finally consider the activation of two very widely used engineering metal-alloys, namely SS-304 and Al-6061. They report that (1) Co-60 is the dominant dose-contributing radionuclide and that (2) long-term activation of Al-alloys is dominated by the initial concentrations of trace-elements — notably Co, Nb and Ag — that are present in the alloy. Finally, they report that the emitted photons from all activated structures that they have measured with gamma-spectrometry were always found to have energies below 3 MeV.

3.5.8 Activation Calculations — Overview of Codes and Nuclear Data

In a presentation titled *Activation Calculations — Present and Future*, (Gallmeier, 2010) gives an overview of calculation tools available for activation calculations. The 2009 versions of the Monte Carlo codes FLUKA and MCNP, as well as GEANT, MARS and PHITS, had activation calculation abilities, but execution times are reported to be intolerably long. He also reports on

the use of the activation code FISPACT-2007⁸ in materials activation calculations. Comment: The experience at Necsa is similar — using Monte Carlo codes for burnup and activation calculations, is prohibitively slow, partly because using the BURN feature in MCNP6.1, 6.11 and 6.2 makes multi-threaded (parallel processing) calculations impossible, so that the code runs in 1 thread in only 1 core of the processor. It is far more sensible to split the activation model from the transport model, as the IAEA indeed advises — refer to Figure 4 on page 27.

3.5.9 Trace-Elements are Often Most Problematic

(Fetter et al., 1988) reports that if the mass-% of the trace-elements niobium (Nb), molybdenum (Mo), silver (Ag), gadolinium (Gd), terbium (Tb), and holmium (Ho) are restricted to very low values (under 1 ppm), then lower levels of long-lived activation products are formed by neutron activation of engineering metals. Comment: The authors have “missed” the highly problematic trace-element Co. Another corrective remark is that Mo is not a particularly activation-hazardous element.

3.5.10 Monte-Carlo Aided Design of Neutron Shielding Concretes

In an article *Monte-Carlo Aided Design of Neutron Shielding Concretes*, (Tefelski et al., 2013) reports that the following long-lived radionuclides are of potential concern in irradiated concretes: H-3, C-14, Na-22, Cl-36, K-40, Ca-41, Ca-45, Mn-54, Fe-55 and Ba-133. Note that these researchers failed to include trace-elements such as Co, Cs and Eu in their material-definitions and therefore “missed” significant problem-nuclides such as Co-60, Cs-134, Eu-152, Eu-154 and Eu-155.

3.5.11 Four Studies on the Neutron Activation of Engineering Materials — Experimental and Computational

(Žagar and Ravnik, 2000), (Žagar et al., 2001), (Žagar and Ravnik, 2002) and (Žagar et al., 2004) irradiated samples of engineering materials in facilities at a TRIGA type reactor, and then

⁸ Comment by co-supervisor TJvR: Since 2012, FISPACT-2007 has been superseded by FISPACT-II version 1.0, then 2.0, then 3.0 (2015), then 3.2 (2017) and 4.0 (2018), i.e. FISPACT-2007 is now (2019/2020) considered to be a thoroughly outdated and obsolete code. Its associated nuclear data is also old and limited in scope.

identified and quantified activation radionuclides by gamma-spectrometry. They also used the activation code ORIGEN to calculate activities of activation nuclides. The following seven long-lived radionuclides are reported as being activated in irradiated concrete samples: ^{54}Mn , ^{60}Co , ^{65}Zn , ^{134}Cs , ^{133}Ba , ^{152}Eu and ^{154}Eu .

3.5.12 Activation calculation for the dismantling and decommissioning of a light water reactor using MCNP with ADVANTG and ORIGEN-S

In an article *Activation calculation for the dismantling and decommissioning of a light water reactor using MCNP with ADVANTG and ORIGEN-S*, (Schlömer et al., 2017) states that, to obtain decommissioning licenses from regulators, neutron-induced activation calculations for the structural components have to be carried out to predict activities in structures and to estimate future costs for conditioning and packaging. The authors continue,

To avoid an overestimation of the radioactive inventory and to calculate the expenses for decommissioning as accurate as possible, modern state-of-the-art Monte-Carlo Techniques (MCNP™) are applied and coupled with present-day activation and decay codes (ORIGEN-S). In this context, ADVANTG is used as weight window generator for MCNP™ i.e. as variance reduction tool to speed up the calculation in deep penetration problems. In this paper, the calculation procedure is described, and the obtained results are presented with a validation along with measured activities and photon dose-rates measured in the post-operational phase. The validation shows that the applied calculation procedure is suitable for the determination of the radioactive inventory of a nuclear power plant. Even the measured gamma dose-rates in the post-operational phase at different positions in the reactor building agree within a factor of 2 to 3 with the calculated results. The obtained results are accurate and suitable to support effectively the decommissioning planning process.

3.5.13 Activation of the Concrete Bio-Shield

The calculations by (Schlömer et al., 2017) for the activation of the concrete bio-shield, identify the following radionuclides as being of concern: H-3, C-14, Mn-54, Co-60, Cs-134, Eu-152 and Eu-154. A noteworthy aspect of this work is the use of the code ADVANTG to “speed up” the convergence of MCNP calculations by the automated generation of optimised variance-reduction parameters for the main MCNP calculation(s).

3.5.14 Activation Neutronics for Swiss Nuclear Power Plants (NPPs)

In a PhD Thesis, (Pantelias Garces, 2013) investigates activation neutronics for Swiss nuclear power plants. He starts by stating:

With an installed capacity of over 3.2 GW_e, the four Swiss Nuclear Power Plants (NPPs) currently supply 40 % of the Swiss electricity demand. In view of future decommissioning liabilities, nuclear utilities are required by law to ensure that adequate financial resources will be available in order to cover the rising costs. In this context, the Swiss National Cooperative for the Disposal of Radioactive Waste (Nagra) periodically performs and updates cost studies relevant to NPP decommissioning and radioactive waste management. An integral aspect of these studies is the radiological characterisation of the NPPs and, more specifically, the calculation of the nuclear activation in reactor components induced by their exposure to neutron radiation. The resulting radiological inventory has a direct effect on the planning of the NPP dismantling and the relevant waste-management considerations.

Just like (Schlömer et al., 2017), the above PhD candidate (Pantelias Garces, 2013) used the code ADVANTG to calculate optimal variance reduction parameters for the Monte Carlo transport code MCNP. In his calculations, he uses the older, now-obsolete 2007 version of FISPACT with the now-deprecated EAF nuclear data, as well as the 2011 version of the SCALE-6.1 code ORIGEN-S⁹. He identifies the following radionuclides of interest: H-3, C-14, Na-22, Cl-36, Ca-41, Mn-54, Fe-55, Co-60, Ni-63, Ni-59, Zn-65, Nb-94, Mo-93, Tc-99, Ag-108m, Ag-110m, Sb-125, Cs-134, Ba-133, Eu-152, Eu-154 and Ho-166m. This list is commendably comprehensive.

⁹ Note by the co-supervisor TJvR: To distinguish the SCALE version of the code ORIGEN from the non-SCALE version of the code ORIGEN, the actively developed version of ORIGEN in SCALE was called ORIGEN-S from circa 1985 until 2016. All development on the version of the ORIGEN code outside the SCALE system, stopped in 1990, so that this “branch” of the ORIGEN code-family fell into disuse and obsolescence. Since 2016, when SCALE 6.2 was released, the SCALE version of the code ORIGEN is simply called ORIGEN, because it was “the only ORIGEN standing.”

3.5.15 A Decade of Japanese Studies on Low-Activation Concrete

In an extensive series of publications spanning a decade, a group of Japanese researchers summarises their work on low-activation concrete — (Kinno et al., 2002), (Morioka et al., 2004), (Hasegawa et al., 2006), (Ogata et al., 2007), (Kakinuma et al., 2007), (Kimura et al., 2007), (Kinno et al., 2007), (Kimura et al., 2009), (Hayashi et al., 2009), (Kinno et al., 2011).

As a rule, the reactor-side or “inner part” of the concrete-and-steel bio-shield around a nuclear reactor becomes so heavily activated that it is classified as radioactive waste its clearance level recommended by the International Atomic Energy Agency (IAEA, 1998, p. 71), (IAEA, 1996) (IAEA, 2004). Here, “clearance” denotes the radioactive classification permissible for disposing of material as non-radioactive waste. The volume and activity of this non-clearable concrete must be minimized. The Japanese research team developed concrete composition “recipes” that they designate as e.g. 1/10, 1/20, 1/30, 1/50, 1/100, 1/300 and 1/1000 specification low-activation concrete (LAC), composed of low-activation raw materials, developed to reduce the generation of residual problematic radionuclides. A 1/100 low-activation concrete will produce a factor 100 times less activity via neutron activation, relative to a reference standard “regular” or “average” ordinary concrete composition. In their work, all concretes are irradiated by an LWR neutron spectrum for 40 years, which is followed by 6 years of “cooling” — a typical timeline for SSCs that must be decommissioned. The Japanese team developed and tested a “low-activation calcium-aluminate-silicate (CAS) additive”. As is the norm, they developed a calculation sequence where transport codes first calculate the neutron fluence-rate $\phi(E)$ through the concrete, and then an activation code uses the multigroup neutron fluence-rate and the material composition of the irradiated structure, to calculate the inventory of activation radionuclides, i.e. the {Nuclide, Activity}-matrix, which is abbreviated as $\{N, A\}$ -matrix. The research team used the transport code DORT and activation code ORIGEN-79; both these codes and their nuclear data date from the early 1980s. The team seems to have commercial interests, though — they claim having compounded excellent low-activation concretes, but give very little if any usable detail about the composition recipes. (Hasegawa et al., 2006) states that Co-60, Eu-152 and Eu-154 were identified as the chief “pest”-radioisotopes and that the foundation of any low-activation concrete composition is the testing for, and strict minimization of, the trace-elements Co and Eu in the raw-materials used to compound the concrete of the reactor’s bioshield. A high alumina content in the cement lowers activation issues. The authors conclude (Hasegawa et al., 2006): “Radioactive analysis showed that Co and Eu were the major target elements which decide the radioactivity level of

reinforced concrete. Material database for the contents of Co and Eu was developed based on the chemical analysis and radio-activation analysis. The correlation between the Co and Eu content was obtained for cement materials. Therefore it was clarified that the low activation cement would be successfully manufactured by adequate selection of raw materials.” (Kinno et al., 2002) states that “low-activation limestone is the most suitable low-activation aggregate and raw material for low-activation cement”, partly because it contains far less Co or Eu than regular raw-materials. They go further by recommending that “nuclear concrete” be manufactured and mixed from special raw materials, which must be identified by geologists:

A notable fact is that the concentrations of both Co and Eu in low-activation limestone associated with schalstein deposits are only 1/10 or so of those in ordinary type of limestone and are particularly low when sandwiched between two beds of schalstein deposits. Such examples of low-activation limestone are all metamorphic and micro-crystallized and are determined to have been accumulated in the Palaeozoic era, mostly in Permian and Carboniferous periods, by identifying fossils found in the same stratum. Schalstein rock is known to be a metamorphosed form of basalt. It can be inferred that the low-activation limestone is closely associated with the process of formation of a schalstein deposit or of a metamorphosed basalt deposit. The foregoing considerations suggest that such forms of limestone bed should be sought for extracting low-activation limestone with which to make low-activation cement. This could lead to further development of ultra-low-activation concrete.

(Uematsu et al., 2008) identify the problems with the decommissioning of concrete-waste as follows:

In decommissioning of nuclear power plants, a large amount of structural material and concrete should be disposed of as radioactive waste. Radioactivity for most of the concrete waste is lower than the clearance level because neutron flux level is relatively low. However, in the present design of BWR plants, in which ordinary concrete such as andesite concrete or sandstone concrete is used as radiation shielding material, part of concrete should be classified to L3 (very low level) radioactive waste. The amount of L3 concrete waste is estimated to be around 1000 tons for one BWR plant.

The sheer cost of disposing of such waste is prohibitive — the 1000 tons of concrete mentioned by the authors will have to be pulverized and drummed in 200-litre steel drums, at a normative disposal cost of around USD 1,000 per single such drum. A quick calculation indicates that a

minimum of approximately 2175 of the 200-litre drums will be required and that the charge levied for the disposal of these drums filled with drummed chunks of radio-activated concrete waste, will typically be 2.2 million USD (at 2020 monetary value).

The same Japanese team (Uematsu et al., 2008) also reports that limestone (mostly CaCO_3) and alumina (mostly Al_2O_3) are the best low-activation admixtures for low-activation concrete and that Co-60, Eu-152 and Eu-154 are the three most problematic activation products, with H-3, C-14, Cl-36, Fe-55, Ni-59, Ni-63, Zn-65 and Cs-134 also being present at levels of potential concern.

(Morioka et al., 2004) reports that the addition of the slow-neutron absorber B-10, in the form of e.g. B_4C powder, significantly lowers neutron activation in concrete. The fluence-rate ϕ of thermal neutrons is suppressed by the presence of an adequate amount of B-10, thereby lowering the values of all reaction-rates that mainly depend on the fluence-rate of slow neutrons. A clear benefit is observed at boron mass-fractions in concrete above approximately 2 %. The authors add that the presence of 2 % added boron in concrete has practically no effect of fast neutron fluence-rates, i.e. the rates of neutron activation reactions driven by fast neutrons, such as e.g. (n, p) , (n, α) and $(n, 2n)$ reactions, will not be lowered by added boron in bio-shield concrete.

(Kimura et al., 2007) state that concrete is a very useful and inexpensive material. However, after long-term use in high neutron fluence-rate areas in an NPP, concrete can become significantly neutron-activated, leading to large future liabilities in the form of high decommissioning costs. The easiest solution is to use low-activation concrete, which will have significantly lower residual radioactivity after 4 to 7 decades of reactor operation, followed by e.g. 6 years of pre-dismantling cooldown-time. In their work, they evaluated fifty raw materials by radiochemical analyses, which assessed the quantities of dominant trace elements such as Co, Eu and Cs, which are problematic activators under thermal-spectrum neutron irradiation conditions. From these investigations, three kinds of aggregates — (1) fused alumina ceramics, (2) silica sand and (3) limestone — and two types of cement — (1) high alumina cement and (2) “white cement”¹⁰ — were selected as best raw materials for low-activation concrete.

¹⁰ “White cement” is made from raw materials containing little or no iron or manganese which is what gives grey cement its colour. It is much finer than grey cement and has higher reflective properties. The production of

Finally, mixing recipes for six types of low-activation concrete and two types of mortar are proposed.

This concludes the discussion of the valuable contributions of the Japanese team, to knowledge about how to produce a dependable and replicable low-activation concrete for use close to nuclear reactors, where relatively intense neutron fields are encountered.

3.5.16 Three Key Concepts:

(1) Activation-Hazardous Elements,

(2) Activation-Hazardous Trace Elements and

(3) Radioactivity-Hazardous Nuclides

(Bylkin et al., 2018) introduces three particularly welcome terms designed to bring conceptual clarity to the relatively young discipline of the decommissioning of nuclear facilities. The concentration of *activation-hazardous elements* in building and construction materials will lead to the formation of *radioactivity-hazardous nuclides*, which is the most important characteristic that will determine the amount and radiological hazard of induced radioactivity. Values of *activation-hazardous trace elements* for the same generic type of material extracted from different geological deposits may differ by one to two orders of magnitude. (Bylkin et al., 2018) shows that the neutron-induced activity in shielding concrete strongly depends on the actual concentrations of activation-hazardous elements in the concrete including ‘trace’ concentrations (other factors being the same). The authors also show that any failure to consider the concentrations of activation-hazardous *trace-elements* will invariably lead to the underestimation of neutron-induced activation levels and amounts of radioactive wastes as well as their clearance-category.

From a literature study and calculations, (Bylkin et al., 2018) identify Eu, Co, Fe, Cs, Ca and Ni as “activation-hazardous elements in concrete and steel compositions of reactor installations”. In response to the above assertion by the authors, we can state that “steel without iron” is a contradiction-in-terms and that “cement without calcium” is also an unattainable goal. Achievable lowering of e.g. the “activation-hazardous element” Ni can be achieved by using

white cement typically needs 40 % more energy than the production of regular grey cement and this contributes to the high price of white cement. Because it contains less Fe and Mn than grey cement, white cement will activate less in a neutron field.

e.g. Duplex stainless steels (SS) such as SS-2205 in preference to high-nickel austenitic stainless steels such as SS-316. We also respond by stating that the greatest reduction in *radioactivity-hazardous nuclides* in metal-alloys and concretes is achieved by reducing the concentration of the trace-elements Eu, Co, Cs, Nb and Ag in raw materials used to make concrete, steel or Al-alloys. Note that our corrected list drops Ca and Fe (because their use is practically unavoidable) and adds two activation-hazardous trace elements, namely Nb and Ag.

3.5.17 The Need for a Systematic Approach to Neutron Activation at NPPs

(Bylkin et al., 2018) state that “significant amounts of radioactive wastes” will be generated during the decommissioning phase of NPPs, from the induced activity of neutron-irradiated structural and shielding materials. An important statement by (Bylkin et al., 2018) is as follows:

Information about concentrations of activation-hazardous elements and radioactivity-hazardous nuclides in radiation shielding materials is fragmented and, as a rule, often unsuitable for practical application.

In other words, (Bylkin et al., 2018) states that there is a need for a systematic approach to neutron activation at NPPs. An express aim of this dissertation is to fill the void by presenting a systematisation of knowledge about activation-hazardous elements and radioactivity-hazardous nuclides of concern in reactor decommissioning.

3.5.18 “Novel Tools for Estimation of Activation Dose” — MCNP, ATTILA, FISPACT-II and ORIGEN

(Pampin and Davis, 2008) presents “Novel tools for estimation of activation dose” and advocate and discuss the use of the radiation transport codes MCNP and ATTILA as well as the activation codes FISPACT and the code ORIGEN in SCALE. A major purpose of this substantial UKAEA report is to advocate the wider use of modern calculation methods to calculate activation source-terms and doses. In essence, the authors are promoting the IAEA’s recommended methodology for materials activation calculations shown in Figure 4 on page 27. This, indeed, is the same calculational methodology followed in this work.

3.5.19 Case-Study: Decommissioning of a VVR-S Research Reactor

(Ionescu et al., 2012) describes the decommissioning of a VVR-S research reactor (which was built during the Soviet era), with emphasis on the radiological characterisation of the reactor block. The “reactor block” presents the major contributor to the overall radioactive inventory of the reactor. Theoretical calculations and gamma spectrometry measurements of representative samples are compared to ensure a validated methodology. The radionuclide inventory of the reactor block and the quantities of radioactive waste and materials which can be released from regulatory control were quantified. The methodology was validated by comparing dose-rate measurements with the results of dose-rate calculations. The authors list H-3, C-14, Fe-55, Co-60, Ni-63, Ni-59, Eu-152, Eu-154 and Eu-155 as activation products of specific radiological concern. Their work suffers from several shortcomings, though:

1. Neutron transport calculations were performed with an obsolete code, namely DORT¹¹, which dates from 1989.
2. An obsolete 1991 version of the activation code ORIGEN is used — this legacy version of this code took only the thermal neutron fluence-rate as input, and then “internally reconstructed” two additional neutron energy groups. In contrast, the latest version of ORIGEN in SCALE 6.2 (ORNL and RSICC, 2018) collapses reaction cross-sections by means of a far more realistic 252-group neutron energy spectrum.

3.5.20 Preliminary Evaluation of Decommissioning Wastes for Nuclear Power Reactors in South Korea

(Lee et al., 2017) presents a *preliminary evaluation of decommissioning wastes for the first commercial nuclear power reactor* in South Korea. MCNP transport calculations that calculate the neutron spectrum, followed by FISPACT activation calculations that calculate the time-dependent $\{N, A\}$ -matrix in irradiated SSCs, were carried out. Only total activities, and not the detailed inventories of problematic radionuclides, are reported. The authors also fail to specify the versions of the codes MCNP and FISPACT, as well as the nuclear data set(s) that were used.

¹¹ Note by co-supervisor TJvR: The discrete-ordinates codes ANISN, DOT, DORT and TORT were widely used during the 1980s and 1990s, until personal computers became fast and powerful enough to allow the use of more accurate Monte Carlo codes and more comprehensive nuclear data sets.

3.5.21 The radionuclide Ca-41 in nuclear reactor concrete

(Hou, 2005) reports on the radiochemical quantification of Ca-41 in nuclear reactor concrete. The latter isotope is formed by the thermal-neutron activation of the target-isotope Ca-40 which typically make up a minimum of 4 % of the mass of concrete. The isotope Ca-40 is an electron-emitter and can neither be identified nor quantified using gamma-spectrometry; radiochemical methods must be used. The Ca in the sample is first dissolved, extracted and then subjected to e.g. X-ray spectrometry and liquid-scintillation counting. Factors responsible for the radiological significance of Ca-41 in concrete, are (1) its long half-life, (2) its high mobility in the environment, coupled to Ca being a nutrient — any Ca-41 that escapes into the environment will readily be incorporated into the bodies of animals and humans.

3.5.22 Decontamination and Dismantling of Radioactive Concrete Structures

In a document spanning 144 pages, (NEA, 2011) presents an overview of the decontamination and dismantling of radioactive concrete structures. The radionuclides that are listed as being significantly present in reactor concrete, are summarised in Table 9 (NEA, 2011).

Table 9: Radionuclides that are significantly present in reactor concrete subjected to neutron irradiation (NEA, 2011)

Nuclide	From reaction	Thermal activation cross section in barn	Half life
^3H	$^6\text{Li}(n,\alpha)^3\text{H}$	953	12.33 a
^{14}C	$^{14}\text{N}(n,p)^{14}\text{C}$	1.81	5730 a
^{39}Ar	$^{39}\text{K}(n,p)^{39}\text{Ar}$	0.1	269 a
^{41}Ca	$^{40}\text{Ca}(n,\gamma)^{41}\text{Ca}$	0.4	$1.03\text{E}+05$ a
^{54}Mn	$^{54}\text{Fe}(n,p)^{54}\text{Mn}$		312 d
^{55}Fe	$^{54}\text{Fe}(n,\gamma)^{55}\text{Fe}$	2.25	2.73 a
^{59}Ni	$^{58}\text{Ni}(n,\gamma)^{59}\text{Ni}$	4.6	$7.6\text{E}+04$ a
^{63}Ni	$^{62}\text{Ni}(n,\gamma)^{63}\text{Ni}$	14.2	100.1 a
^{60}Co	$^{59}\text{Co}(n,\gamma)^{60}\text{Co}$	18.7	5.27 a
^{65}Zn	$^{64}\text{Zn}(n,\gamma)^{65}\text{Zn}$	0.76	244 d
^{133}Ba	$^{132}\text{Ba}(n,\gamma)^{133}\text{Ba}$?	10.5 a
^{134}Cs	$^{133}\text{Cs}(n,\gamma)^{134}\text{Cs}$	29	2.1 a
^{152}Eu	$^{151}\text{Eu}(n,\gamma)^{152}\text{Eu}$	$9.2\text{E}+03$	13.5 a
^{154}Eu	$^{153}\text{Eu}(n,\gamma)^{154}\text{Eu}$	312	8.6 a
^{155}Eu	$^{154}\text{Eu}(n,\gamma)^{155}\text{Eu}$	85	4.76 a
$^{166}\text{Ho}^m$	$^{165}\text{Ho}(n,\gamma)^{166m}\text{Ho}$	64.7	1 200 a

There are several omissions or “gaps” in the above table. Firstly, the important isotope Na-22 is not listed. Secondly, the authors neglect to consider that all nuclear reactions of the type (z, t) , (where z signifies an arbitrary projectile, e.g. a neutron), will produce H-3 (because tritium (t) is identical to H-3); the single pathway to H-3 listed in Table 9 is therefore incomplete. (Nuclear reactions of the type (z, t) are normally threshold reactions, and in such cases, the tritium-producing exit-channel only opens energetically once the energy of the incident neutron exceeds the threshold-energy. Two examples of “missed” tritium-producing reactions are $^9_4\text{Be}(n, t)^7_3\text{Li}$ and $^6_3\text{Li}(n, t)^4_2\text{He}$; in general all $X(z_1, z_2)Y$ nuclear reactions where either z_2 is t or Y is H-3, produce tritium. The third and final omission identified in Table 9 is the nuclide Nb-94. Steel rebar and stainless-steel cooling pipes used in the concrete bio-shield of the reactor will typically contain trace amounts of Nb, which will activate to Nb-94 — the only stable isotope of Nb is Nb-93, which activates to Nb-94 by the reaction $^{93}_{41}\text{Nb}(n, \gamma)^{94}_{41}\text{Nb}$, which is exothermic, as are all (n, γ) -reactions. For thermal neutrons, the

cross-section of the latter reaction, as specified in ENDF/B-7.1, is approximately 1.2 b (Soppera et al., 2013).

3.5.23 Decommissioning Planning for an Austrian MTR

Two Austrian authors, (Mück and Casta, 2000), treat the planning for the decommissioning of the ASTRA Reactor, a 10 MW multipurpose MTR research reactor at the Austrian Research Center in Seibersdorf, which was to be decommissioned after 39 years of successful operation. An initial step was the estimate of the total activity content and the waste volumes to be expected. Each component, device or structural element was surveyed, its chemical composition estimated and the approximate total neutron fluence at its site in the reactor reconstructed. Of importance in this context were trace elements with high neutron activation cross-sections. From long-term experience with most of these materials, from activation analysis performed before some of the materials had been deployed in the reactor and from measurements performed in the context of the study in a few cases where no data were available, the activity of these components was estimated. Where no measurements were available, activities were calculated using activation tables taken from a publication dating from 1976. The authors did not perform any neutron transport or activation calculations. Their list of radioisotopes-of-interest contains the by-now-familiar ^3H , ^{14}C , ^{54}Mn , ^{55}Fe , ^{60}Co , ^{59}Ni , ^{63}Ni , ^{133}Ba and ^{152}Eu . A nuclide not encountered in previous references is ^{178}Hf (hafnium-178), which is expected to be present in the absorber-rods (i.e. control-rods) used in this specific MTR design; reactors that do not use Hf in neutron absorber materials, will not produce ^{178}Hf . The authors conclude as follows: “A preliminary evaluation of the arising radioactive waste was performed. The estimates amount to approximately 320 kg of medium-level radioactive waste and about 60 tonnes of contaminated and 100 tonnes of activated low-level radioactive waste. The activity inventory is roughly 200 TBq in the medium-level waste and 6 GBq in the low-level waste.”

The above estimate of 160 tonnes of radioactive waste that will fail clearance criteria, can be used in a rough cost estimate. Assume that the average mass-density of the radioactive waste is 2.3 g cm^{-3} , that the waste must be disposed of in 200-litre drums and that the disposal cost per single such drum amounts to USD 1000. Then the number of drums calculates to at least 350 and the associated disposal cost charged by a radioactive waste repository will be in the order of 350,000 USD. Suppose now that prior knowledge of low-activation materials selection had been used to design and construct the nuclear facility and that this had reduced the volume

of radioactive waste that had to be disposed of in 200-litre drums, by 50%. This would have reduced the disposal cost for low-level radioactive waste by approximately USD 175,000.

3.5.24 Reactor Decommissioning Experience in the UK

(Westall and Tawton, 2012) presents an overview of decommissioning experience in the UK, specifically for Magnox reactors. Ever pragmatic, they stress the need for performing measurements to validate neutron activation calculations. For all components within the steel bio-shield, shortly after final shutdown, Fe-55 was the most significant radionuclide in terms of inventory, i.e. total activity. However, its half-life is relatively short at 2.7 years so that after 20-30 years the longer-lived Ni-63 becomes the radionuclide with the highest activity; its 100-year half-life results in a much slower reduction of activity with time. The other significant radionuclides are H-3, Co-60, long-lived Ca-41 in concrete and C-14 in graphite. The authors state that the activity of activation products will decay by approximately two orders of magnitude within circa 50 years, after which the rate of decrease becomes much slower. Amongst the emitters of penetrating ionising photons that contribute to worker exposure, Co-60 is found to be the most significant isotope for approximately the first 100 years. After the elapse of this duration of time, the activity of Co-60 will drop to below that of other gamma-emitting, long-lived radionuclides such as Eu-152, Nb-94 and Ag-108m. Over the first century, the activity of Co-60 inventory will decrease by approximately five orders of magnitude (i.e. a factor of 10^5), and the dose-rate from activation products will therefore also drop by several orders of magnitude over the first century of radioactive decay.

3.5.25 Implementation of the Decommissioning of Two Research Reactors in France

(Lopes and Pillette-Cousin, 2003) sets forth the implementation of stage-3 decommissioning of the Triton Facility in France. This facility was built in the late 1950s. The Triton “pile” i.e. nuclear reactor was first operated in June 1959. It was a 6 MW research reactor working with high-enrichment uranium (HEU) as fuel, and light water as moderator and coolant. The Nereide “pile” (i.e. reactor) was first operated in 1960. It was a 600-kW reactor that also used enriched uranium as fuel and light water as moderator and coolant. The Triton reactor was used mainly for radionuclide production, radiation shielding studies, neutron diffraction experiments and fundamental physics experiments. Five neutron beam ports were built in the concrete radiation shielding around the Triton water-pool, to enable neutron experiments.

Calculations were used to obtain a profile of the spatial distribution of neutron activation inside the radiation shielding. This was accomplished by using the TRIPOLI-4 Monte Carlo radiation transport code to compute neutron fluence-rate distributions, and the activation code DARWIN-PEPIN-2 to calculate the activities of activation products in structures irradiated by neutrons originating from the reactor. Experimental studies were also performed — dozens of core drillings and samplings were performed in irradiated structures such as the concrete bio-shield. The activities of beta and beta-gamma emitters were determined by laboratory methods. Both in the calculation and in the measurements, the predominant activation radionuclides were found to be Eu-152, Eu-154, Co-60, Ni-63, Fe-55 and H-3 (Lopes and Pillette-Cousin, 2003). The calculated profile of the radionuclide distribution in the concrete shielding was in good agreement with experimental results.

3.5.26 Decommissioning Experience in Pakistan

(Israr et al., 2003) reported on the partial decommissioning of the Pakistan Research Reactor-1 (PARR-1). Analysis of decommissioning debris showed the presence of the following isotopes: Eu-152, Eu-154, Zn-65, Ca-41, Ag-108m and Ag-110m. The activity per unit mass in the debris was in the order of 2.2 Bq/g.

3.5.27 A Good Practice Guide for Radiological Sentencing

(NISDF, 2017) is a *Good Practice Guide* that details the principles, practices and processes to be used when determining whether an object may be released from any further controls based on radiological protection considerations. “It identifies approaches to segregate radioactive or potentially radioactive substances and articles from non-radioactive (or ‘out of scope’) substances and articles.” Table 3 on page 4 was prepared from information on pages 181 — 183 in this Guide.

3.5.28 Decommissioning Plan for the Trojan PWR

(Portland General Electric Company, 2001) deals with the Trojan Nuclear Plant (TNP) Decommissioning Plan. TNP is in Columbia County, Oregon, USA. TNP achieved initial criticality in December 1975 and began commercial operation in May 1976. The reactor output was rated at 3411 MW_t with an approximate net electrical output rating of 1130 MW_e. The nuclear steam supply system was a four-loop pressurized water reactor (PWR) designed by Westinghouse Electric Corporation. TNP was shut down for the last time in November 1992.

In January 1993, after approximately 17 years of operation, PGE notified the Nuclear Regulatory Commission (NRC), USA, of its decision to permanently cease power operations.

The TNP decommissioning plan states that the extent of neutron activation of the concrete in the containment wall, secondary shield wall, and reactor vessel missile shield were determined by core-bore analysis. The primary radionuclides identified were Co-60 and Eu-152. Another concrete core-bore sample was taken from the reactor vessel shield wall, close to the centreline of the reactor vessel. The core-sample was segmented and analyzed for gamma-ray emitting radioisotopes. Predominant radionuclides identified were Co-60, Eu-152, Eu-154, Eu-155 and Cs-134. Radioactivity was detected to a depth of approximately 125 cm (the total shielding thickness is 260 cm). Close agreement was noted between the calculated neutron activation results and the measured activation values. Agreement between calculations and experimental results was particularly good for Eu-152, at shallow depths into the concrete. Deeper into the concrete, the agreement between calculations and laboratory results was not as good, although the calculated values were conservative, i.e. the calculations tended to overestimate the activity of activation radionuclides. Neutron transport calculations were performed with the code ANISN and activation calculations with the code ORIGEN. Both these codes date from the late 1970s and early 1980s and are, in retrospect, antiquated and obsolete. PGE (2001) lists the following additional radionuclides of concern: Mn-54, Fe-55, Ni-63, Ag-108m, Ag-110m and Sb-125.

3.5.29 Clearance Levels for the Recycling of Metallic Scrap

(Lentijo, 2002) is a very valuable, fact-laden source of information on the following decommissioning topics:

- Clearance levels
- Unconditional clearance levels
- Conditional clearance levels
- Metallic material release — nuclide-specific clearance levels for metal scrap recycling
- Nuclide-specific clearance levels for direct reuse of metals items
- Building release
- Radionuclide-specific clearance levels for building reuse or demolition

- Radionuclide-specific clearance levels for building demolition
- Radionuclide-specific clearance levels for building rubble
- Verification of clearance levels
- Site release.

(Lentijo, 2002) specifies clearance levels for the recycling of metal scrap, as summarised in Table 10.

Table 10: Clearance levels for metal scrap recycling (Lentijo, 2002)

Nuclide	Activity per unit mass ($Bq\ g^{-1}$)	Activity per unit surface area ($Bq\ cm^{-1}$)
Na-22	1	10
Sc-46	1	10
Mn-54	1	10
Co-56	1	10
Co-58	1	10
Co-60	1	10
Zr-95	1	10
Nb-94	1	10
Ru-106	1	10
Ag-108m	1	10
Ag-110m	1	10
K-40	1	100
Zn-65	1	100
Se-75	1	100
Sr-85	1	100
Sr-90	10	10
Cl-36	10	100
Co-57	10	100
Y-91	10	100
Zr-93	10	100
C-14	100	1000
As-73	100	1000
Mo-93	100	1000
Tc-99	100	1000
Ca-45	1.0E3	100
S-35	1.0E3	1.0E3
Tc-97	1.0E3	1.0E3
Tc-97m	1.0E3	1.0E3
H-3	1.0E3	1.0E4
Nb-93m	1.0E3	1.0E4

Nuclide	Activity per unit mass ($Bq g^{-1}$)	Activity per unit surface area ($Bq cm^{-1}$)
Fe-55	1.0E4	1.0E4
Ni-59	1.0E4	1.0E4
Ni-63	1.0E4	1.0E4
Mn-53	1.0E4	1.0E5

To guide the eye, five distinct hazard-classes of radionuclides have been colour-coded in Table 10.

There is a good qualitative and quantitative agreement between Table 1 (page 2), Table 3 (page 4) and Table 10.

The clearance levels of one particular radionuclide — Ca-41 — has not been found in IAEA publications. It is, however, specified in (NEA, 2011: 57) as 1.0E5 Bq/g for the “release value of rubble”. This is a very “liberal” value. The underlying physical reason for the low hazard of Ca-41 is as follows: Ca-41 has a long half-life of circa 1E5 years, but emits only low-energy electrons and photons, having low penetrating abilities. This isotope of Ca emits circa 0.1218 ionising photons per nuclear transition, all at energies below 3.56E-03 MeV; it further emits just below 0.771 electrons per nuclear transition, all at energies below 3.53E-03 MeV (ENDF/B-7.1 nuclear data). These are very low energies, i.e. the penetrating ability and biological hazard is markedly low.

This concludes the “survey phase” of the literature study. The final step is to systematise and summarise the information about (1) problematic, high-activation target materials, and (2) the radionuclides that will make the dominant contributions to dose-rate fields and related radiological concerns during reactor decommissioning activities.

3.6 Summary and Conclusions: Literature Survey

In a comprehensive survey of technical literature, the long-lived activation radionuclides summarised in Table 11 have been found to be problematic at nuclear facilities at the decommissioning time; this table also contains the elements in which the radioisotopes are produced via neutron activation.

Table 11: Summary of long-lived activation-radionuclides and the materials in which they are produced, during the operation of a nuclear power plant (NPP)

Nuclide	Irradiated target material in which the radionuclide is formed	Severe Clearance Limitations?	Producer of Intense, Penetration Ionising Photons?
Na-22	Na	Y	Y
Mn-54	Fe and Mn	Y	Y
Co-60	Co and Ni; also Fe, Mn and Cr at $\phi \geq 10^{13}$	Y	Y
Zn-65	Zn and Cu	Y	Y
Nb-94	Nb and Mo	Y	Y
Ag-108m	Ag and Cd	Y	Y
Ag-110m	Ag and Cd	Y	Y
Cs-134	Cs	Y	Y
Cs-137	Ba	Y	γ^{12}
Ba-133	Ba	Y	Y
Eu-152	Eu, Sm and Nd	Y	Y
Eu-154	Eu, Sm and Gd	Y	Y
Ho-166m	Ho and Dy	Y	Y
Eu-155	Eu, Sm and Gd	Y	Y
H-3	All $X(z_1, z_2)Y$ nuclear reactions ¹³ where either z_2 is t or Y is H-3	N	N
C-14	N and C	N	N
Cl-36	Cl and K	N	N
Ca-41	Ca	N	N
Fe-55	Fe and Ni	N	N
Ni-59	Ni	N	N
Ni-63	Ni and Cu	N	N
Mo-93	Mo and Ru	N	N
Tc-99	Mo and Ru	N	N

In Table 11, Ho-166m was included within the “red category” clearance level radionuclides. This isotope has a half-life of 1200 yr \pm 180 yr (ENDF/B-7.1 (2011)). It emits several high-energy photons at energies as high as 0.810276 MeV, as well as electrons up to an energy of 1.23 MeV. The clearance level of Ho-166m is not specified in IAEA (International Atomic Energy Agency) or NEA (Nuclear Energy Agency) literature, but its high half-life and

¹² The radioactive progeny isotope of Cs-137, namely Ba-137m, emits the dominant penetrating ionising photons.

¹³ Note that tritium (t) is ^3H i.e. H-3.

penetrating, high-energy photon and electron emissions, will most certainly place it in the “red” category in Table 11, where we have indeed inserted it. It will only be produced in notable quantity from the irradiation of the element Ho, in which event Ho-166m will be by far the dominant radionuclide (this statement is based on FISPACT-II calculations). Ho-166m can also be produced, albeit at lower activities per unit mass of material, from the irradiation of the element Dy by neutrons. As a final remark, it should be noted that the elements Ho and Dy not “engineering elements” but merely unwanted, unnecessary trace-elements in Al-alloys, Ni-alloys and Fe-alloys as well as concrete at nuclear reactor facilities, so that Ho-166m will never be dominant in irradiated materials within the timespan of the first 100 years after cessation of reactor operation.

During the investigation behind the completion of Table 11, many pathway-analysis calculations were performed with the code FISPACT-II and it was found that neutron irradiation of Ba produces notable activities of the highly problematic radionuclide Cs-137, via two nuclear reactions:

Two Ba-isotopes contribute to the production of Cs-137: Ba-137 and Ba-138. The natural abundance of Ba-137 is 11.23 % and that of Ba-138 is 71.7 % — cf. (Meija et al., 2016) and (Holden et al., 2018).

A fraction of 89.2 % of the inventory of Cs-137 as neutron activation product is produced via the (n,p) -reaction, $^{137}_{56}\text{Ba} (n,p) ^{137}_{55}\text{Cs}$. This is a threshold reaction with a negligible cross-section for $E \leq 7 \text{ MeV}$.

The balance of 10.8 % of the Cs-137 is produced by (n,np) - and (n,d) -reactions on Ba-138. The nuclear reaction $^{138}\text{Ba} (n,d) ^{137}\text{Cs}$ is a threshold reaction with a negligible cross-section for $E \leq 10 \text{ MeV}$. The nuclear reaction $^{138}\text{Ba} (n,np) ^{137}\text{Cs}$ is also a threshold reaction with a negligible cross-section for $E \leq 12.3 \text{ MeV}$ (Soppera et al., 2013).

Insight into the existence of this pathway for the production of Cs-137 from Ba is absent in the published literature. High levels of Ba are found in barite shielding concrete, which uses high-grade barite ore, which typically contains at least 90 % BaSO₄. In a typical LWR neutron

spectrum, only a small fraction¹⁴ of the neutrons will have energies capable of producing Cs-137 from Ba. The induced activity of Cs-137 (half-life 30.08064 yr) will therefore always be low relative to that of other long-lived radionuclides formed by thermal neutrons. From this, it follows that barite concrete is not suitable for deployment in parts of a reactor building where notable neutron fluence-rates may be encountered, because it will lead to the formation of high activities of Ba-133 as well as smaller activities of the even longer-lived Cs-137. According to FISPACT-II calculations, the $\{N, A\}$ -matrix for the irradiation of a mass of 100 g Ba under scenario **DECO_60yr_6yr_1E9** is

$$\begin{bmatrix} {}^{133}\text{Ba} & 1.334E6 \text{ Bq} \\ {}^{137}\text{Cs} & 42.15 \text{ Bq} \\ {}^{137m}\text{Ba} & 39.77 \text{ Bq} \\ {}^{134}\text{Cs} & 10.63 \text{ Bq} \end{bmatrix}$$

from which it is seen that the activity of Cs-137 and its progeny Ba-137m is 4 to 5 orders of magnitude lower than that of Ba-133 which is produced by an (n, γ) -reaction, which is always exothermic i.e. it has no energy-threshold.

The target-elements that can, upon irradiation by typical neutrons with an LWR spectrum, only produce low-hazard radionuclides having liberal clearance-levels, are

C, N, Cl, K and Ca

while target-elements that can, upon irradiation by typical LWR spectrum neutrons, form high-hazard, very restrictive clearance-level radionuclides, are

Na, Mn, Fe, Co, Ni, Cu, Zn, Nb, Mo, Ru, Ag, Cd, Cs, Ba, Nd, Sm, Eu, Gd and Ho.

The final part of the literature survey will be to present a summary of the radiological “fingerprint” of each of the problematic radionuclides listed in Table 11. Information was taken from (Soppera et al., 2013) and (ICRP, 2008).

Na-22 has a half-life of 2.60276 yr and emits a high yield of high-energy photons at $E_\gamma = 1.27453$ MeV. It also emits circa 0.9 positrons per nuclear transition, each of which will produce two annihilation photons of energy 0.511 MeV.

¹⁴ According to a calculation by TJvR: approximately 0.2 %.

Mn-54 has a half-life of 0.854365 yr and emits a high yield of high-energy photons at up to 0.834848 MeV.

Co-60 has a half-life of 5.27124 yr and emits a high yield of high-energy photons at up to 1.33249 MeV.

Zn-65 has a half-life of 0.667858 yr and emits a high yield of high-energy photons at up to 1.11554 MeV.

Nb-94 has a half-life of 2.03004E4 yr (i.e. more than twenty thousand years) and emits a high yield of high-energy photons at up to 0.871091 MeV.

Ag-108m has a half-life of 438.00844 yr and emits a high yield of high-energy photons at up to 0.722907 MeV.

Ag-110m has a half-life of 0.68382 yr and emits a high yield of high-energy photons at up to 1.50503 MeV.

Cs-134 has a half-life of 2.06524 yr and emits a high yield of high-energy photons at up to 0.795864 MeV.

Cs-137 has a half-life of 30.08064 yr and emits a high yield of high-energy photons at up to 0.661657 MeV.

Ba-133 has a half-life of 10.51631 yr and emits a high yield of medium energy photons at up to 0.356013 MeV.

Eu-152 has a half-life of 13.53729 yr and emits a high yield of high-energy photons at up to 1.40801 MeV.

Eu-154 has a half-life of 8.60118 yr and emits a high yield of high-energy photons at up to 1.27444 MeV.

Eu-155 has a half-life of 4.7531 yr and emits a high yield of lower energy photons at up to 0.105305 MeV. As a result of the lower energy of the emitted photons, Eu-155 is less dangerous than Eu-152 and Eu-154.

Ho-166m has a half-life of 1200 yr and emits a high yield of high-energy photons at up to 0.810276 MeV.

4 CALCULATION MODELS: NEUTRON ACTIVATION

4.1 First Step in a Neutron Activation Calculation: Evaluating of the Neutron Spectrum

The first step in an activation calculation is to use a radiation transport code such as MCNP, FLUKA, TRIPOLI or GEANT4 to calculate representative multigroup neutron spectra in all irradiated components of interest. In this investigation, a standard LWR neutron spectrum in two circa 2.3 m long Al-rods, each with a diameter of 2.5 cm, located a few cms outside the northern core-box facet of the SAFARI-1 reactor, inside the reactor water pool, was used as the standardised LWR neutron spectrum — refer to (Van Rooyen, 2015) and (T.J. Van Rooyen, 2017). A top-view of the two Al-rods in the water-pool next to the LWR is shown in Figure 5. This drawing was generated by using the code MCNP's built-in plotter to draw the geometry of an x - y view of the geometry of the reactor, the water pool and the beam tubes, as incorporated in the MCNP model of the reactor (Zamonsky, 2019a).

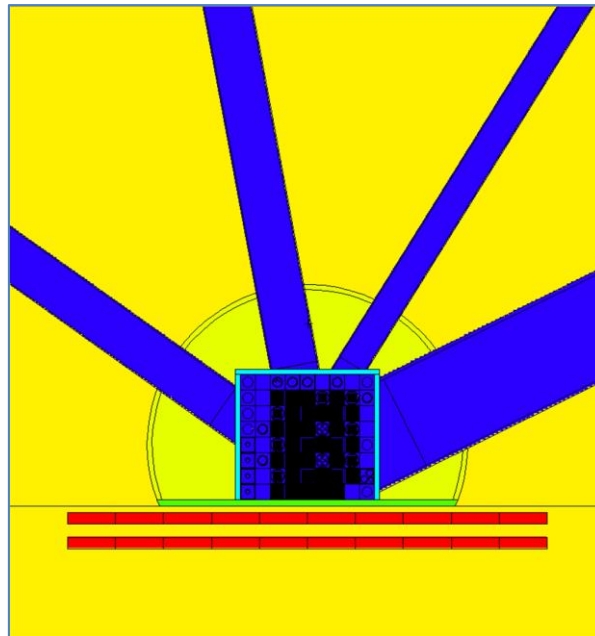






Figure 5: Two Al-rods in water-pool just outside the core of the SAFARI-1 reactor

Legend:

	Reactor core and neutron beamlines
	Core-box
	Water
	Aluminium rods

The energy spectrum $\phi(E)$ of the neutron fluence-rate in the irradiated Al-structure, is shown in Figure 6.

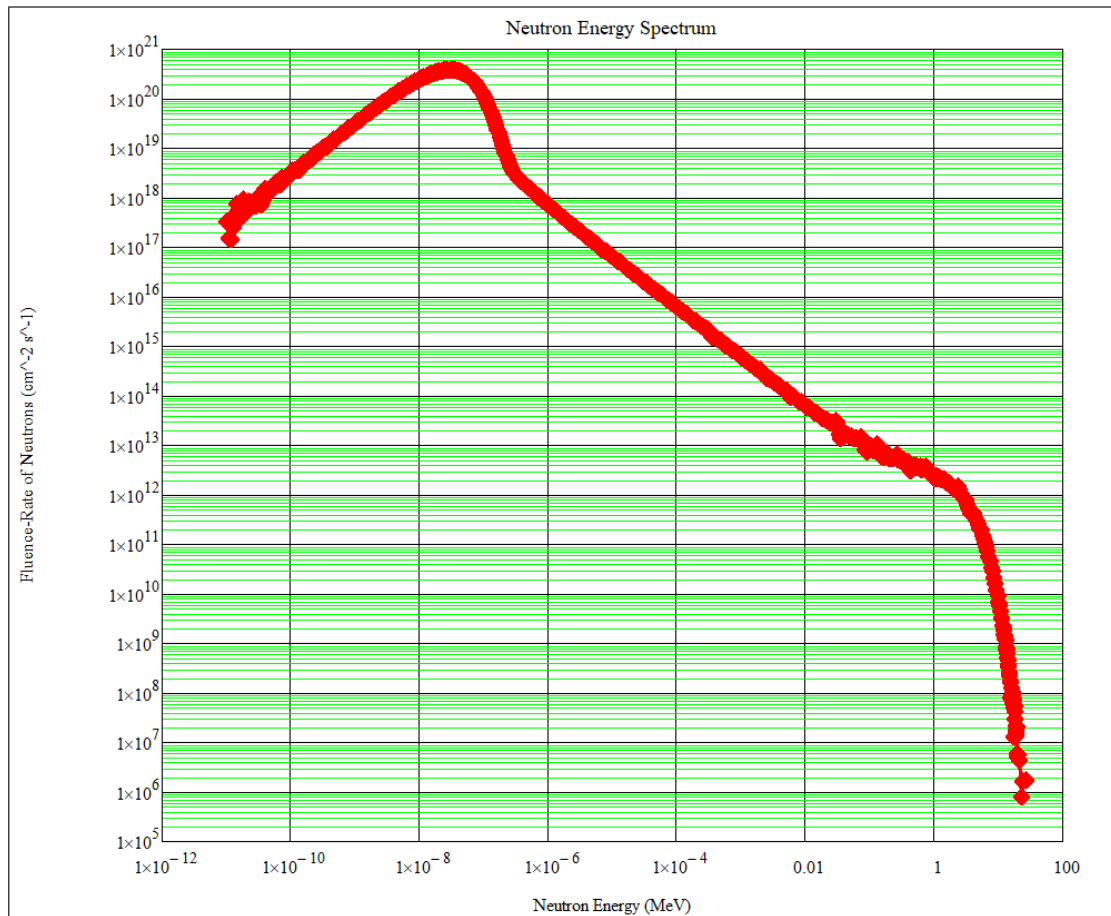


Figure 6: Neutron spectrum in the irradiated Al-rods in the water pool close to the SAFARI-1 reactor

This standard, full moderated LWR neutron spectrum $\phi(E)$ was calculated with the code MCNP 6.2 (LANL, 2018a) using ENDF/B-8.0 nuclear data (Brown et al., 2018), converted into ACE formatted cross-section files (ACE is an initialism for “A Compact ENDF”) by the MCNP-team at LANL for use by the code MCNP (Conlin et al., 2018). Where available, special thermal treatment cross-sections (Parsons, 2018) were used (see below). The MCNP calculation model was developed by Necsa’s Dr Oscar M. Zamonsky (Zamonsky, 2019a). The neutron spectrum was converged in 709 neutron energy groups; the latter neutron energy partition is specified in the FISPACT-II 3.00 User’s Manual (Sublet et al., 2015). All activation calculations in this project used this LWR activation spectrum, and always in 709 neutron energy groups.

The following special thermal treatment cross-sections from LANL, based on ENDF/B-8.0 nuclear data, were used (Parsons, 2018) in Rev. 3.00 of the MCNP calculation model of the SAFARI-1 reactor. This improves the accuracy of the calculated neutron spectrum $\phi(E)$ in the energy-region where the cross-sections of (n, γ) cross-sections tend to have high values. All reaction-rate integrals for neutron activation reactions have products of type $\sigma(E) \phi(E)$ in their integrands, so that the improved quantification of both $\sigma(E)$ and $\phi(E)$ in the low-energy range will improve the accuracy of neutron activation calculations.

The specification `MT100 AL-27.83T` was used to request special thermal treatment of neutron scattering for all Al-alloy structures—a dominant metal in SSC of the SAFARI-1 reactor.

The specification `MT120 H-H2O.83T` was used to request special thermal treatment of neutron scattering for all hydrogen in in-core and ex-core water (H₂O).

The specification `MT130 BE-MET.81T` was used to request special thermal treatment of neutron scattering for the beryllium metal in the reflector.

The specification `MT11 FE-56.83T` was used to request special thermal treatment of neutron scattering for all Fe in steel-alloys such as e.g. SS-314L.

The spectrum in Figure 6 is close to a “textbook” LWR neutron energy spectrum in the light water moderator. Above circa 1.4 MeV, the spectral shape approaches that of a Watt prompt fission neutron spectrum. Below 0.3 eV, the spectral shape approaches a Maxwellian thermal neutron spectrum. Between 0.3 eV and 1.4 MeV, the shape is a slowing-down neutron spectrum, characteristic of an LWR, as a result of neutron moderation via elastic scattering by H-1, the dominant scattering nuclide.

The neutron spectrum in Figure 6 will be observed practically unchanged in structures inside the reactor water pool, on condition that (1) the material structure is immersed in light water, (2) is relatively thin, and (3) the ratio $\frac{\sigma_s}{\sigma_a}$ for the irradiated material must be reasonably high over the neutron energy range, i.e. neutron scattering (cross-section σ_s) must dominate vis-a-vis neutron absorption (cross-section σ_a). Examples of structures that conform to the above requirements are in-pool rigs manufactured from aluminium and stainless-steel alloys, where the material diameter thickness does not exceed e.g. 10 cm at the thickest places. The core-box, the grid-plate, in-pool rigs as well as the neutron beam entering the NRAD (Neutron

Radiography) facility on the beam-port floor level, will all “see” the neutron spectrum of Figure 6, with minor localised variations. Examples of structures that do NOT conform to the above requirements would be irradiated structures containing strong neutron absorbers such as boron, cadmium or gadolinium, or very thick irradiated structures that do not contain the neutron scatterer H-1. Measured at a time 15 years after construction, typical ordinary concrete will contain approximately 5 % water by mass (Shultis and Faw, 2000), i.e. it contains a high enough number-fraction of H-1 to sustain the classical LWR neutron spectrum observed in Figure 6. This single, representative, “classical” LWR neutron spectrum was used in all activation calculations in this work.

The assertion that there exists a “classical LWR” neutron spectrum, requires substantiation through case-studies. Using the approved MCNP calculation model of the SAFARI-1 reactor developed at Necsra RRT (Zamonsky, 2019a) the co-supervisor of this dissertation calculated 6 neutron spectra, each in 709 energy groups, in a number of structures in and around the SAFARI-1 reactor at Necsra, and these spectra are clearly almost identical — see Figure 7. Whether the neutron spectrum is evaluated in the cladding of a target-plate, in a watery uranic slurry, in the beryllium reflector (BER), in the core-box, in the grid-plate or in an Al-rod in the water-pool adjacent to the reactor, the neutron spectrum remains basically the same.

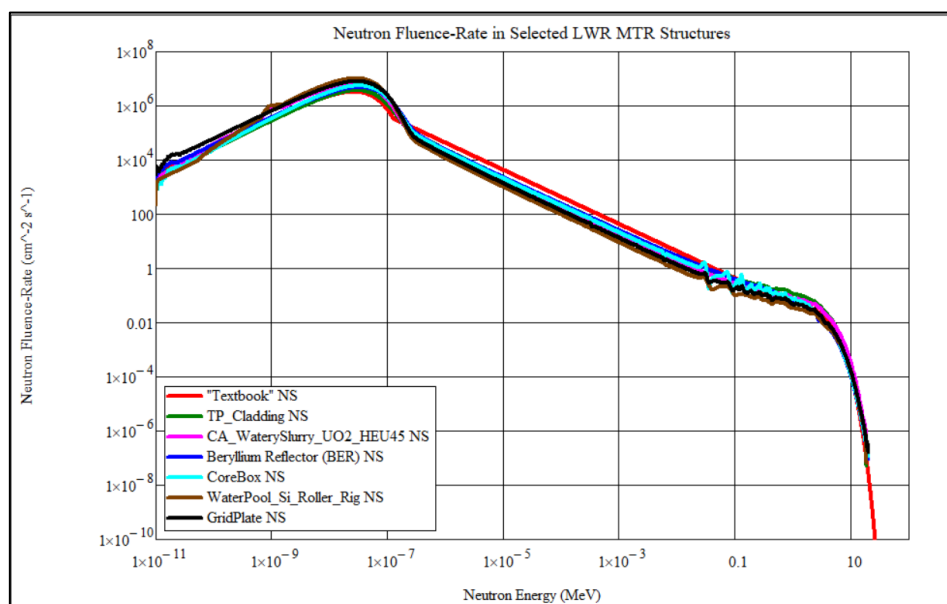


Figure 7: Calculated neutron spectra in 6 structures in and around the SAFARI-1 reactor core

Abbreviations:

NS: Neutron Spectrum

TP: Target Plate

CA: Criticality Accident

The seven neutron spectra shown in Figure 7 are clearly very similar, i.e. there indeed exists a “classical” LWR neutron spectrum.

Note: The “ideal NS” in Figure 7 is a simplistic neutron spectrum (NS) that is fully Maxwellian in the thermal neutron energy range (here $E \leq 0.125 \text{ eV}$), has a perfect $1/E$ shape in the slowing-down energy range (here $0.125 \text{ eV} \leq E \leq 0.8208 \text{ MeV}$) and an uncollided Watt prompt fission neutron (PFN) spectrum shape in the higher energy range (here $E \geq 0.8208 \text{ MeV}$). The MathCAD implementation of this spectrum¹⁵ is shown in Figure 8.

Mathematical form of the “ideal neutron spectrum”:	
$\varphi_{\text{tfr}}(E) :=$	$E \cdot \exp\left(\frac{-E}{2.58522 \cdot 10^{-8}}\right) \text{ if } (10^{-15} \leq E \leq 0.125 \cdot 10^{-6})$
	$\frac{(1.2414 \cdot 10^{-16})}{E} \text{ if } (0.125 \cdot 10^{-6} \leq E \leq 0.8208)$
	$(1.9228 \cdot 10^{-16}) \cdot \exp\left(\frac{-E}{0.965}\right) \cdot \sinh(\sqrt{2.29 \cdot E}) \text{ if } (E \geq 0.8208)$

Figure 8: Mathematical form of the “ideal neutron spectrum”, coded in MathCAD 14

In conclusion, one can say that a neutron spectrum that is highly representative of structures and components in and around the SAFARI-1 reactor core, was calculated. The calculated spectrum was validated against several other neutron spectra and found to be very similar, and therefore highly representative of LWR neutron spectra.

¹⁵ Note by co-supervisor TJvR: This spectrum was fitted as a continuous function using a legacy computer-algebra system named REDUCE, and then coded in Fortran as well as MathCAD by the co-supervisor, back in 1986. (Implementations of REDUCE are available on most variants of Unix, Linux, Microsoft Windows, or Apple Macintosh systems by using an underlying Portable Standard Lisp or Codemist Standard LISP implementation. REDUCE has also been translated into the coding language Julia, developed at MIT, USA.)

4.2 The Radiation Transport Code MCNP6.2 and the Calculation Model of the SAFARI-1 Reactor used to Calculate the Neutron Fluence-Rate

The Monte Carlo radiation transport code MCNP has been under development at Los Alamos National Laboratory (LANL) for many decades. It is a Monte Carlo code that simulates radiation transport for many different particles, including neutrons, photons, electrons, protons and alpha-particles. The latest version of MCNP is MCNP6.2 (LANL, 2018b). The use of the code for nuclear fission reactors is very well established. In such devices, neutron energies span the energy range up to 20 MeV, while the maximum photon energy is consistently below 15 MeV. At these relatively low neutron energies, tabular ACE format cross-section data are used, and there is no need to switch to the use of “model physics” i.e. the use of nuclear models when tabular XS data is absent. At neutron energies below circa 4 eV, the code can be instructed to switch from free-gas cross-sections to bound-state thermal scattering law cross-sections, also called $S(\alpha, \beta)$ cross-sections, for selected materials such as ^1H in H_2O , as well as for Al in Al-alloys and for Fe in steel-alloys, and more — refer to (Parsons, 2018).

Version 3.00 of the standard Necsra RRT MCNP model of the SAFARI-1 reactor, was used. This model is described in (Zamonsky, 2019a). The code-validation conformance of the code MCNP6.2 (which was used to execute the SAFARI-1 calculation model) to NNR RG-0016 standards, is set forth in (Zamonsky, 2019b). The only modifications made to the baseline MCNP model of the SAFARI-1 reactor, were (1) a switch to ENDF/B-8.0 (Conlin et al., 2018) cross-sections and (2) ENDF/B-8.0 thermal neutron scattering data (Parsons, 2018), and (3) the addition of an MCNP type-F4 tally for the fluence-rate two Al-rods, containing embedded information about the energy-boundaries of the 709-group energy-partition.

4.3 The Activation Code FISPACT-II

The activation code FISPACT-II 3.00 (Sublet et al., 2015) was used in this study. FISPACT-II is an inventory code capable of performing modelling of activation, transmutations and depletion induced by neutron, proton, alpha, deuteron or gamma particles incident on matter.

FISPACT-II is written in object-style Fortran-2003 and has full dynamic memory allocation. It uses an accurate ODE solver and can perform pathways, uncertainty and sensitivity calculations. All these can be used in multi-pulse irradiation calculations, including those where the fluence-rate spectrum $\phi(E)$ changes from irradiation pulse to pulse. It reads the modern,

ENDF-format data libraries such as the latest TALYS-based TENDL-2017 evaluated nuclear data libraries. The code can use probability table data to account for self-shielding effects, i.e. a decrease in effective 1-group neutron cross-sections caused by “dips” in the function $\phi(E)$ at the energies where absorption resonance peaks strongly deplete neutrons.

The four principal tasks that FISPACT-II can perform, are:

1. Collapses problem-independent ENDF format multigroup reaction cross-sections to problem-dependent 1-group binary-format reaction cross-section libraries (COLLAPX). Also extracts and consolidates ENDF format fission-yield, half-life and radiation emission data into ARRAYX binary-format libraries.
2. Construction and solution of rate-equations to calculate the time evolution of the nuclide inventory in response to different irradiation scenarios. These scenarios include:
 - A cooling-only calculation
 - A single irradiation pulse followed by cooling
 - Multiple irradiation pulses where only flux amplitudes, and not the energy-spectrum of the flux, change, followed by cooling
 - Multi-step irradiation where flux amplitude, flux spectra and collapsed 1-group cross-sections can change from step to step, followed by cooling
 - Multi-projectile simulation.
3. Computation and output of derived radiological quantities.
4. Subsidiary calculations to identify the key reactions and decays, and to assess the quality of the predictions. The four main subsidiary items are
 - Pathways analysis
 - Uncertainty calculations from pathways
 - Reduced model calculations
 - Monte-Carlo sensitivity and uncertainty calculations.

The library preparation task comprises reading and “collapsing” the cross-section data, reading, “condensing” and storing the decay data and fission-fragment yield data, and storing the regulatory radiological data (potential biological hazards, clearance data and legal transport data).

FISPACT-II constructs effective 1-group cross-sections by *collapsing* the energy-dependent cross-sections in the ENDF libraries, i.e., taking the weighted average over the energy variable E of the cross-section $\sigma(E)$ weighted by the irradiating projectile fluence-rate $\phi(E)$, where the projectiles may be neutrons, protons, deuterons, alpha-particles or gamma-rays.

4.4 Details of FISPACT Calculations

Details of how neutron activation calculations are performed with FISPACT-II 3.00 are given and discussed in Annexure A starting on page 190.

5 RESULTS

5.1 Research Question RQ₁:

Neutron Activation: A Non-Linear Function of Neutron Fluence-Rate ϕ

5.1.1 Case-Study to Demonstrate the Non-Linearity of Neutron Activation as a Function of the Fluence-Rate ϕ

A very important finding is that neutron activation is a non-linear function of the magnitude of the neutron fluence-rate ϕ_n . Using FISPACT-II 3.00, the following all-element material, as specified in Table 12, was activated, first at an integral¹⁶ neutron fluence-rate of

$$\phi = 10^{13} \text{ cm}^{-2}\text{s}^{-1}$$

and then at a fluence-rate

$$\phi = 10^{14} \text{ cm}^{-2}\text{s}^{-1}$$

i.e. at a value of ϕ that is 10 times higher than before. The investigated irradiation scenario was the decommissioning scenario, i.e. 60 yr of irradiation followed by 6 years of cooling.

Table 12: Specification of an “All-Element” Material that Contains 100 g of Every Chemical Element Found in Nature

```
<< Target Material Spec >>
<< Total Mass in kg; Number of Elements in mtl>>
MASS  8.10      83
H      1.2345679
HE     1.2345679
LI     1.2345679
BE     1.2345679
B      1.2345679
C      1.2345679
N      1.2345679
O      1.2345679
F      1.2345679
NE     1.2345679
NA     1.2345679
MG     1.2345679
AL     1.2345679
SI     1.2345679
P      1.2345679
S      1.2345679
```

¹⁶ When the neutron fluence-rate function $\phi(E)$ is integrated over the energy domain, the integral neutron fluence-rate ϕ is obtained — it is simply the total neutron fluence-rate over all neutron energies.

CL	1.2345679
AR	1.2345679
K	1.2345679
CA	1.2345679
SC	1.2345679
TI	1.2345679
V	1.2345679
CR	1.2345679
MN	1.2345679
FE	1.2345679
CO	1.2345679
NI	1.2345679
CU	1.2345679
ZN	1.2345679
GA	1.2345679
GE	1.2345679
AS	1.2345679
SE	1.2345679
BR	1.2345679
KR	1.2345679
RB	1.2345679
SR	1.2345679
Y	1.2345679
ZR	1.2345679
NB	1.2345679
MO	1.2345679
TC	0.0000000
RU	1.2345679
RH	1.2345679
PD	1.2345679
AG	1.2345679
CD	1.2345679
IN	1.2345679
SN	1.2345679
SB	1.2345679
TE	1.2345679
I	1.2345679
XE	1.2345679
CS	1.2345679
BA	1.2345679
LA	1.2345679
CE	1.2345679
PR	1.2345679
ND	1.2345679
PM	0.0000000
SM	1.2345679
EU	1.2345679
GD	1.2345679
TB	1.2345679
DY	1.2345679
HO	1.2345679
ER	1.2345679
TM	1.2345679
YB	1.2345679
LU	1.2345679
HF	1.2345679
TA	1.2345679
W	1.2345679
RE	1.2345679
OS	1.2345679

IR	1.2345679
PT	1.2345679
AU	1.2345679
HG	1.2345679
TL	1.2345679
PB	1.2345679
BI	1.2345679

The material specified in Table 12 is, essentially, 0.10 kg of each of the chemical elements ranging from H to Bi, excluding Tc and Pm — because the latter two elements are practically absent in nature. The number 1.2345679 that follows the standard chemical names of the 81 elements that are present, represents the mass-percentage of each element in the irradiated mixture of $83 - 2 = 81$ elements, because $\frac{100\%}{81} = 1.2345679\%$; the mass-% values add up to 100 %.

The investigated irradiation scenario was the decommissioning scenario, i.e. 60 years of irradiation followed by 6 years of cooling, which is specified as follows to FISFACT-II.

```
<< Start: Irradiation >>
FLUX  1.00E13
TIME  60  YEARS  ATOMS
<< End: Irradiation >>
<< Start: Cooling >>
FLUX  0.0
ZERO
TIME  6  YEARS  ATOMS
<< End: Cooling >>
```

and

```
<< Start: Irradiation >>
FLUX  1.00E14
TIME  60  YEARS  ATOMS
<< End: Irradiation >>
<< Start: Cooling >>
FLUX  0.0
ZERO
TIME  6  YEARS  ATOMS
<< End: Cooling >>
```

Note that the keyword “ATOMS” is a request to the code FISFACT-II to print a complete set of results at a given point in the timeline.

Results are summarised in Table 13.

Table 13: Activities at $\phi = 1E14 \text{ cm}^{-2} \text{ s}^{-1}$ compared to activities at $\phi = 1E13 \text{ cm}^{-2} \text{ s}^{-1}$, for the activation of an all-element target material in the high fluence-rate domain

Radionuclide	Ratio $\left(\frac{Act(\phi=1E14 \text{ cm}^{-2} \text{ s}^{-1})}{Act(\phi=1E13 \text{ cm}^{-2} \text{ s}^{-1})} \right)$
H3	1.1E+00
Co60	3.4E-01
Cs134	1.8E-01
Eu154	4.3E-02
Tm170	2.7E+00
Eu155	7.5E-02
Tl204	5.0E+00
Pt193	1.3E+00
Ta182	8.8E-01
Tm171	4.2E+00
Tb160	1.2E+00
Ag110m	5.8E-01
Ni63	3.2E+00
Zn65	6.3E+00
Fe55	7.2E+00
Pm147	9.2E+00
C14	9.0E+00
Ag109m	9.4E+00
Cd109	9.4E+00
Ir192	8.1E+00
Kr85	1.2E+01
Se75	1.1E-02
Sb124	5.2E+00
Pm145	2.6E+00
S35	9.1E-01
Nb93m	7.0E+00
Cd113m	4.2E+00
Sm145	5.0E+00
Ag108m	1.8E-02
Cs137	1.1E+01
W185	4.4E+01
Ba137m	1.1E+01
Sm151	1.5E-01
Sb125	1.3E+01
Ca45	9.4E+00
Hf181	1.9E+01
Cl36	3.0E-01
Ba133	4.8E+00
Ag110	5.8E-01
Te123m	1.2E+01
Hg203	1.1E+01
Tb157	1.8E-02

Radionuclide	Ratio $\left(\frac{Act(\phi=1E14\text{ cm}^{-2}\text{ s}^{-1})}{Act(\phi=1E13\text{ cm}^{-2}\text{ s}^{-1})}\right)$
Te125m	1.6E+01
Lu177m	1.0E+00
In114m	1.6E+00
Ho166m	8.4E-02
In114	1.6E+00
Nb94	4.4E+00
Po210	1.1E+01
Hf177m	1.0E+00
Dy159	2.9E-02
W181	4.5E-02
Ni59	1.0E+00
Sn119m	9.0E+00
Ag108	1.8E-02
In113m	8.6E+00
Sn113	8.6E+00
Sn121m	2.5E+00
Gd153	4.2E-03
Ce141	1.2E+01
Ar39	3.0E+00
Sn121	2.5E+00
Ru103	1.2E+01
Rh103m	1.2E+01
Lu177	1.0E+00
Tb158	7.3E-02
Sc46	3.2E+01
Nb95	2.0E+01
Ce139	5.6E+00
Mn54	6.9E+00
Lu174	5.5E-01
Co58	3.1E+00
Ca41	3.9E+00
Sn123	1.1E+01
Zr95	9.9E+00
Te127m	2.4E+00
Te127	2.4E+00
I125	5.1E-05
Eu152	1.5E-02
Pm146	2.6E+00
Mo93	6.1E+00
Sr85	8.7E+00
Kr81	1.3E+01
Cr51	1.9E+00
Ho163	1.2E-01
Cd115m	1.1E+01
Sr89	1.1E+01

Radionuclide	Ratio $\left(\frac{Act(\phi=1E14\text{ cm}^{-2}\text{ s}^{-1})}{Act(\phi=1E13\text{ cm}^{-2}\text{ s}^{-1})}\right)$
Ar37	6.4E+00
Lu174m	7.4E-01
Co57	5.5E+00
Fe59	1.4E+02
Os194	6.7E+01
Ir194	6.7E+01
Cs135	8.1E+00
Se79	1.2E+01
Te121	6.8E+00
Te121m	6.8E+00
Rh102	5.5E-01
Pm148m	2.1E+01
Hf175	1.6E+00
Tc99	3.7E+00
Re188	2.8E+00
W188	2.8E+00
Tm168	2.7E+00
La137	1.4E+00
Os185	1.7E+00
Y88	8.6E+00
Rh102m	4.0E-01
Be10	1.0E+01
Xe127	6.9E+00
Nb95m	9.9E+00
P33	3.6E+00
Zr93	9.5E+00
Re184m	7.8E-01
Re184	7.9E-01
V49	1.7E+00
Ta179	1.3E+00
Lu173	8.4E-01
Te129m	1.1E+01
Tc97m	1.9E+01
Nb91	6.3E+00
Eu156	7.4E-01
Pd107	1.2E+01
Pm148	2.1E+01
Re186	1.9E-01
Re186m	1.9E-01
Rb86	9.5E+00
Pm143	7.8E+00
Te129	1.1E+01
Bi207	7.0E+00
Pb207m	7.0E+00
Hf178m	1.8E+00

Radionuclide	Ratio $\left(\frac{Act(\phi=1E14\text{ cm}^{-2}\text{ s}^{-1})}{Act(\phi=1E13\text{ cm}^{-2}\text{ s}^{-1})}\right)$
Hf178n	1.8E+00
Pm144	1.2E+01
Y91	6.9E+01
Tc97	4.1E+00
P32	9.0E+01
Si32	9.4E+01
Sc45m	9.4E+00
Ce144	9.3E+01
Pr144	9.3E+01
K40	2.4E+00
Os191	1.6E+01
Ir191m	1.6E+01
Na22	9.8E-01
Eu150	6.0E-05
I129	3.5E+00
Yb169	3.9E+00
Y90	9.6E+01
Sr90	9.6E+01
Bi208	6.8E+00
Ir192n	4.8E+00
Au195	1.6E-01
Rh101	6.7E+00
Nb91m	9.9E+00
Tl206	5.6E+00
Bi210m	5.6E+00
Ar42	9.5E+01
K42	9.5E+01
Rb84	9.4E+00
Tc98	5.1E+01
Gd151	2.4E-01
Rb87	9.8E-01
Hf182	7.4E+01
Re187	1.2E-02
Rb83	8.7E+00
Pb205	3.4E+01
Kr83m	8.7E+00
Ge73m	1.5E-02
As73	1.5E-02
Pd103	8.0E+00
Ru106	9.1E+01
Rh106	9.1E+01
Re183	2.7E+00
Hf179n	4.6E+00
Tc95m	9.4E+00
In115m	1.1E+01

Radionuclide	Ratio $\left(\frac{Act(\phi=1E14\text{ cm}^{-2}\text{ s}^{-1})}{Act(\phi=1E13\text{ cm}^{-2}\text{ s}^{-1})}\right)$
Y89m	1.1E+01
Ag105	8.7E+00
Pr144m	9.3E+01
Sm147	6.5E-02
Sm146	2.0E+01
Fe60	9.2E+01
Co60m	9.2E+01
Pr143	9.3E+00
Cs136	8.1E+01
Po209	7.5E+01
Nb92	4.6E+00
Ge71	1.2E+01
Tc95	9.4E+00
Zr88	9.8E+00
Sn117m	1.2E+01
As74	5.7E+00
Lu176	1.0E-01
Co56	5.6E+00
Mn53	1.4E+00
Nd147	2.0E+01
Bi210	8.4E+01
Pb210	8.4E+01
Al26	9.8E-01
Cs131	2.9E+00
Gd150	2.6E-02
Xe131m	2.2E+01
La138	2.9E-01
Sn126	8.5E+01
Sb126m	8.5E+01
Ir193m	7.7E+01
Sb126n	8.5E+01
Er169	3.7E+01
Tl202	2.7E+01
I126	1.0E+00
Pb202	2.8E+01
Ba131	2.9E+00
Po208	1.2E+02
Sb126	8.7E+01
Eu149	1.4E-01
Nd144	2.4E+00
In115	2.4E-02
Au194	2.2E-02
Hg194	2.2E-02
Lu172	1.9E-03
Lu172m	1.9E-03

Radionuclide	Ratio $\left(\frac{Act(\phi=1E14 \text{ cm}^{-2} \text{ s}^{-1})}{Act(\phi=1E13 \text{ cm}^{-2} \text{ s}^{-1})}\right)$
Hf172	1.9E-03
Os186	1.8E-01
Sm148	1.2E+00
Pt190	2.4E-05
Ce136	3.9E-01

The nuclide activity ratio $\left(\frac{A(\phi_n=10^{14} \text{ cm}^{-2} \text{ s}^{-1})}{A(\phi_n=10^{13} \text{ cm}^{-2} \text{ s}^{-1})}\right)$ ranges between values as low as 2.38E-5 to as high as 138 when the magnitude of ϕ_n is increased by a factor 10. This means that neutron activation is a non-linear phenomenon, at least in the upper part of the domain of realistic fluence-rates ϕ . The reasons for this non-linearity will be explained below. The practical implication of this finding is that one cannot “solve” a neutron activation problem at a reference neutron fluence-rate ϕ_{ref} and then linearly “scale up” or “scale down” answers such as activities, dose-rates and heat-deposition rates, as a linear function of the fluence-rate ϕ . In other words, neutron activation problems must be solved on a one-by-one i.e. an individual basis, for every value of ϕ .

On the other hand, neutron activation is a fully linear function of the mass of the irradiated material, at a constant neutron fluence-rate ϕ , if we ignore self-shielding related spectral shift effects in bulk samples.

The next calculational experiment was to investigate whether neutron activation is a linear phenomenon in the lower fluence-rate domain of concern. The “all-element material” defined in Table 12 above was irradiated for 7 days and then cooled off for 1 year at $\phi_{lo} = 1.0E8 \text{ cm}^{-2} \text{ s}^{-1}$ and at $\phi_{hi} = 1.0E9 \text{ cm}^{-2} \text{ s}^{-1}$. The reason for the short irradiation period (7 days) was to prevent depletion of target isotopes, while the reasoning behind the relatively long cooling time (1 year), was to eliminate short-lived radionuclides from the picture. Results are summarised in Table 14.

Table 14: Activities at $\phi = 1E9 \text{ cm}^{-2} \text{ s}^{-1}$ compared to activities at $\phi = 1E8 \text{ cm}^{-2} \text{ s}^{-1}$ for the activation of an all-element target material in the low neutron fluence-rate domain

Nuclide	Activity Ratio $\left(\frac{A(\phi_n=10^9 \text{ cm}^{-2} \text{ s}^{-1})}{A(\phi_n=10^8 \text{ cm}^{-2} \text{ s}^{-1})}\right)$
Eu152	1.00E+01
H3	1.00E+01
Tm170	1.00E+01
Ir192	1.00E+01

Eu154	1.00E+01
Co60	1.00E+01
Cs134	1.00E+01
Ta182	1.00E+01
Tb160	1.00E+01
Ag110m	1.00E+01
Gd153	1.00E+01
Tl204	1.00E+01
Zn65	1.00E+01
Tm171	1.00E+01
Se75	1.00E+01
Eu155	1.00E+01
Re187	1.00
Rb87	1.00
Sb124	1.00E+01
S35	1.00E+01
Lu177m	1.00E+01
Hf177m	1.00E+01
Hf175	1.00E+01
Os185	1.00E+01
Fe55	1.00E+01
Hf181	1.00E+01
Sm151	1.00E+01
Pm147	1.00E+01
W185	1.00E+01
W181	1.00E+01
Lu177	1.00E+01
Sm147	1.00
Hg203	1.00E+01
In114m	1.00E+01
In114	1.00E+01
Ca45	1.00E+01
Ag110	1.00E+01
Sm145	1.00E+01
I125	1.00E+01
Dy159	1.00E+01
Lu176	1.00
Ce141	1.00E+01
Ni63	1.00E+01
Yb169	1.00E+01
Ru103	1.00E+01
Rh103m	1.00E+01
K40	1.00
Po210	1.00E+01
Ho166m	1.00E+01
Te123m	1.00E+01

In113m	1.00E+01
Sn113	1.00E+01
Sb125	1.00E+01
Ag109m	1.00E+01
Cd109	1.00E+01
Kr85	1.00E+01
Co58	1.00E+01
Nb95	1.00E+01
Te125m	1.00E+01
C14	1.00E+01
Sn119m	1.00E+01
Cd113m	1.00E+01
Cr51	1.00E+01
Ce139	1.00E+01
Nb93m	1.00E+01
Ag108m	1.00E+01
Zr95	1.00E+01
Te127m	1.00E+01
Te127	1.00E+01
Pm145	1.00E+01
Pt193	1.00E+01
Sr85	1.00E+01
Mn54	1.00E+01
Sn123	1.00E+01
Cs137	1.00E+01
Ba137m	1.00E+01
Ba133	1.00E+01
Ar37	1.00E+01
Cl36	1.00E+01
Sr89	1.00E+01
Cd115m	1.00E+01
Tb157	1.00E+01
Fe59	1.00E+01
La138	1.00
Lu174	1.00E+01
Ar39	1.00E+01
Tm168	1.00E+01
Lu174m	1.00E+01
Ag108	1.00E+01
Sc46	1.00E+01
Ni59	1.00E+01
Nb94	1.00E+01
Sn121m	1.00E+01
Te121	1.00E+01
Te121m	1.00E+01
Rh102m	1.00E+01

In115	1.00
Co57	1.00E+01
Sn121	1.00E+01
Rh102	1.00E+01
Xe127	1.00E+01
Re184	1.00E+01
Re184m	1.00E+01
Y88	1.00E+01
Nb95m	1.00E+01
Rb86	1.00E+01
Ca41	1.00E+01
Te129m	1.00E+01
Te129	1.00E+01
Ho163	1.00E+01
Eu150	1.00E+01
Mo93	1.00E+01
Tb158	1.00E+01
Pt190	1.00
Tc97m	1.00E+01
Os191	1.00E+01
Ir191m	1.00E+01
Nd144	1.00
V49	1.00E+01
Ta179	1.00E+01
Kr81	1.00E+01
Na22	1.00E+01
Sm149	1.00
Lu173	1.00E+01
Ir192n	1.00E+01
Pm143	1.00E+01
Au195	1.00E+01
Se79	1.00E+01
Ce136	1.00
Y91	1.00E+01
Sc45m	1.00E+01
Cd113	1.00
Rb84	1.00E+01
Nb91m	1.00E+01
Pm144	1.00E+01
Gd152	1.00
Tc99	1.00E+01
Gd151	1.00E+01
Sm148	1.00
Re186	1.00E+01
Re186m	1.00E+01
P32	1.00E+01

P33	1.00E+01
La137	1.00E+01
Xe134	1.00
Er162	1.00
Re183	1.00E+01
Yb168	1.00
Eu149	1.00E+01
Pd103	1.00E+01
Os186	1.00
Xe124	1.00
Be10	1.00E+01
Cd114	1.00
Ge73m	1.00E+01
As73	1.00E+01
Os184	1.00
Rb83	1.00E+01
Ce142	1.00
Zr93	1.00E+01
Hf179n	8.34
Kr83m	1.00E+01
Y89m	1.00E+01
Tc95m	1.00E+01
Gd160	1.00
In115m	1.00E+01
Bi207	1.00E+01
Nb91	1.00E+01
Rh101	1.00E+01
Hf178m	1.00E+01
Hf178n	1.00E+01
Pb207m	1.00E+01
W183	1.00
Pd107	1.00E+01
Ag105	1.00E+01
Pr143	1.00E+01
Sn124	1.00
Hf174	1.00
W184	1.00
Cs135	1.00E+01
Pm148m	1.00E+01
W186	1.00
Tc97	1.00E+01
Hf179m	1.00
Ge71	1.00E+01
Pd110	1.00
I129	1.00E+01
Pm146	1.00E+01

Te123	1.00
Bi208	1.00E+01
As74	1.00E+01
Pb204	1.00
Tl206	1.00E+01
Bi210m	1.00E+01
Tc95	1.00E+01
Sn117m	1.00E+01
Ta180m	1.00
V50	1.00
Zr88	1.00E+01
Bi209	1.00
Nd147	1.00E+01
Re188	100.0
W188	100.0
Cd108	1.00
Pm148	1.00E+01
Cs131	1.00E+01
Y90	1.00E+01
Sr90	1.00E+01
Mo100	1.00
Nd148	1.00
Co56	1.00E+01
Xe131m	1.00E+01
Ce144	1.05E+01
Pr144	1.05E+01
Ru106	1.00E+01
Rh106	1.00E+01
Lu172	1.00E+01
Lu172m	1.00E+01
Hf172	1.00E+01
Nd150	1.00
Pb205	1.00E+01
Ba131	1.00E+01
Cd116	1.00
Gd150	1.00E+01
Cd106	1.00
Os194	100.0
Ir194	100.0
Zr96	1.00
Er169	1.00E+01
Ir193m	1.00E+01
I126	1.00E+01
Dy156	1.00
Te130	1.00
Nb92	1.00E+01

Ca48	1.00
Al26	1.00E+01
Ir190	1.00E+01
Tl202	1.00E+01
Si32	1.02E+01
Pr144m	1.05E+01

In Table 14, ratios between approximately 8 and 10.5 (which signifies linear and near-linear activation behaviour) are colour-coded in green. Values below 2 indicate non-linear activation and are in red; values above approximately 12 also indicate non-linear activation and are highlighted in yellow. Practically all the radiologically important isotopes identified in the literature survey are found to activate linearly (colour-coding: green). Only 4 isotopes — Os-194, Ir-194, Re-188 and W-188 — activate as a function of ϕ^2 , i.e. they display clear quadratic behaviour. The activities of a surprising number of isotopes appear to depend on $\phi^0 = 1$, which is unexpected, anomalous behaviour.

An analysis of the isotopes in Table 14 whose activities appear not to depend on ϕ (i.e. the ratio $\left(\frac{A(\phi_n=10^9 \text{ cm}^{-2} \text{ s}^{-1})}{A(\phi_n=10^8 \text{ cm}^{-2} \text{ s}^{-1})}\right) = 1$), indicate that they all have extremely long half-lives; some examples are:

Re-187 — T_half = 4.1E10 yr

Rb-87 — T_half = 4.923E10 yr

Sm147 — T_half = 1.06E11 yr

Ca-48 — T_half = 4.4E19 yr

Te-130 — T_half = 7.9E23 yr

Dy-156 — T_half = 1.0E18 yr

Zr-96 — T_half = 3.9E19 yr

It is evident that a numerical quirk in the LODE (Linear Ordinary Differential Equations) solver of FISPACT-II 3.00 (released in 2015) is responsible for the unexpected, illogical “fluence-rate

independent” activation behaviour¹⁷ highlighted in red in Table 14. None of the radionuclides of concern in decommissioning scenarios is implicated in the numerical quirk discovered in the code FISPACT-II 3.00, i.e. the soundness of computed results and the validity of recommendations are not affected.

All four radionuclides whose activity depends on ϕ^2 do not have direct precursors found in nature; all their isotopic precursors are “two steps away” from the end-product radionuclide and this causes the activation to depend on ϕ^2 . Such non-linear phenomena are investigated and explained below, for the neutron activation of elements such as Cr (see page 93), Mn (see page 91) and Fe (see page 88).

5.1.2 Reason for the non-linearity of neutron activation as a function of ϕ , especially at higher fluence-rates φ

The non-linearity of neutron activation as a function of ϕ can be understood by considering an example. Consider the formation of ${}^{60}_{27}\text{Co}$ with the irradiation of a sample of pure Fe in a neutron field ϕ_n . At $t = 0$, there is no ${}^{59}\text{Co}$ present in the sample. When irradiation starts, the radionuclide ${}^{59}_{26}\text{Fe}$ is formed via the neutron activation of the stable Fe isotope ${}^{58}\text{Fe}$; this process is Rapid and is called an R-process. The ${}^{59}\text{Fe}$ then radioactively transitions to stable ${}^{59}\text{Co}$ (i.e. it is a β -delayed, i.e. a Slow or S-process¹⁸). The ${}^{59}\text{Co}$ then activates to the long-lived and radiologically hazardous and problematic radionuclide ${}^{60}\text{Co}$. In other words, *both* (1) the number of target atoms ${}^{59}\text{Co}$ as well as (2) the reaction rate $\phi_n \sigma N$ of the nuclear reaction ${}^{59}\text{Co} + n \rightarrow {}^{60}\text{Co}$, depend on ϕ and thus the non-linearity manifests because the effective reaction rate for the production of ${}^{60}\text{Co}$ depends on $\phi \times \phi = \phi^2$ when Fe is the target-material

At low fluence-rates, the non-linearity of neutron activation is far less pronounced than at high values of ϕ .

¹⁷ Note by co-supervisor TJvR: FISPACT-II is a very expensive code and Necsa was unable to afford versions 3.20 (2016) and 4.00 (2018). The UKAEA team mentioned that “numerous bug fixes” had been done in the most recent releases of this activation code.

¹⁸ In stellar nucleogenesis, the terms R-process and S-process are used to describe Rapid (R) and Slow (S) nuclear processes.

5.1.3 Burnup of Target-Isotopes in Irradiated Materials

One reason for the observed non-linearity of neutron activation is the burn-away of target-isotopes with high neutron transmutation cross-sections, over long irradiation periods and at high fluence-rates. Consider e.g. the irradiation of a hypothetical material that contains 100 g of every chemical element found on earth — from H to Bi, with the exclusion of Tc and Pm — in a fluence-rate of $\phi = 1.0E14 \text{ cm}^{-2} \text{ s}^{-1}$. After 60 years of neutron irradiation, (1) many initially present nuclides will either be severely depleted or markedly augmented, and (2) initial natural abundances of the isotopes of the elements will be completely perturbed, through transmutation reactions. The decrease in the masses of some elements and the increase of the masses of others is illustrated in Table 15.

Table 15: Mass-depletion and mass-augmentation in a hypothetical material that initially contains all terrestrial elements, and is irradiated under scenario

DECO_60yr_1E14

Element	Mass initially present (g)	Mass present after 60 years of irradiation (g)	Relative change in mass (%)
H	100	113.480	13.48
He	100	113.720	13.72
Li	100	105.690	5.69
Be	100	99.7450	-0.255
B	100	81.7170	-18.28
C	100	119.850	19.85
N	100	80.2220	-19.78
O	100	99.9980	-0.002
F	100	99.8410	-0.159
Ne	100	100.010	0.01
Na	100	93.9540	-6.046
Mg	100	106.340	6.34
Al	100	97.2540	-2.746
Si	100	105.700	5.70
P	100	98.0710	-1.929
S	100	138.830	38.83
Cl	100	62.8670	-37.13
Ar	100	97.2850	-2.72

Element	Mass initially present (g)	Mass present after 60 years of irradiation (g)	Relative change in mass (%)
K	100	103.810	3.81
Ca	100	100.090	0.09
Sc	100	0.07215	-99.93
Ti	100	101.160	1.16
V	100	57.1190	-42.88
Cr	100	144.020	44.0
Mn	100	20.6050	-79.40
Fe	100	181.970	81.97
Co	100	2.33710	-97.66
Ni	100	216.810	116.81
Cu	100	68.6220	-31.38
Zn	100	114.090	14.09
Ga	100	77.5670	-22.43
Ge	100	123.090	23.10
As	100	56.8580	-43.14
Se	100	147.540	47.54
Br	100	48.9380	-51.06
Kr	100	152.300	52.3
Rb	100	95.7620	-4.24
Sr	100	105.620	5.62
Y	100	85.6400	-14.36
Zr	100	114.470	14.47
Nb	100	91.8580	-8.14
Mo	100	107.730	7.73
Tc	0	0.53525	#DIV/0!
Ru	100	93.4150	-6.59
Rh	100	0.39027	-99.61
Pd	100	188.130	88.13
Ag	100	1.46990	-98.53
Cd	100	218.590	118.59
In	100	0.68417	-99.32
Sn	100	203.200	103.20
Sb	100	40.5760	-59.42

Element	Mass initially present (g)	Mass present after 60 years of irradiation (g)	Relative change in mass (%)
Te	100	161.980	61.98
I	100	36.3980	-63.60
Xe	100	159.820	59.82
Cs	100	23.6000	-76.40
Ba	100	177.710	77.71
La	100	35.1910	-64.81
Ce	100	123.720	23.72
Pr	100	48.6770	-51.32
Nd	100	191.180	91.18
Pm	0	0.20413	#DIV/0!
Sm	100	34.3030	-65.70
Eu	100	0.39960	-99.60
Gd	100	250.410	150.41
Tb	100	10.7760	-89.22
Dy	100	9.30610	-90.69
Ho	100	7.20620	-92.79
Er	100	333.130	233.13
Tm	100	6.77060	-93.23
Yb	100	218.690	118.69
Lu	100	8.40450	-91.60
Hf	100	126.480	26.48
Ta	100	40.4910	-59.51
W	100	241.940	141.94
Re	100	2.55820	-97.44
Os	100	178.590	78.59
Ir	100	4.08650	-95.91
Pt	100	261.010	161.0
Au	100	0.38289	-99.62
Hg	100	191.430	91.43
Tl	100	93.50600	-6.49
Pb	100	124.230	24.23
Bi	100	99.603	-0.40

An entry `#DIV/0!` in the final column of Table 15, indicates that the initial mass of the element was zero so that an attempt to calculate the relative change in mass will result in division by zero.

Elements that are substantially *depleted* by neutron irradiation and associated transmutation, are highlighted in red blocks, while elements that are substantially *replenished* by neutron irradiation and associated transmutation, are highlighted in green blocks in Table 15. It is seen that, over long irradiation times and at high values of ϕ as is prevalent in an MTR, the engineering elements V, Cr, Mn, Fe and Ni will undergo vast decreases or increases in mass-%, which will undoubtedly undermine the metallurgical integrity of steel and stainless steel structures. It is also seen that elements such as Eu, Ir, Co, Re, Rh, Ag and Au are practically completely burned up. In contrast, a low net change in mass-% is seen for the elements Be, O, Mg, Al, Si, Ca, Ti, Zr, Nb, Mo, Ru and Bi. In principle, a metal alloy composed of one or more of the elements Be, Mg, Al, Si, Ti, Zr and Mo, should have higher mechanical integrity over extended irradiation times in an intense neutron fluence-rate (with a characteristic LWR energy-spectrum $\phi(E)$), compared to e.g. Fe-alloys. (Fe-alloys can be deployed in e.g. pressure-vessels for PWRs and BWRs, because in such structures $\phi < 10^{10} \text{ cm}^{-2} \text{ s}^{-1}$).

Another point that is best illustrated by an example, is the alteration in the isotopic composition of elements after exposure to intense neutron irradiation. This is illustrated for Fe in a fluence-rate of $\phi = 10^{14} \text{ cm}^{-2} \text{ s}^{-1}$ for 60 years, followed by 1 year of cooling and is summarised in Table 16.

There are four stable isotopes of Fe, namely Fe-54 (natural abundance 5.845 %), Fe-56 (natural abundance 91.754 %), Fe-57 (natural abundance 2.1191 %) and Fe-58 (natural abundance 0.2819 %). Here and in the entire manuscript, all natural-abundance data for terrestrial isotopes, are taken from the most recent, official IUPAC publications, notably (Meija et al., 2016) and (Holden et al., 2018).

Table 16: Typical change in the isotopic composition of Fe undergoing intense neutron irradiation in scenario `DECO_60yr_6yr_1E14`

Fe Isotope	Mass-% before irradiation	Mass-% after irradiation
Fe-54	5.8450	4.30138
Fe-55	0.0000	0.05663

Fe Isotope	Mass-% before irradiation	Mass-% after irradiation
Fe-56	91.754	67.9572
Fe-57	2.1191	23.3882
Fe-58	0.2819	4.29536
Fe-59	0.0000	0.00001
Fe-60	0.0000	0.00130

In Table 16 it is seen that the mass-% of both stable isotopes Fe-54 and Fe-56 are significantly lowered by prolonged and intense neutron irradiation, while that of the stable isotopes Fe-57 and Fe-58 are drastically increased. The general finding is that intense neutron irradiation perturbs the isotopic composition of chemical elements. Even if it is chemically purified to contain only the element Fe, neutron-irradiated Fe will neutronically behave differently compared to natural, terrestrial Fe (^{nat}Fe), because the neutron exposure has left it with an altered isotopic composition. The general pattern is that, for an element with several isotopes, the neutron-field will deplete the isotopes with lower mass-numbers *A* and add to the mass-% of the isotopes with higher mass-numbers — see Table 16. The element Fe has 4 stable isotopes. During neutron irradiation, the abundances of Fe-54 and Fe-56 are lowered while the abundances of Fe-57 and Fe-58 are increased by the high (*n, γ*)-reaction rate.

The information presented in Table 16 is graphically displayed in Figure 9.

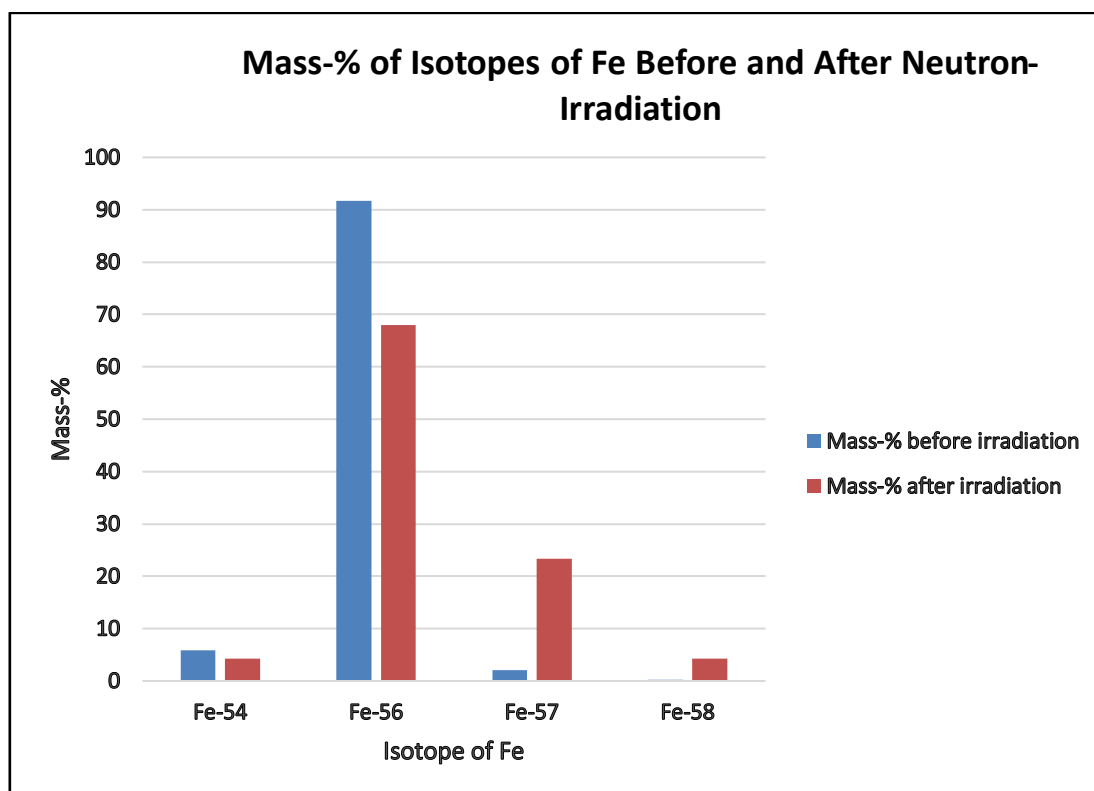


Figure 9: Mass-% of the stable isotopes of Fe before and after prolonged exposure to intense irradiation by neutrons — the isotopic composition of the element Fe is markedly perturbed by the exposure to neutrons

5.1.4 Non-linearity in the Neutron Activation of Iron (Fe; $Z = 26$)

The non-linearity of neutron activation is now investigated further, but now for three separate single-element samples that are irradiated for $T_{irr} = 7$ days at

$$\phi_{hi} = 10^{14} \text{ cm}^{-2} \text{ s}^{-1}$$

and at

$$\phi_{lo} = 10^{13} \text{ cm}^{-2} \text{ s}^{-1}$$

and then cooled off for $T_{cool} = 1$ year. The three elements that will be investigated, are Fe, Mn and Cr, i.e. the three elements placed “just to the left of” Co in the Periodic Table of the elements. The short irradiation time (7 days) was selected to eliminate target-element burn-away (i.e. depletion) considerations. The long cooling time was selected to eliminate short-lived radionuclides.

The activities of the induced radionuclides for an irradiated reference sample of 100 g of Fe, are given in Table 17.

Table 17: Activities of induced radionuclides for the irradiation of a 100 g sample of Fe at two integral neutron fluence-rates that differ by a factor 10 in magnitude, namely $\phi_{lo} = 1E13 \text{ cm}^{-2} \text{ s}^{-1}$ and $\phi_{hi} = 1E14 \text{ cm}^{-2} \text{ s}^{-1}$

$\phi_{lo} = 10^{13} \text{ cm}^{-2} \text{ s}^{-1}$		$\phi_{hi} = 10^{14} \text{ cm}^{-2} \text{ s}^{-1}$		Activation Product	Ratio $\frac{A(\phi_{hi})}{A(\phi_{lo})}$
Nuclide	Activity (Bq)	Nuclide	Activity (Bq)		
Fe55	3.4197E+10	Fe55	3.4188E+11	Fe55	1.0E+01
Mn54	3.2946E+08	Mn54	3.2923E+09	Mn54	1.0E+01
Fe59	8.9322E+07	Fe59	8.9330E+08	Fe59	1.0E+01
Cr51	1.1672E+04	Co60	1.4725E+05	Co60	1.0E+02
Co60	1.4730E+03	Cr51	1.1669E+05	Cr51	1.0E+01
H3	9.6295E+01	H3	9.6429E+02	H3	1.0E+01
Mn53	7.4682E-01	Mn53	7.4587E+00	Mn53	1.0E+01
Co60m	5.4895E-02	Co60m	5.4898E+00	Co60m	1.0E+02
Fe60	5.4895E-02	Fe60	5.4898E+00	Fe60	1.0E+02
Co58	1.8621E-03	Co58	1.7998E-01	Co58	1.0E+02
V49	4.3570E-07	V49	4.3545E-05	V49	1.0E+02
Sc46	1.7461E-12	Ni63	3.2911E-09	Ni63	1.0E+05
Co57	1.3664E-12	Co57	1.3262E-09	Co57	1.0E+03
Ni63	3.2917E-14	Sc46	1.7451E-10	Sc46	1.0E+02
Ca45	2.8511E-14	Ca45	2.8502E-11	Ca45	1.0E+03
Ni59	4.3778E-15	Ni59	4.3744E-12	Ni59	1.0E+03
V50	9.0597E-16	Mn52	2.7406E-14	Mn52	2.0E+03
Mn52	1.5106E-17	V50	9.0526E-15	V50	1.0E+01
V48	1.2375E-17	V48	1.2361E-15	V48	1.0E+02
Sc45m	5.4171E-19	Sc45m	5.4153E-16	Sc45m	1.0E+03

An entry $\#N/A$ in the final column indicates that the nuclide is not present for both values of ϕ so that activities cannot be compared¹⁹. In the final column, entries highlighted in a red cell, indicate a non-linear dependence of activity on ϕ .

From Table 17 it is evident that straight-forward neutron absorption reactions with isotopes that are abundantly present in the pre-irradiated sample, lead to product yields that are a linear function of ϕ . Fe-54 is present in the sample and it activates to the radionuclide Fe-55 by a simple neutron absorption reaction. Therefore, the activity of Fe-55 depends linearly on the neutron fluence-rate ϕ . The same holds for the simple nuclear reactions that produce Mn-54, Fe-59, Cr-51, H-3 and Mn-53. On the other hand, the activities of Co-60 and Co-60m and Fe-

¹⁹ The comparison uses EXCEL's VLOOKUP function.

60 are upped by a factor 100 when ϕ increases by a factor 10. The underlying reason is as stated above — both (1) the number of target-nuclides as well as (2) the rate of formation of the activation product, depend on ϕ so that the activities of the last group of nuclides will increase as a function of $\phi \times \phi = \phi^2$. If ϕ therefore changes by a factor 10, the activities of Co-60 and Co-60m and Fe-60 are increased by a factor of $10 \times 10 = 10^2 = 100$.

FISPACT-II 3.00 summarises the pathways for the formation of the nuclides seen in the irradiated sample, as summarised in Table 18.

Table 18: Summary by FISPACT-II of the pathways for the formation of selected radio-nuclides in a Fe sample irradiated at a high neutron fluence-rate

Target nuclide Fe 59	99.999% of inventory given by 1 path		

path 1	99.999% Fe 58	---(R)---	Fe 59 ---(L)---
	100.00%(n,g)		
Target nuclide Fe 55	99.982% of inventory given by 1 path		

path 1	99.982% Fe 54	---(R)---	Fe 55 ---(L)---
	100.00%(n,g)		
Target nuclide Mn 54	100.000% of inventory given by 1 path		

path 1	100.000% Fe 54	---(R)---	Mn 54 ---(L)---
	100.00%(n,p)		
Target nuclide Cr 51	100.000% of inventory given by 1 path		

path 1	100.000% Fe 54	---(R)---	Cr 51 ---(L)---
	100.00%(n,a)		
Target nuclide Co 60m	100.000% of inventory given by 1 path		

path 1	100.000% Fe 58	---(R)---	Fe 59 ---(D)---
	100.00%(n,g)	100.00%(b-)	Co 59 ---(R)---
			Co 60m---(S)---
			100.00%(n,g)
Target nuclide Co 60	100.000% of inventory given by 2 paths		

path 1	61.684% Fe 58	---(R)---	Fe 59 ---(D)---
	100.00%(n,g)	100.00%(b-)	Co 59 ---(R)---
			Co 60m---(b)---
			Co 60 ---(L)---
			100.00%(IT)
			0.00%(n,E)
			0.00%(n,n)
path 2	38.316% Fe 58	---(R)---	Fe 59 ---(D)---
	100.00%(n,g)	100.00%(b-)	Co 59 ---(R)---
			Co 60 ---(L)---
			100.00%(n,g)
Target nuclide H 3	99.812% of inventory given by 3 paths		

path 1	1.751% Fe 54	---(R)---	H 3 ---(L)---
	41.05%(n,t)		
	58.95%(n,t)m		

path 2	72.035%	Fe 56	---(R)---	H 3	---(L)---
			100.00%(n,t)		
path 3	26.026%	Fe 57	---(R)---	H 3	---(L)---
			100.00%(n,t)		
Target nuclide Fe 60 100.000% of inventory given by 1 path					

path 1	100.000%	Fe 58	---(R)---	Fe 59	---(R)---
			100.00%(n,g)		100.00%(n,g)
Target nuclide Mn 53 100.000% of inventory given by 2 paths					

path 1	99.184%	Fe 54	---(R)---	Mn 53	---(L)---
			98.15%(n,np)		
			1.85%(n,d)		
path 2	0.815%	Fe 54	---(R)---	Fe 53	---(b)---
			100.00%(n,2n)		100.00%(b+)
					0.00%(n,p)

FISPACT-II's report of the *pathway summary* for Co-60 is given in Table 19.

Table 19: Pathway summary for the formation of the radionuclide Co-60 from the irradiation of a sample that initially contained 100% pure Fe, by an intense field of LWR neutrons

Target nuclide Co 60 100.000% of inventory given by 1 path					
path 1	100.000%	Fe 58	---(R)---	Fe 59	---(D)---
				Co 59	---(R)---
					Co 60
					---(L)---
This generic pathway is the sum of 2 pathways					

A comparison of Table 17 with Table 18 and Table 19 brings the following principle to light: The formation of Fe-59, Fe-55, Mn-54 and Cr-51 involves a 1-step reaction where the parent-isotope is initially present in the sample of pure Fe. In the formation of Co-60 is, by contrast, the direct precursor-isotope Co-59 is initially absent and must first be “bred” in the irradiated Fe-sample. The reaction-rate for the formation of Co-60 is, therefore, the product of the reaction-rate for the formation of Co-59, multiplied by the reaction-rate for the activation of Co-60 from Co-59. Both these reaction-rates are linear functions of ϕ so that the reaction-rate for the generation of Co-60 will be proportional to $\phi \times \phi = \phi^2$.

5.1.5 Non-linearity in the Neutron Activation of Manganese (Mn; Z = 25)

We now step down by 1 on the atomic number scale, from $Z = 26$ to $Z = 25$ to investigate the neutron activation of the element Mn, which is widely used in many steel-alloys at typical mass-concentrations as high as 3 %. As before, sample 1 is irradiated for $T_{irr} = 7$ days at $\phi_{hi} =$

$10^{14} \text{ cm}^{-2} \text{ s}^{-1}$ while sample 2 is irradiated at $\phi_{lo} = 10^{13} \text{ cm}^{-2} \text{ s}^{-1}$ and then cooled off for $T_{cool} = 1$ year.

We have seen that the neutron activation of Fe ($Z = 26$) can “breed” Co ($Z = 27$) under intense neutron irradiation, even if the initial concentration of Co in a sample is zero. The “suspicion” is therefore that elements such as Mn ($Z = 25$), Cr ($Z = 24$), and even V ($Z = 23$) — which are located to the left of Fe on the Periodic Table of the Elements, can do the same, i.e. also “breed” Co-59 under intense neutron irradiation, enabling the latter stable isotope to then activate to the long-lived, radiologically problematic radioisotope Co-60.

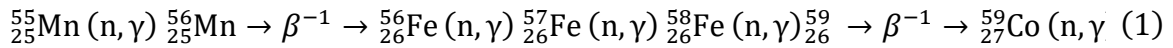
There is only a single stable isotope of Mn, namely $^{55}_{25}\text{Mn}$. The radionuclides and their activities, for the irradiation of reference sample of 100 g Mn by neutrons having an LWR energy-spectrum, are given in Table 20.

Table 20: Activities of induced radionuclides for the irradiation of a 0.1 kg sample of Mn at two neutron fluence-rates that differ by a factor 10 in magnitude

$\phi_{lo} = 10^{13} \text{ cm}^{-2} \text{ s}^{-1}$		$\phi_{hi} = 10^{14} \text{ cm}^{-2} \text{ s}^{-1}$		Activation Product	Ratio $\frac{A(\phi_{hi})}{A(\phi_{lo})}$
Nuclide	Activity (Bq)	Nuclide	Activity (Bq)		
Mn54	2.7869E+07	Mn54	2.7844E+08	Mn54	1.E+01
H3	2.3129E+03	H3	2.3125E+04	H3	1.E+01
Fe55	1.6542E+02	Fe55	1.6536E+04	Fe55	1.E+02
Fe59	6.9437E-06	Fe59	7.0364E-02	Fe59	1.E+04
Cr51	5.0496E-07	Cr51	6.3094E-05	Cr51	1.E+02
Mn53	4.9562E-09	Co60	2.2814E-06	Co60	1.E+05
Co60	2.2938E-11	Mn53	4.9492E-07	Mn53	1.E+02
Sc47	1.1937E-12	Mn56	5.0890E-08	Mn56	#N/A
V49	1.7880E-15	Co60m	1.7081E-10	Co60m	1.E+05
Co60m	1.7106E-15	Fe60	1.7081E-10	Fe60	1.E+05
Fe60	1.7106E-15	Co58	2.8396E-12	Co58	1.E+05
Mn52	1.2171E-16	V49	1.7864E-12	V49	1.E+03
Ca45	3.3511E-17	Sc48	1.2352E-12	Sc48	#N/A
Co58	2.9203E-17	Ca45	3.3502E-14	Ca45	1.E+03
Sc46	1.7665E-19	Sc46	1.7664E-16	Sc46	1.E+03
Ca47	7.7884E-20	Co58m	8.1249E-19	Co58m	#N/A
Sc45m	6.3672E-22	Sc45m	6.3653E-19	Sc45m	1.E+03
V50	1.0188E-22	Ni63	1.7833E-20	Ni63	1.E+08
Co57	1.2250E-26	Co57	1.1820E-20	Co57	1.E+06
Ni63	1.8378E-28	V50	1.0179E-20	V50	1.E+02

An entry $\boxed{\#N/A}$ in the final column indicates that the nuclide is not present for both values of ϕ so that activities cannot be compared. In the final column, entries highlighted in a red cell, indicate a non-linear dependence of activity on ϕ .

From Table 20 it is evident that straight-forward neutron absorption reactions with target-isotopes that are abundantly present in the pre-irradiated sample, lead to product yields that are a linear function of the integral fluence-rate ϕ . Mn-55 is present in the sample and the formation of Mn-54 and H-3 will be a linear function of ϕ . On the other hand, the “breeding” of the problematic long-lived isotope Co-60 in a sample of pure Mn, shows a substantial dependence on ϕ namely by a factor ϕ^5 . This is because of the long chain of (n, γ) -reactions leading from Mn-55 to Co-60, which is shown in Eq. (1).



Because the concentrations of a total of 4 target-isotopes, namely Fe-56, Fe-57, Fe-58, Co-59 as well as the rate of the last reaction step, ${}^{59}_{27}\text{Co} (n, \gamma) {}^{60}_{27}\text{Co}$, all depend nearly linearly on ϕ , it follows that the rate of formation of Co-60 will depend on $\phi^4 \times \phi = \phi^5$, i.e. if ϕ is increased by a factor 10, then the irradiated sample can contain up to 10^5 times more Co-60 activity. This “breeding” of Co-60 in a sample that initially contains 100 % pure Mn, is therefore of substantial radiological importance at high neutron fluence-rates but will be comparatively negligible at lower neutron fluence-rates, i.e. it is a very “steep” function of ϕ .

5.1.6 Non-linearity of the neutron activation of Chromium (Cr; $Z = 24$)

We now step down by 1 on the atomic number scale, from $Z = 25$ (Mn) to $Z = 24$ (Cr) to investigate the neutron activation of the element Cr, which is widely used in many stainless-steel-alloys at mass-percentages typically ranging between 11 % and 20 %. As before, sample 1 is irradiated for $T_{irr} = 7$ days at $\phi_{hi} = 10^{14} \text{ cm}^{-2} \text{ s}^{-1}$ while sample 2 is irradiated at $\phi_{lo} = 10^{13} \text{ cm}^{-2} \text{ s}^{-1}$ and then cooled off for $T_{cool} = 1$ year.

The reason for investigating Cr is that we have seen that the neutron activation of Fe, as well as Mn, can “breed” Co under intense irradiation conditions, even if the initial concentration of Co in a sample is zero. The “suspicion” is therefore that even the element Cr — which is located to the left of Fe and Mn on the Periodic Table of the Elements, can do the same, i.e. also “breed” Co-59 under intense neutron irradiation, which then activates to the long-lived, problematic isotope Co-60.

There are four stable isotopes of Cr in nature — Cr-50 (natural abundance 4.3452 %), Cr-52 (natural abundance 83.7895 %), Cr-53 (natural abundance 9.5006 %) and Cr-54 (natural abundance 2.3647%) (Meija et al., 2016). The activities of the induced radionuclides for a reference sample of 100 g Cr, as calculated with FISPACT-II, are given in Table 21.

Table 21: Activities of induced radionuclides for the irradiation of a 0.1 kg sample of the element Cr at two neutron fluence-rates that differ by a factor 10 in magnitude

$\phi_{lo} = 10^{13} \text{ cm}^{-2} \text{ s}^{-1}$		$\phi_{hi} = 10^{14} \text{ cm}^{-2} \text{ s}^{-1}$		Activation Product	Ratio $\frac{A(\phi_{hi})}{A(\phi_{lo})}$
Nuclide	Activity (Bq)	Nuclide	Activity (Bq)		
Cr51	8.5747E+07	Cr51	8.5705E+08	Cr51	1.0E+01
V49	6.6645E+04	V49	6.6623E+05	V49	1.0E+01
H3	1.0759E+01	H3	1.0763E+02	H3	1.0E+01
Mn54	5.5690E-02	Mn54	5.5705E+00	Mn54	1.0E+02
Sc46	1.7567E-02	Sc46	1.7591E-01	Sc46	1.0E+01
V48	3.9489E-06	Fe55	2.1521E-04	Fe55	1.0E+03
Fe55	2.1513E-07	V48	3.9421E-05	V48	1.0E+01
Ca45	8.7001E-08	Ca45	8.9454E-06	Ca45	1.0E+02
V50	2.5087E-10	V50	2.5060E-09	V50	1.0E+01
Sc45m	1.6530E-12	Fe59	5.6355E-10	Fe59	1.0E+05
Fe59	5.6341E-15	Sc45m	1.6996E-10	Sc45m	1.0E+02
Ar39	8.8890E-18	Co60	1.3013E-14	Co60	1.0E+06
Mn53	6.5906E-18	Mn53	6.5879E-15	Mn53	1.0E+03
K42	8.5704E-20	Ar39	8.8312E-16	Ar39	9.9E+01
Ar42	8.5700E-20	K42	3.9747E-17	K42	4.6E+02
Co60	1.3014E-20	Ar42	3.9745E-17	Ar42	4.6E+02
Sc44	9.1572E-24	Co60m	1.1381E-18	Co60m	1.0E+06
Ti44	9.1572E-24	Fe60	1.1381E-18	Fe60	1.0E+06
Co60m	1.1378E-24	Co58	1.6253E-20	Co58	#N/A
Fe60	1.1378E-24	Sc44	9.1534E-21	Sc44	1.0E+03

As before, an EXCEL results-code #N/A in the final column indicates that the nuclide is not present for both values of ϕ so that activities cannot be compared. In the final column, entries highlighted in a red cell, indicate a non-linear dependence of activity on ϕ .

From Table 21 it is evident that straight-forward neutron absorption reactions with isotopes that are abundantly present in the pre-irradiated sample, lead to linear product yields. Cr-50 is present in the sample and it activates to Cr-51 by a simple neutron absorption reaction. As a

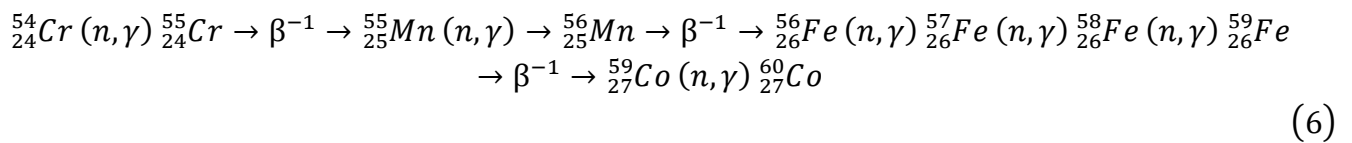
result, the concentration of Cr-51 depends linearly on the neutron fluence-rate ϕ . On the other hand, the activity of Mn-54 is upped by a factor 100 when ϕ increases by a factor 10. The underlying reason is as follows: FISPACT gives the pathway for the formation of Mn-54 as follows:

Target nuclide Mn 54	99.903% of inventory given by 1 path							
path 1	99.903% Cr 54	---(R)---	Cr 55	---(d)---	Mn 55	---(R)---	Mn 54	---(L)---
	100.00%(n,g)		100.00%(b-)		100.00%(n,2n)			

Because there is no initial Mn in the irradiated Cr sample, both (1) the number of target-nuclides Mn-55 as well as (2) the rate of formation of the activation product Mn-54 via the nuclear reaction ${}^{55}_{25}\text{Mn}(n,2n){}^{54}_{25}\text{Mn}$, depends on ϕ , so that the activity Mn-54 will be a function of $\phi \times \phi = \phi^2$. If ϕ therefore changes by a factor 10, the activity of Mn-54 is increased by a factor $10^2 = 100$.

Rule: The rule that emerges is that one simply counts the number of (n, z) -reactions²⁰ in the pathway. If there are n such reactions in the path, then the formation of the product nuclide will be a function of ϕ^n .

For the “breeding” of the problematic long-lived isotope Co-60 in a sample of pure, Cr a massively high dependence by a factor ϕ^6 is observed. This is because of the long chain of neutron-absorption transmutation-reactions leading from Cr-54 to Co-60, which is shown in Eq. (6).



Because the concentrations of 5 target isotopes, namely Mn-55, Fe-56, Fe-57, Fe-58, Co-59 as well as the rate of the last reaction step, ${}^{59}_{27}\text{Co}(n,\gamma){}^{60}_{27}\text{Co}$, all depend nearly linearly on ϕ , it follows that the activity of Co-60 will depend on ϕ^6 , i.e. if ϕ is increased by a factor 10, then the irradiated sample can contain up to 10^6 times more Co-60. The “rule” works well — in Eq. (6) there are 6 reactions of type (n, z) in the “isotopic ancestry” of Co-60, so that the formation-rate of the latter problematic radionuclide will depend on ϕ^6 . This “breeding” of

²⁰ In this standard nuclear-reaction nomenclature, z signifies an arbitrary exit-entity.

Co-60 in Cr is therefore of importance at high neutron fluence-rates, but should be negligible at lower neutron fluence-rates — the dependence of the formation rate of Co-60 is a very steep function of ϕ .

5.1.7 Non-linearity in the Neutron Activation of Vanadium (V; Z = 23)

Similar non-linearities will be observed for the breeding of Co-60 in vanadium at high neutron fluence-rates. According to FISPACT-II calculations, the $\{N, A\}$ -matrix for the irradiation of a mass of 100 g V under scenario **DECO_60yr_6yr_1E14** is

$$\begin{bmatrix} {}^{60}\text{Co} & 1.0\text{E}6 \text{ Bq} \\ {}^3\text{H} & 5.5\text{E}5 \text{ Bq} \\ {}^{55}\text{Fe} & 1.3\text{E}4 \text{ Bq} \\ {}^{54}\text{Mn} & 3.6\text{E}3 \text{ Bq} \\ {}^{49}\text{V} & 8.2\text{E}2 \text{ Bq} \\ {}^{63}\text{Ni} & 1.8\text{E}1 \text{ Bq} \end{bmatrix}$$

i.e. Co-60 remains the dominant long-lived radionuclide that will be formed in V at high values of ϕ and extended irradiation times.

5.1.8 Non-linearity in the Neutron Activation of Titanium (Ti; Z = 22)

High non-linearities will also be observed for the breeding of Co-60 in titanium at high neutron fluence-rates and long irradiation times. According to FISPACT-II calculations, the $\{N, A\}$ -matrix for the irradiation of a mass of 100 g Ti under scenario **DECO_60yr_6yr_1E14** is

$$\begin{bmatrix} {}^3\text{H} & 3.5\text{E}5 \text{ Bq} \\ {}^{45}\text{Ca} & 3.6\text{E}4 \text{ Bq} \\ {}^{46}\text{Sc} & 1.7\text{E}2 \text{ Bq} \\ {}^{60}\text{Co} & 1.4\text{E}2 \text{ Bq} \\ {}^{55}\text{Fe} & 3.1 \text{ Bq} \end{bmatrix}$$

i.e. Co-60 remains a relatively noteworthy long-lived radionuclide that will be formed in Ti at very high values of ϕ sustained over extended irradiation times.

5.1.9 Conclusions: Non-linearity of Neutron Activation

Neutron activation is not a linear process; at high neutron fluence-rates, non-linear behaviour can be extreme, but at low neutron fluence-rates, a more linear or fully linear behaviour of

activation becomes the norm. It is, therefore, wrong to perform neutron activation calculations at a reference neutron fluence-rate and then simply scale activities and dose-rates linearly to other values of ϕ . Every neutron activation problem, characterised by the composition and mass of the irradiated material, together with the problem's parameters ϕ , ϕ and T_{irrad} , must be treated as unique and should, therefore, be solved on a case-by-case basis, without attempting to take “clever shortcuts” based on the intuitive yet incorrect assumption of a linear dependence of the activated $\{N, A\}$ - matrix on the variable ϕ .

5.2 Research Question RQ_2 :

Ranking of the Elements in a Decommissioning Irradiation Scenario

Research Question RQ_2 is: For the general *Decommissioning Scenario* DECO_60yr_6yr_φ defined in § 2.9.2 on page 21, calculate the ranking order of all irradiated elements in terms of the photon dose-rate at a distance of 1 m from a reference mass of 1 g of each irradiated chemical element, at $T_{\text{cool}} = 6$ yr, for all integral fluence-rates ϕ that are investigated. This gives a direct indication of the intensity of the dose-rate field that will prevail around activated materials, at decommissioning time.

5.2.1 Ranking of the Elements According to the Dose-Rates from the Irradiation-and-Cooldown Scenario DECO_60yr_6yr_1E14

For the irradiation of 100 g of each of the natural terrestrial elements, in an LWR neutron spectrum at $\phi = 1.0E14 \text{ cm}^{-2} \text{ s}^{-1}$, for 60 years, followed by a cooling time of 6 years, the ranking order of the elements in terms of the photon dose-rate at 1 m in a vacuum from a point-source 1 g mass of irradiated material, is summarised in Table 22.

Table 22: Radiological ranking of the elements for an irradiation scenario

DECO_60yr_6yr_1E14

Z	Element	DR at 1 m from 1 g at $T_{\text{cool}} = 6$ yr (Sv/h)
27	Co	7.26E-02
26	Fe	2.89E-03
55	Cs	2.06E-03
54	Xe	1.50E-03

Z	Element	DR at 1 m from 1 g at $T_{cool} = 6$ yr (Sv/h)
28	Ni	9.59E-04
25	Mn	7.60E-04
62	Sm	4.00E-04
60	Nd	2.11E-04
41	Nb	1.35E-04
76	Os	1.21E-04
77	Ir	7.67E-05
75	Re	7.26E-05
50	Sn	6.29E-05
56	Ba	5.59E-05
51	Sb	4.54E-05
47	Ag	2.76E-05
74	W	1.67E-05
30	Zn	1.62E-05
53	I	1.49E-05
80	Hg	1.45E-05
52	Te	1.36E-05
81	Tl	1.30E-05
46	Pd	1.04E-05
29	Cu	7.64E-06
59	Pr	7.29E-06
78	Pt	3.79E-06
36	Kr	3.66E-06
35	Br	2.34E-06
42	Mo	2.07E-06
65	Tb	1.23E-06
68	Er	1.06E-06
58	Ce	7.43E-07
48	Cd	6.29E-07
66	Dy	5.39E-07
64	Gd	5.30E-07
24	Cr	4.90E-07
79	Au	4.48E-07
73	Ta	3.96E-07
67	Ho	3.59E-07
63	Eu	1.86E-07
57	La	9.00E-08
72	Hf	6.43E-08
70	Yb	5.34E-08
71	Lu	4.76E-08
44	Ru	3.65E-08
83	Bi	3.51E-08
20	Ca	3.00E-08
69	Tm	1.75E-08

Z	Element	DR at 1 m from 1 g at $T_{cool} = 6$ yr (Sv/h)
45	Rh	1.26E-08
34	Se	9.68E-09
18	Ar	3.74E-09
40	Zr	3.06E-09
23	V	3.04E-09
21	Sc	2.94E-09
37	Rb	2.77E-09
17	Cl	2.24E-09
11	Na	3.44E-10
49	In	3.01E-10
19	K	2.56E-10
82	Pb	7.16E-11
38	Sr	1.71E-11
16	S	1.25E-11
33	As	6.34E-12
39	Y	3.90E-12
22	Ti	8.71E-13
10	Ne	2.07E-13
13	Al	1.98E-13
32	Ge	9.40E-14
12	Mg	3.73E-14
31	Ga	9.10E-15
15	P	8.16E-16
14	Si	1.48E-18
9	F	4.31E-20
8	O	4.53E-28
7	N	1.22E-38
5	B	2.24E-42
4	Be	2.56E-49
6	C	5.10E-51
1	H	1.00E-99
2	He	1.00E-99
3	Li	1.00E-99

One apparent anomaly in Table 22 is that Eu is ranked very low, whereas the extensive literature survey consistently indicates that Eu is a highly problematic activator. The answer is that at the high fluence-rate $\phi = 1.0E14$ cm⁻² s⁻¹ and long irradiation time $T_{irr} = 60$ yr, the initially present Eu is quickly burned away, so that only a fraction 7.1050E-8 of the initial mass of this high-activation element remains, according to FISPACT-II calculation. Close to 98 % of the Co has also burned away, but this happens more gradually and linearly, and Co is, therefore, the top-ranked activator in the case under assessment.

Examples of the practical use of the information in Table 22:

- The engineering metals Co, Fe, Mn and Ni are high-activators at $\phi = 1.0E14 \text{ cm}^{-2} \text{ s}^{-1}$ and $T_{irr} = 60 \text{ yr}$. In contrast, Be, Si, C, O, Mg, Al and Ti are low-activators. Wherever possible, structures should be manufactured from these low-activator chemical elements, while the use of high-activator chemical elements should be minimised.
- For the modelled exposure-scenario (i.e. fluence-rate and timeline), raw materials should be tested to contain as little as possible of the trace elements Co, Cs, Sm, Nd and Nb.

5.2.2 Ranking of the Elements According to the Dose-Rates from the Irradiation-and-Cooldown Scenario **DECO_60yr_6yr_1E13**

For the irradiation of 100 g of each of the natural terrestrial elements, in an LWR neutron spectrum at $\phi = 10^{13} \text{ cm}^{-2} \text{ s}^{-1}$, for $T_{irrad} = 60 \text{ yr}$, followed by a cooling time $T_{cool} = 6 \text{ yr}$, the ranking order of the elements in terms of the photon dose-rate at 1 m in a vacuum from a point source 1 g mass of irradiated material, is summarised in Table 23.

Table 23: Radiological ranking of the elements for an irradiation scenario

DECO_60yr_6yr_1E13

Z	Element	DR at 1 m from 1 g at T_cool = 6yr (Sv/h)
27	Co	2.30E-01
55	Cs	1.76E-02
62	Sm	9.29E-03
63	Eu	3.99E-03
77	Ir	2.00E-04
47	Ag	1.41E-04
54	Xe	8.29E-05
60	Nd	6.18E-05
41	Nb	2.66E-05
26	Fe	1.78E-05
28	Ni	1.59E-05
66	Dy	1.43E-05
76	Os	1.38E-05
67	Ho	1.01E-05
56	Ba	9.77E-06
50	Sn	7.25E-06
81	Tl	5.34E-06
78	Pt	5.12E-06
30	Zn	3.14E-06

Z	Element	DR at 1 m from 1 g at T_cool = 6yr (Sv/h)
64	Gd	3.09E-06
46	Pd	2.76E-06
51	Sb	9.36E-07
29	Cu	6.71E-07
65	Tb	5.75E-07
68	Er	4.33E-07
36	Kr	3.87E-07
42	Mo	3.42E-07
80	Hg	3.12E-07
48	Cd	1.59E-07
71	Lu	1.05E-07
35	Br	9.87E-08
69	Tm	9.80E-08
45	Rh	7.28E-08
73	Ta	5.56E-08
25	Mn	2.43E-08
70	Yb	2.22E-08
75	Re	1.86E-08
52	Te	1.82E-08
72	Hf	8.32E-09
20	Ca	7.76E-09
17	Cl	7.68E-09
21	Sc	5.70E-09
83	Bi	5.06E-09
58	Ce	3.34E-09
44	Ru	3.27E-09
34	Se	2.94E-09
74	W	7.81E-10
40	Zr	3.60E-10
11	Na	3.54E-10
37	Rb	3.03E-10
19	K	9.51E-11
18	Ar	3.96E-11
53	I	2.09E-11
82	Pb	5.42E-12
57	La	3.10E-12
79	Au	2.93E-12
24	Cr	2.15E-12
59	Pr	2.03E-12
38	Sr	1.26E-12
16	S	8.43E-13
49	In	7.98E-13
39	Y	4.53E-13
13	Al	2.03E-13
33	As	1.89E-13
23	V	1.27E-13
22	Ti	4.58E-14

Z	Element	DR at 1 m from 1 g at T_cool = 6yr (Sv/h)
12	Mg	3.60E-14
10	Ne	2.06E-14
32	Ge	2.64E-16
31	Ga	1.80E-16
14	Si	1.29E-18
15	P	2.92E-20
9	F	4.25E-24
8	O	4.44E-33
7	N	4.06E-50
1	H	1.00E-99
2	He	1.00E-99
3	Li	1.00E-99
4	Be	1.00E-99
5	B	1.00E-99
6	C	1.00E-99

For the modelled exposure scenario (i.e. fluence-rate and timeline), the top-most activators are Co, Cs, Sm, Eu, Ir, Ag, Nd, Nb, Fe, Ni, Dy, Os, and Ho.

The apparent anomalously low ranking of Eu is still observed in Table 23. At the modelled high value of ϕ , and protracted irradiation time of 60 years, about 97 % of the Eu has been burned away, more than 30 % of Cs while 35 % of Co is burned up.

Examples of the practical use of the information in Table 23:

- The commonly used engineering metals Co, Fe and Ni are high-activators at $\phi = 10^{13} \text{ cm}^{-2} \text{ s}^{-1}$ and $T_{irr} = 60 \text{ yr}$. In contrast, Be, Si, Mg, Ti, V, Al and Cr are low-activators in the case under assessment, as are the elements C, B and O. Wherever possible, structures should be manufactured from these low-activators and engineers must attempt to minimise the use of high-activator chemical elements.
- Note that the use of the alloying metal Cr is not advised at $\phi \geq 10^{14} \text{ cm}^{-2} \text{ s}^{-1}$ but is advised at $\phi \leq 10^{13} \text{ cm}^{-2} \text{ s}^{-1}$; at high values of ϕ , the irradiation of Cr can “breed” Co-60, as explained § 5.1.6 on page 93 above.
- Note that the use of the alloying metal V is not advised at $\phi \geq 10^{14} \text{ cm}^{-2} \text{ s}^{-1}$ but is advised at $\phi \leq 10^{13} \text{ cm}^{-2} \text{ s}^{-1}$; at high values of ϕ , the irradiation of V by LWR neutrons can “breed” Co-60, as explained above.
- For the modelled exposure scenario (i.e. fluence-rate and time-line), raw materials should be tested to contain as little as possible of the high-activation trace elements such as Co, Cs, Sm, Eu, Ag, Nd, Nb, Dy, Ho, Ba and Sn.

5.2.3 Ranking of the Elements According to the Dose-Rates from the Irradiation-and-Cooldown Scenario **DECO_60yr_6yr_1E12**

For the irradiation of 100 g of each of the natural terrestrial elements, in an LWR neutron spectrum at $\phi = 10^{12} \text{ cm}^{-2} \text{ s}^{-1}$, for an irradiation time of 60 years, followed by a cooling time of 6 years, the ranking order of the elements in terms of the photon dose-rate at 1 m in a vacuum from a point source 1 g mass of irradiated material, is summarised in Table 24.

Table 24: Radiological ranking of the elements for irradiation scenario

DECO_60yr_6yr_1E12

Z	Element	DR at 1 m from 1 g at T_cool = 6 yr (Sv/h)
63	Eu	3.56E-02
27	Co	3.33E-02
62	Sm	3.15E-03
55	Cs	2.79E-03
47	Ag	4.24E-05
64	Gd	3.68E-05
67	Ho	2.28E-05
77	Ir	1.55E-05
66	Dy	6.88E-06
54	Xe	3.95E-06
41	Nb	2.88E-06
56	Ba	9.29E-07
50	Sn	7.38E-07
78	Pt	7.24E-07
81	Tl	6.16E-07
60	Nd	6.06E-07
26	Fe	6.03E-07
30	Zn	3.43E-07
28	Ni	1.83E-07
76	Os	7.03E-08
29	Cu	6.14E-08
46	Pd	5.24E-08
68	Er	5.23E-08
65	Tb	4.93E-08
45	Rh	3.90E-08
42	Mo	3.61E-08
36	Kr	3.59E-08
71	Lu	1.61E-08
73	Ta	1.60E-08
48	Cd	1.56E-08
51	Sb	1.01E-08
69	Tm	5.69E-09
80	Hg	3.42E-09

Z	Element	DR at 1 m from 1 g at T_cool = 6 yr (Sv/h)
35	Br	1.16E-09
17	Cl	1.12E-09
20	Ca	8.74E-10
21	Sc	7.70E-10
34	Se	5.83E-10
72	Hf	5.61E-10
83	Bi	5.27E-10
75	Re	4.18E-10
58	Ce	4.18E-10
70	Yb	3.71E-10
25	Mn	3.40E-10
11	Na	2.70E-10
44	Ru	2.27E-10
52	Te	4.04E-11
40	Zr	3.67E-11
37	Rb	3.06E-11
74	W	1.38E-11
19	K	1.20E-11
18	Ar	4.00E-13
82	Pb	3.88E-13
57	La	1.75E-13
13	Al	1.38E-13
24	Cr	1.24E-13
38	Sr	1.21E-13
49	In	8.40E-14
39	Y	4.60E-14
12	Mg	2.73E-14
23	V	2.07E-14
79	Au	1.91E-14
53	I	1.35E-14
16	S	1.07E-14
22	Ti	4.55E-15
33	As	2.75E-15
10	Ne	1.55E-15
59	Pr	1.89E-16
31	Ga	1.97E-18
14	Si	8.67E-19
32	Ge	3.67E-19
15	P	1.01E-22
9	F	3.06E-28
8	O	1.92E-33
7	N	3.56E-51
1	H	1.00E-99
2	He	1.00E-99
3	Li	1.00E-99
4	Be	1.00E-99
5	B	1.00E-99

Z	Element	DR at 1 m from 1 g at T_cool = 6 yr (Sv/h)
6	C	1.00E-99

For the modelled exposure scenario (i.e. fluence-rate and timeline), the top-most activators are (in order) Eu, Co, Sm, Cs, Ag, Gd and Ho. Then comes (in order) Ir, Dy, Nb, Ba, Sn and Pt.

Examples of the practical use of the information in Table 24:

- For the modelled exposure scenario (i.e. fluence-rate and timeline), the top-tier activators are (in order) Eu, Co, Sm, Cs, Ag, Gd and Ho.
- The second-tier activators are (in order) Ir, Dy, Nb, Ba, Sn and Pt.
- At $\phi = 10^{12} \text{ cm}^{-2} \text{ s}^{-1}$ and $T_{irr} = 60 \text{ yr}$, the commonly used engineering metals Fe, Ni and Mn are now mid-to-low activators because they cannot “breed” much Co-60 at these lower fluence-rates.
- The metal Mo remains a useful, well-below-average activator.
- The “dependable lowest-activator” elements are O, Si, Ti, V, Mg, Cr, Al and Zr. Wherever possible, structures should be manufactured from these low-activators and engineers must attempt to avoid or minimise the inclusion of the high-activators.
- Raw materials should be tested to contain as little as possible of the high-activation trace elements Eu, Co, Sm, Cs, Ag, Gd, Ho, Ir, Dy, Nb, Ba, Sn and Pt.

5.2.4 Ranking of the Elements According to the Dose-Rates from the Irradiation-and-Cooldown Scenario DECO_60yr_6yr_1E11

For the irradiation of 100 g of each of the natural terrestrial elements, in an LWR neutron spectrum at $\phi = 10^{11} \text{ cm}^{-2} \text{ s}^{-1}$, for an irradiation time of 60 years, followed by a cooling time of 6 years, the ranking order of the elements in terms of the photon dose-rate at 1 m in vacuum from a point source 1 g mass of irradiated material, is summarised in Table 25.

Table 25: Radiological ranking of the elements for the irradiation scenario

DECO_60yr_6yr_1E11

Z	Element	DR at 1m from 1 g at T_cool = 6 yr (Sv/h)
63	Eu	2.93E-02
27	Co	3.45E-03
55	Cs	2.92E-04

Z	Element	DR at 1m from 1 g at T_cool = 6 yr (Sv/h)
62	Sm	7.09E-05
67	Ho	1.02E-05
47	Ag	4.79E-06
64	Gd	9.92E-07
66	Dy	4.70E-07
54	Xe	3.51E-07
41	Nb	2.90E-07
77	Ir	2.30E-07
56	Ba	9.21E-08
78	Pt	7.51E-08
50	Sn	7.40E-08
60	Nd	7.06E-08
81	Tl	6.25E-08
26	Fe	4.78E-08
30	Zn	3.46E-08
28	Ni	1.42E-08
29	Cu	6.07E-09
65	Tb	5.29E-09
68	Er	4.93E-09
45	Rh	4.62E-09
42	Mo	3.63E-09
36	Kr	3.53E-09
71	Lu	2.36E-09
73	Ta	1.86E-09
48	Cd	1.53E-09
46	Pd	6.05E-10
69	Tm	2.37E-10
17	Cl	1.16E-10
76	Os	1.09E-10
51	Sb	1.06E-10
20	Ca	8.84E-11
11	Na	7.94E-11
21	Sc	7.93E-11
34	Se	6.25E-11
75	Re	5.58E-11
83	Bi	5.29E-11
72	Hf	5.27E-11
58	Ce	4.27E-11
80	Hg	3.46E-11
25	Mn	3.44E-11
44	Ru	2.05E-11
35	Br	1.18E-11
70	Yb	3.83E-12
52	Te	3.80E-12

Z	Element	DR at 1m from 1 g at T_cool = 6 yr (Sv/h)
40	Zr	3.68E-12
37	Rb	3.07E-12
19	K	1.74E-12
74	W	1.24E-12
57	La	1.31E-13
82	Pb	3.71E-14
13	Al	2.17E-14
24	Cr	1.22E-14
38	Sr	1.20E-14
49	In	8.68E-15
12	Mg	8.03E-15
39	Y	4.60E-15
18	Ar	4.21E-15
79	Au	2.18E-15
23	V	2.17E-15
22	Ti	4.54E-16
53	I	1.40E-16
16	S	1.10E-16
10	Ne	4.40E-17
33	As	2.86E-17
59	Pr	1.78E-17
14	Si	1.37E-19
31	Ga	1.99E-20
32	Ge	7.00E-22
15	P	1.37E-24
9	F	7.98E-33
8	O	8.00E-44
7	N	6.97E-54
1	H	1.00E-99
2	He	1.00E-99
3	Li	1.00E-99
4	Be	1.00E-99
5	B	1.00E-99
6	C	1.00E-99

Examples of the practical use of the information in Table 25:

- For the modelled exposure scenario (i.e. fluence-rate and timeline), the top-most activators are (in order) Eu, Co, Cs, Sm, Ho, and Ag.
- The second-tier activators are (in order) Gd, Dy, Nb, Ir, Ba, Pt and Sn.
- At $\phi \approx 10^{11} \text{ cm}^{-2} \text{ s}^{-1}$ and $T_{irr} = 60 \text{ yr}$, the commonly used engineering metals Fe and Ni are now mid-to-low activators, because they cannot “breed” Co-60 at such low fluence-rates.

- The metal Mo remains a useful, well-below-average activator.
- The “dependable lowest-activator” elements are, C, Be, O, Si, Ti, V, Mg, Cr, Al, Zr and Mn. Note that Mn, which is a high-activator at high values of ϕ , has now become a low-activator at $\phi \leq 10^{11} \text{ cm}^{-2} \text{ s}^{-1}$. Wherever possible, structures should be manufactured from alloys or blends of these low-activator elements and engineers must attempt to avoid high-activator elements.
- Raw-materials should be tested to contain as little as possible of the high-activation trace elements (in order of radiological concern): Eu, Co, Cs, Sm, Ho, Ag, Gd, Dy, Nb, Ba, Pt and Sn.

5.2.5 Ranking of the Elements According to the Dose-Rates from the Irradiation-and-Cooldown Scenario DECO_60yr_6yr_1E10

The order of severity in which the elements activate, as well as “Lessons learned” are essentially identical to what was observed at $\phi = 10^{11} \text{ cm}^{-2} \text{ s}^{-1}$ (Table 25 on page 105).

(Note: the process of extracting dose-rates or activities from hundreds of FISPACT-II outputs is (still) a non-automated, manual and therefore extremely time-consuming process.)

5.2.6 Ranking of the Elements According to the Dose-Rates from the Irradiation-and-Cooldown Scenario DECO_60yr_6yr_1E9

The order of severity in which the elements activate, as well as “Lessons learned” are essentially identical to what was observed at $\phi = 10^{11} \text{ cm}^{-2} \text{ s}^{-1}$ (Table 25 on page 105).

5.2.7 Ranking of the Elements According to the Dose-Rates from the Irradiation-and-Cooldown Scenario DECO_60yr_6yr_1E8

The order of severity in which the elements activate, as well as “Lessons learned” are essentially identical to what was observed at $\phi = 10^{11} \text{ cm}^{-2} \text{ s}^{-1}$ (Table 25 on page 105).

5.2.8 Ranking of the Elements According to the Dose-Rates from the Irradiation-and-Cooldown Scenario **DECO_60yr_6yr_1E7**

The order of severity in which the elements activate, as well as “Lessons learned” are essentially identical to what was observed at $\phi = 10^{11} \text{ cm}^{-2} \text{ s}^{-1}$ (Table 25 on page 105).

5.3 Research Question RQ_3 :

Ranking of the Elements in a Fuel-Assembly (FA) End-Adapter Exposure Scenario

DECO_1yr_6yr_1E14

Research Question RQ_3 is as follows: For the fuel-assembly end-adapter (“nozzle”) exposure scenario **DECO_1yr_6yr_1E14** defined in § 2.9.3 on page 22, calculate the radiological ranking order of all irradiated chemical elements in terms of the dose-rate at a distance of 1 m from a reference mass of 1 g, for each irradiated chemical element, for $T_{irrad} = 1 \text{ yr}$ and at $T_{cool} = 6 \text{ yr}$, for the integral fluence-rate $\phi = 10^{14} \text{ cm}^{-2} \text{ s}^{-1}$ — realistic irradiation conditions for FA end-adaptors. Results are summarised in Table 26.

Table 26: Radiological ranking of the elements in a fuel-assembly end-adaptor irradiation scenario **DECO_1yr_6yr_1E14**

Z	Element	DR at 1m from 1 g at T_cool = 6 yr (Sv/h)
27	Co	4.10E-01
63	Eu	9.84E-02
55	Cs	7.04E-02
62	Sm	1.24E-02
47	Ag	4.49E-04
54	Xe	2.19E-05
67	Ho	2.17E-05
51	Sb	1.72E-05
77	Ir	1.67E-05
50	Sn	1.59E-05
30	Zn	1.55E-05
26	Fe	1.15E-05
81	Tl	1.01E-05
66	Dy	8.16E-06
41	Nb	6.68E-06

Z	Element	DR at 1m from 1 g at T_cool = 6 yr (Sv/h)
69	Tm	6.34E-06
56	Ba	5.90E-06
64	Gd	5.42E-06
28	Ni	3.53E-06
60	Nd	3.22E-06
46	Pd	3.06E-06
78	Pt	1.71E-06
68	Er	1.21E-06
45	Rh	8.18E-07
29	Cu	7.95E-07
48	Cd	3.78E-07
71	Lu	3.40E-07
76	Os	2.05E-07
36	Kr	1.95E-07
73	Ta	1.25E-07
65	Tb	8.78E-08
21	Sc	7.24E-08
42	Mo	5.61E-08
34	Se	4.22E-08
80	Hg	3.77E-08
25	Mn	1.83E-08
70	Yb	9.20E-09
35	Br	3.19E-09
72	Hf	2.67E-09
17	Cl	1.82E-09
20	Ca	1.44E-09
83	Bi	1.41E-09
58	Ce	1.16E-09
52	Te	9.24E-10
74	W	7.86E-10
44	Ru	6.79E-10
75	Re	6.13E-10
11	Na	3.67E-10
37	Rb	1.95E-10
18	Ar	1.15E-10
40	Zr	2.07E-11
19	K	1.97E-11
57	La	8.60E-12
24	Cr	6.64E-12
39	Y	4.11E-12
53	I	4.03E-12
49	In	2.31E-12
79	Au	1.36E-12
23	V	1.11E-12
82	Pb	9.63E-13
38	Sr	8.07E-13
22	Ti	4.30E-13

Z	Element	DR at 1m from 1 g at T_cool = 6 yr (Sv/h)
33	As	2.14E-13
13	Al	1.72E-13
12	Mg	3.71E-14
16	S	1.59E-14
59	Pr	5.22E-15
10	Ne	3.52E-15
31	Ga	9.91E-17
32	Ge	3.52E-17
14	Si	1.09E-18
15	P	2.32E-22
9	F	3.25E-27
8	O	3.59E-28
7	N	5.62E-47
1	H	1.00E-99
2	He	1.00E-99
3	Li	1.00E-99
4	Be	1.00E-99
5	B	1.00E-99
6	C	1.00E-99

For the modelled scenario, circa 45 % of irradiated Eu, 6 % of Cs and 4 % of Co are transmuted, i.e. burned up by neutron-induced nuclear reactions.

Examples of the practical use of the information in Table 26:

- For the modelled exposure scenario **DECO_1yr_6yr_1E14**, the top-tier activators are (in order) Co, Eu, Cs, Sm and Ag.
- The second-tier activators are (in order) Ho, Sb, Ir, Sn, Zn, Fe, Tl, Dy, Nb, Tm, Ba, Gd, Ni, Nd, Pd and Pt.
- The commonly used engineering metal Fe ranks as a high-activator because it “breeds” Co-60 at the high fluence-rate. In Fe, the activity per unit mass of Co-60 will be 3.95 MBq/g — more than a factor million times higher than unconditional clearance levels.
- The metals Mo and Mn are useful, well-below-average activators.
- The “dependable lowest-activator” elements are C, Be, O, Si, Mg, Al, Ti, V, Cr and Zr. Wherever possible, structures should be manufactured from alloys or blends of these low-activators and engineers must attempt to avoid the high-activators.

- Raw materials should be tested to contain as little as possible of the high-activation trace elements (in order of radiological concern): Co, Eu, Cs, Sm, Ag, Ho, Sb, Ir, Sn, Zn, Fe, Tl, Dy, Nb, Tm, Ba, Gd, Ni, Nd, Pd and Pt.

The end-adapters of the fuel-assemblies of the SAFARI-1 reactor are manufactured from Al-alloy 6082, which is the strongest generally available 6000-series Al-alloy at heat-treatment temper T6. This alloy’s elemental composition is given in Table 27; the mass-% values for the trace-elements S, Ca, P, Na, K and Co are “educated guesses” and will differ between manufacturers, geographical areas and also from batch to batch — see e.g. the PhD thesis *Trace Elements in Al-Si Foundry Alloys* (Ludwig, 2013).

Table 27: FISPACT input specification for Al-6082

AL	95.20
SI	1.30
MG	1.20
MN	1.00
FE	0.50
CR	0.25
ZN	0.20
CU	0.10
TI	0.10
S	0.030
CA	0.030
P	0.030
NA	0.025
K	0.025
CO	0.010

The 7000-series Al-alloys typically contain at least 5% Zn, which is a high-activator element. It follows that 6000-series Al-alloys will be lower activators than (the mechanically stronger) 7000-series Al-alloys and are the best-suited group of Al-alloys for use in nuclear applications involving exposure to high neutron fluence-rates — see e.g. (Luzginova et al., 2014).

5.4 Research Question RQ_4 :

Ranking of the Elements in a Neutron Radiography (NRAD) Exposure Scenario

Research Question RQ_4 is: For the two Neutron Radiography (NRAD) irradiation-and-cooldown scenarios defined in § 2.9.4 on page 22, calculate the ranking order of all irradiated elements in terms of the photon dose-rate at a distance of 1 m from a reference mass of 1 g of each irradiated chemical element, at $T_{cool} = 30$ days, for an integral fluence-rate of $\phi = 10^9 \text{ cm}^{-2} \text{ s}^{-1}$. This involves two discrete irradiation times: 1 hour and 24 hours (i.e. 1 day).

5.4.1 Ranking of the elements in a Neutron Radiography (NRAD) Exposure Scenario

NRAD_1h_30d_1E9

The ranking order of the elements in terms of the photon dose-rate at 1 m in vacuum from a point source with a mass of 1 g, is summarised in Table 28.

Table 28: Radiological ranking of the elements in the irradiation scenario

NRAD_1h_30d_1E9

Z	Element	DR at 1m from 1 g at $T_{cool} = 30$ days (Sv/h)
77	Ir	2.41E-08
21	Sc	1.60E-08
63	Eu	7.21E-09
65	Tb	3.18E-09
73	Ta	2.24E-09
27	Co	1.13E-09
55	Cs	8.20E-10
51	Sb	5.63E-10
47	Ag	3.54E-10
72	Hf	3.41E-10
70	Yb	2.39E-10
71	Lu	2.10E-10
76	Os	7.98E-11
79	Au	6.28E-11
44	Ru	5.43E-11
69	Tm	5.00E-11
58	Ce	4.40E-11
34	Se	4.10E-11
80	Hg	3.69E-11
64	Gd	1.68E-11

Z	Element	DR at 1m from 1 g at T_cool = 30 days (Sv/h)
24	Cr	1.40E-11
37	Rb	1.16E-11
49	In	1.14E-11
32	Ge	1.04E-11
75	Re	9.95E-12
60	Nd	7.26E-12
54	Xe	5.54E-12
52	Te	3.87E-12
28	Ni	2.85E-12
30	Zn	2.85E-12
62	Sm	2.37E-12
40	Zr	1.98E-12
26	Fe	1.62E-12
56	Ba	1.34E-12
38	Sr	8.86E-13
50	Sn	6.68E-13
74	W	6.32E-13
57	La	6.31E-13
46	Pd	6.02E-13
19	K	5.74E-13
66	Dy	3.81E-13
67	Ho	2.58E-13
78	Pt	1.71E-13
48	Cd	1.13E-13
42	Mo	9.31E-14
22	Ti	9.16E-14
81	Tl	5.48E-14
41	Nb	4.10E-14
35	Br	3.41E-14
68	Er	3.21E-14
53	I	2.62E-14
18	Ar	2.48E-14
33	As	2.29E-14
45	Rh	2.01E-14
39	Y	1.59E-14
20	Ca	1.03E-14
25	Mn	3.88E-15
29	Cu	1.98E-15
31	Ga	1.98E-15
36	Kr	4.33E-16
11	Na	1.49E-16
59	Pr	3.56E-17
83	Bi	1.50E-17
23	V	4.08E-18

Z	Element	DR at 1m from 1 g at T_cool = 30 days (Sv/h)
17	Cl	2.22E-18
82	Pb	1.29E-18
12	Mg	1.51E-20
13	Al	4.76E-22
7	N	2.47E-25
3	Li	1.91E-26
14	Si	5.95E-27
10	Ne	7.99E-31
4	Be	5.17E-31
16	S	4.44E-36
15	P	1.29E-36
1	H	1.00E-99
2	He	1.00E-99
5	B	1.00E-99
6	C	1.00E-99
8	O	1.00E-99
9	F	1.00E-99

Examples of the practical use of the information presented in Table 28:

- For the modelled exposure scenario (i.e. fluence-rate and timeline), the top-tier activators are (in order) Ir, Sc, Eu, Tb, Ta, Co, Cs, Sb, Ag, Hf, Yb and Lu.
- The second-tier activators are (in order) Os, Au, Ru, Tm, Ce, Se, Hg, Gd, Cr, Rb, In, Ge, Re, Nd, Xe, Te, Ni, Zn, Sm, Zr, Fe, Ba.
- For this NRAD irradiation scenario, the commonly used engineering metals Fe ranks as a medium-high activator, because its top-3 activation products — Fe-59, Mn-54 and Cr-51 — have half-lives that range between 27 days and 312 days, i.e. dose-rates at $T_{cool} = 30$ days will still be considerable.
- The “dependable lowest-activator” elements are O, C, B, H, P, S, Be, Si, N, Al, Mg, Pb, V, Cu, Mn and Ca. Wherever practical, structures should be manufactured from alloys or blends of these low-activators and engineers must attempt to avoid the high-activators.
- Biological samples undergoing neutron tomography will typically contain mostly O, C, N, H, P, S, Si, Mg and Ca and will be benign activators.
- The neutron-irradiation of steel-alloys, which are rich in Fe, Mn, Cr, Ni and Mo, may present significant activities and dose-rates from neutron-activation products.

- Al-alloys will activate far less than Fe-alloys (steels), provided that the content of Co, Cr, Ni, Zn and Fe be as low as possible. Al-alloys of the 7000-series contain up to 7% Zn and will activate worse than the 6000-series Al-alloys which are largely Al-Mg-Si alloys, i.e. more benign activators.

5.4.2 Radiological Ranking of the Elements in a Neutron Radiography (NRAD) Exposure

Scenario **NRAD_1d_30d_1E9**

The ranking order of the elements in terms of the photon dose-rate at 1 m in vacuum from a point source 1 g mass of each irradiated material, is summarised in Table 29.

Table 29: Radiological ranking of the elements in an NRAD irradiation scenario

NRAD_1d_30d_1E9

Z	Element	DR at 1m from 1 g at T_cool = 30 days (Sv/h)
77	Ir	5.77E-07
21	Sc	3.82E-07
63	Eu	1.73E-07
65	Tb	7.60E-08
73	Ta	5.35E-08
27	Co	2.72E-08
55	Cs	1.97E-08
51	Sb	1.34E-08
47	Ag	8.47E-09
72	Hf	8.13E-09
70	Yb	5.64E-09
71	Lu	4.74E-09
76	Os	1.89E-09
79	Au	1.34E-09
44	Ru	1.29E-09
69	Tm	1.20E-09
58	Ce	1.05E-09
34	Se	9.82E-10
80	Hg	8.78E-10
30	Zn	4.57E-10
64	Gd	4.01E-10
24	Cr	3.32E-10
37	Rb	2.73E-10
49	In	2.72E-10
32	Ge	2.42E-10
75	Re	2.19E-10
60	Nd	1.69E-10

Z	Element	DR at 1m from 1 g at T_cool = 30 days (Sv/h)
54	Xe	1.31E-10
52	Te	8.98E-11
28	Ni	6.81E-11
62	Sm	5.34E-11
40	Zr	4.76E-11
26	Fe	3.86E-11
56	Ba	3.13E-11
38	Sr	2.12E-11
50	Sn	1.59E-11
74	W	1.51E-11
46	Pd	1.40E-11
57	La	1.01E-11
66	Dy	9.13E-12
67	Ho	6.19E-12
78	Pt	3.71E-12
48	Cd	2.59E-12
22	Ti	2.19E-12
42	Mo	2.06E-12
81	Tl	1.31E-12
41	Nb	9.60E-13
68	Er	7.58E-13
35	Br	6.59E-13
53	I	6.12E-13
18	Ar	5.89E-13
19	K	5.74E-13
33	As	5.38E-13
45	Rh	4.80E-13
39	Y	3.81E-13
20	Ca	2.40E-13
25	Mn	9.30E-14
29	Cu	4.75E-14
36	Kr	9.97E-15
11	Na	3.57E-15
59	Pr	8.47E-16
83	Bi	3.58E-16
23	V	7.20E-17
17	Cl	5.34E-17
82	Pb	2.88E-17
12	Mg	3.61E-19
31	Ga	2.30E-19
13	Al	1.06E-20
7	N	1.04E-24
14	Si	1.12E-25
10	Ne	4.74E-28

Z	Element	DR at 1m from 1 g at T_cool = 30 days (Sv/h)
8	O	2.07E-29
16	S	6.12E-32
15	P	1.28E-34
1	H	1.00E-99
2	He	1.00E-99
3	Li	1.00E-99
4	Be	1.00E-99
5	B	1.00E-99
6	C	1.00E-99
9	F	1.00E-99

Examples of the practical use of the information in Table 29:

- For the modelled exposure scenario (i.e. fluence-rate and timeline), the top-tier activators are (in order) Ir, Sc²¹, Eu, Tb, Ta, Co, Cs and Sb.
- The second-tier activators are (in order) Ag, Hf, Yb, Lu, Os, Au, Ru, Tm, Ce, Zn and Cr.
- Intermediate level activators are Ni, Sm, Zr, Fe, Ba, Sn and W.
- For this NRAD irradiation scenario, the commonly used engineering metals Cr ranks as a medium-high activator, because its main activation product, Cr-51, has a half-life of circa 27 days, i.e. the dose-rate at $T_{cool} = 30$ days will still be considerable.
- The “dependable low-activator” elements are C, B, Be, H, P, S, O, Al, Mg, Pb, V, Cu, Mn, Ca, Mo and Ti. Wherever practical, structures should be manufactured from alloys or blends of these low-activators and engineers must attempt to avoid the high-activators.

²¹ Note by co-supervisor TjvR: Here and elsewhere in this work, the element scandium (Sc) is ignored because it is very scarce and also not used in nuclear reactor materials.

5.5 Research Question RQ_5 :

Graphing Activities and Dose-Rates of selected elements used in engineering materials, for decommissioning scenarios

DECO_60yr_50yr_φ

Research Question RQ_5 entails the calculation and plotting of the (1) total induced activity in irradiated samples, and (2) the photon dose-rate at 1 m from a 1 g irradiated sample, for all integral fluence-rates under investigation, for a standardised selection of important elements present in engineering materials such as concretes, steel-alloys and Al-alloys, as a function of cooling time, from $T_{cool} = 0$ to $T_{cool} = 50$ yr. The irradiation scenario is **DECO_60yr_50yr_φ** and neutron fluence-rates span the range from $\phi = 10^{14} \text{ cm}^{-2} \text{ s}^{-1}$ down to $\phi = 10^7 \text{ cm}^{-2} \text{ s}^{-1}$.

When interpreting the dose-rate graphs presented in this section, two reference dose-rates must always be kept in mind for quantitative orientation:

- A dose-rate of approximately **1 μSv/h** represents a dose-rate below which the access control and radiological monitoring of staff can be relaxed or waived.
- The dose-rate of approximately **0.1 μSv/h** represents the average *natural background dose-rate* (NBDR) on the surface of planet earth, i.e. it is the dose-rate below which an activated component will not add any significant dose to nearby people.

Following the graphs that are presented below, the elements will be classified as *high-activators*, *medium-activators* and, finally, *low-activators*. The activities and dose-rates at cooling times between 5 and 10 years were used in this qualitative classification.

A final point is that the high-activators Eu and Cs are not commonly encountered as trace-elements in metal-alloys such as the Al-alloys in reactor SSCs that are exposed to $\phi \geq 10^{11} \text{ cm}^{-2} \text{ s}^{-1}$ and will, therefore, be left out of the graphs for $\phi \geq 10^{11} \text{ cm}^{-2} \text{ s}^{-1}$.

5.5.1 Plots of Activity and Dose-Rates for Scenario **DECO_60yr_50yr_1E14**

The time-dependence $A(t)$ of total activities produced by the neutron irradiation of selected elements, for a scenario **DECO_60yr_50yr_1E14** are shown in Figure 10.

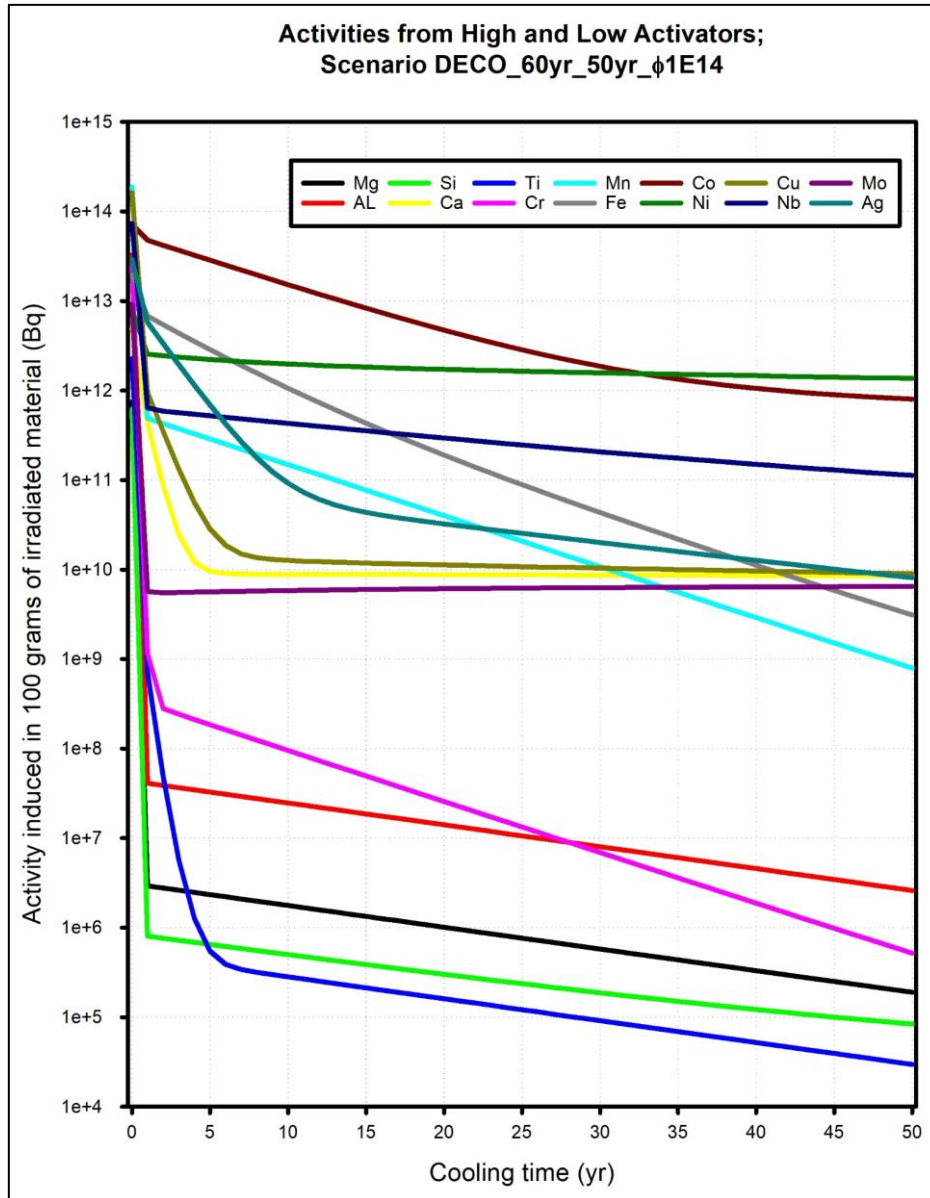


Figure 10: Activities produced by the neutron irradiation of selected elements for an irradiation scenario DECO_60yr_50yr_1E14

In Figure 10 is seen that the activities of all nuclides remain above 10^4 Bq over the first 50 years after irradiation of the 100 g samples. The problematic, high-activators are the elements Co, Ni, Nb; activities per unit mass of these elements remain above 10^9 Bq/g even after 50 years of cooling time. The second-tier activators are Fe, Ag, Cu, Mn and Ca. The lowest activators are Cr, AL, Mg, Si and Ti. As from $T_{cool} \approx 6$ yr, the lowest activity is observed for Ti, followed by Si and Mg.

The time-dependence of the functions $DR(t)$ of dose-rates at 1 m from a 1 g sample of selected elements irradiated under scenario DECO_60yr_50yr_1E14 are shown in Figure 10.

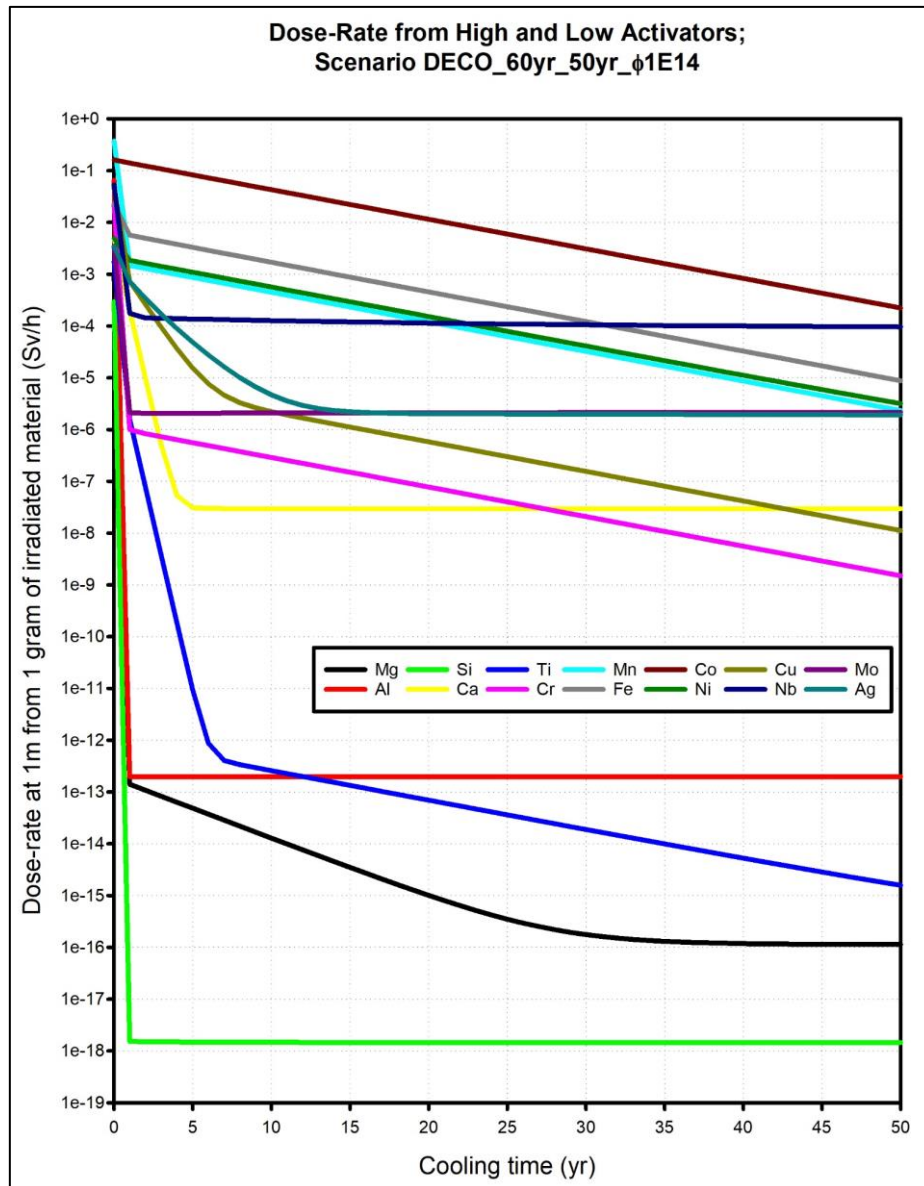


Figure 11: Dose-rates produced by the neutron irradiation of selected elements, for scenario DECO_60yr_50yr_1E14

In Figure 11 it is seen that the top-tier, problematic activators are Co, Nb, Fe, Mn, Mo and Ag. The second-tier, intermediate activators are Cu, Ca and Cr. The lowest-tier, most benign activators are Al, Ti, Mg and Si.

5.5.2 Plots of Activity and Dose-Rates for Scenario DECO_60yr_50yr_1E13

The time-dependence $A(t)$ of the activities induced by the neutron irradiation of selected elements, for scenario DECO_60yr_50yr_1E13, are shown in Figure 12.

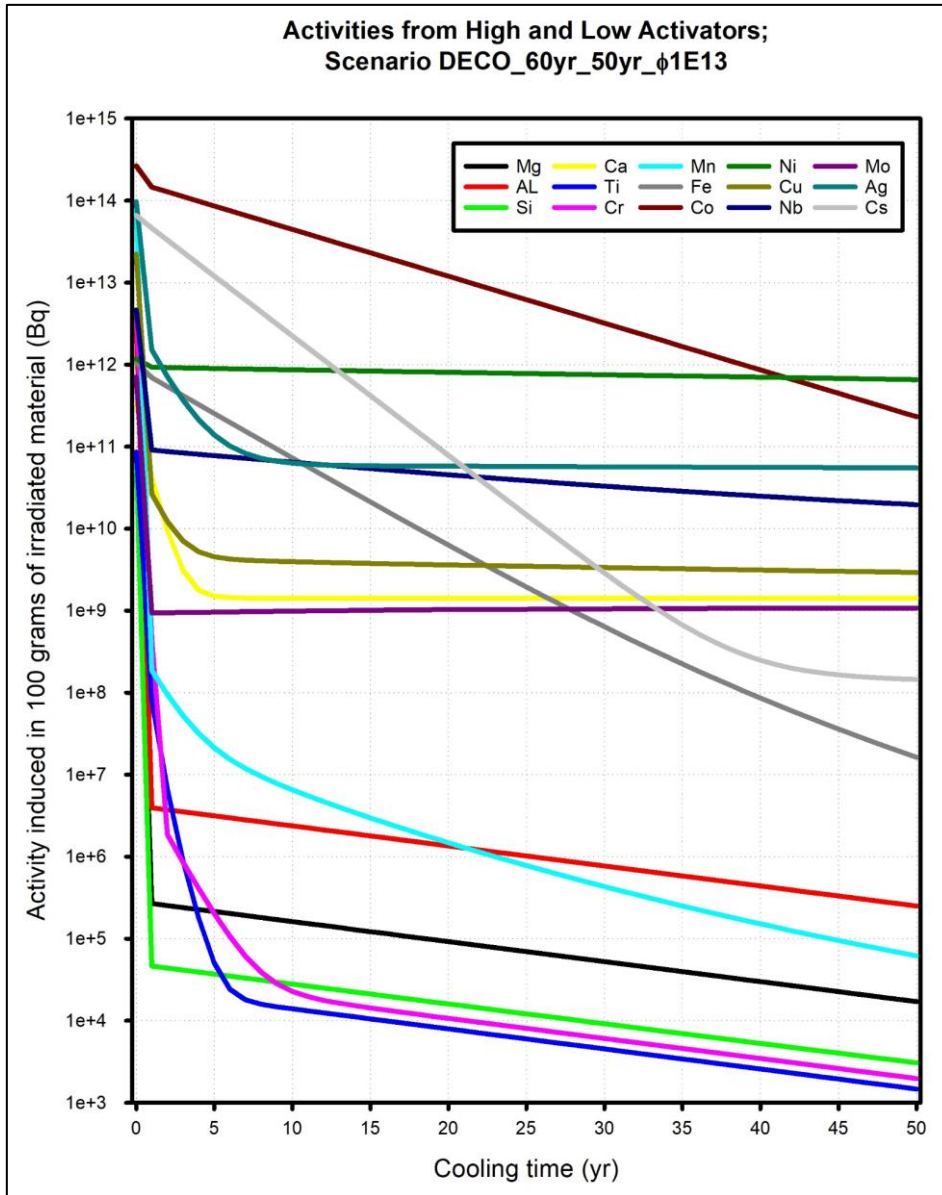


Figure 12: Activities produced by the neutron irradiation of selected elements, for scenario DECO_60yr_50yr_1E13

In Figure 12, the top-tier activating elements for scenario DECO_60yr_50yr_1E13, from the viewpoint of induced activity $A(t)$, are Co, Ni, Ag and Nb. Activities per unit mass of high-activator elements remain above 10^8 Bq/g even after 50 years of cooling time. The second-tier activators are Cu, Ca, Mo and Fe. The lowest activators are Al, Mn, Mg, Cr, Si and Ti. As from $T_{cool} \approx 6$ yr, the lowest activity is achieved by irradiated Ti. In all irradiation cases, the superiority of Ti as a low-activator is pronounced and remarkable. Titanium-alloys are known to be very strong, and component designs that replace Fe-alloys in high neutron fluence-rate regions with Ti-alloys, will result in a valuable lowering of long-term neutron activation issues.

Figure 13 displays the dose-rates at 1 m from 1 g masses of selected elements irradiated under scenario **DECO_60yr_50yr_1E13**.

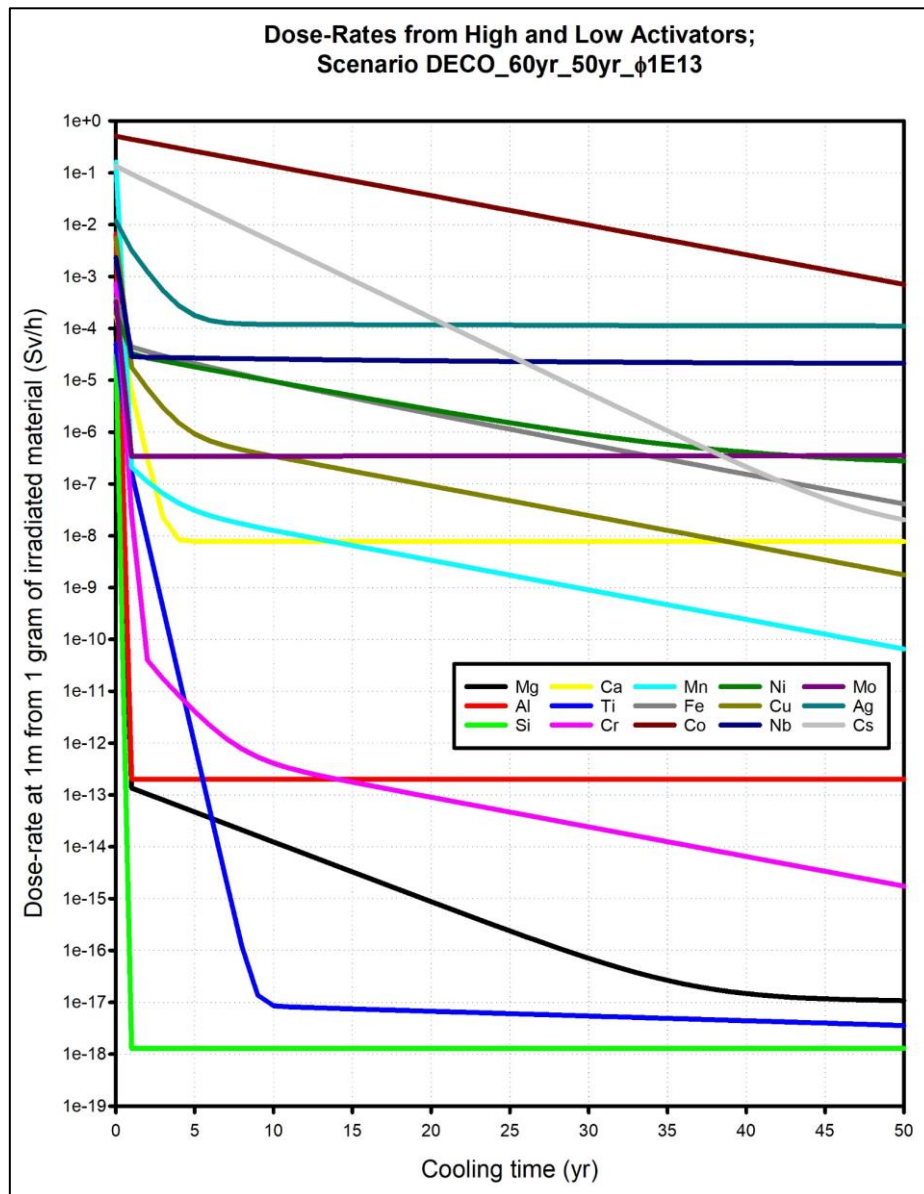


Figure 13: Dose-rates produced by the neutron irradiation of selected elements, for scenario **DECO_60yr_50yr_1E13**

In Figure 13 the top-tier activating elements for scenario **DECO_60yr_50yr_1E13**, from the viewpoint of the dose-rate functions $DR(t)$, are Co, Cs, Ag and Nb. The second-tier activators are Ni, Fe, Mo, Cu, Mn and Ca. The lowest activators are Cr, Al, Mg, Ti and Si. As from $T_{cool} \approx 1$ yr, the lowest dose-rate is seen for the activation of Si. The low activation of Si and the even lower activation of oxygen (O) shows that high-purity sand and sandstone (SiO_2) will be a very low-activator mineral. An ordinary concrete that contains more than circa 85 % SiO_2

by mass, is a candidate for a low-activation material if the presence of high-activator trace-elements is minimised.

5.5.3 Plots of Activity and Dose-Rates for Scenario **DECO_60yr_50yr_1E12**

The high-activator element Eu is not encountered as a noteworthy trace-element in most metal alloys, but only in concretes — refer to e.g. (Ludwig, 2013) and (Stephens Jr and Pohl, 1978). At nuclear reactor facilities in South Africa, concretes are never exposed to neutron fluence-rates above circa $10^{11} \text{ cm}^{-2} \text{ s}^{-1}$. For this reason, Eu was left out of the graphs of the high-flux scenarios **DECO_60yr_50yr_1E14** and **DECO_60yr_50yr_1E13**. As from **DECO_60yr_50yr_1E12**, the element Eu is now introduced to the list of elements-of-interest.

The time-dependence $A(t)$ of the activities induced by the neutron irradiation of selected elements, for scenario **DECO_60yr_50yr_1E12**, are shown in Figure 14.

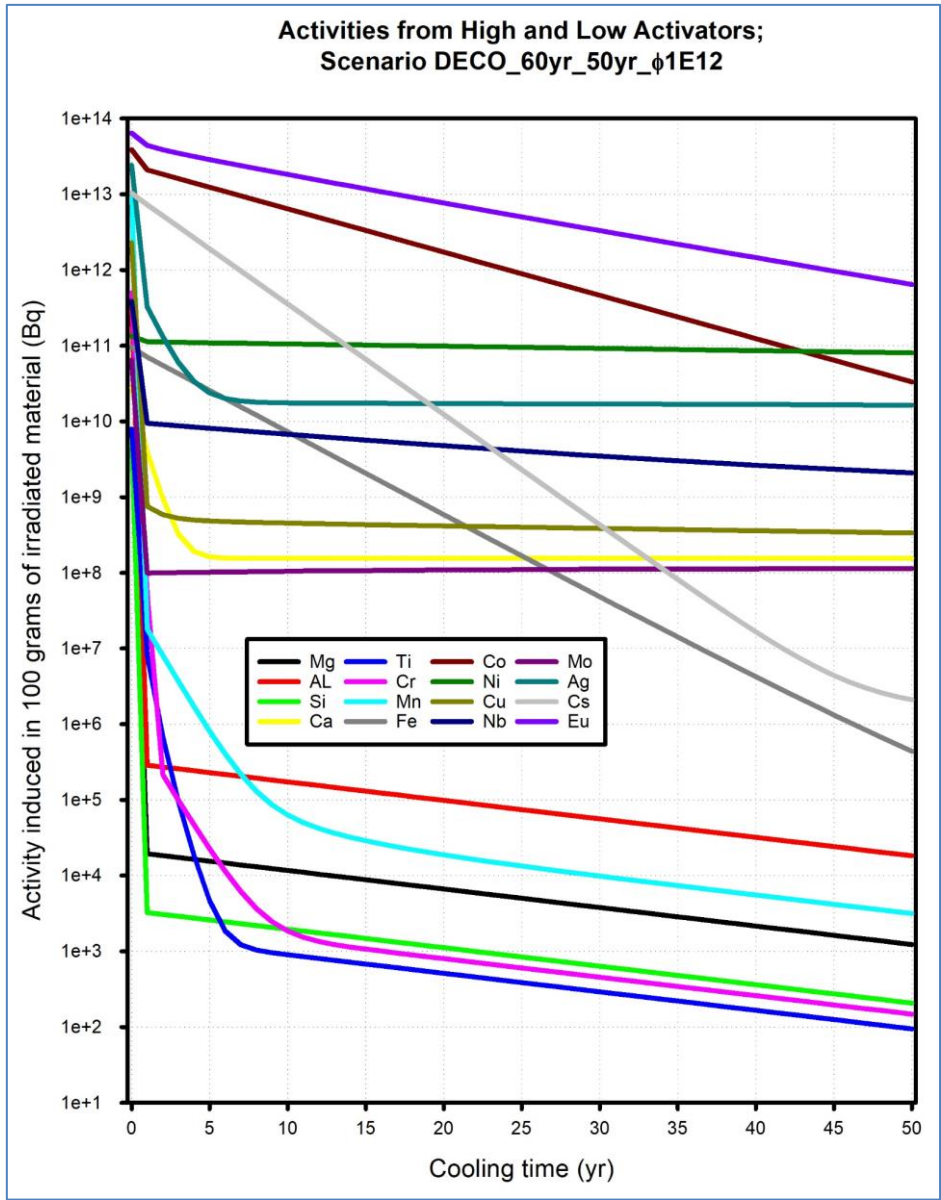


Figure 14: Activities produced by the neutron irradiation of selected elements, for scenario DECO_60yr_50yr_1E12

In Figure 14, the top-tier activating elements for scenario DECO_60yr_50yr_1E12, from the viewpoint of the induced activity $A(t)$, are Eu, Co, Cs, Ni, Ag and Nb. The second-tier activators are Fe, Cu, Ca and Mo. The lowest activators are Al, Mn, Mg, Cr, Si and Ti. As from $T_{cool} \approx 6$ yr, the lowest activity is achieved by the irradiation of Ti.

Figure 15 displays the dose-rates at 1 m from 1 g masses of selected elements irradiated under scenario DECO_60yr_50yr_1E12.

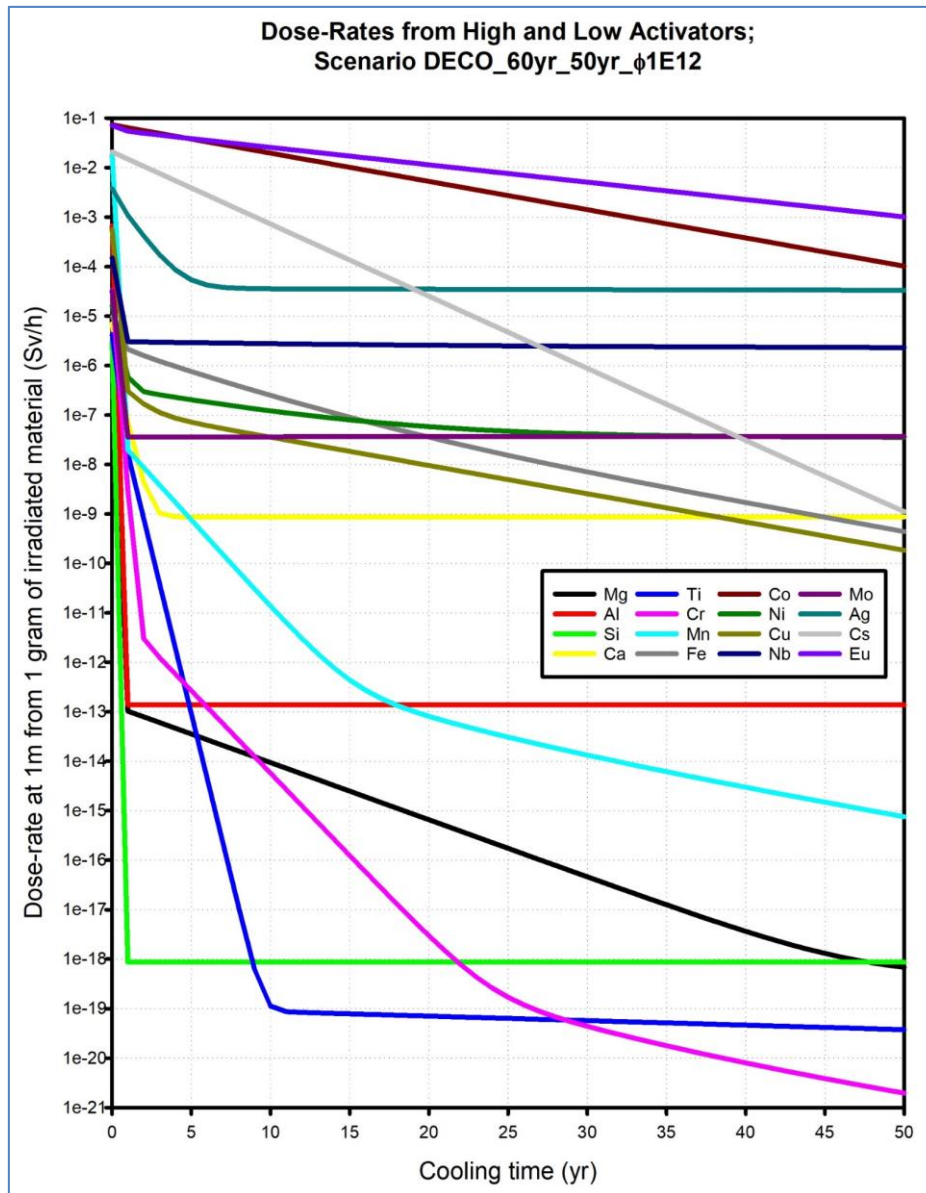


Figure 15: Dose-rates produced by the neutron irradiation of selected elements, under scenario DECO_60yr_50yr_1E12

In Figure 15 the top-tier activating elements for scenario DECO_60yr_50yr_1E12, from the viewpoint of the dose-rate $DR(t)$, are Eu, Co, Cs, Ag and Nb. The second-tier dose-rate producing activators are Fe, Ni, Mo, Cu, Ca and Mn. The lowest dose-rate producing activator elements are Al, Mg, Cr, Si and Ti. Initially, Si cools off fastest, but at approximately 9 years, the dose-rate from Ti becomes lower, and as from approximately 30 years, the dose-rate from irradiated Cr is lowest.

5.5.4 Plots of Activity and Dose-Rates for Scenario **DECO_60yr_50yr_1E11**

The time-dependence $A(t)$ of the activities induced by the neutron irradiation of selected elements, for scenario **DECO_60yr_50yr_1E11**, are shown in Figure 16.

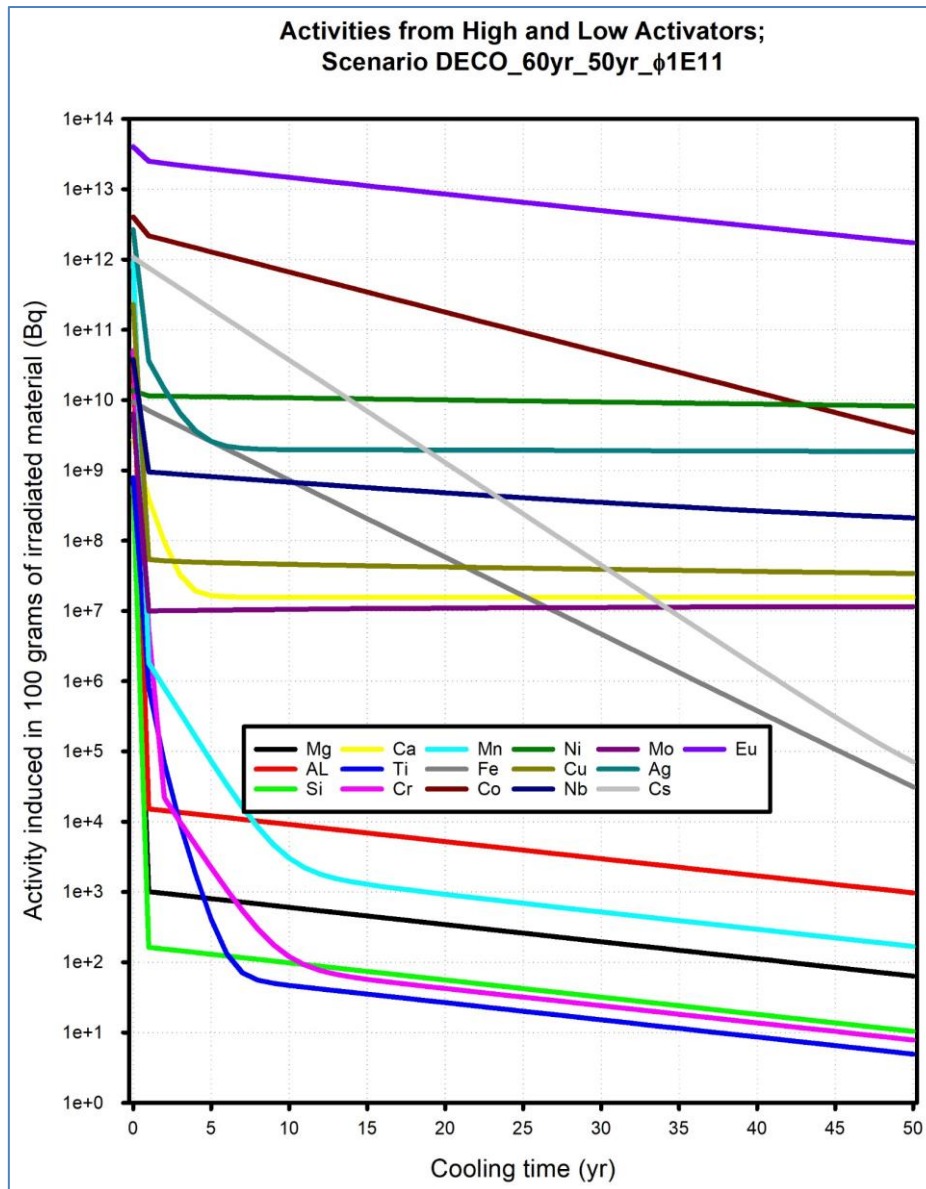


Figure 16: Activities produced by the neutron irradiation of selected elements, for scenario **DECO_60yr_50yr_1E11**

In Figure 16, the top-tier activating elements for scenario **DECO_60yr_50yr_1E11**, from the viewpoint of the induced activity $A(t)$, are Eu, Co, Cs, Ni, Ag, Fe and Nb. The second-tier activators are Cu, Ca and Mo. The lowest activators are Al, Mn, Mg, Cr, Si and Ti. As from $T_{cool} \approx 7$ yr, the lowest activity is achieved by the irradiation of the element Ti.

Figure 17 displays the dose-rates at 1 m from 1 g masses of selected elements irradiated under scenario **DECO_60yr_50yr_1E11**.

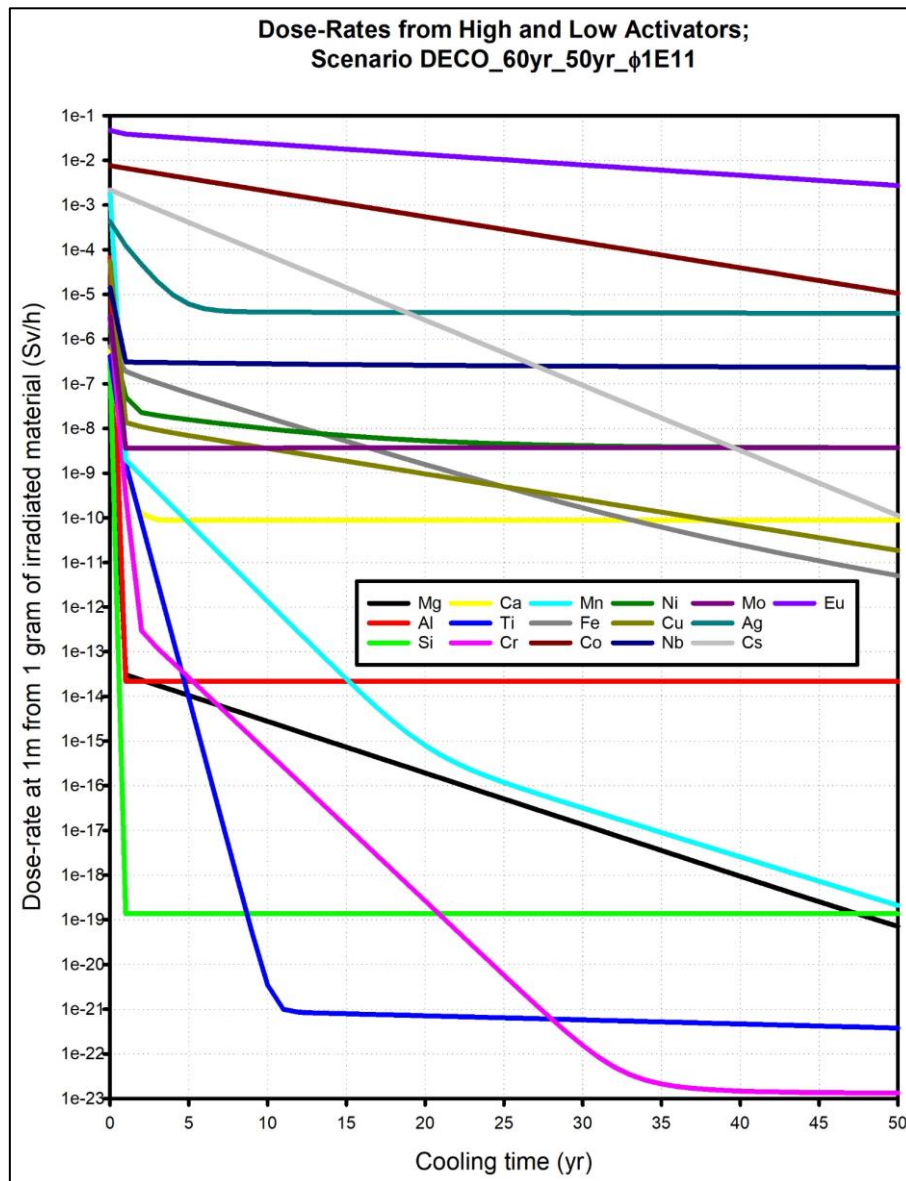


Figure 17: Dose-rates produced by the neutron irradiation of selected elements, for scenario **DECO_60yr_50yr_1E11**

In Figure 17 the top-tier activating elements for scenario **DECO_60yr_50yr_1E11**, from the viewpoint of the dose-rate $DR(t)$, are Eu, Co, Cs, Ag and Nb. The second-tier dose-rate producing activators are Fe, Ni, Mo, Cu and Ca. The lowest dose-rate producing activator elements are Mn, Al, Mg, Cr, Si and Ti.

5.5.5 Plots of Activity and Dose-Rates for Scenario **DECO_60yr_50yr_1E10**

The time-dependence $A(t)$ of the activities induced by the neutron irradiation of selected elements, for scenario **DECO_60yr_50yr_1E10**, are shown in Figure 18.

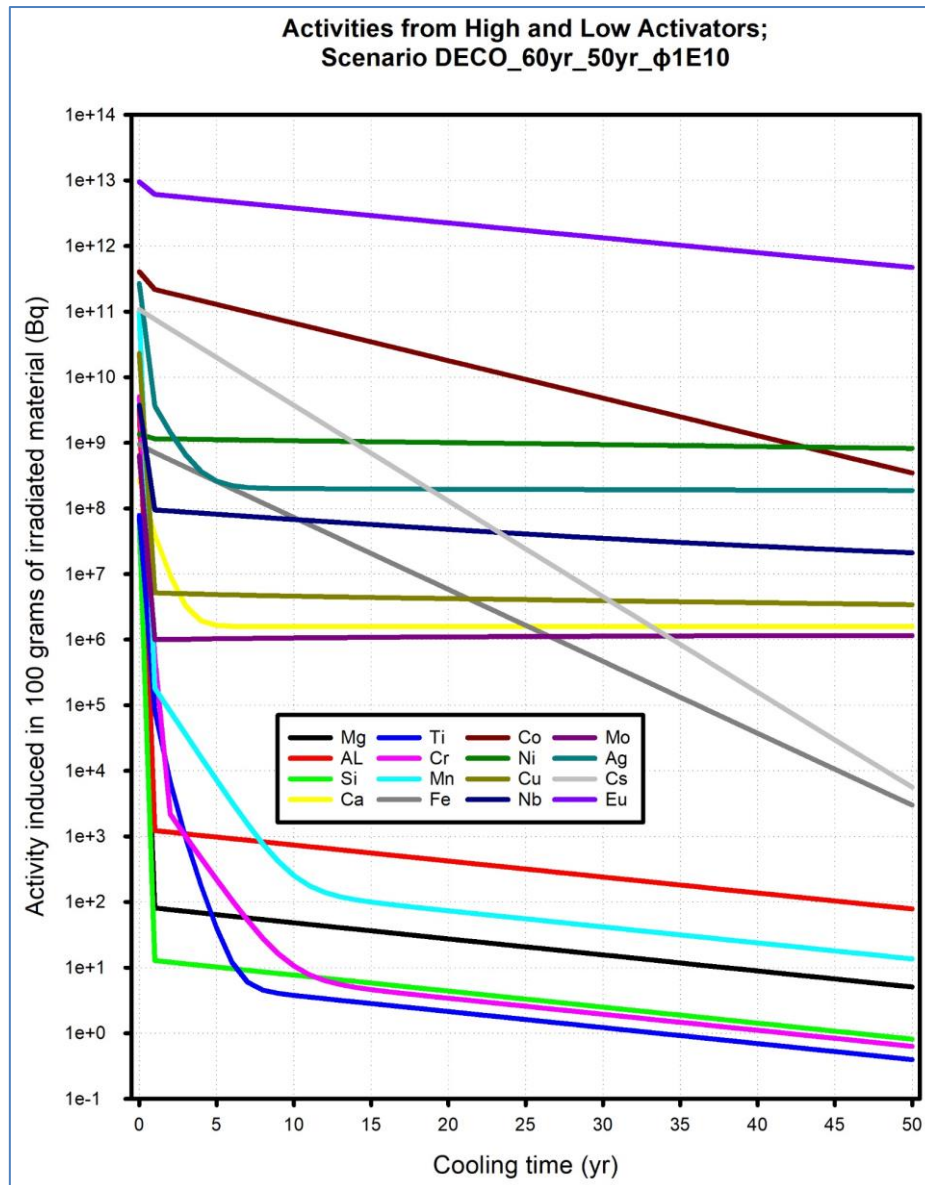


Figure 18: Activities produced by the neutron irradiation of selected elements, for scenario **DECO_60yr_50yr_1E10**

In Figure 18, the top-tier activating elements for scenario **DECO_60yr_50yr_1E10**, from the viewpoint of the induced activity $A(t)$, are Eu, Co, Cs, Ni, Ag, Fe and Nb. The second-tier activators are Cu, Ca and Mo. The lowest activators are Al, Mn, Mg, Cr, Si and Ti. As from $T_{cool} \approx 7$ yr, the lowest activity is achieved by the irradiation of the element Ti.

Figure 19 displays the dose-rates at 1 m from 1 g masses of selected elements irradiated under scenario **DECO_60yr_50yr_1E10**.

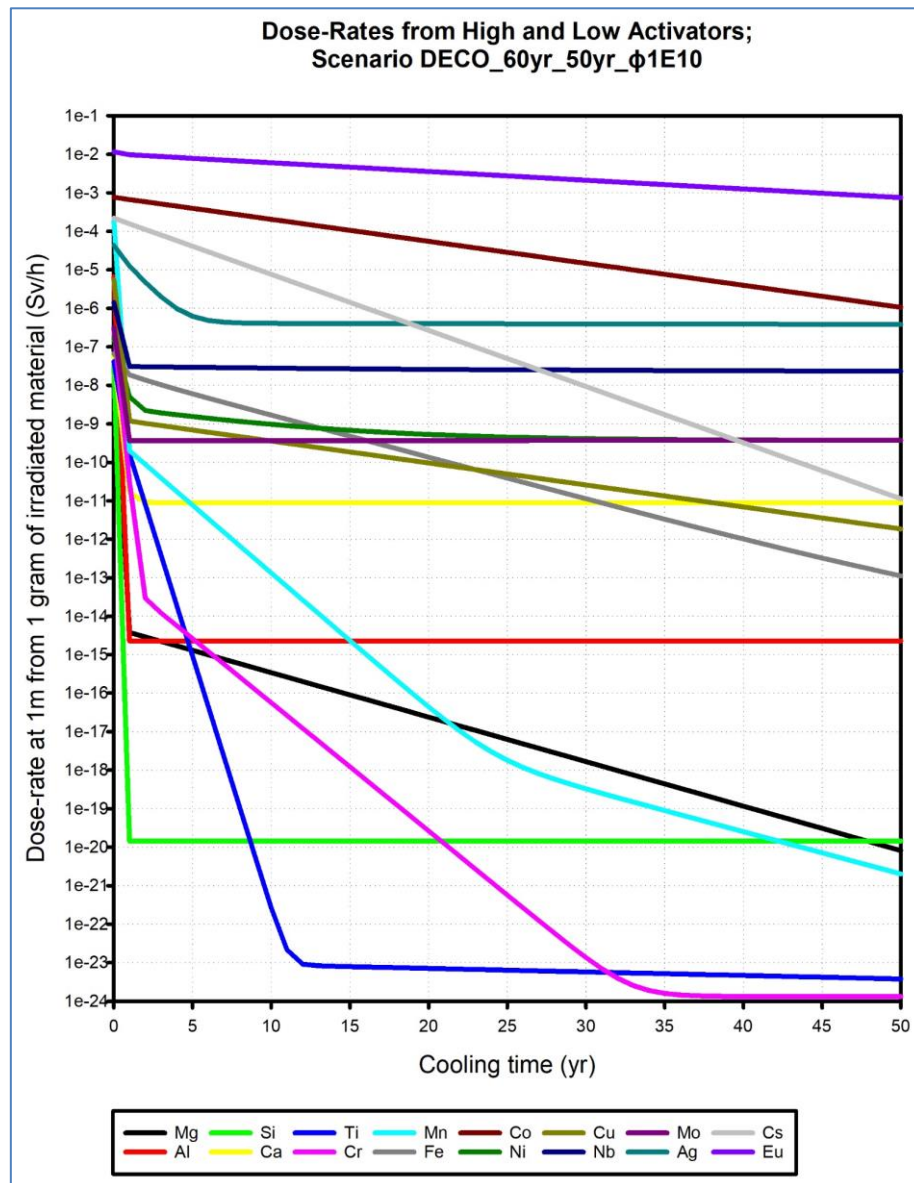


Figure 19: Dose-rates produced by the neutron irradiation of selected elements, for scenario **DECO_60yr_50yr_1E10**

In Figure 19 the top-tier activating elements for scenario **DECO_60yr_50yr_1E10**, from the viewpoint of the dose-rate $DR(t)$, are Eu, Co, Cs, Ag and Nb. The second-tier dose-rate producing activators are Fe, Ni, Mo, Cu and Ca. The lowest dose-rate producing activator elements are Mn, Al, Mg, Cr, Si and Ti. As from $T \approx 32$ yr, the lowest dose-rate is seen for the irradiation of Cr.

5.5.6 Plots of Activity and Dose-Rates for Scenario **DECO_60yr_50yr_1E9**

The time-dependence $A(t)$ of the activities induced by the neutron irradiation of selected elements, for scenario **DECO_60yr_50yr_1E9**, are shown in Figure 20.

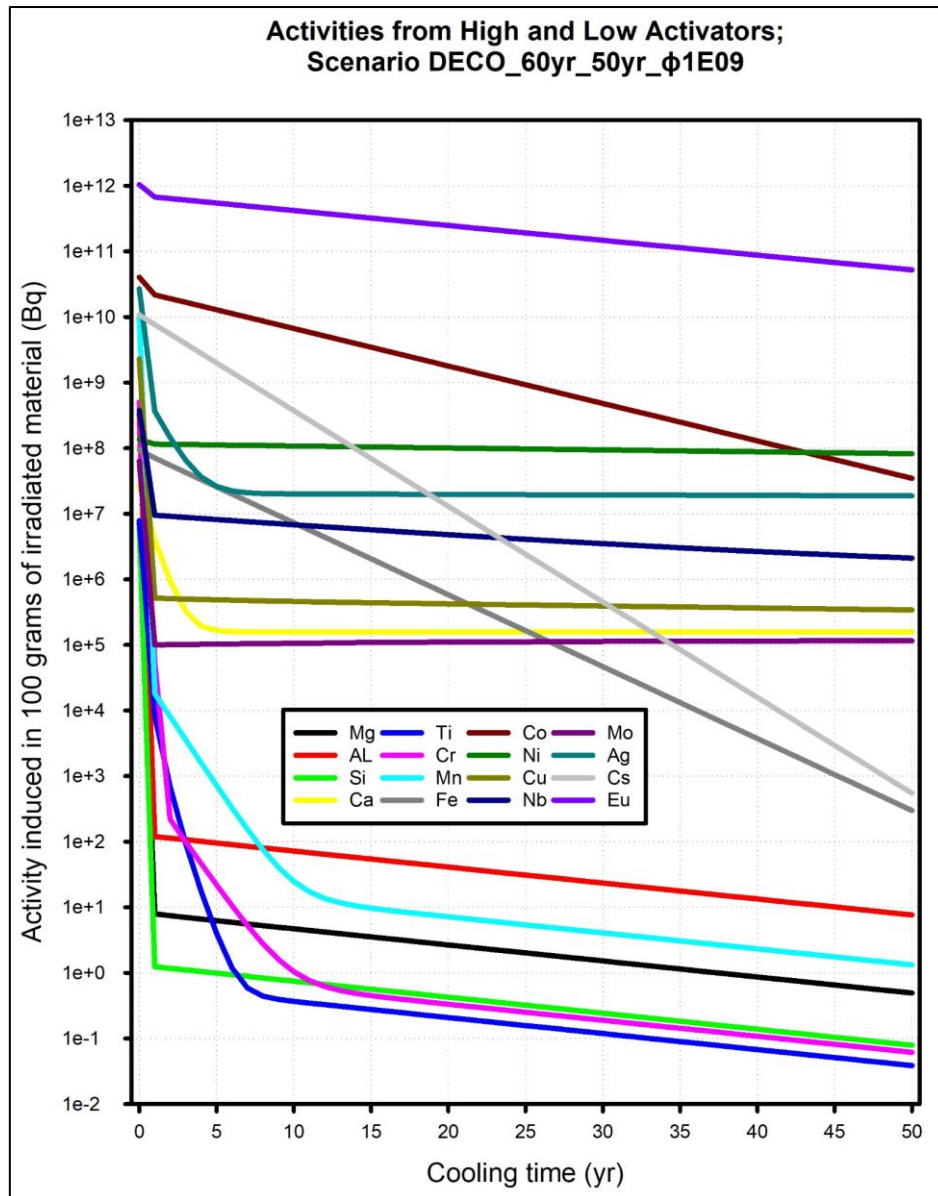


Figure 20: Activities produced by the neutron irradiation of selected elements, for scenario **DECO_60yr_50yr_1E9**

In Figure 20, the top-tier activating elements for scenario **DECO_60yr_50yr_1E9**, from the viewpoint of the induced activity $A(t)$, are Eu, Co, Cs, Ni, Ag, Fe and Nb. The second-tier activators are Cu, Ca and Mo. The lowest activators are Al, Mn, Mg, Cr, Si and Ti. As from $T_{cool} \approx 6$ yr, the lowest activity is achieved by the irradiation of the element Ti.

Figure 21 displays the dose-rates at 1 m from 1 g masses of selected elements irradiated under scenario **DECO_60yr_50yr_1E9**.

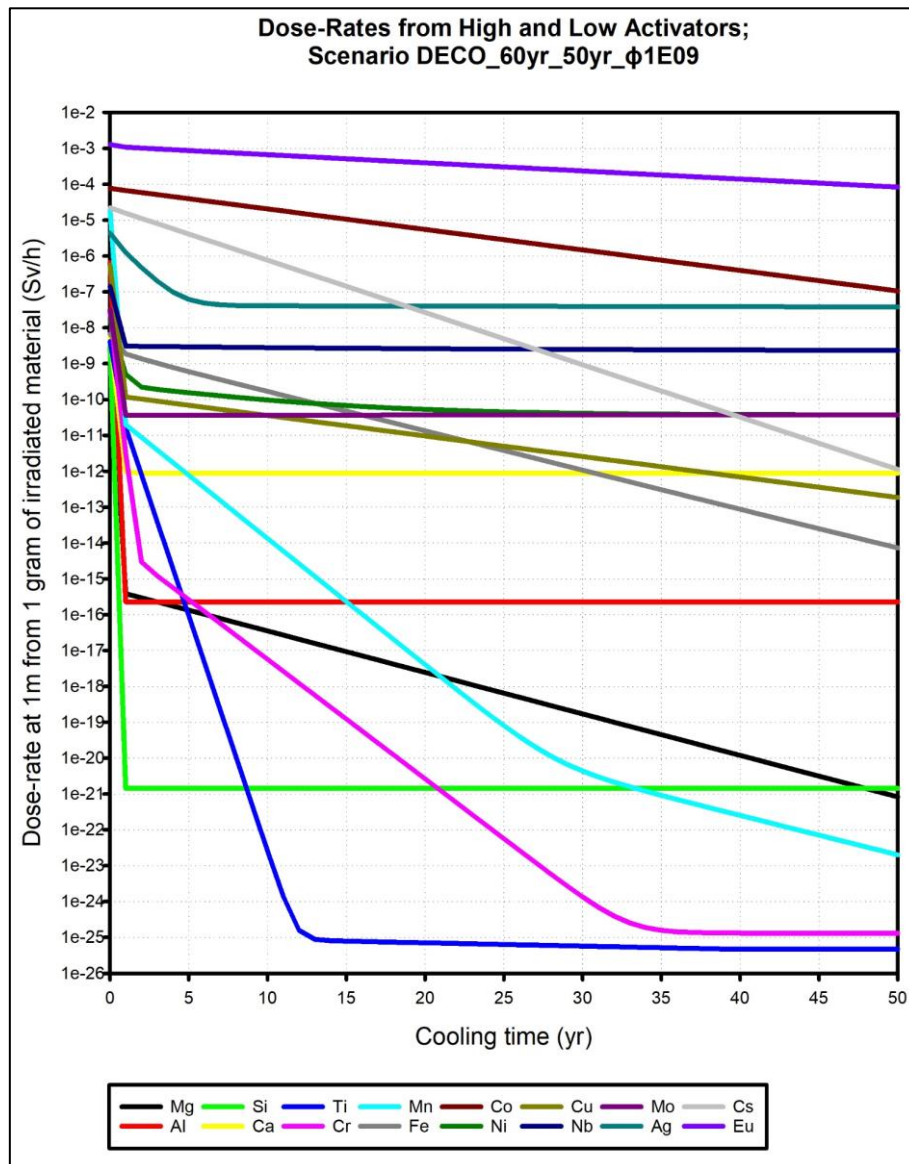


Figure 21: Dose-rates produced by the neutron irradiation of selected elements, for scenario **DECO_60yr_50yr_1E9**

In Figure 21 the top-tier activating elements for scenario **DECO_60yr_50yr_1E9**, from the viewpoint of the dose-rate $DR(t)$, are Eu, Co, Cs, Ag and Nb. The second-tier dose-rate producing activators are Fe, Ni, Mo, Cu and Ca. The lowest dose-rate producing activator elements are Mn, Al, Mg, Cr, Si and Ti. As from $T \approx 8$ yr, the lowest dose-rate is seen for the irradiation of the element Ti.

5.5.7 Plots of Activity and Dose-Rates for Scenario **DECO_60yr_50yr_1E8**

The time-dependence $A(t)$ of the activities induced by the neutron irradiation of selected elements, for scenario **DECO_60yr_50yr_1E8**, are shown in Figure 22.

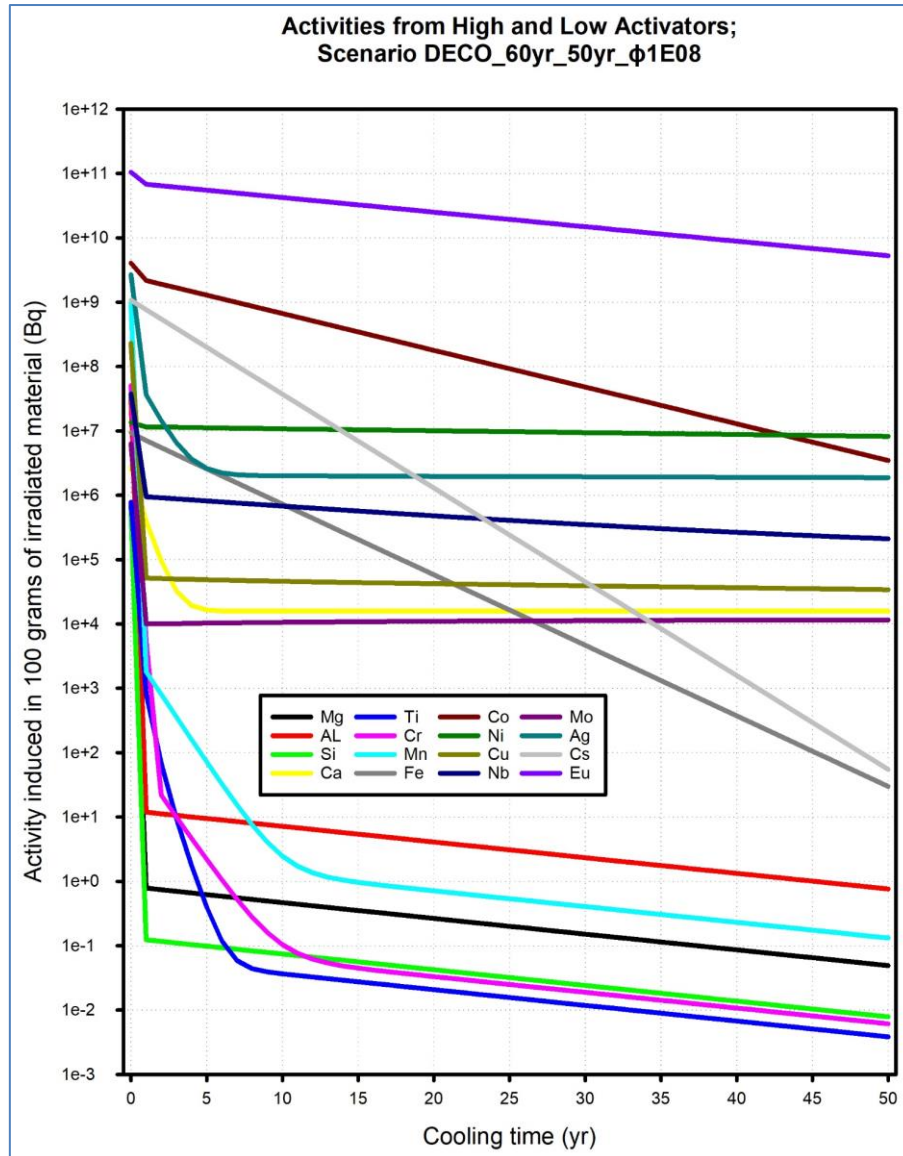


Figure 22: Activities produced by the neutron irradiation of selected elements, for scenario **DECO_60yr_50yr_1E8**

In Figure 22, the top-tier activating elements for scenario **DECO_60yr_50yr_1E8**, from the viewpoint of the induced activity $A(t)$, are Eu, Co, Cs, Ni, Ag, Fe and Nb. The second-tier activators are Cu, Ca and Mo. The lowest activators are Al, Mn, Mg, Cr, Si and Ti. As from $T_{cool} \approx 6$ yr, the lowest activity is achieved by the irradiation of the element Ti.

Figure 23 displays the dose-rates at 1 m from 1 g masses of selected elements irradiated under scenario **DECO_60yr_50yr_1E8**.

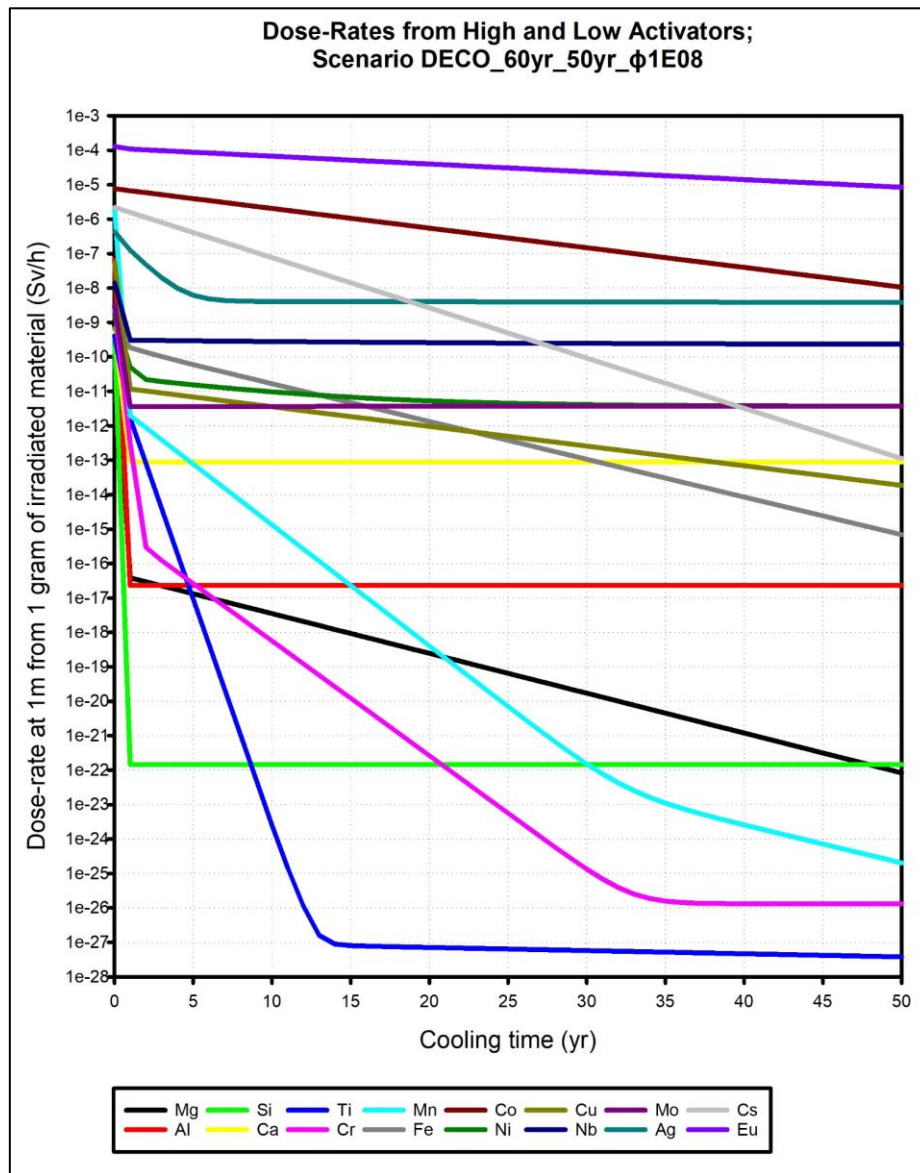


Figure 23: Dose-rates produced by the neutron irradiation of selected elements, for scenario **DECO_60yr_50yr_1E8**

In Figure 23 the top-tier activating elements for scenario **DECO_60yr_50yr_1E8**, from the viewpoint of the dose-rate $DR(t)$, are Eu, Co, Cs, Ag and Nb. The second-tier dose-rate producing activators are Fe, Ni, Mo, Cu and Ca. The lowest dose-rate producing activator elements are Mn, Al, Mg, Cr, Si and Ti. As from $T \approx 8$ yr, the lowest dose-rate is seen for the irradiation of the element Ti.

5.5.8 Plots of Activities and Dose-Rates for Scenario **DECO_60yr_50yr_1E7**

All results for **DECO_60yr_50yr_1E7** are simply approximately 10 times lower than for **DECO_60yr_50yr_1E8** and all conclusions are identical — in this fluence-rate domain, neutron activation behaves in a linear manner.

5.6 Research Question RQ_6 :

Plots of Activities and Dose-Rates for Scenarios **DECO_1yr_50yr_1E15** and **DECO_1yr_50yr_1E14** for the Fuel-Assembly End-Adaptors

5.6.1 Plots of Activities and Dose-Rates for Scenario **DECO_1yr_50yr_1E15** for MTR Fuel-Assemblies

The time-dependence $A(t)$ of the activities induced by the neutron irradiation of selected elements, for scenario **DECO_1yr_50yr_1E15**, are shown in Figure 24. This irradiation scenario is representative for the central, peak-fluence parts of the structural Al-alloy in SAFARI-1 fuel-assemblies, e.g. the fuel cladding.

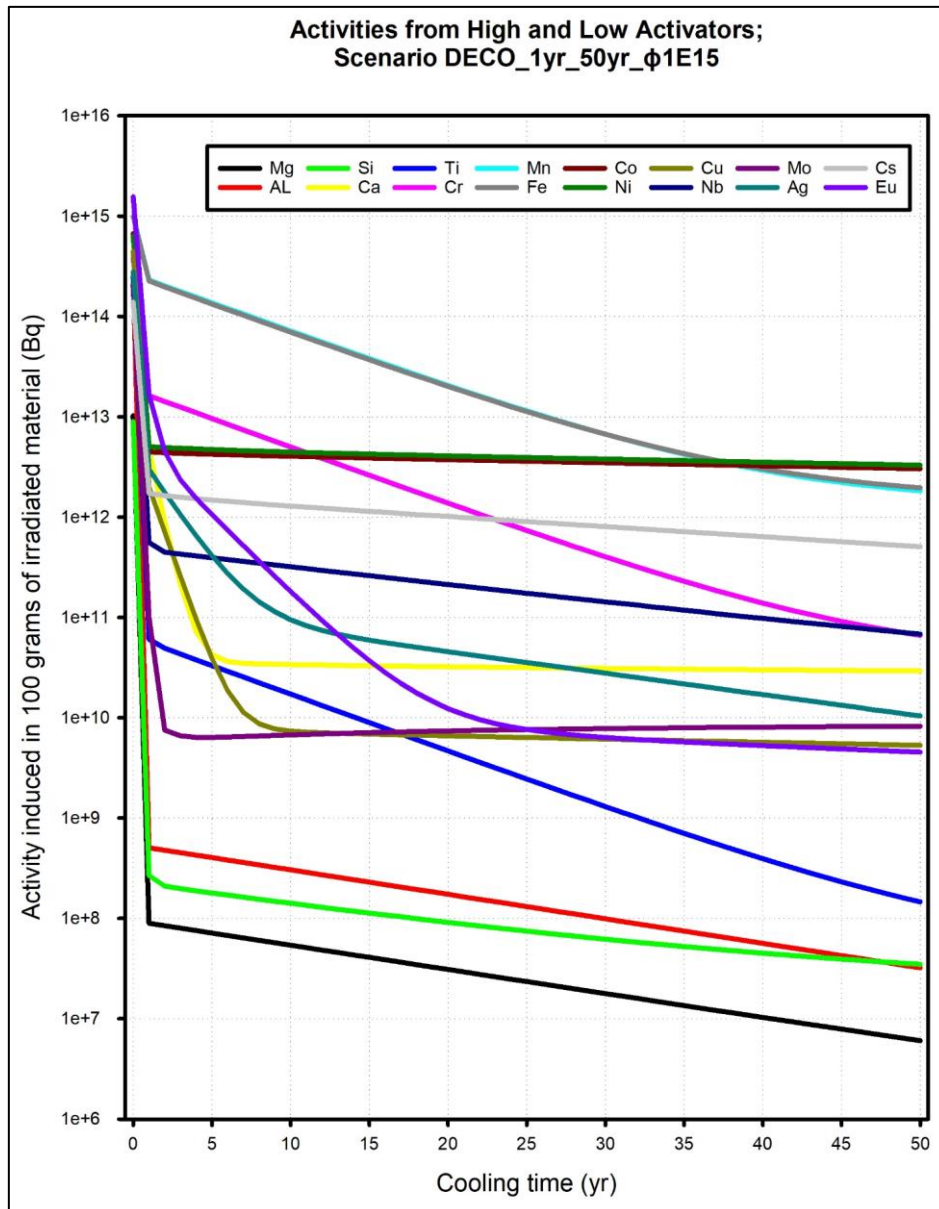


Figure 24: Activities produced by the neutron irradiation of selected elements, for highly exposed Al-alloy in an MTR fuel-assembly that is exposed under irradiation scenario DECO_1yr_50yr_1E15

In Figure 24, the top-tier activating elements for scenario DECO_1yr_50yr_1E15, from the viewpoint of the induced activity $A(t)$, are Mn, Fe, Co, Ni and Cr. (Note that the curves for Fe and Mn are coincident and cannot be spatially distinguished.) The second-tier activators are Cs, Nb, Ag and Ca. The lowest activators are Mg, Si and Al. This ranking is unusual and therefore requires explanation. The usual top-activators —Eu and Co — are “burned up” over 1 year of exposure to the extremely high fluence-rate of $\phi = 1E15 \text{ cm}^{-2} \text{ s}^{-1}$ and are therefore not high-activators in this extreme exposure scenario. Mn, Fe and Cr are high-activators because they “breed” Co-60 — high activities of Co-60 are activated in Cr, Mn and Fe — as

explained in § 5.1.6 (page 93), § 5.1.5 (page 91) and § 5.1.4 (page 88). Even Ti “breeds” some Co-60 and therefore loses its usual status as a very low-activator, at very high neutron fluence-rates, as is accounted for in § 5.1.8 on page 96. The only class of engineering metal that can readily withstand the “hammering” of neutron fluence-rates as high as $1\text{E}15\text{ cm}^{-2}\text{ s}^{-1}$ for times as long as 1 year, is Al-alloys composed almost exclusively of Al, Mg and Si — the three consistently performing and trustworthy low-activator elements under all realistic neutron fluence-rate scenarios. The 6-series of Al-alloys are Al-Mg-Si alloys and are best suited to withstand very high neutron fluence-rates — refer to e.g. (Kolluri, n.d.), (Kapusta et al., 2003), (Farrell and King, 2009) and (Weeks et al., 1990).

Figure 25 displays the dose-rates at 1 m from 1 g masses of selected elements irradiated under scenario **DECO_1yr_50yr_1E15**.

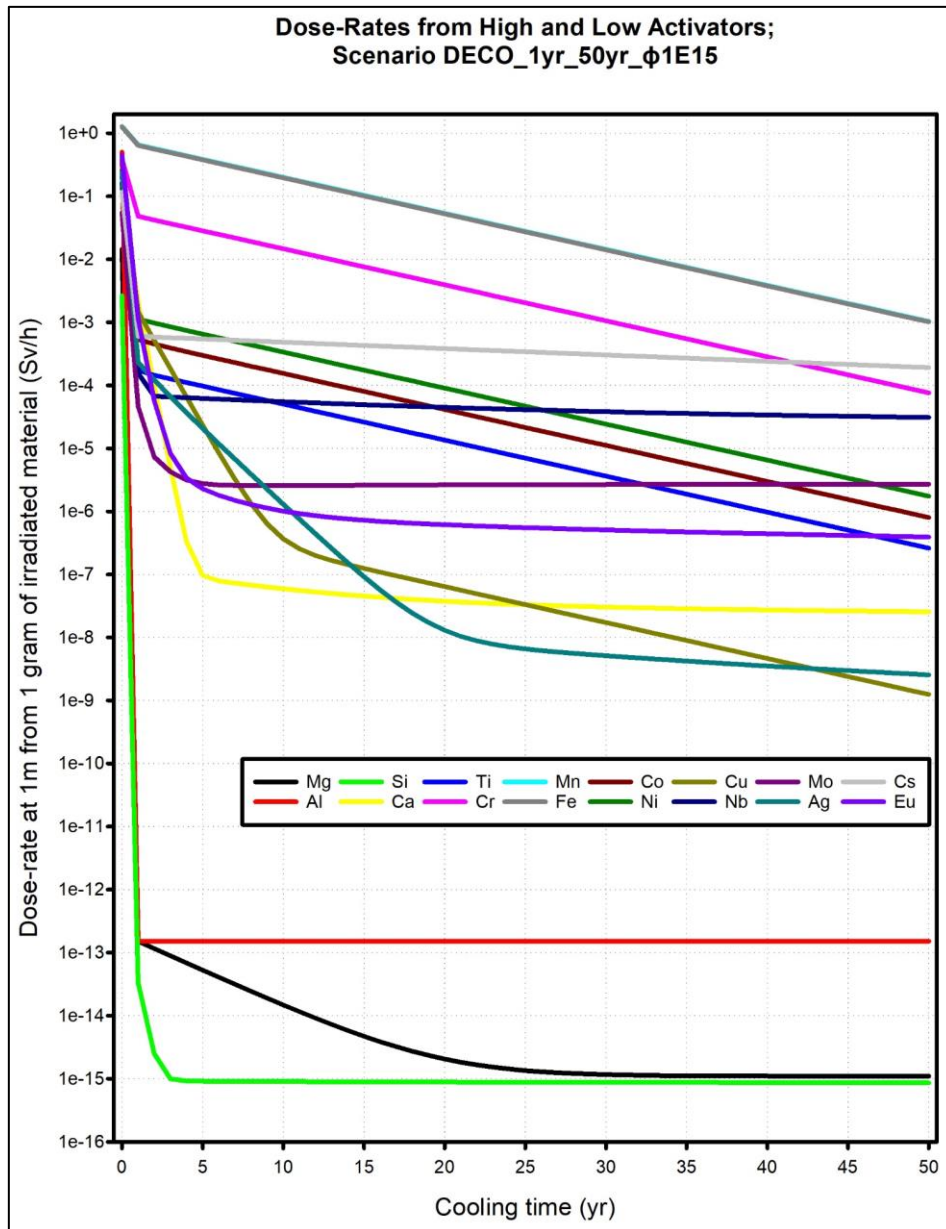


Figure 25: Dose-rates produced by the neutron irradiation of selected elements, for a fuel-assembly end-adaptor irradiation scenario DECO_1yr_50yr_1E15

In Figure 25 the top-tier activating elements for scenario DECO_1yr_50yr_1E15, from the viewpoint of the dose-rate $DR(t)$, are Mn, Fe, Cr and Cs. The second-tier dose-rate producing activators are Ni, Co, Nb, Mo, Eu and Ti. The lowest dose-rate producing activator elements are Al, Mg and Si. Again, it is seen that under very intense neutron irradiation, Ti loses its status as a low-activator element, while Al, Mg and Si are consistent low-activators. At the extremely high fluence-rate, Co and Eu are burned up and therefore do not figure amongst the ranks of the high-activators in Figure 25.

5.6.2 Plots of Activities and Dose-Rates for Scenario **DECO_1yr_50yr_1E14** for MTR Fuel-Assemblies

The time-dependence $A(t)$ of the activities induced by the neutron irradiation of selected elements, for scenario **DECO_1yr_50yr_1E14**, are shown in Figure 26. This irradiation scenario is representative for the end-adapters on SAFARI-1 fuel-assemblies.

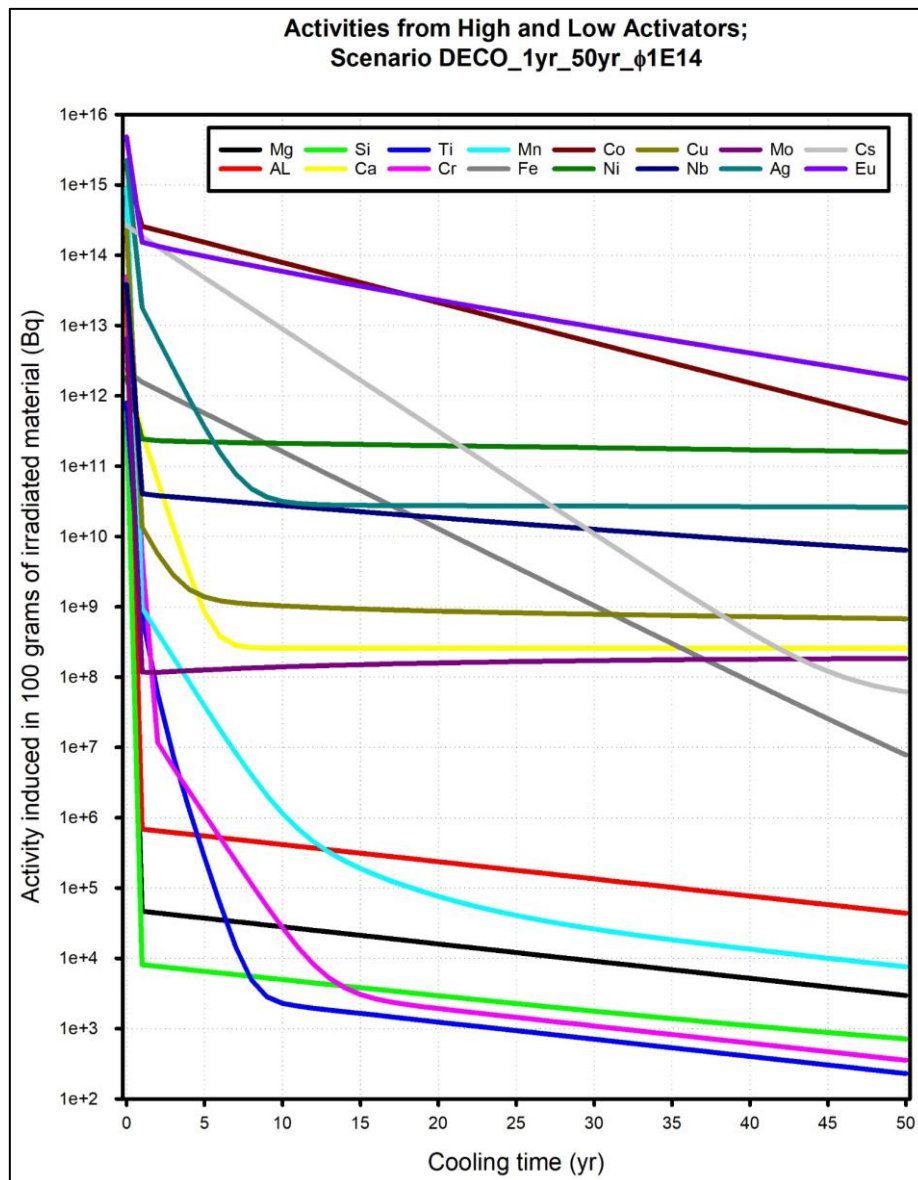


Figure 26: Activities produced by the neutron irradiation of selected elements, for a fuel-assembly end-adaptor irradiation scenario **DECO_1yr_50yr_1E14**

In Figure 26, the top-tier activating elements for scenario **DECO_1yr_50yr_1E14**, from the viewpoint of the induced activity $A(t)$, are Co, Eu, Cs, Ni, Fe, Ag and Nb. The second-tier

activators are Cu, Ca and Mo. The lowest activators are Mn, Al, Mg, Cr, Si and Ti. As from $T_{\text{cool}} \approx 8$ yr, the lowest activity is achieved for the irradiation of the element Ti.

Remarkable, qualitative differences are observed between Figure 24 and Figure 26 — at very high neutron fluence-rates ($10^{15} \text{ cm}^{-2}\text{s}^{-1}$; Figure 24), target-atoms with high neutron capture cross-sections are depleted, and non-linear “breeding” of Co-60 is seen in the 5 elements to the left of Co in the Periodic Table. When the fluence-rate is decreased by a factor 10 ($10^{14} \text{ cm}^{-2}\text{s}^{-1}$; Figure 26), these phenomena subside and the “usual” elements are found to be high-activators, medium-activators and low-activators.

Figure 27 displays the dose-rates at 1 m from 1 g masses of selected elements irradiated under scenario DECO_1yr_50yr_1E14.

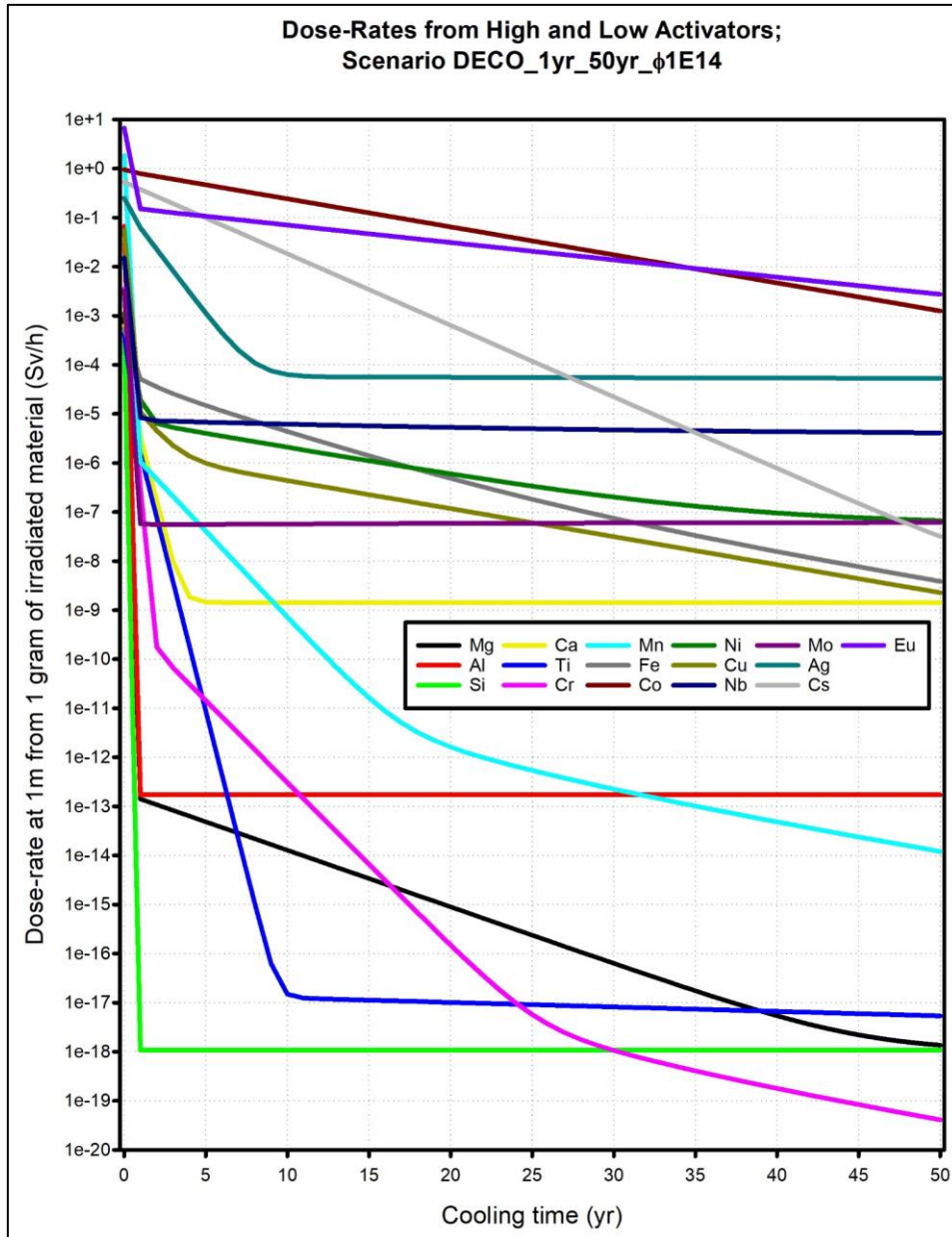


Figure 27: Dose-rates produced by the neutron irradiation of selected elements, for a fuel-assembly end-adaptor irradiation scenario DECO_1yr_50yr_1E14

In Figure 27 the top-tier activating elements for scenario DECO_1yr_50yr_1E14, from the viewpoint of the dose-rate $DR(t)$, are Co, Eu, Cs, Ag and Nb. The second-tier dose-rate producing activators are Fe, Ni, Mo, Cu and Ca. The lowest dose-rate producing activator elements are Mn, Al, Mg, Cr, Ti and Si. As from $T \approx 1$ yr to $T \approx 30$ yrs, the lowest dose-rate is seen for the irradiation of the element Si. Beyond $T \approx 30$ yrs, the lowest dose-rate is seen for the irradiation of the element Cr.

This concludes the presentation of results for scenarios of type **DECO_1yr_50yr_φ**, which are mainly of importance for the neutron activation of fuel-assemblies, specifically the end-adaptors, which are detached from FAs before the latter are put in long-term dry-storage.

5.7 Research Question *RQ*₇:

Plots of Activities and Dose-Rates for Neutron Radiography Irradiation Scenarios

5.7.1 Plots of Activities and Dose-Rates for the NRAD irradiation scenario

NRAD_1h_1000d_1E9

The time-dependence $A(t)$ of the activities induced by the neutron irradiation of selected elements, for scenario **NRAD_1h_1000d_1E9**, are shown in Figure 28. Note that the time-axes in Figure 28, Figure 29, Figure 30 and Figure 31 have a logarithmic scale, to enable insight into the activation-behaviour in the first minutes and hours after irradiation stops

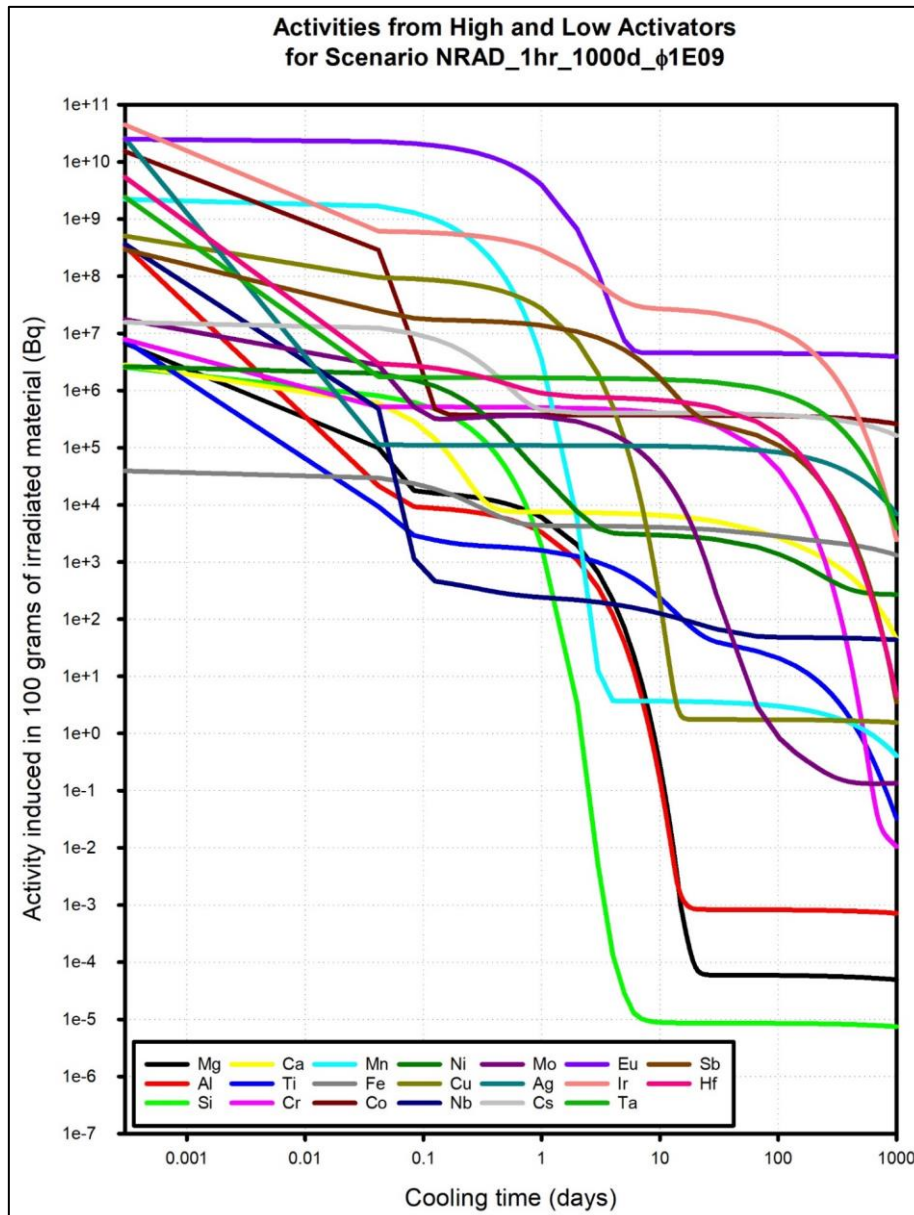


Figure 28: Activities produced by the neutron irradiation of selected elements, for a neutron radiography (NRAD) irradiation scenario NRAD_1h_30d_1E9

In Figure 28, the top-tier activating elements²² for scenario NRAD_1h_30d_1E9, from the viewpoint of the induced activity $A(t)$, evaluated at $T_{cool} = 10$ days, are Eu, Co, Cs, Cr, Ag and Mo. The second-tier activators are Ca, Fe, Ni, Ti, Cu and Nd. The lowest activators are Mn, Mg, Al and Si.

²² Note by co-supervisor TJvR: The element Ir is known to be a high activator under scenario NRAD_1h_30d_1E9 and also NRAD_1d_30d_1E9. However, it is extremely rare in nature, except in geological layers that contain fallout from asteroid or meteor impacts.

Figure 29 displays the dose-rates at 1 m from 1 g masses of selected elements irradiated under scenario `NRAD_1h_30d_1E9`.

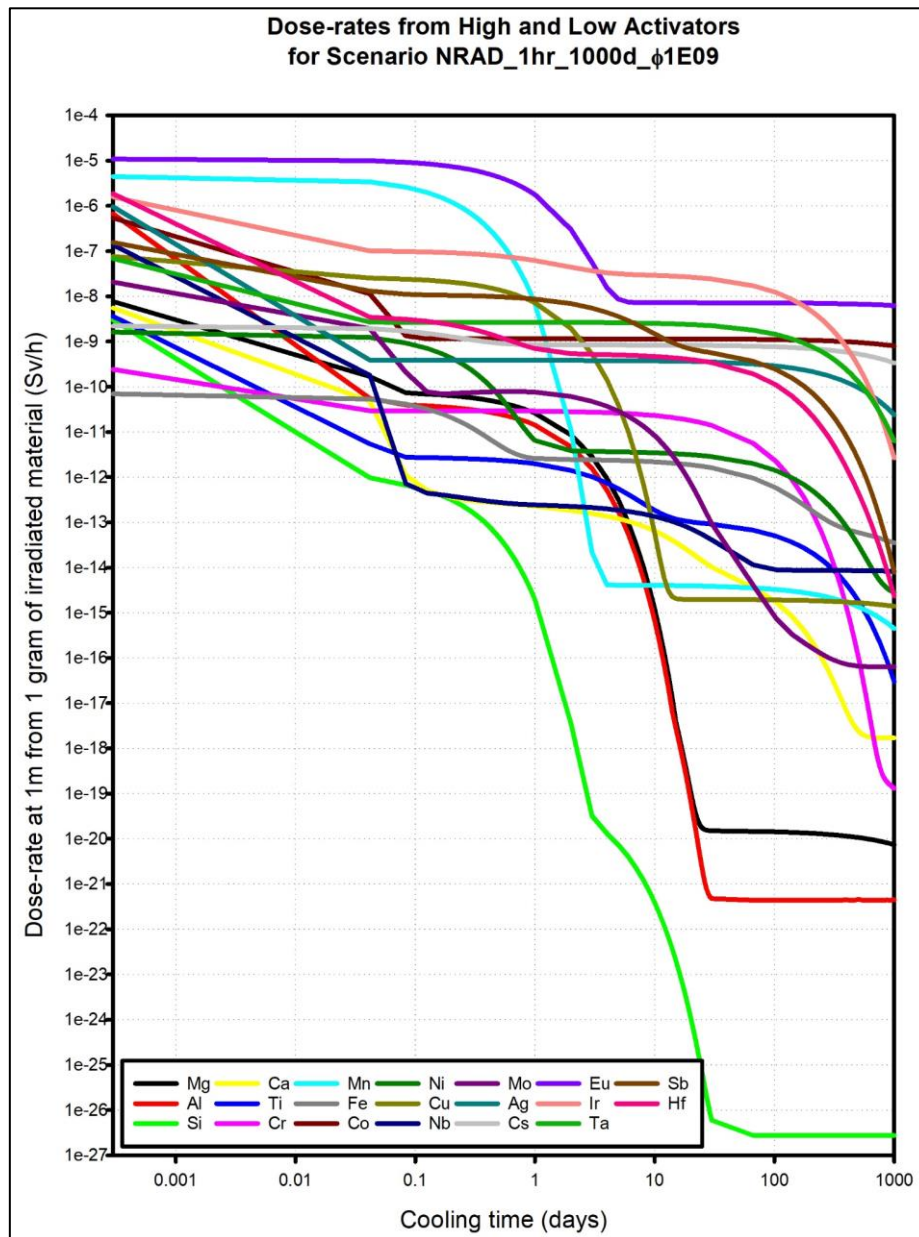


Figure 29: Dose-rates produced by the neutron irradiation of selected elements, for a neutron radiography irradiation scenario `NRAD_1h_30d_1E9`

In Figure 29 the top-tier activating elements for scenario `NRAD_1hr_30d_1E9`, from the viewpoint of the dose-rate $DR(t)$, evaluated at a cooling time of 10 days, are Ir, Eu, Ta, Co, Cs, Ag and Hf. The second-tier dose-rate producing activators are Cr, Mo, Ni, Fe, Ti, Nb, Cu, Ca and Mn. The lowest dose-rate producing activator elements are Si, Mg and Al. Note that Mn activates intensely to produce very high dose-rates in the first few hours, but at a cooling time

of 10 days the radioisotope Mn-56 (half-life 2.5789 h), which is responsible for this phenomenon, has decayed to negligible activities.

5.7.2 Plots of Activities and Dose-Rates for the NRAD irradiation scenario

NRAD_1d_30d_1E9

The time-dependence $A(t)$ of the activities induced by the neutron irradiation of selected elements, for scenario **NRAD_1d_30d_1E9**, are shown in Figure 30.

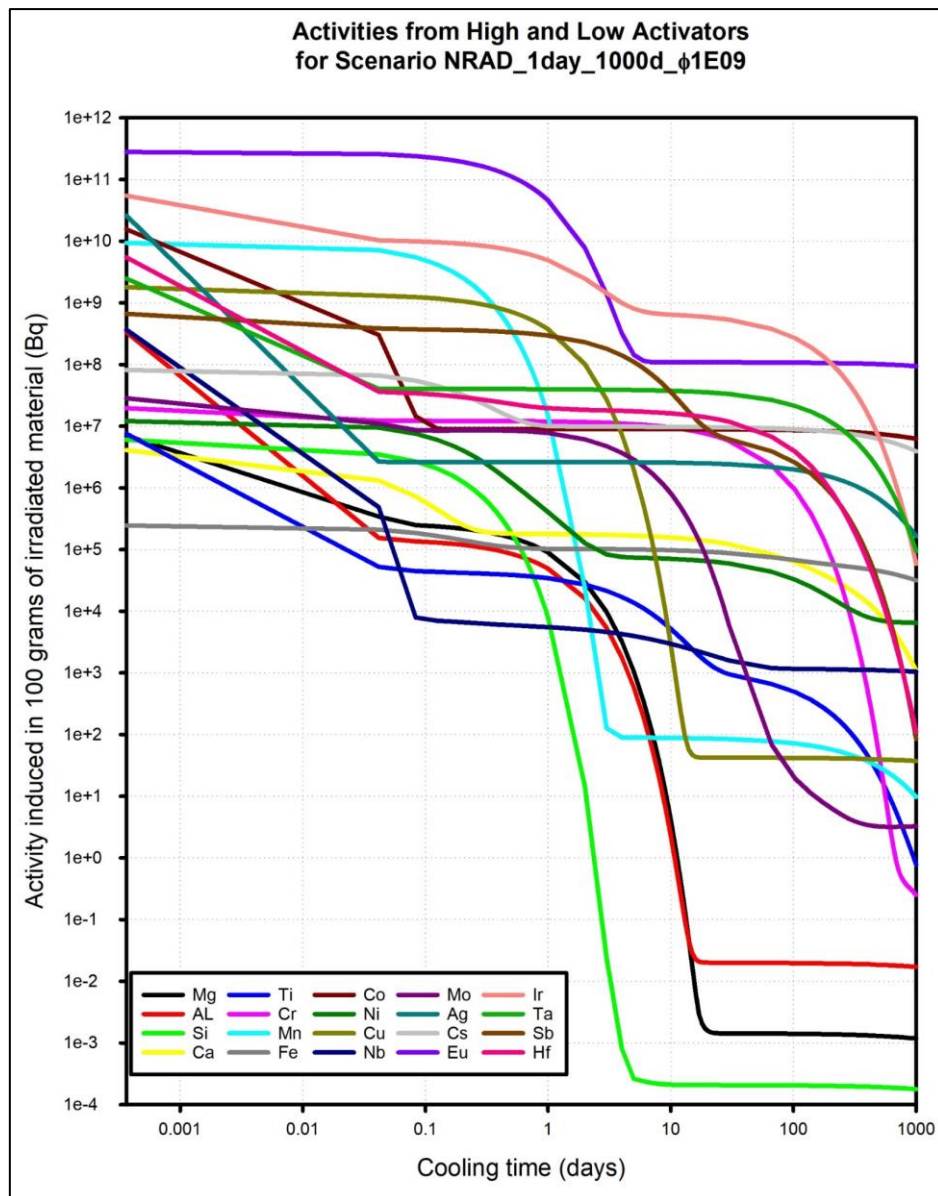


Figure 30: Activities produced by the neutron irradiation of selected elements, for a neutron radiography (NRAD) irradiation scenario **NRAD_1d_30d_1E9**

In Figure 30 the top-tier activating elements for scenario `NRAD_1d_30d_1E9`, from the viewpoint of the induced activity $A(t)$, evaluated at $T_{cool} = 10$ days, are Eu, Co, Cs, Cr, Ag and Mo. The second-tier activators are Ca, Fe, Ni, Ti, Cu and Nd. The lowest activators are Mn, Mg, Al and Si.

Figure 31 displays the dose-rates at 1 m from 1 g masses of selected elements irradiated under scenario `NRAD_1d_30d_1E9`.

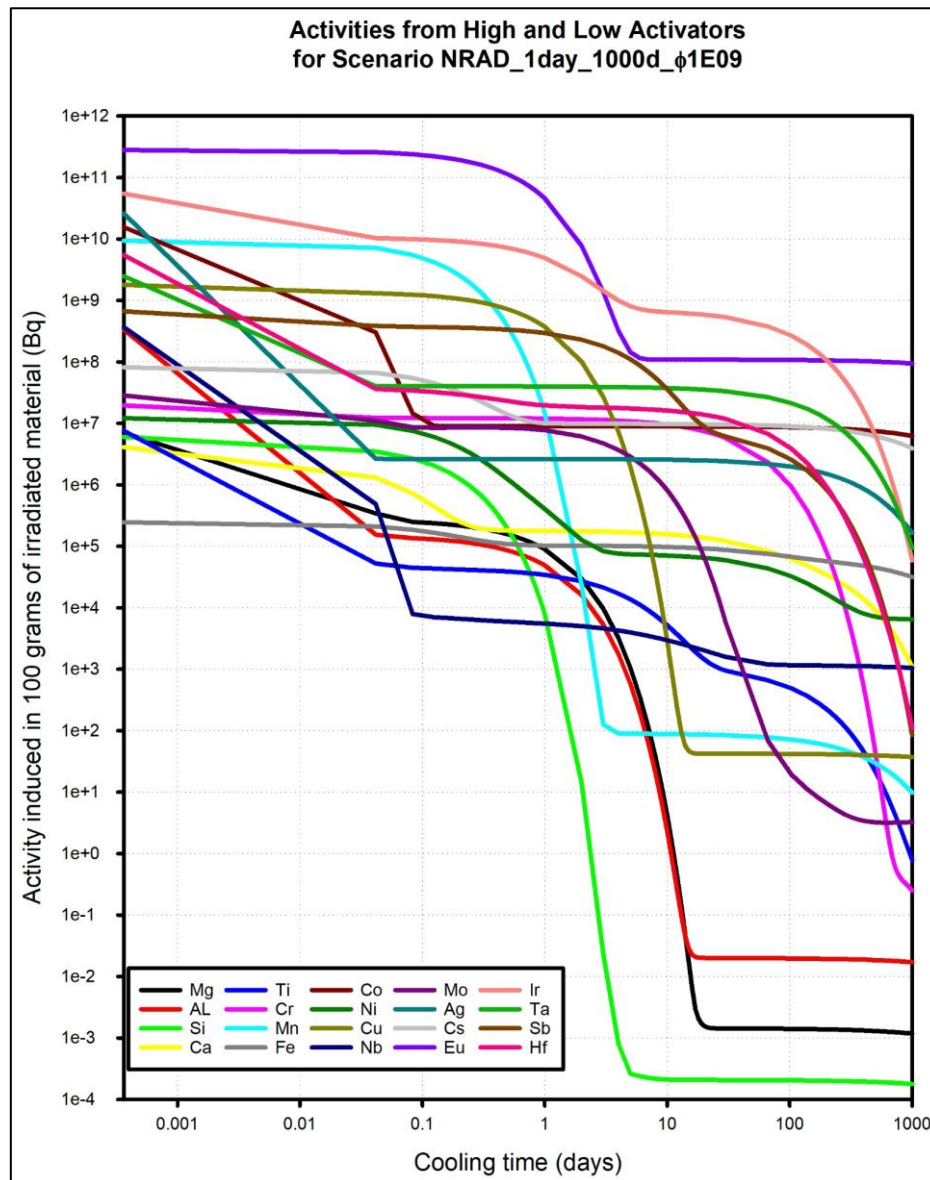


Figure 31: Dose-rates produced by the neutron irradiation of selected elements, for a neutron radiography irradiation scenario `NRAD_1d_30d_1E9`

In Figure 31 the top-tier activating elements for scenario `NRAD_1d_30d_1E9`, from the viewpoint of the dose-rate $DR(t)$, evaluated at a cooling time of 10 days, are Ir, Eu, Sb, Ta, Hf,

Co, Cs, Ag and Cr. The second-tier dose-rate producing activators are Mo, Ni, Fe, Ti, Nb, Cu, Ca and Mn. The lowest dose-rate producing activator elements are Mg, Al, and Si.

5.8 Research Question RQ_8 : Completeness of the Lists of High-Activator Chemical Elements and Problematic Activation Radionuclides

5.8.1 Defining the Completeness Issue

The literature survey identified a list of problematic, high-activator elements, along with a list of the most problematic radionuclides formed by neutron activation. These are summarised in Table 11 on page 55. The results of the exhaustive set of FISPACT-II neutron-activation calculation models — a separate model for every element in the periodic table, at many integral fluence-rates and for many irradiation scenarios — must now be used to test whether the above two lists — (1) problematic target-element and (2) problematic product-radionuclides — are complete, i.e. without omissions or “gaps”. This research question is called the “completeness issue”. Problematic radionuclides are characterised by (1) long half-lives, (2) the emission of penetrating ionising photons. If (3) such a radionuclide also belongs to an element that is a nutrient or a nutrient-analogue (e.g. B, C, Na, Mg, P, S, Cl, K, Ca, Cr, Mn, Fe, Cu, Zn, Se, Rb²³, Sr²⁴, Mo, I and Cs²⁵), clearance levels will be even more restrictive because the release of the radionuclide into the biosphere may or will eventually lead to its incorporation into the food-chain.

5.8.2 Addition #1: Ba as a Parent of Cs-137

During the investigation behind the completion of Table 11 on page 55, many pathway analysis calculations were performed with the code FISPACT-II and it was found that neutron

²³ Note by co-supervisor TjvR: Chemically, Rb mimics the nutrient K.

²⁴ Note by co-supervisor TjvR: Chemically, Sr mimics the nutrients Mg and Ca.

²⁵ Note by co-supervisor TjvR: Chemically, Cs mimics the nutrient K.

irradiation of Ba produces notable activities of the highly problematic radionuclide Cs-137 (half-life 30.08064 yr), via two nuclear reactions: (1) A fraction 89.2 % of Cs-137 is produced via the (n, p) reaction, $^{137}_{56}\text{Ba}(n, p)^{137}_{55}\text{Cs}$ while (2) 10.8 % of the Cs-137 is produced by (n, np) and (n, d) reactions on Ba-138. The natural abundance of Ba-137 is 11.23 % and that of Ba-138 is 71.7 % — cf. (Meija et al., 2016) and (Holden et al., 2018). Insight into the existence of this pathway for the production of Cs-137 from Ba is absent in the published literature. High levels of Ba are found in barite shielding concrete, which uses barite ore, which contains at least 80 % BaSO_4 . From this, it follows that barite concrete is not suitable for deployment in parts of the reactor building where notable neutron fluence-rates may be encountered, because it will lead to the formation of the problematic radionuclide Cs-137 in the concrete matrix. The use of barites concrete should be restricted to the shielding of sources of gamma-photons.

5.8.3 {Nuclide, Activity}-matrices or NA-matrices for Discrete Irradiation Scenarios

For each discrete irradiation scenario, every element has an associated characteristic activation matrix. By this is meant a {Nuclide-Activity}-matrix or $\{N, A\}$ -matrix of the radionuclides and their activities that will be present in the reference mass of 100 g i.e. 0.1 kg of target-material. A selection of $\{N, A\}$ activation matrices, all computed with FISPACT-II 3.00 using the reference LWR neutron energy spectrum $\phi_{LWR}(E)$, are now presented.

5.8.4 Activation Matrices for Selected Elements Under Irradiation Scenario

DECO_60yr_6yr_1E14

The $\{N, A\}$ *activation matrix* for the irradiation of 0.1 kg of the element magnesium (Mg), is shown in Table 30.

Table 30: Activation matrix for the element Mg, under irradiation scenario

DECO_60yr_6yr_1E14

Nuclide	Activity per 100 g	Half-Life
H3	2.2113E+06	12.32 yr
C14	4.3218E+03	5700 yr
Na22	1.3436E+01	2.6018 yr
Al26	3.5784E-02	7.17E5 yr

Magnesium is found as an important alloying element in all 5-series, all 6-series and all 7-series Al-alloys. At the SAFARI-1 reactor at Necsa, the core-box is manufactured of Al-5052

(SAFARI-1, 2005), while the Silicon Roller Assembly (SRA) deployed a few cms outside the core-box, inside the water-pool surrounding the reactor, uses Al-6261 and Al-6082 alloys (Van Rooyen, 2015). The top and bottom nozzles, more specifically termed *end-adaptors*, of SAFARI-1 fuel-assemblies, are manufactured from Al-6082 (SAFARI-1, 2005). Al-6082 contains circa 1.3 % Si and 1.2 % Mg, while Al-6261 contains circa 0.7 % Si and 1.0 % Mg. Al-5052 may contain up to 2.8 % Mg and must contain less than 0.25 % Si. The grid-plate of the SAFARI-1 reactor is manufactured from Al-alloy 2014, which contains in the order of 0.6 % Mg (Van Rooyen, 2019).

The radionuclides H-3 and C-14 — which are seen in Table 30 as activation radionuclides produced from neutron irradiation of Mg — emit no ionising photons, but only low-energy β -electrons, and enjoy reasonably liberal clearance-levels — see Table 1 on page 2; their presence in irradiated Mg is therefore of little concern from the perspective of the external dose-rate. However, the concentrations of H-3 and C-14 are far above the unconditional clearance levels set by the IAEA i.e. Mg irradiated at the fluence-rate under consideration, on the fixed decommissioning timescale used for the analysis, will have to be treated as radioactive waste and sent to a national disposal facility, because the half-life of H-3 is 12.32 years and that of C-14 is 5700 years. The nuclide Na-22 is a potentially problematic emitter of positrons, which will annihilate by producing 0.511 MeV gamma-rays; its half-life is 2.6 years. However, the induced activity is 134 Bq per 1000 g, which is 0.134 Bq/g, which is marginally above the unconditional clearance level of 0.1 Bq/g for Na-22. Waiting an additional year or two will enable the Na-22 in the irradiated Mg to reach the unconditional clearance level of 0.1 Bq/g. The last isotope in the above activation matrix is Al-26; in IAEA publications this is not a “listed” problematic radionuclide and its concentration of 3.6E-4 Bq/g is below any clearance-related radiological concerns.

The *Activation Matrix* for the irradiation of 0.1 kg of the element aluminium (Al), under irradiation scenario **DECO_60yr_6yr_1E14**, is shown in Table 31.

Table 31: Activation matrix for the element Al, under irradiation scenario **DECO_60yr_6yr_1E14**

Nuclide	Activity per 100 g	Half-Life
H3	3.0941E+07	12.32 yr
Al26	6.2025E+01	7.17E5 yr
P32	1.5605E-01	14.268 days

Nuclide	Activity per 100 g	Half-Life
Si32	1.5601E-01	153.0 yr
C14	3.1941E-02	5700 yr
Na22	1.4435E-02	2.6018 yr

Aluminium (Al) is the preferred engineering metal in MTR designs where internal temperatures at the metal-to-water interface do not exceed circa 110° C. In the SAFARI-1 reactor at Necsa, Al-alloys are used in the fuel-assemblies, for the core-box, the core grid-plate and the reactor tank.

Looking at the nuclides in Table 31, the presence of H-3 and C-14 is, as before, not problematic from an external dose-rate perspective, BUT the concentration of H-3 is 3.1E5 Bq/g, which exceeds the maximum unconditional clearance level of 1E4 Bq/g for this isotope, by a factor 31 — refer to Table 1 on page 2. The concentrations of all other radionuclides are far below the unconditional clearance levels as set by the IAEA and present no clearance-related issues.

The *Activation Matrix* for the irradiation of 0.1 kg of the element silicon (Si), under irradiation scenario **DECO_60yr_6yr_1E14**, is shown in Table 32.

Table 32: Activation matrix for the element Si, under irradiation scenario

DECO_60yr_6yr_1E14

Nuclide	Activity per 100 g	Half-Life
H3	5.7234E+05	12.32 yr
P32	2.1825E+04	14.268 days
Si32	2.1820E+04	153.0 yr
Cl36	3.0687E-01	3.01007E5 yr

Si is very abundant in ordinary concrete and is also found in many Al-alloys up to mass-percentages reaching as high as 4 %. None of the radionuclides in Table 32 exceeds the IAEA's unconditional clearance levels set forth in Table 1 on page 2, i.e. Si is a remarkably low-activator element.

The *Activation Matrix* for the irradiation of 0.1 kg of the element calcium (Ca), under irradiation scenario **DECO_60yr_6yr_1E14**, is shown in Table 33.

Table 33: Activation matrix for the element Ca, under irradiation scenario**DECO_60yr_6yr_1E14**

Nuclide	Activity per 100 g	Half-Life
Ca41	5.3144E+09	9.9400E4 yr
Ar39	3.5917E+09	269.0 yr
Ca45	1.4577E+08	162.61 yr
H3	3.6005E+06	12.32 yr
Cl36	4.3094E+04	3.0130E5 yr
Sc46	2.1643E+04	83.80 d
K42	1.0560E+04	Effective: 32.9 yr
Ar42	1.0559E+04	32.9 yr
K40	9.1398E+03	1.24799861785E9 yr
Sc45m	2.7697E+03	Effective: 162.61 yr
P32	9.9113E+01	14.268 days
Si32	9.9087E+01	153.0 yr
S35	6.0665E+01	87.37 days

Ca is prevalent in concrete, cement and grouting. Its “top” activation products reach very high activities but are very weak emitters of ionising radiation: Ca-41, Ar-39 and H-3 emit no gamma-photons and very low-energy, low-intensity electrons. Cl-36 produces annihilation photons (energy 0.511 MeV) from positron annihilation, but at a very low positron emission yield of only $Y = 1.38976E-4$. Ca-45 emits no ionising photons and only low-energy β -electrons at energies below 0.26 MeV. The first nuclide of note in Table 33 is Sc-46, which does emit intense and penetrating ionising photons at energies of 1.12055 MeV and 0.889277 MeV; however, the half-life of this radionuclide is short so that at $T_{cool} = 12$ yr it has essentially decayed away. K-42 is also an emitter of intense ionising photons, with energy 1.5246 MeV and a positron emission-yield of 0.1808, i.e. 18.08 %. It must be kept in mind that the half-life of K-42 is very short (12.4 h), but it is a transition-product of its precursor-isotope Ar-42 so that K-42 will take on the effective half-life of its longer-lived precursor (32.9 yr). Ar-42 does not emit any photons. Furthermore, the long-lived noble-gas isotope Ar-42 will tend to diffuse out of the concrete or cement so that the realistic activity concentrations of Ar-42 and K-42 will be somewhat lower than the values listed in Table 33. Sc-45m emits only exceedingly feeble ionising radiation — the maximum emitted photon energy is only 12.4 keV

and the emission yield is very low at circa 0.24 %. None of the nuclides listed in Table 33 exceeds the IAEA's explicit clearance level criteria.

The presence of two radionuclides in Table 33 requires some clarification: Sc-46 and Cl-36.

FISPACT-II gives the following pathway information for the formation of the radionuclide Sc-46 (half-life 83.8 days) from the irradiation of elemental Ca:

path 1	2.060%	Ca 43	---(R)---	Ca 44	---(R)---	Ca 45	---(d)---	Sc 45	---(R)---	Sc 46	---(S)---
			100.00%(n,g)		100.00%(n,g)		100.00%(b-)		100.00%(n,g)		
path 2	0.602%	Ca 43	---(R)---	Ca 44	---(R)---	Ca 45	---(d)---	Sc 45	---(R)---	Sc 46m	---(b)---
---(S)---			100.00%(n,g)		100.00%(n,g)		100.00%(b-)		100.00%(n,g)		100.00%(IT)
											0.00%(n,E)
											0.00%(n,n)
path 3	74.751%	Ca 44	---(R)---	Ca 45	---(d)---	Sc 45	---(R)---	Sc 46	---(S)---		
			100.00%(n,g)		100.00%(b-)		100.00%(n,g)				
path 4	21.854%	Ca 44	---(R)---	Ca 45	---(d)---	Sc 45	---(R)---	Sc 46m	---(b)---	Sc 46	---(S)---
			100.00%(n,g)		100.00%(b-)		100.00%(n,g)		100.00%(IT)		
											0.00%(n,E)
											0.00%(n,n)

FISPACT-II gives the following pathway information for the formation of the radionuclide Cl-36 (half-life 3.0130E5 yr) from the irradiation of elemental Ca:

Target nuclide Cl 36	99.015% of inventory given by 3 paths											
path 1	78.401%	Ca 40	---(R)---	Ca 41	---(R)---	Ar 38	---(R)---	S 35	---(d)---	Cl 35	---(R)---	Cl 36
---(L)---			100.00%(n,g)		100.00%(n,a)		100.00%(n,a)		100.00%(b-)		100.00%(n,g)	
												0.00%(n,pt)
path 2	18.637%	Ca 40	---(R)---	Ar 37	---(r)---	S 34	---(R)---	S 35	---(d)---	Cl 35	---(R)---	Cl 36
---(L)---			100.00%(n,a)		100.00%(n,a)		100.00%(n,g)		100.00%(b-)		100.00%(n,g)	
												0.00%(n,pt)
path 3	1.976%	Ca 40	---(R)---	Cl 36	---(L)---							
			100.00%(n,pa)									

This ends the analysis of the activation of the element Ca under irradiation scenario **DECO_60yr_6yr_1E14**.

The *Activation Matrix* for the irradiation of 0.1 kg of the element titanium (Ti), under irradiation scenario **DECO_60yr_6yr_1E14**, is shown in Table 34.

Table 34: Activation matrix for the element Ti, under irradiation scenario **DECO_60yr_6yr_1E14**

Nuclide	Activity per 100 g	Half-Life
H3	3.5311E+06	12.32 yr

Nuclide	Activity per 100 g	Half-Life
Ca45	3.5707E+05	162.61 yr
Sc46	1.7161E+03	83.80 d
Co60	1.4380E+03	5.2712 yr
Fe55	3.0596E+01	2.744 yr
K42	1.8748E+01	Effective: 32.9 yr
Ar42	1.8747E+01	32.9 yr
Mn54	1.0975E+01	312.2 d

Titanium (Ti) is an excellent engineering metal and its use is mainly limited by its high cost, compared to e.g. steel-alloys.

The two radionuclides of note in Table 34 are Sc-46, which does emit intense and penetrating ionising photons at energies of 1.12055 MeV and 0.889277 MeV, and a relatively small activity of Co-60. The activity of the Co-60 will keep the induced activity in the highly irradiated Ti above the unconditional clearance level, for a number of decades, i.e. Co-60 will be the limiting radionuclide activated in the target Ti, under irradiation scenario **DECO_60yr_6yr_1E14**.

In Table 34 and in the following few tables, the radioisotope Co-60 will figure prominently. Based on Table 1, Table 2 and Table 3, we assume its clearance level to be 1 g/cm⁻³.

The *Activation Matrix* for the irradiation of 0.1 kg of the element vanadium (V), under irradiation scenario **DECO_60yr_6yr_1E14**, is shown in Table 35.

Table 35: Activation matrix for the element vanadium (V), under irradiation scenario **DECO_60yr_6yr_1E14**

Nuclide	Activity (Bq) per 100 g	Half-Life
Co60	1.0010E+06	5.2712 yr
H3	5.5298E+05	12.32 yr
Fe55	1.3320E+04	2.744 yr
Mn54	3.6299E+03	312.2 d
V49	8.2328E+02	330 day
Ni63	1.7656E+01	101.2 yr
Co60m	1.8789E-01	Effective: 2.6E6 yr
Fe60	1.8789E-01	2.6E6 yr

In Table 35 it is clear that the level of induced activity of Co-60 in vanadium (V) irradiated under irradiation scenario **DECO_60yr_6yr_1E14**, will be approximately a factor 1E4 above the criterion for unconditional clearance, i.e. highly neutron irradiated vanadium alloys will present a long-term radioactivity burden and will have to be disposed of as radioactive waste.

Clearance-level criteria for the radionuclide Co-60 will only be met after the elapse of a certain time interval. We now derive a mathematical expression for the calculation of this time-interval. Let A_{Co60} be the total activity of Co-60 in the irradiated sample, and let M be the sample's mass. Let CL_{Co60} be the clearance-level (1 Bq/g) for Co-60. Let N be the number of half-lives that must pass before the clearance-level criterion is met. The required number of half-lives, N is then calculated by solving for N in Eq. (7).

$$\left(\frac{1}{2}\right)^N = \left(\frac{CL_{Co60}}{\left(\frac{A_{Co60}}{M}\right)}\right) \quad \text{Eq. (7)}$$

The MathCAD implementation of the expression in Eq. (7) is shown in Figure 32.

Cooling time required for Co-60 to meet Clearance Levels

Given

$$\left(\frac{1}{2}\right)^{NN} = \frac{CL_{Co60}}{\left(\frac{A_{Co60}}{M}\right)}$$

$$\text{Find}(NN) \rightarrow \log\left(\frac{CL_{Co60} \cdot M}{A_{Co60}}, \frac{1}{2}\right)$$

$A_{Co60} := 1.0010E+06 \cdot Bq$

$M := 100 \cdot gm$

$CL_{Co60} := 1 \cdot \frac{Bq}{gm}$

$T_{halfCo60} := 5.27124 \cdot yr$

$$T_{cool} := \log\left(\frac{CL_{Co60} \cdot M}{A_{Co60}}, \frac{1}{2}\right) \cdot T_{halfCo60}$$

Required cooling time:

$\frac{T_{cool}}{yr} = 70.1$

Figure 32: Mathcad-14 implementation of Eq. (7) (page 154) — calculation of the cooling time required to meet regulatory clearance levels

Clearance level criteria for the radionuclide Co-60 will only be met after approximately $T_{cool} \approx 71$ years of storage.

The *Activation Matrix* for the irradiation of 0.1 kg of the element chromium (Cr), under irradiation scenario **DECO_60yr_6yr_1E14**, is shown in Table 36.

Table 36: Activation matrix for the element chromium (Cr), under irradiation scenario **DECO_60yr_6yr_1E14**

Nuclide	Activity (Bq) per 100 g	Half-Life
Co60	1.6065E+08	5.2712 yr
Fe55	6.2993E+05	2.744 yr

Nuclide	Activity (Bq) per 100 g	Half-Life
H3	2.4848E+05	12.32 yr
V49	1.5660E+05	330 day
Mn54	8.4008E+04	312.2 d
Ni63	7.0803E+03	101.2 yr
Co60m	2.9036E+01	Effective: 2.6E6 yr
Fe60	2.9036E+01	2.6E6 yr

In Table 36 it is clear that the level of induced activity of Co-60 in chromium (Cr) under irradiation scenario **DECO_60yr_6yr_1E14**, will be a factor 1.6065E6 above the criterion for unconditional clearance, i.e. highly neutron irradiated chromium alloys will present a long-term radioactivity burden and will have to be disposed of as radioactive waste. Using Eq. (7) (page 154) it is calculated that unconditional clearance-level criteria for Co-60 will only be reliably met after a cooling period of approximately $T_{cool} \approx 110$ years of storage.

The *Activation Matrix* for the irradiation of 0.1 kg of the element manganese (Mn), irradiated under irradiation scenario **DECO_60yr_6yr_1E14**, is shown in Table 37.

Table 37: Activation matrix for the element manganese (Mn), under irradiation scenario **DECO_60yr_6yr_1E14**

Nuclide	Activity (Bq) per 100 g	Half-Life
Co60	2.5232E+11	5.2712 yr
Fe55	2.3027E+08	2.744 yr
Ni63	2.4168E+07	101.2 yr
Mn54	5.7945E+06	312.2 d
H3	2.9268E+06	12.32 yr
Co60m	4.6097E+04	Effective: 2.6E6 yr
Fe60	4.6097E+04	2.6E6 yr
Ni59	10.114	7.60017E4 yr
Zn65	6.3274	243.92998 d

In Table 37 it is clear that the level of induced activity of Co-60 in manganese (Mn) irradiated under decommissioning scenario 1, will be a factor 2.523E9 above the criterion for unconditional clearance, i.e. highly neutron irradiated manganese alloys will present a long-term radioactivity burden and will have to be disposed of as radioactive waste. Using Eq. (7)

(page 154) it is calculated that unconditional clearance-level criteria for Co-60 will only be reliably met after a cooling period of approximately $T_{cool} \approx 165$ years of storage.

The *Activation Matrix* for the irradiation of 0.1 kg of the element iron (Fe), irradiated under irradiation scenario **DECO_60yr_6yr_1E14**, is shown in Table 38.

Table 38: Activation matrix for the element iron (Fe), under irradiation scenario **DECO_60yr_6yr_1E14**

Nuclide	Activity (Bq) per 100 g	Half-Life
Fe55	1.4005E+12	2.744 yr
Co60	9.3873E+11	5.2712 yr
Ni63	2.8663E+08	101.2 yr
Mn54	2.5882E+08	312.2 d
H3	6.1189E+05	12.32 yr
Co60m	1.9071E+05	Effective: 2.6E6 yr
Fe60	1.9071E+05	2.6E6 yr
Mn53	2.1362E+02	3.70008E6 yr
Zn65	1.3811E+02	243.92998 d
Ni59	6.4094E+01	7.60017E4 yr

The level of induced activity of Co-60 in a reference mass of iron (Fe) irradiated under irradiation scenario **DECO_60yr_6yr_1E14**, will be a factor 9.387E10 above the criterion for unconditional clearance, i.e. highly neutron irradiated Steel-alloys will present a long-term radioactivity burden and will have to be disposed of as radioactive waste. Using Eq. (7) (page 154) it is calculated that unconditional clearance-level criteria for Co-60 will only be reliably met after a cooling period of approximately $T_{cool} \approx 175$ years of storage.

The *Activation Matrix* for the irradiation of a reference mass of 0.1 kg of the element cobalt (Co), under irradiation scenario **DECO_60yr_6yr_1E14**, is shown in Table 39.

Table 39: Activation matrix for the element cobalt (Co), under irradiation scenario **DECO_60yr_6yr_1E14**

Nuclide	Activity (Bq) per 100 g	Half-Life
Co60	2.4182E+14	5.2712 yr
Ni63	9.8533E+12	101.2 yr
H3	1.4105E+07	12.32 yr

Nuclide	Activity (Bq) per 100 g	Half-Life
Zn65	1.0147E+07	243.92998 d
Co60m	8.1845E+05	Effective: 2.6E6 yr
Fe60	8.1845E+05	2.6E6 yr
Ni59	5.4420E+05	7.60017E4 yr
Fe55	2.3852E+03	2.744 yr

The level of induced activity of Co-60 in cobalt (Co) irradiated under irradiation scenario **DECO_60yr_6yr_1E14**, will be a factor 2.418E12 above the criterion for unconditional clearance, i.e. highly neutron irradiated cobalt-based alloys will present a long-term radioactivity burden and will have to be disposed of as radioactive waste. Using Eq. (7) (page 154) it is calculated that unconditional clearance-level criteria for Co-60 will only be reliably met after a cooling period of approximately $T_{cool} \approx 220$ years of storage.

The *Activation Matrix* for the irradiation of a reference mass of 0.1 kg of the element nickel (Ni) under irradiation scenario **DECO_60yr_6yr_1E14**, is shown in Table 40.

Table 40: Activation matrix for the element Nickel (Ni), under irradiation scenario **DECO_60yr_6yr_1E14**

Nuclide	Activity (Bq) per 100 g	Half-Life
Ni63	1.8357E+13	101.2 yr
Co60	3.1666E+12	5.2712 yr
Ni59	7.1272E+10	7.60017E4 yr
Fe55	5.6272E+10	2.744 yr
Zn65	1.4315E+08	243.92998 d
Co57	6.8623E+07	271.74005 d
H3	1.6433E+07	12.32 yr
Mn54	8.3229E+04	312.2 d
Co60m	2.7878E+04	Effective: 2.6E6 yr
Fe60	2.7878E+04	2.6E6 yr
Co58	9.3821E+02	70.86 d

The level of induced activity of Co-60 in Ni irradiated under scenario **DECO_60yr_6yr_1E14**, will be a factor 3.167E11 above the criterion for unconditional clearance, i.e. highly neutron irradiated Ni-rich alloys such as SS-316L or NA-690 will present a long-term radioactivity burden and will have to be disposed of as radioactive waste. For the irradiated Ni-alloys,

unconditional clearance level criteria for Co-60 will only be reliably met after circa 200 years of storage at a national radioactive waste-disposal facility.

5.8.5 A Shorter Route to Answer Research Question RQ_8 — the Completeness Issue

The above “activation matrix” analysis method proved to be too cumbersome and slow to serve as a practical, quick analysis-tool to ascertain the completeness of the list of (1) problematic radionuclides and (2) problematic target-materials, which we have called Research Question RQ_8 .

To answer the “completeness issue” of Research Question RQ_8 within a tolerable time, a calculational experiment was designed. As a first step, the (72) elements that will be readily encountered in metal alloys, metal oxides and concretes used in the high neutron fluence-rate zones at a nuclear reactor facility, were identified as being H, Li, Be, B, C, N, O, F, Na, Mg, Al, Si, P, S, Cl, K, Ca, Ti, V, Cr, Mn, Fe, Co, Ni, Cu, Zn, Ga, Ge, As, Se, Sr, Zr, Nb, Mo, Ru, Rh, Pd, Ag, Cd, In, Sn, Sb, Te, I, Cs, Ba, La, Ce, Pr, Nd, Sm, Eu, Gd, Tb, Dy, Ho, Er, Tm, Yb, Lu, Hf, Ta, W, Re, Os, Ir, Pt, Au, Hg, Tl, Pb And Bi. Next, an “importance-weighting factor for use in engineering materials” with values restricted to the set {1, 5, 10, 25, 100} was allocated to each of the above elements. Elements such as C, O, Al, Cr, Fe, Ni and Zr received a weight of 100; elements such as Be, B, Mg, Ca, Ti, Mo, Cd, In, Si and Ba received a weight of 25, etc. Rare-earth elements, as well as uncommon elements such as Ga, Ge, As, Se, Re, Os, Ir and Pt, received a weight of 1. The composite 72-element material shown in Table 41 that contains “all important elements weighted according to usage” was now prepared for an irradiation scenario **DECO_60yr_6yr_1E10** calculation using FISPACT-II. The integral fluence-rate $\phi = 10^{10} \text{ cm}^{-2} \text{ s}^{-1}$ was selected to be representative of conditions in e.g. the reactor pressure vessel (RPV) and the reactor pressure vessel head (RPVH) at a PWR, as well as in the most highly irradiated concrete zones adjacent to the RPV at such a facility.

Table 41: FISPACT-II material input for the calculational experiment designed to identify problematic long-lived radionuclides produced at LWR facilities

MASS	0.10	72
H	1.14574E-01	
LI	1.14574E-01	
BE	2.86435E+00	
B	2.86435E+00	
C	2.86435E+00	
N	1.14574E-01	
O	1.14574E+01	

F	1.14574E-01
NA	1.14574E-01
MG	2.86435E+00
AL	1.14574E+01
SI	1.14574E+01
P	1.14574E-01
S	1.14574E-01
CL	1.14574E-01
K	1.14574E-01
CA	1.14574E+00
TI	1.14574E+00
V	1.14574E+00
CR	1.14574E+01
MN	1.14574E+00
FE	1.14574E+01
CO	1.14574E-01
NI	2.86435E+00
CU	1.14574E+00
ZN	5.72869E-01
GA	1.14574E-01
GE	1.14574E-01
AS	1.14574E-01
SE	1.14574E-01
SR	1.14574E+00
ZR	1.14574E+01
NB	1.14574E+00
MO	1.14574E+00
RU	1.14574E-02
RH	1.14574E-02
PD	1.14574E-02
AG	1.14574E-01
CD	1.14574E+00
IN	1.14574E+00
SN	1.14574E-01
SB	1.14574E-01
TE	1.14574E-02
I	1.14574E-02
CS	1.14574E-01
BA	1.14574E+00
LA	1.14574E-02
CE	1.14574E-02
PR	1.14574E-02
ND	1.14574E-02
SM	1.14574E-02
EU	1.14574E-02
GD	1.14574E-02
TB	1.14574E-02
DY	1.14574E-02
HO	1.14574E-02
ER	1.14574E-02
TM	1.14574E-02
YB	1.14574E-02
LU	1.14574E-02
HF	1.14574E-01
TA	1.14574E-02
W	1.14574E-02
RE	1.14574E-02
OS	1.14574E-02
IR	1.14574E-02
PT	1.14574E-02

AU	1.14574E-01
HG	1.14574E-02
TL	1.14574E-02
PB	1.14574E+00
BI	1.14574E-02

The second column specifies the mass-% of each element and is required to add up to 100 %. The total mass of the irradiated 72-element sample is 0.1 kg i.e. 100 g.

The results of the FISPACT calculation is shown in Table 42. In the final column of this table, radio-isotopes that are far from reaching clearance-levels, are in red cells; isotopes that are marginally above clearance levels are in white cells, while isotopes that meet clearance levels are in green cells.

Table 42: Identification of problematic, long-lived radionuclides produced at LWR plants

Isotope	Activity (Bq)	Clearance level (Bq/g)	Activity per unit mass (Bq/g)	Radiological sentencing	Exceeds clearance level by a factor
H3	3.199E+09	25000	3.199E+07	Too high to be cleared	1.28E+03
Eu152	5.085E+08	2	5.085E+06	Too high to be cleared	2.54E+06
Co60	1.296E+08	1	1.296E+06	Too high to be cleared	1.30E+06
Ni63	3.151E+07	3000	3.151E+05	Too high to be cleared	1.05E+02
Eu154	2.985E+07	1.8	2.985E+05	Too high to be cleared	1.66E+05
Fe55	2.297E+07	1500	2.297E+05	Too high to be cleared	1.53E+02
Cs134	1.637E+07	1.6	1.637E+05	Too high to be cleared	1.02E+05
Sm151	1.199E+06	3200	1.199E+04	Too high to be cleared	3.75E+00
Cd113m	9.585E+05	100	9.585E+03	Too high to be cleared	9.59E+01
Nb93m	7.825E+05	1000	7.825E+03	Too high to be cleared	7.83E+00
C14	5.449E+05	770	5.449E+03	Too high to be cleared	7.08E+00
Eu155	3.320E+05	41	3.320E+03	Too high to be cleared	8.10E+01
Ni59	3.243E+05	7100	3.243E+03	May be disposed	4.57E-01
Tl204	2.561E+05	310	2.561E+03	Too high to be cleared	8.26E+00
Ag108m	2.116E+05	1.3	2.116E+03	Too high to be cleared	1.63E+03
Ba133	1.540E+05	10	1.540E+03	Too high to be cleared	1.54E+02
Nb94	1.247E+05	1.4	1.247E+03	Too high to be cleared	8.91E+02
Ho166m	6.893E+04	5	6.893E+02	Too high to be cleared	1.38E+02
Cl36	5.689E+04	15	5.689E+02	Too high to be cleared	3.79E+01
Tm171	4.255E+04	3200	4.255E+02	May be disposed	1.33E-01
Zn65	2.610E+04	6.3	2.610E+02	Too high to be cleared	4.14E+01
Ag110m	2.451E+04	1.3	2.451E+02	Too high to be cleared	1.89E+02
Ag108	1.925E+04	10	1.925E+02	Too high to be cleared	1.93E+01

Isotope	Activity (Bq)	Clearance level (Bq/g)	Activity per unit mass (Bq/g)	Radiological sentencing	Exceeds clearance level by a factor
Ca41	1.797E+04	10	1.797E+02	Too high to be cleared	1.80E+01
Pm147	1.664E+04	1000	1.664E+02	May be disposed	1.66E-01
Pt193	1.456E+04	100	1.456E+02	Too high to be cleared	1.46E+00
Ag109m	1.235E+04	10	1.235E+02	Too high to be cleared	1.24E+01
Cd109	1.235E+04	91	1.235E+02	Too high to be cleared	1.36E+00
Sb125	1.219E+04	5.2	1.219E+02	Too high to be cleared	2.34E+01
Pm145	1.134E+04	100	1.134E+02	Too high to be cleared	1.13E+00
Gd153	7.114E+03	31	7.114E+01	Too high to be cleared	2.29E+00
Mo93	6.894E+03	170	6.894E+01	May be disposed	4.06E-01
Sn121m	5.904E+03	10	5.904E+01	Too high to be cleared	5.90E+00
Sn121	4.582E+03	10	4.582E+01	Too high to be cleared	4.58E+00
Mn54	4.271E+03	3.7	4.271E+01	Too high to be cleared	1.15E+01
Te125m	2.986E+03	10	2.986E+01	Too high to be cleared	2.99E+00
Tb157	2.711E+03	10	2.711E+01	Too high to be cleared	2.71E+00
Zr93	6.094E+02	290	6.094E+00	May be disposed	2.10E-02
Tc99	5.220E+02	570	5.220E+00	May be disposed	9.16E-03
Be10	3.505E+02	100	3.505E+00	May be disposed	3.51E-02
Ag110	3.333E+02	10	3.333E+00	May be disposed	3.33E-01
Tm170	2.556E+02	660	2.556E+00	May be disposed	3.87E-03
Ca45	1.815E+02	1200	1.815E+00	May be disposed	1.51E-03
Sm145	1.725E+02	100	1.725E+00	May be disposed	1.73E-02
Sn119m	1.080E+02	100	1.080E+00	May be disposed	1.08E-02
Lu174	1.041E+02	100	1.041E+00	May be disposed	1.04E-02
Se79	9.337E+01	100	9.337E-01	May be disposed	9.34E-03
Ho163	9.037E+01	100	9.037E-01	May be disposed	9.04E-03
Tb158	5.071E+01	100	5.071E-01	May be disposed	5.07E-03
Nb91	4.250E+01	100	4.250E-01	May be disposed	4.25E-03
Eu150	3.916E+01	100	3.916E-01	May be disposed	3.92E-03
Co57	3.805E+01	30	3.805E-01	May be disposed	1.27E-02
Ir192	1.847E+01	9.2	1.847E-01	May be disposed	2.01E-02
Ir192n	1.835E+01	10	1.835E-01	May be disposed	1.84E-02
Rh102	1.640E+01	10	1.640E-01	May be disposed	1.64E-02
Ta182	1.343E+01	4.2	1.343E-01	May be disposed	3.20E-02
Re187	1.176E+01	10	1.176E-01	May be disposed	1.18E-02
V49	1.149E+01	10	1.149E-01	May be disposed	1.15E-02
Lu177m	9.526E+00	10	9.526E-02	May be disposed	9.53E-03
Se75	9.461E+00	14	9.461E-02	May be disposed	6.76E-03
Hf177m	7.373E+00	10	7.373E-02	May be disposed	7.37E-03
Re186	4.989E+00	10	4.989E-02	May be disposed	4.99E-03

Isotope	Activity (Bq)	Clearance level (Bq/g)	Activity per unit mass (Bq/g)	Radiological sentencing	Exceeds clearance level by a factor
Re186m	4.989E+00	10	4.989E-02	May be disposed	4.99E-03
Cs137	4.829E+00	3.7	4.829E-02	May be disposed	1.31E-02
Ba137m	4.557E+00	5	4.557E-02	May be disposed	9.11E-03
K40	4.416E+00	10	4.416E-02	May be disposed	4.42E-03
Na22	4.088E+00	1.1	4.088E-02	May be disposed	3.72E-02
Y90	3.542E+00	5	3.542E-02	May be disposed	7.08E-03
Sr90	3.541E+00	15	3.541E-02	May be disposed	2.36E-03
La137	3.466E+00	10	3.466E-02	May be disposed	3.47E-03
Lu177	2.246E+00	10	2.246E-02	May be disposed	2.25E-03
Hf178m	1.984E+00	10	1.984E-02	May be disposed	1.98E-03
Hf178n	1.984E+00	10	1.984E-02	May be disposed	1.98E-03
Sm147	1.411E+00	10	1.411E-02	May be disposed	1.41E-03

In Table 42, the clearance levels were either taken from Table 1, Table 2 or Table 3. Where no published values existed, an “educated guess” was made based on the following criteria: (1) Is the element a nutrient or a nutrient-analogue (see page 147) for which mammals will have a metabolic affinity and the (2) energies of emitted ionising radiations. The radionuclides that were found to exceed clearance limits, are summarised in Table 43 and are also colour-coded in four bins that indicate by which factor clearance levels are exceeded.

Table 43: Radionuclides found to exceed clearance limits in a DECO_60yr_6yr_1E10 irradiation-cooling scenario

Isotope	Exceeds clearance level by a factor
Eu152	2.54E+06
Co60	1.30E+06
Eu154	1.66E+05
Cs134	1.02E+05
Ag108m	1.63E+03
H3	1.28E+03
Nb94	8.91E+02
Ag110m	1.89E+02
Ba133	1.54E+02
Fe55	1.53E+02
Ho166m	1.38E+02

Isotope	Exceeds clearance level by a factor
Ni63	1.05E+02
Cd113m	9.59E+01
Eu155	8.10E+01
Zn65	4.14E+01
Cl36	3.79E+01
Sb125	2.34E+01
Ag108	1.93E+01
Ca41	1.80E+01
Ag109m	1.24E+01
Mn54	1.15E+01
Tl204	8.26E+00
Nb93m	7.83E+00
C14	7.08E+00
Sn121m	5.90E+00
Sn121	4.58E+00
Sm151	3.75E+00
Te125m	2.99E+00
Tb157	2.71E+00
Gd153	2.29E+00
Pt193	1.46E+00
Cd109	1.36E+00
Pm145	1.13E+00

The list of problematic radionuclides in Table 43 includes Eu-152, Co-60, Eu-154, Cs-134, Ag-108m, H-3, Nb-94, Ag-110m, Ba-133, Fe-55, Ho-166m, Ni-63, Cd-113m, Eu-155, Zn-65, Cl-36, Sb-125, Ag-108, Ca-41, Ag-109m and Mn-54 in the groups that will exceed clearance levels by more than a factor 10 after 6 years of cooling. Almost all these radionuclides have been identified in the research literature, except for Cd-113m, Ag-108 and Ag-109m. Attention will now turn to these three “newly emerged” candidate radionuclides.

According to a pathway & uncertainty analysis performed with FISPACT-II, the nuclide Cd-113m (half-life 14.1003 yr) is practically only formed from the irradiation of Cd by neutrons:

Target nuclide Cd113m	99.829% of inventory given by 2 paths

path	1	90.133%	Cd112	---(R)---	Cd113m---	(S)---
				100.00%(n,g)		
path	2	9.696%	Cd113	---(R)---	Cd113m---	(S)---
				100.00%(n,n)		

The element Cd is, however, not an important trace-element in engineering metals or concretes. In other words, Cd-113m will be confined to Cd-containing control-rods or control-assemblies, so that it will not normally be important.

Next, we turn to Ag-108. Its half-life is only 2.4 minutes, so it cannot possibly survive in isolation for more than 1 day. The reason for its presence is that it is the transition-product of the long-lived isotope Ag-108m (half-life 438.00844 years) which transitions to the radionuclide Ag-108 with a branching ratio of 8.7 %. Whenever and wherever Ag-108m is present, Ag-108 will also be present and will make a small addition to the dose-rate. The final “verdict” is that it is not necessary to list Ag-108 separately as a “problematic” radionuclide because it is a byproduct of the radioactive transition of Ag-108m. In other words, in irradiated materials that have cooled down for some time, Ag-108 will only be present if its precursor Ag-108m is also present.

The FISPACT calculation gives no pathway for the formation of the nuclide Ag-109m. With Ag present in the irradiated material, the activity of Ag-109m that was formed is 1.235E+04 Bq. By eliminating the element Ag from the irradiated material, the activity Ag-109m formed was only slightly lower at 7.117E3 Bq, i.e. the formation of Ag-109m is largely independent of the presence of initial Ag in the material. By now eliminating Cd from the initial composition of the irradiated material, the activity of Ag-109m fell to a low 32.44 Bq. It stands to reason that Ag-109 is mostly formed from the activation of Cd which is, as argued above, not an abundant trace-element in engineering materials.

As a result of the elimination of all 3 of the “new, additional candidates” for “long-lived, problematic” radionuclides, the list of problematic radionuclides identified by the calculational experiment, reduces to the list presented in Table 44.

Table 44: Final, verified list of radionuclides of highest concern, at times 6 years or longer after reactor shutdown, from the viewpoint of ease-of-clearance of long-term irradiated engineering materials

Radionuclide	Half-Life (yr)
Eu-152	13.525
Co-60	5.271
Eu-154	8.601
Cs-134	2.065
Ag-108m	418.01
H-3	12.32
Nb-94	2.04E4
Ag-110m	0.683875
Ba-133	10.551
Fe-55	2.744
Ho-166m	1200.0
Ni-63	101.202
Eu-155	4.753
Zn-65	0.668
Cl-36	3.013E5
Sb-125	2.759
Ca-41	9.94E4
Mn-54	0.855

All the problematic radionuclides listed in Table 44 have indeed been identified in published technical literature dealing with the decommissioning of LWR facilities — refer to the “red entries” in Table 11 on page 55. That is, there are no important radionuclides missing from our list of problematic, long-lived radionuclides that will be encountered in LWR decommissioning work. With this, Research Question RQ_8 has been answered, i.e. we have indeed, and in a demonstrable and defensible manner, arrived at a complete list of problematic, long-lived radionuclides that must be considered in reactor decommissioning work. This entails that Table 11 on page 55 is a comprehensive listing of all potentially problematic radioisotopes that may be encountered during decommissioning work. Table 44 (page 166) should be read as the most likely radionuclides that will be encountered in decommissioning practice, given that many chemical elements are not normally present in engineering materials, except as undesired trace elements.

5.9 Revisiting Research Question RQ_1 : Linearity or Non-Linearity

5.9.1 The Design of a Calculational Experiment to Probe the Linearity Issue

In the tables and graphs that summarise results about neutron activation, it consistently appears that neutron activation behaves linearly at low neutron fluence-rates, but non-linearly at high fluence-rates.

A calculational experiment was devised to investigate the question of linearity. Ten chemical elements — Ti, Cr, Mn, Fe, Co, Ni, Cu, Ag, Cs and Eu — were individually irradiated under seven irradiation scenarios, summarised in Table 45.

Table 45: Seven irradiation scenarios used to investigate whether neutron activation behaves linearly

Number	Irradiation Scenario
1	DECO_1yr_50yr_φ1E09
2	DECO_1yr_50yr_φ1E10
3	DECO_1yr_50yr_φ1E11
4	DECO_1yr_50yr_φ1E12
5	DECO_1yr_50yr_φ1E13
6	DECO_1yr_50yr_φ1E14
7	DECO_1yr_50yr_φ1E15

5.9.2 Linear and Non-Linear Neutron Activation Behaviour of Titanium (Ti)

When Ti is exposed to the neutron irradiation scenarios listed in Table 45, the activity ratios

$\left(\frac{A(t) \text{ for } \phi_{hi}}{A(t) \text{ for } \phi_{lo}}\right)$ behave as shown in the subsequent figures.

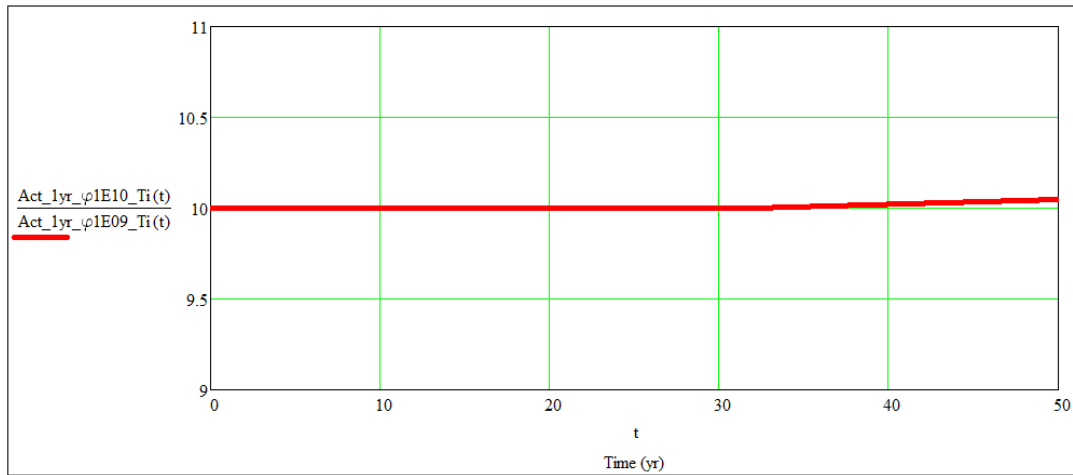


Figure 33: Ratio of activities $A(t)$ induced in Ti by neutron activation at $\phi = 1E10 \text{ cm}^{-2} \text{ s}^{-1}$ and at $\phi = 1E9 \text{ cm}^{-2} \text{ s}^{-1}$ i.e. in the low fluence-rate domain; a ratio of 10 indicates linear behaviour

Across the fluence-rate range from $\phi = 1E10 \text{ cm}^{-2} \text{ s}^{-1}$ through $\phi = 1E11 \text{ cm}^{-2} \text{ s}^{-1}$ through $\phi = 1E12 \text{ cm}^{-2} \text{ s}^{-1}$ to $\phi = 1E13 \text{ cm}^{-2} \text{ s}^{-1}$, the activation behaviour of Ti remains linear.

At $\phi = 1E14 \text{ cm}^{-2} \text{ s}^{-1}$ some initial evidence of the breakthrough of imminent non-linear activation behaviour is first observed — see Figure 34.

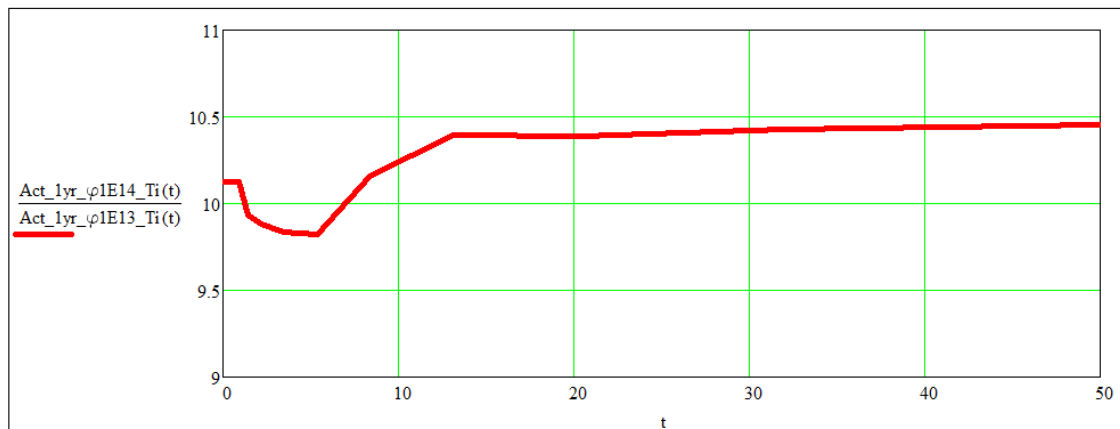


Figure 34: Ratio of activities $A(t)$ induced in Ti by neutron activation at $\phi = 1E14 \text{ cm}^{-2} \text{ s}^{-1}$ and at $\phi = 1E13 \text{ cm}^{-2} \text{ s}^{-1}$ i.e. in the medium-high fluence-rate domain; a ratio of 10 indicates linear behaviour

Above $\phi = 1E14 \text{ cm}^{-2} \text{ s}^{-1}$ the neutron activation behaviour of Ti suddenly becomes extremely non-linear, as is clear in Figure 35.

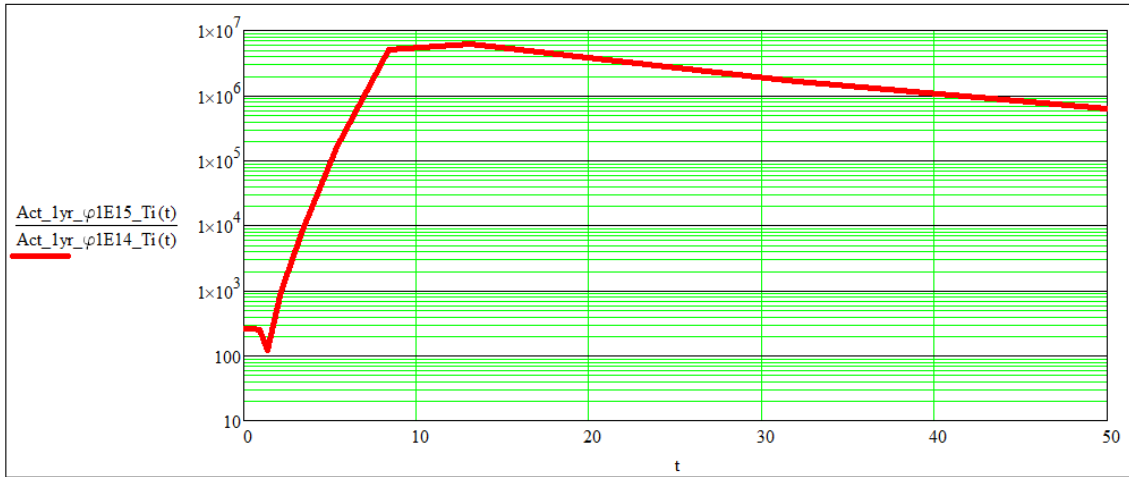


Figure 35: Ratio of activities $A(t)$ induced in Ti by neutron activation at $\phi = 1E15 \text{ cm}^{-2} \text{ s}^{-1}$ and at $\phi = 1E14 \text{ cm}^{-2} \text{ s}^{-1}$ i.e. in the high fluence-rate domain

It is clear that the neutron activation of Ti, over a duration of 1 year, behaves quite linearly up to a neutron fluence-rate of approximately $\phi = 1E14 \text{ cm}^{-2} \text{ s}^{-1}$. At higher fluence-rates, linear neutron-activation behaviour suddenly breaks down quite spectacularly when the fluence-rate becomes high enough to transmute Ti to V and then transmute V to Cr and then transmute Cr to Mn and then transmute Mn to Fe which then transmutes to stable Co-59 which subsequently activates to Co-60. In other words, the onset of the “chain-breeding” of Co-60 is sudden and marks the point of departure from linearity in the activation behaviour of the element Ti, as is seen in Figure 35.

5.9.3 Linear and Non-Linear Neutron Activation Behaviour of Chromium (Cr)

When the element Cr is exposed to the neutron irradiation scenarios listed in Table 45, the activity-ratios $\left(\frac{A(t) \text{ for } \phi_{hi}}{A(t) \text{ for } \phi_{lo}}\right)$ behave as shown in the following figures.

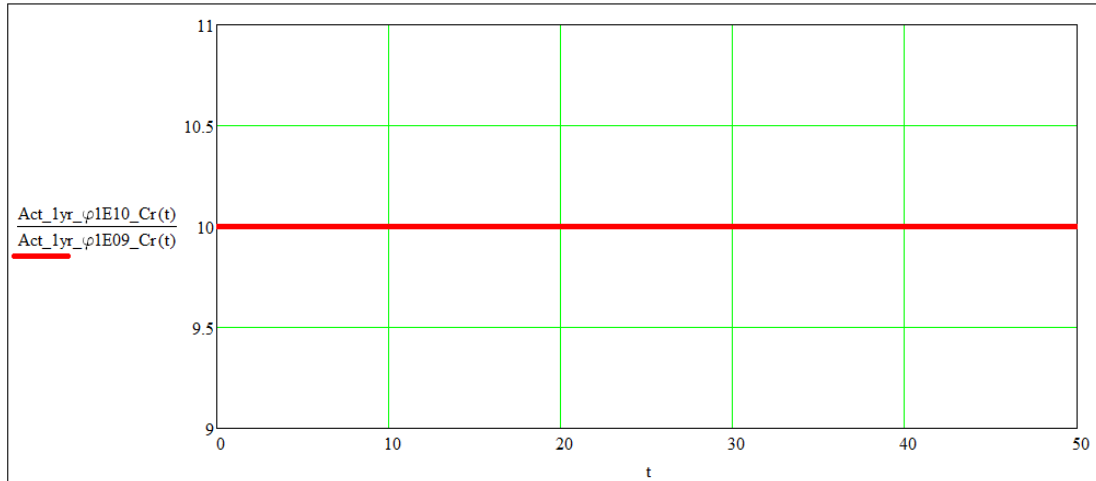


Figure 36: Ratio of activities A(t) induced in Cr by neutron activation at $\phi = 1E10 \text{ cm}^{-2} \text{ s}^{-1}$ and at $\phi = 1E9 \text{ cm}^{-2} \text{ s}^{-1}$ i.e. in the low fluence-rate domain; a ratio of 10 indicates linear behaviour

Across the fluence-rate range from $\phi = 1E10 \text{ cm}^{-2} \text{ s}^{-1}$ through $\phi = 1E11 \text{ cm}^{-2} \text{ s}^{-1}$ through $\phi = 1E12 \text{ cm}^{-2} \text{ s}^{-1}$ to $\phi = 1E13 \text{ cm}^{-2} \text{ s}^{-1}$, the activation behaviour of Cr remains linear.

At $\phi = 1E14 \text{ cm}^{-2} \text{ s}^{-1}$ some initial evidence of the breakthrough of imminent non-linear activation behaviour is first observed for the neutron-irradiation of Cr — see Figure 34.

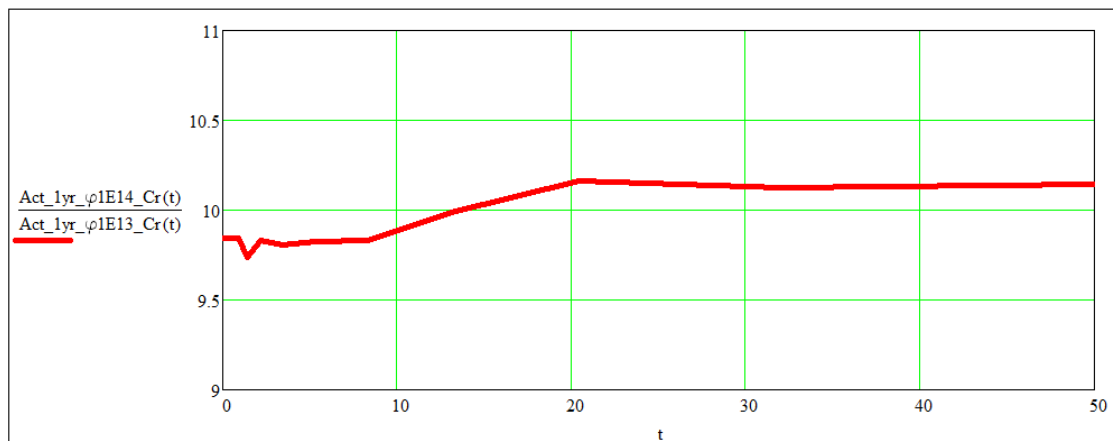


Figure 37: Ratio of activities A(t) induced in Cr by neutron activation at $\phi = 1E14 \text{ cm}^{-2} \text{ s}^{-1}$ and at $\phi = 1E13 \text{ cm}^{-2} \text{ s}^{-1}$ i.e. in the medium-high fluence-rate domain; a ratio of 10 indicates linear behaviour

Above $\phi = 1E14 \text{ cm}^{-2} \text{ s}^{-1}$ the neutron activation behaviour of Cr suddenly becomes completely non-linear, as is clear in Figure 35.

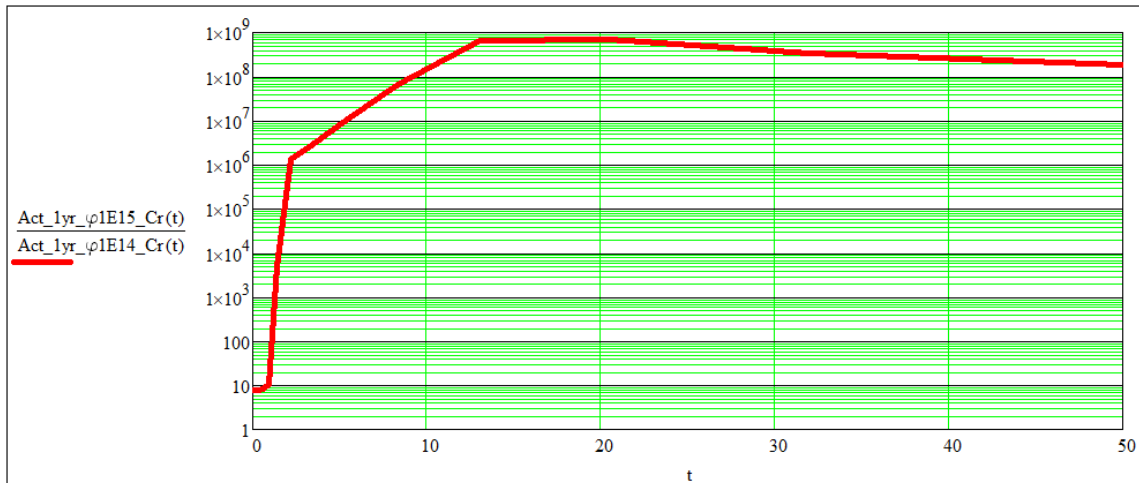


Figure 38: Ratio of activities $A(t)$ induced in Cr by neutron activation at $\phi = 1E15 \text{ cm}^{-2} \text{ s}^{-1}$ and at $\phi = 1E14 \text{ cm}^{-2} \text{ s}^{-1}$ i.e. in the high fluence-rate domain

It is clear that the neutron activation of Cr, over a duration of 1 year, behaves quite linearly up to a neutron fluence-rate of approximately $\phi = 1E14 \text{ cm}^{-2} \text{ s}^{-1}$. At higher fluence-rates, linear neutron-activation behaviour suddenly breaks down quite spectacularly when the fluence-rate becomes high enough to transmute Cr to Mn, then transmute Mn to Fe which then transmutes to stable Co-59 which subsequently activates to Co-60. In other words, the onset of the “chain-breeding” of Co-60 is sudden and marks the point of departure from linearity in the activation behaviour of the element Cr, as is seen in Figure 35.

5.9.4 Linear and Non-Linear Neutron Activation Behaviour of Manganese (Mn)

The neutron activation of the element Mn remains linear up to approximately $\phi = 1E12 \text{ cm}^{-2} \text{ s}^{-1}$. At $\phi = 1E13 \text{ cm}^{-2} \text{ s}^{-1}$ the non-linear behaviour shown in Figure 39 is observed.

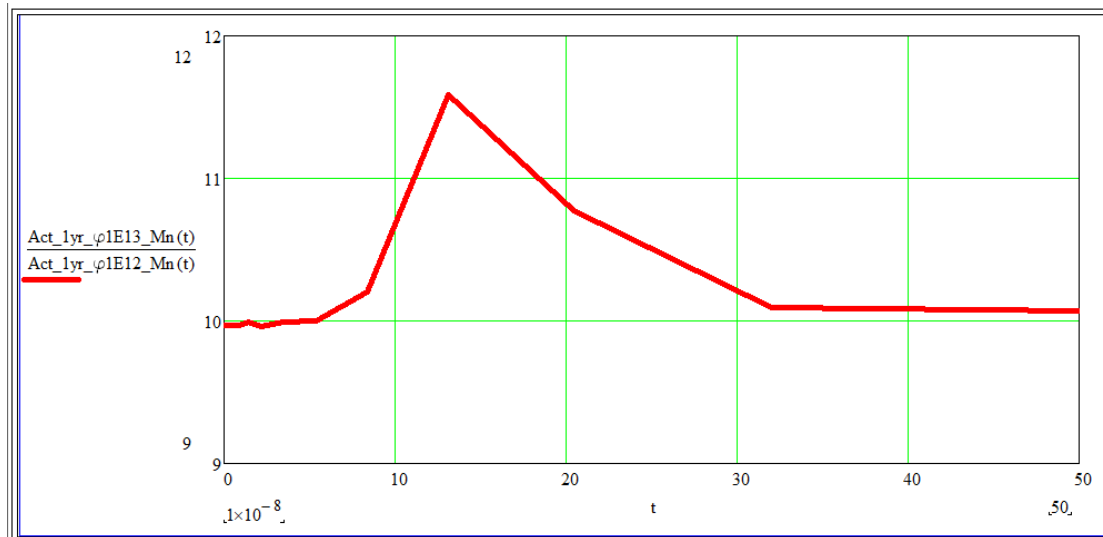


Figure 39: Ratio of activities $A(t)$ induced in Mn by neutron activation at $\phi = 1E13 \text{ cm}^{-2} \text{ s}^{-1}$ and at $\phi = 1E12 \text{ cm}^{-2} \text{ s}^{-1}$ i.e. in the intermediate fluence-rate domain; a ratio of 10 indicates linear behaviour

At $\phi = 1E14 \text{ cm}^{-2} \text{ s}^{-1}$ clearer evidence of increasingly stronger departure from linear activation behaviour is observed for the neutron-irradiation of Mn — see Figure 40.

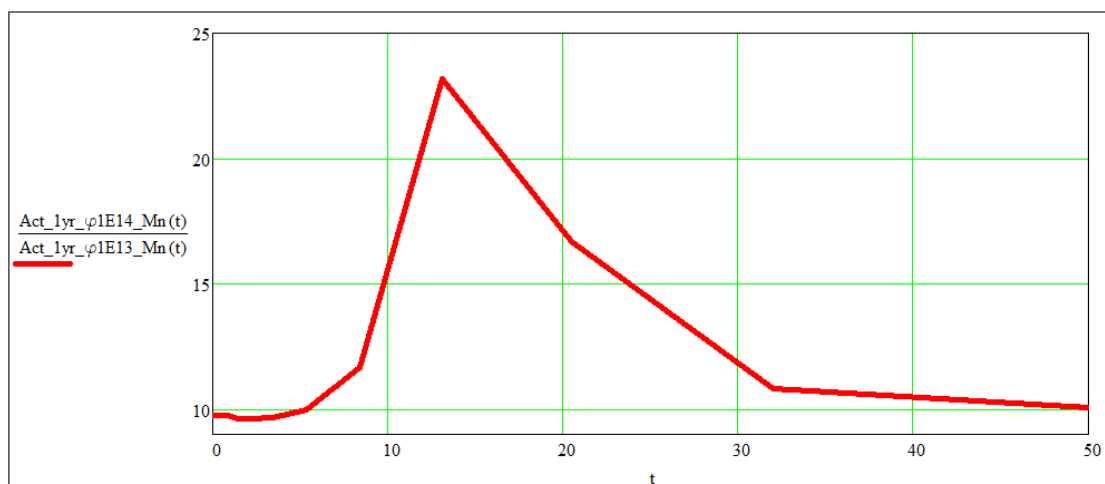


Figure 40: Ratio of activities $A(t)$ induced in Mn by neutron activation at $\phi = 1E14 \text{ cm}^{-2} \text{ s}^{-1}$ and at $\phi = 1E13 \text{ cm}^{-2} \text{ s}^{-1}$ i.e. in the medium-high fluence-rate domain; a ratio of 10 indicates linear behaviour

Above $\phi = 1E14 \text{ cm}^{-2} \text{ s}^{-1}$ the neutron activation behaviour of Mn suddenly becomes extremely non-linear, as is clear in Figure 41.

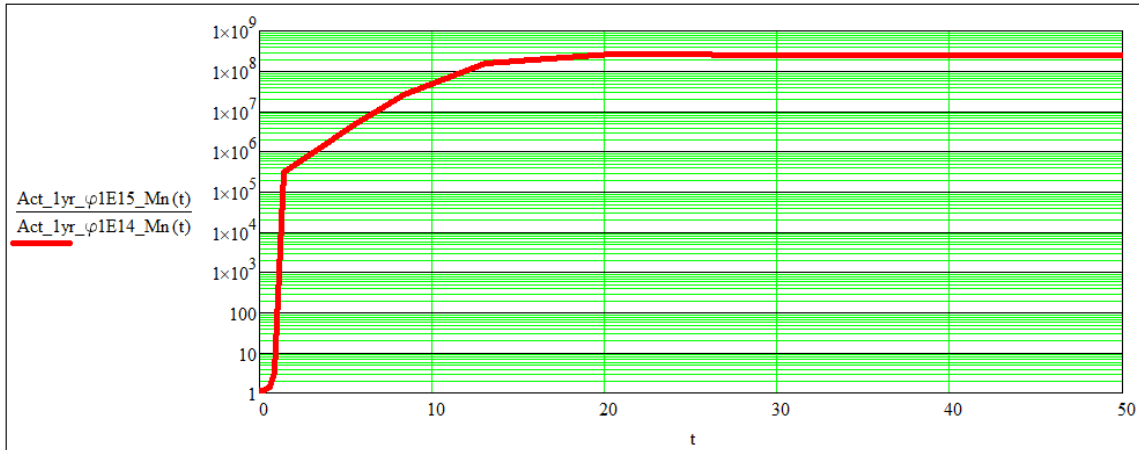


Figure 41: Ratio of activities $A(t)$ induced in Mn by neutron activation at $\phi = 1E15 \text{ cm}^{-2} \text{ s}^{-1}$ and at $\phi = 1E14 \text{ cm}^{-2} \text{ s}^{-1}$ i.e. in the high neutron fluence-rate domain

It is clear that the neutron activation of Mn, over a duration of 1 year, behaves reasonably linear up to a neutron fluence-rate of approximately $\phi = 1E13 \text{ cm}^{-2} \text{ s}^{-1}$, and later near-linear, up to a neutron fluence-rate of approximately $\phi = 1E14 \text{ cm}^{-2} \text{ s}^{-1}$. At higher fluence-rates, linear and near-linear neutron-activation behaviour suddenly breaks down quite spectacularly. The cause of the observed phenomenon is that very high neutron fluence-rates are capable of setting the following “chain-breeding” cascade in motion: The neutrons transmute stable Mn-55 to radioactive Mn-56 which quickly transitions to Fe-56 which then absorbs, in succession, 2 neutrons to become stable Fe-58 which absorbs a neutron to become radioactive Fe-59 which β -transitions (half-life: 44.495 days) to stable Co-59 which absorbs a neutron to activate to the long-lived radionuclide Co-60. In other words, the onset of the “chain-breeding” of Co-60 is sudden and marks the point of departure from linearity in the activation behaviour of the element Mn, as is seen in Figure 41.

5.9.5 Linear and Non-Linear Neutron Activation Behaviour of Iron (Fe)

The neutron activation of the element Fe remains linear up to $\phi = 1E13 \text{ cm}^{-2} \text{ s}^{-1}$. At $\phi = 1E14 \text{ cm}^{-2} \text{ s}^{-1}$ the slight non-linear behaviour shown in Figure 42 is observed.

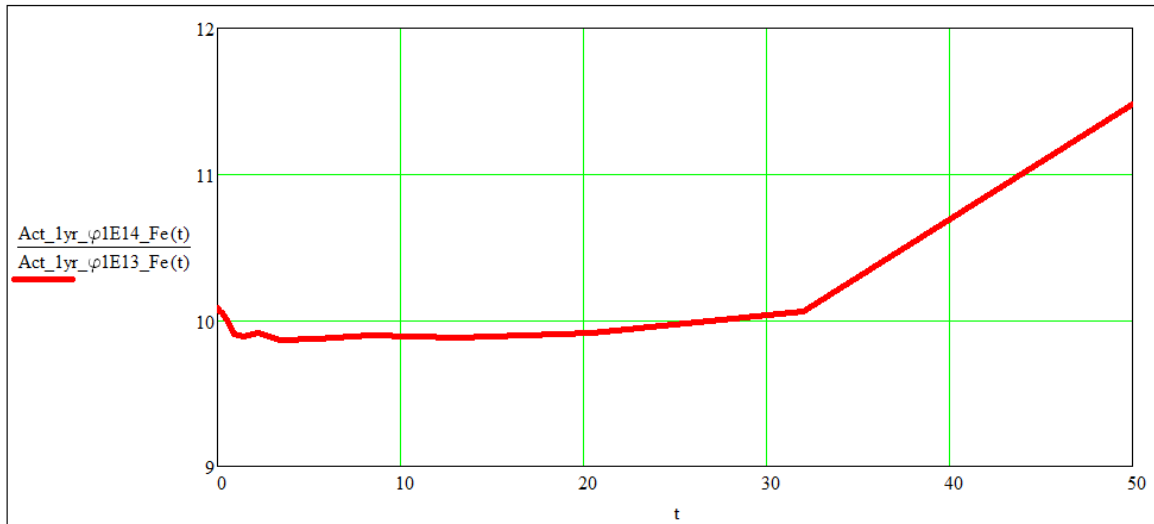


Figure 42: Ratio of activities $A(t)$ induced in Fe by neutron activation at $\phi = 1E14 \text{ cm}^{-2} \text{ s}^{-1}$ and at $\phi = 1E13 \text{ cm}^{-2} \text{ s}^{-1}$ i.e. in the medium-high fluence-rate domain; a ratio of 10 indicates linear behaviour

Above $\phi = 1E14 \text{ cm}^{-2} \text{ s}^{-1}$ the neutron activation behaviour of Fe suddenly becomes radically non-linear, as is clear in Figure 43.

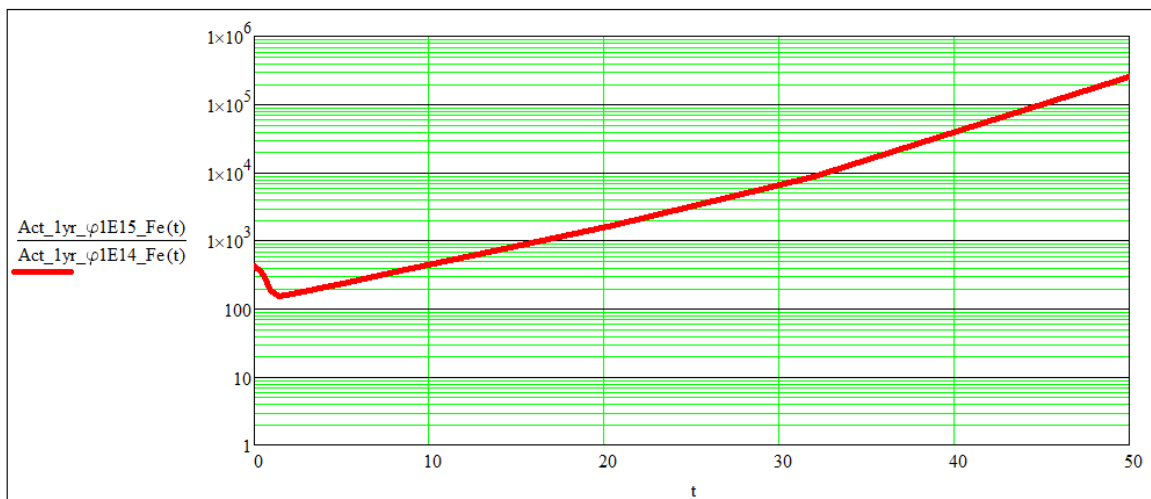


Figure 43: Ratio of activities $A(t)$ induced in Fe by neutron activation at $\phi = 1E15 \text{ cm}^{-2} \text{ s}^{-1}$ and at $\phi = 1E14 \text{ cm}^{-2} \text{ s}^{-1}$ i.e. in the high neutron fluence-rate domain; a ratio of 10 indicates linear activation behaviour

It is clear that the neutron activation of Fe, over a duration of 1 year, behaves reasonably linear and later off-linear, up to a neutron fluence-rate of approximately $\phi = 1E14 \text{ cm}^{-2} \text{ s}^{-1}$. At higher fluence -rates, linear or near-linear neutron-activation behaviour breaks down quite abruptly when the fluence-rate becomes high enough to transmute the stable isotopes of Fe to

stable Co-59 which subsequently activates to the long-lived radionuclide Co-60. In other words, the onset of the “chain-breeding” of Co-60 in irradiated Fe is sudden and marks the point of departure from linearity in the activation behaviour of the element Fe, as is seen in Figure 43.

5.9.6 Linear and Non-Linear Neutron Activation Behaviour of Cobalt (Co)

The neutron activation behaviour of the element Co is remarkably linear up to $\phi = 1E14 \text{ cm}^{-2} \text{ s}^{-1}$. At $\phi = 1E15 \text{ cm}^{-2} \text{ s}^{-1}$ some mild non-linear behaviour is observed, which is related to (1) the depletion of the reactant, Co, at high values of ϕ and (2) some “chain-breeding” of the long-lived radionuclide Ni-63 — see Figure 44.

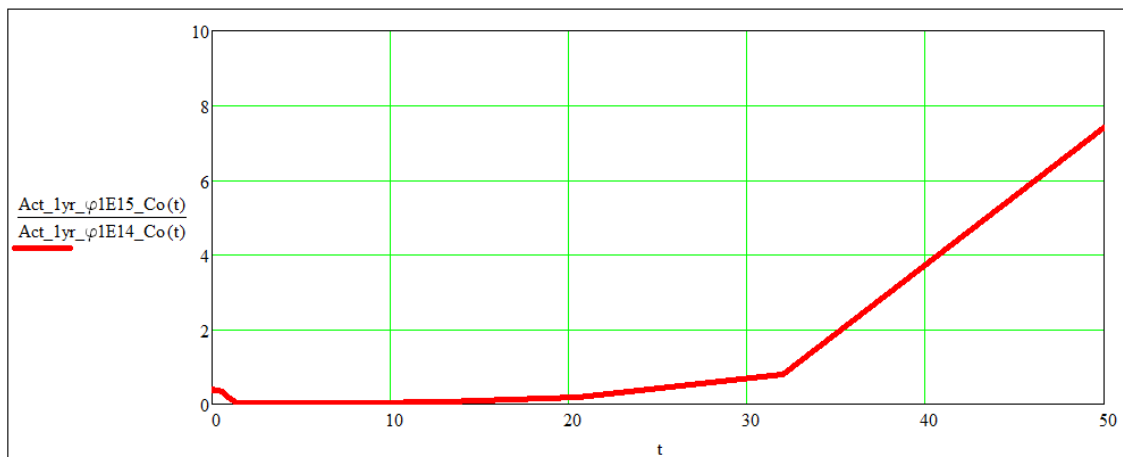


Figure 44: Ratio of activities A(t) induced in Co by neutron activation at $\phi = 1E15 \text{ cm}^{-2} \text{ s}^{-1}$ and at $\phi = 1E14 \text{ cm}^{-2} \text{ s}^{-1}$ i.e. in the high neutron fluence-rate domain; a ratio of 10 indicates linear activation behaviour

When 100 g Co is irradiated at $\phi = 1E15 \text{ cm}^{-2} \text{ s}^{-1}$ for 1 year, only a few milligrams of Co remains, while 64.3 g Ni, 21.76 g Cu and 21.666 g Zn will have been produced via transmutation.

5.9.7 Linear and Non-Linear Neutron Activation Behaviour of Nickel (Ni)

The neutron activation behaviour of Ni remains reasonably linear up to $\phi = 1E14 \text{ cm}^{-2} \text{ s}^{-1}$ but at $\phi = 1E15 \text{ cm}^{-2} \text{ s}^{-1}$ there is a significant departure from linearity, as seen in Figure 45.

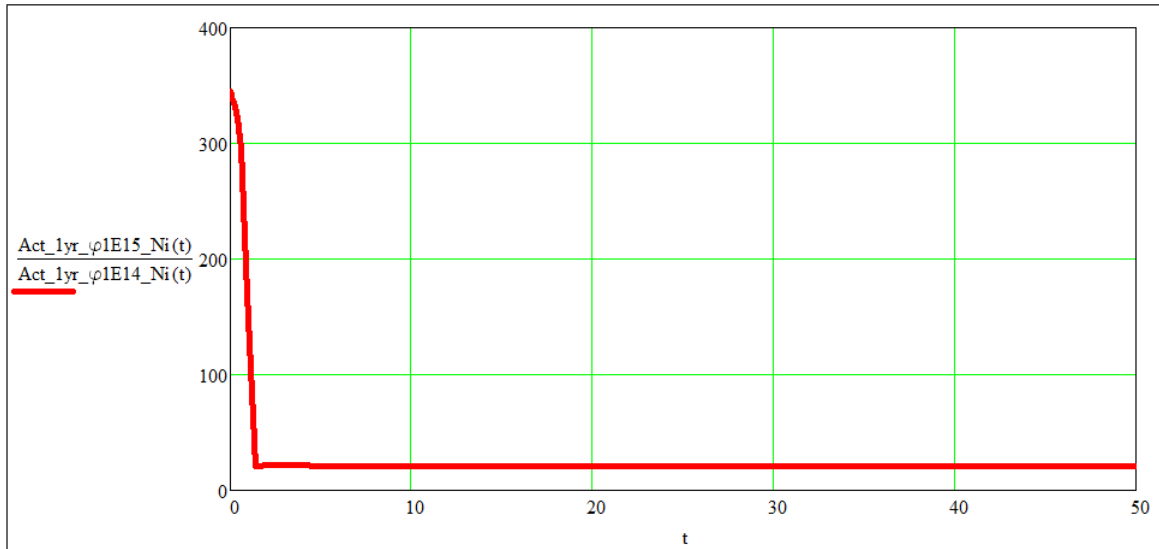


Figure 45: Ratio of activities $A(t)$ induced in Ni by neutron activation at $\phi = 1E15 \text{ cm}^{-2} \text{ s}^{-1}$ and at $\phi = 1E14 \text{ cm}^{-2} \text{ s}^{-1}$ i.e. in the high neutron fluence-rate domain; a ratio of 10 indicates linear behaviour

5.9.8 Linear and Non-Linear Neutron Activation Behaviour of Copper (Cu)

The neutron activation behaviour of Cu remains reasonably linear up to $\phi = 1E14 \text{ cm}^{-2} \text{ s}^{-1}$ but at $\phi = 1E15 \text{ cm}^{-2} \text{ s}^{-1}$ there is evidence of mild, temporally transient non-linearity, as seen in Figure 46.

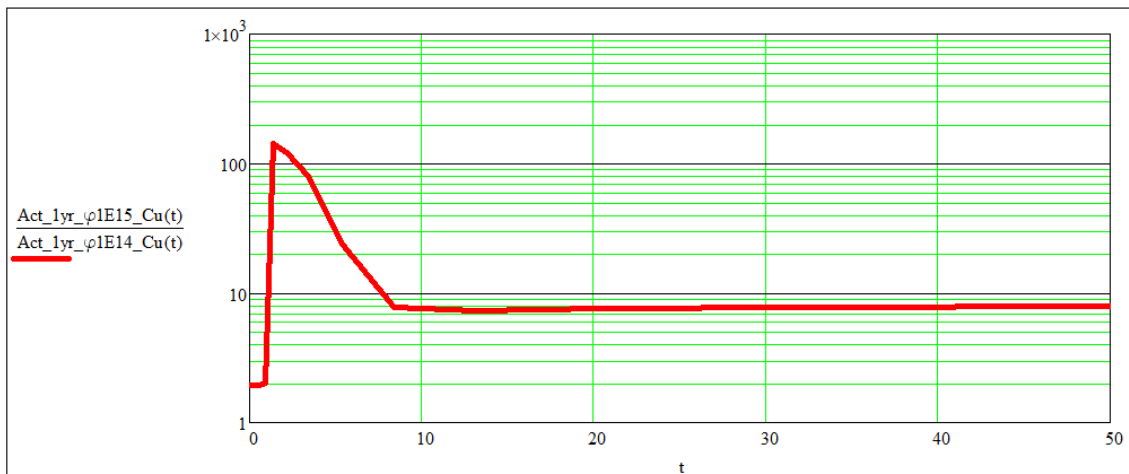


Figure 46: Ratio of activities $A(t)$ induced in Cu by neutron activation at $\phi = 1E15 \text{ cm}^{-2} \text{ s}^{-1}$ and at $\phi = 1E14 \text{ cm}^{-2} \text{ s}^{-1}$ i.e. in the high neutron fluence-rate domain; a ratio of 10 indicates linear activation behaviour

5.9.9 Linear and Non-Linear Neutron Activation Behaviour of Silver (Ag)

The neutron activation behaviour of Ag remains reasonably linear up to $\phi = 1E14 \text{ cm}^{-2} \text{ s}^{-1}$ but at $\phi = 1E15 \text{ cm}^{-2} \text{ s}^{-1}$ the reactant Ag becomes depleted, forcing depletion-driven sub-linear activation behaviour — see Figure 47.

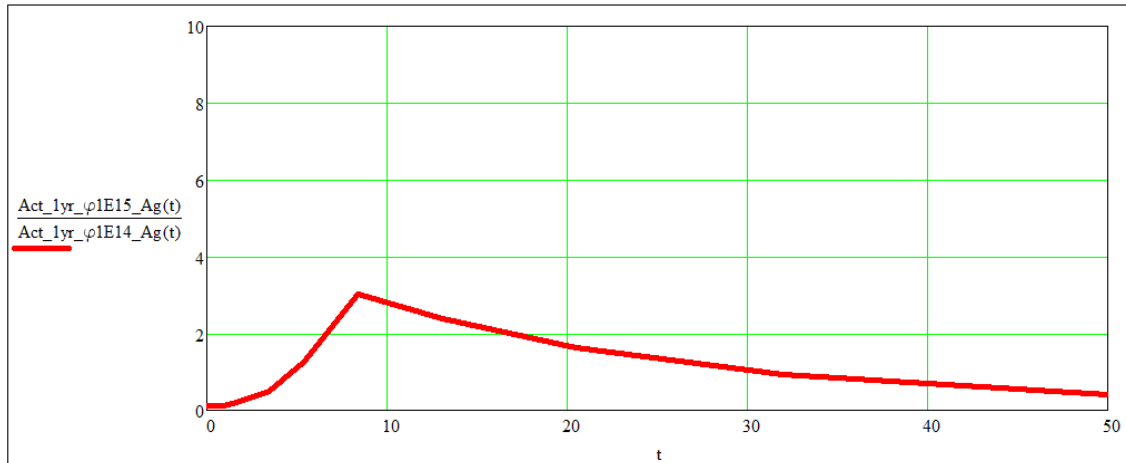


Figure 47: Ratio of activities A(t) induced in Ag by neutron activation at $\phi = 1E15 \text{ cm}^{-2} \text{ s}^{-1}$ and at $\phi = 1E14 \text{ cm}^{-2} \text{ s}^{-1}$ i.e. in the high neutron fluence-rate domain; a ratio of 10 indicates linear behaviour

5.9.10 Linear and Non-Linear Neutron Activation Behaviour of Caesium (Cs)

The neutron activation behaviour of the chemical element Cs remains reasonably linear up to $\phi = 1E13 \text{ cm}^{-2} \text{ s}^{-1}$ but at $\phi = 1E14 \text{ cm}^{-2} \text{ s}^{-1}$ there is some mild departure from linearity, as seen in Figure 48.

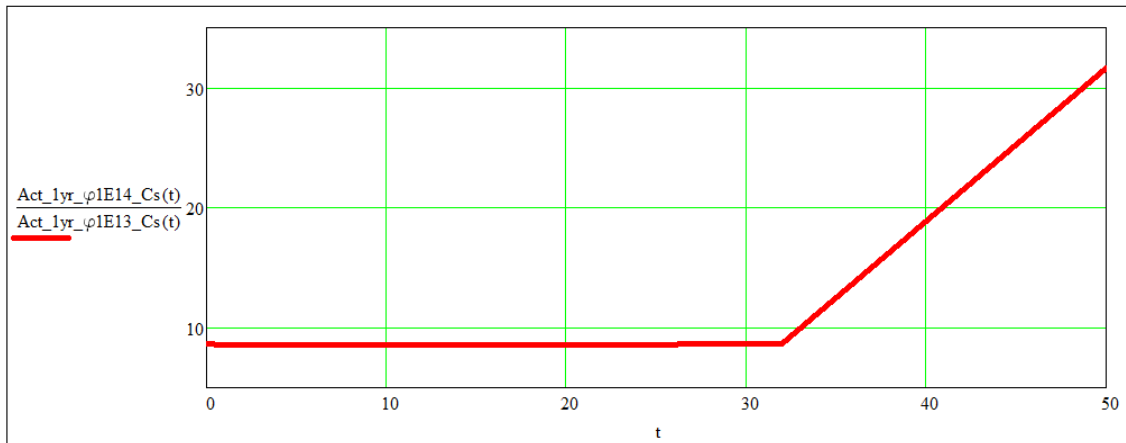


Figure 48: Ratio of activities $A(t)$ induced in the element caesium (Cs) by neutron activation at $\phi = 1E14 \text{ cm}^{-2} \text{ s}^{-1}$ and at $\phi = 1E13 \text{ cm}^{-2} \text{ s}^{-1}$ i.e. in the medium-high fluence-rate domain; a ratio of 10 indicates linear behaviour

Above $\phi = 1E14 \text{ cm}^{-2} \text{ s}^{-1}$ there is a significant, sharp departure from linearity, as seen in Figure 49.

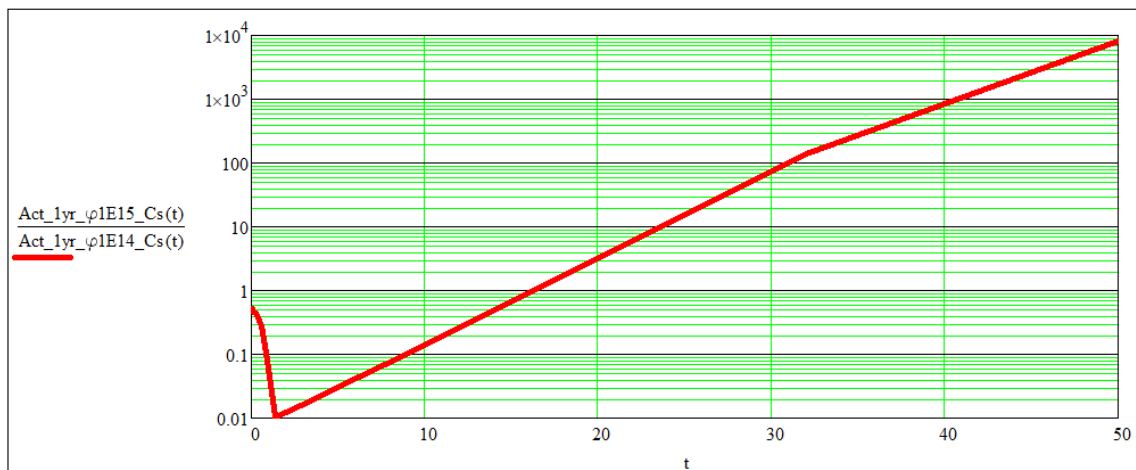


Figure 49: Ratio of activities $A(t)$ induced in Cs by neutron activation at $\phi = 1E15 \text{ cm}^{-2} \text{ s}^{-1}$ and at $\phi = 1E14 \text{ cm}^{-2} \text{ s}^{-1}$ i.e. in the high neutron fluence-rate domain

The reason for the sudden onset of the steep non-linearity observed in Figure 49 is that at very high fluence-rates, the 4-step “*non-linear ladder-breeding*” of the long-lived isotope Cs-137 from the only stable isotope of Cs, namely Cs-133, becomes possible. FISPACT-II calculations indicate that, at a cooling time of 40 years, 99.96 % of the activity present in a sample of Cs irradiated for 1 year at $\phi = 1E15 \text{ cm}^{-2} \text{ s}^{-1}$, is attributable to Cs-137 and its short-lived equilibrium radioactive progeny, Ba-137m. In sharp contrast, the joint percentage contributions of Cs-137 and Ba-137m is only 0.00363 % at $\phi = 1E13 \text{ cm}^{-2} \text{ s}^{-1}$.

The above phenomenon is called *non-linear ladder-breeding* or *non-linear ladder-activation* and not “chain”-breeding, because it is intra-element (Cs only) activation and not inter-element activation (e.g. $\text{Cr} \rightarrow \text{Mn} \rightarrow \text{Fe} \rightarrow \text{Co-59} \rightarrow \text{Co-60}$).

5.9.11 Linear and Non-Linear Neutron Activation Behaviour of Europium (Eu)

The non-linearity observed in the neutron activation of europium (Eu) is caused by the burn-away, i.e. depletion, of the stable reactant isotopes — Eu-151 and Eu-153. This depletion-driven sub-linear activation behaviour is seen in is observed in Figure 50.

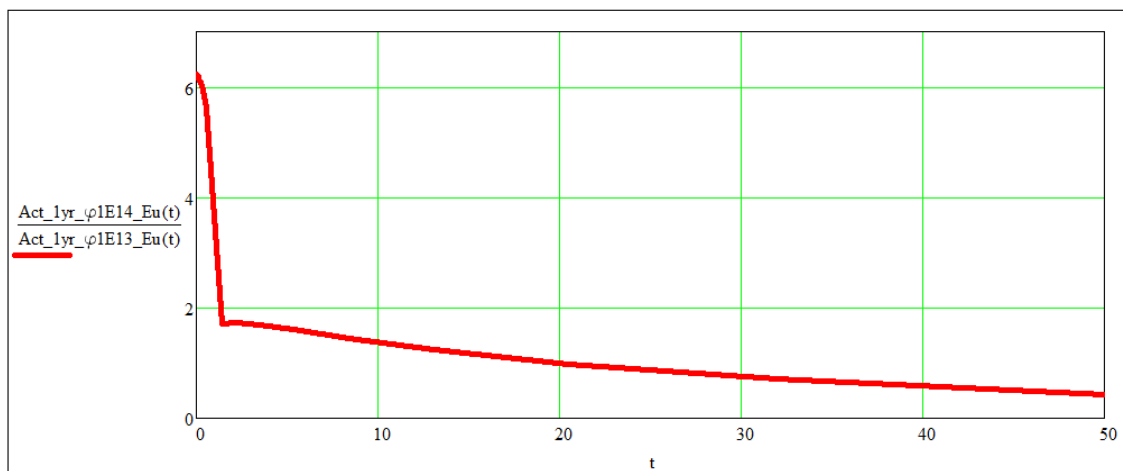


Figure 50: Ratio of activities $A(t)$ induced in the element europium (Eu) by neutron activation at $\phi = 1\text{E}14 \text{ cm}^{-2} \text{ s}^{-1}$ and at $\phi = 1\text{E}13 \text{ cm}^{-2} \text{ s}^{-1}$ i.e. in the medium-high fluence-rate domain; a ratio of 10 indicates linear behaviour

5.9.12 Clusters of Technologically Important and Abundant Elements that “Chain-Breed” Towards a Long-Lived Radionuclide of an Element to their RHS in the Periodic Table (PT)

A cluster of 5 elements that are relatively abundant in the crust of the earth (see Figure 1 on page 13), and also have excellent engineering properties, are found with atomic numbers ranging from $Z = 22$ to $Z = 26$. These five elements are Ti ($Z = 22$), V ($Z = 23$), Cr ($Z = 24$), Mn ($Z = 25$) and Fe ($Z = 26$). The radioisotopes of these elements are generally not long-lived and do not present decommissioning issues. However, just to the RHS of this cluster of elements, in the Periodic Table (PT), there is the element cobalt (Co) which champions a long-lived radioisotope that also emits penetrating ionising photons — Co-60.

This cluster of “chain-breeders of Co-60” under extremely high neutron fluence-rate conditions, is seen in columns 4, 5, 6, 7 and 8 of row 4 in the PT — see Figure 51.

IUPAC Periodic Table of the Elements

Key:
 atomic number
 Symbol
 name
 standard atomic weight

INTERNATIONAL UNION OF PURE AND APPLIED CHEMISTRY

Figure 51: The Periodic Table of the Elements (Holden et al., 2018)

At high neutron fluence-rates — generally above $\phi = 1E13 \text{ cm}^{-2} \text{ s}^{-1}$ or $\phi = 1E14 \text{ cm}^{-2} \text{ s}^{-1}$, the elements Ti, V, Cr, Mn and Fe begin to “chain-breed” Co-60 in a process that has been demonstrated to be highly non-linear.

The above clustering of five technologically important and abundant elements (Ti, V, Cr, Mn and Fe) that “chain-breed” a long-lived radionuclide (Co-60), is unique in the PT of elements. One less important analogous case is found in the neutron-activation of the element Zr, which is used very abundantly as the fuel cladding material in PWRs and BWRs. For the irradiation of 100 g of Zr in neutron fluence-rates of, respectively, $\phi_{lo} = 1E13 \text{ cm}^{-2} \text{ s}^{-1}$ or $\phi_{hi} = 1E15 \text{ cm}^{-2} \text{ s}^{-1}$, for 1 yr, followed by 50 years of cooling, the induced activities of several radionuclides display highly non-linear ratios, as summarised in Table 46.

Table 46: Non-linearity in the activation of the element zirconium (Zr)

Radionuclide	Ratio $\frac{A(\phi_{hi}=1E15 \text{ cm}^{-2} \text{ s}^{-1})}{A(\phi_{lo} = 1E13 \text{ cm}^{-2} \text{ s}^{-1})}$ at $T_{cool} = 50 \text{ yr}$
Zr-93	3.275E+03
Nb-93m	3.353E+03
Y-90	3.573E+04

Radionuclide	Ratio $\frac{A(\phi_{hi}=1E15 \text{ cm}^{-2} \text{ s}^{-1})}{A(\phi_{lo} = 1E13 \text{ cm}^{-2} \text{ s}^{-1})}$ at $T_{cool} = 50 \text{ yr}$
Sr-90	3.573E+04
H-3	6.056E+03
Nb-94	1.306E+06
Tc-99	1.356E+10
Kr-85	6.875E+06

In the event of linearity in neutron activation behaviour, the expected activity ratio would be

$\frac{\phi_{hi}}{\phi_{lo}} = \frac{1E15 \text{ cm}^{-2} \text{ s}^{-1}}{1E13 \text{ cm}^{-2} \text{ s}^{-1}} = 100$. Instead one finds activity-ratios of approximately 3.6E4 for Sr-90 (half-life 28.79061 yr), 1.3E6 for Nb-94 (half-life 2.03004E4 yr) and 1.35E10 for Tc-99 (half-life 2.11105E5 yr). At very high fluence-rates, it is evident that zirconium isotopes ($Z = 40$) begin to chain-breed, in a highly non-linear fashion, the long-lived radionuclides $^{94}_{41}\text{Nb}$ (half-life 2E4 yr) and $^{99}_{43}\text{Tc}$ (half-life 2.11E5 yr).

5.9.13 Conclusions about the Non-Linearity of Neutron Activation

Neutron activation can sometimes depend profoundly non-linearly on the neutron fluence-rate. For this reason, it is incorrect and dangerous to perform a neutron activation calculation at a chosen reference integral fluence-rate ϕ_{ref} and then to attempt to scale activities and dose-rates linearly for other fluence-rates. There are no “shortcuts” i.e. every neutron activation problem must be modelled individually.

5.10 Proposed Terminology (Addition by the Co-Supervisor, TJvR)

During the course of this study, apt descriptions were encountered in published literature, and two additional descriptive terms were coined. The following phrases can improve the conceptual clarity and brevity of communication about neutron activation and reactor decommissioning.

Useful new terms found in published literature:

- *Activation-Hazardous Elements* (page 44)
- *Activation-Hazardous Trace Elements* (page 44)
- *Radioactivity-Hazardous Nuclides* (page 44).

Potentially useful terms proposed in this dissertation:

- *Chain-Breeding* or *Chain-Activation* (of e.g. Co-60 from Ti, V, Cr, Mn and Fe) (page 167 – 181)
- *Ladder-Breeding* or *Ladder-Activation* (of e.g. Cs-137 from Cs-133) (pages 32 & 177).

6 SUMMARY AND CONCLUSIONS

6.1 General Summary

At nuclear reactor facilities, intense neutron radiation fields are encountered inside and around reactor vessels. Engineering materials exposed to the neutron field absorb neutrons in nuclear reactions, and radioisotopes are produced in this way. This process is termed *neutron activation*. Neutron activation produces radionuclides in irradiated materials, i.e. the irradiated materials will become radioactive. Most radionuclides produced by neutron activation are undesired and will place a radioactive waste burden on the licensed facility, adding to total operational costs and inflating future liabilities. After irradiation by the neutron field ends, long-lived radionuclides will remain present in irradiated materials and will present radiological and radioactive waste-disposal problems such as e.g. (1) a field of ionising radiation will be present around the activated material and will expose workers to doses of ionising radiation, and (2) some activated material may not pass clearance level criteria set by e.g. the IAEA and will therefore have to be disposed of as radioactive waste, at a significant cost.

An inquiry into the systematics of neutron activation showed that the dependence of neutron activation levels on the neutron fluence-rate can sometimes behave in profoundly non-linear ways. For this reason, it is futile and dangerous to attempt to perform a neutron activation calculation at a chosen reference integral fluence-rate ϕ_{ref} and then attempt to scale activities and dose-rates linearly for other fluence-rates. There are no “shortcuts” i.e. every neutron activation problem is unique and must, therefore, be modelled individually, or at least must be derived from simulations at similar neutron fluence-rates.

Using a representative neutron spectrum calculated for a typical LWR, a total of 81 chemical elements were irradiated and subsequently allowed to cool down under specific scenarios that represent important decommissioning and operational scenarios. For selected scenarios of practical importance, the elements were ranked in terms of the dose-rate at 1 m from a reference mass of 1 g of each irradiated chemical element. These tables clearly show which elements are high-activators, which elements are intermediate activators and which elements are low-activators. This information may be used to select low-activation materials for new reactor facilities, and for components that must be replaced in existing nuclear facilities. The tabulated results can guide decommissioning engineers, project managers, radiation protection specialists, neutron radiography teams and even reactor design teams.

A comprehensive literature study was undertaken and presented. From the literature-study emerged a list of high-activator elements as well as problematic, long-lived radioisotopes formed by neutron activation. Approximately 1600+ calculations with the activation code FISPACT-II 3.00 were performed, in order to describe the systematics of neutron activation in realistic irradiation-and-cooldown scenarios. The full set of systematic FISPACT-II calculations served to verify and validate the list of high-activation materials and problematic long-lived radionuclides gathered from the literature survey.

A comprehensive set of graphs were presented to show how induced activities and photon dose-rate fields will evolve over e.g. the first 50 years after the end of irradiation, for elements used in important engineering materials such as carbon steel-alloys, stainless-steel alloys, nickel alloys, ordinary concrete, magnetite concrete and hematite concrete. The durations of these irradiations range from 1 hour to 60 years.

A notable result was that, for a decommissioning scenario, titanium-alloys are significantly more benign neutron activators compared to steel-alloys. Problematic elements that are high-activators are europium (Eu), cobalt (Co), caesium (Cs), silver (Ag) and niobium (Nb). The testing of raw materials used in concrete close to a nuclear reactor must be designed to minimise the amount of the above high-activators in the concrete. Al-alloys and steel-alloys used in intense neutron fields must also be tested to minimise the high-activators. Where possible, aluminium-alloys and titanium-alloys must be preferred in areas where significant neutron fluence-rates are expected.

6.2 Major Summary and Conclusion (SC) Points

The major Summary and Conclusion (“SC”) points that follow from this study of the systematics of neutron activation, are as follows:

SC₁ Neutron activation can sometimes depend profoundly non-linearly on the neutron fluence-rate. For this reason, it is incorrect and dangerous to perform a neutron activation calculation at a chosen reference integral fluence-rate ϕ_{ref} and then to attempt to scale activities and dose-rates linearly for other fluence-rates. There are no “shortcuts” i.e. every neutron activation problem must be modelled individually.

SC₂ For decommissioning-related irradiation-and-cooldown scenarios

DECO_60yr_6yr_φ, the photon dose-rates from radionuclides produced by the irradiation of

a reference mass of each element found in nature were calculated and sorted for

$$\phi = 10^{14} \text{ cm}^{-2} \text{ s}^{-1}$$

$$\phi = 10^{13} \text{ cm}^{-2} \text{ s}^{-1}$$

$$\phi = 10^{12} \text{ cm}^{-2} \text{ s}^{-1}$$

$$\phi = 10^{11} \text{ cm}^{-2} \text{ s}^{-1}.$$

Design engineers, decommissioning engineers and radiation protection specialists can use this information to (1) select low-activation materials for new reactor facilities or components that are replaced, and (2) know in advance which irradiated reactor components will produce high dose-rate fields from an internal burden of radionuclides produced by activation. The tabulated ranking-order of the elements can e.g. be used to identify radiologically meaningful *material-substitutions*. Because Ti is much lower on the list of activators than e.g. Fe, for all scenarios of class DECO_60yr_6yr_φ, it stands to reason that replacing or *substituting* Fe-alloys with Ti-alloys will lower inventories of activation products and also lower dose-rates. Likewise, substituting Fe-alloys as far as possible with Al-Mg-Si-Cr-Ti alloys will also lower the long-term inventory of radionuclides that will have to be dealt with at decommissioning time.

SC₃ For neutron radiography related irradiation-and-cooldown scenarios NRAD_1h_30d_1E9 and NRAD_1d_30d_1E9, the photon dose-rates from radionuclides produced by the irradiation of a reference mass of each element found in nature were calculated and sorted in ranking tables. Neutron Radiography teams can use this information to e.g. (1) select low-activation construction materials, (2) plan for extended cooldown periods if e.g. cobalt-containing alloys are irradiated and (3) construct radiological safety-cases for submission to regulators. NRAD scientists can also use this information to anticipate, in advance, that investigated structures with high mass-% contents of e.g. the metallic elements Ir, Cr and Co will be radiologically “very hot” after neutron tomography sessions.

SC₄ Lists of (1) problematic, high-activation elements (Table 11, page 55) and (2) long-lived, problematic activation radionuclides (Table 44, page 166) have been compiled from the literature and a large number of activation calculations. The most problematic neutron activators are Eu, Co, Cs, Ag and Nb.

SC₅ A list of consistently low-activator elements emerged. The most consistent benign, low-activator elements are Ti, Al, Mg and Si. When the neutron fluence-rate is consistently below $10^{10} \text{ cm}^{-2} \text{ s}^{-1}$, the elements Cr, V and Mn also behave as low-activators, i.e. the use of Ti-Al-

V-Cr alloys in the place of steel-alloys at a nuclear reactor facility will lower the burden of activation products at decommissioning time.

SC₆ A set of graphs have been constructed to graphically and intuitively show how different chemical elements will respond radiologically under commonly encountered neutron irradiation scenarios, as a function of elapsed time after irradiation. These graphs may prove useful for decommissioning planners.

SC₇ A field of knowledge that was previously imperfectly documented, has now been summarised in a comprehensive and up-to-date literature survey (Chapter 3) which surpasses — in both scope and depth — most comparable endeavours. By means of 1600+ carefully designed calculation models using the state-of-the-art activation code, FISPACT-II, the “systematics” of the neutron activation of engineering materials, from a practical reactor decommissioning perspective, have now been uncovered, systematised and documented. The need for such a systematisation is expressed by e.g. (Bylkin et al., 2018) — see § 3.5.17 on page 45.

SC₈ The Research Hypothesis (§ 1.3 on page 10) has been proven to be viable and correct — see § 6.3 below.

SC₉ A number of little-known or previously unknown and undocumented activation phenomena have been discovered, described and named — see § 6.4 below.

6.3 Research Hypothesis Proven

In § 1.3 on page 10, the *research hypothesis* at the foundation of this investigation was formulated. This research hypothesis has been proven to be robust and correct. It was possible to successfully characterise the neutron activation “fingerprints” of the chemical elements in preparation for nuclear reactor decommissioning. It was possible to individually investigate every chemical element via calculational experiments and then to sort or order the elements from *high-activator* to *low-activator* as well as into subsets such as e.g. *highly problematic activators*, *somewhat problematic activators* and *benign, low-activators*, for different practical, nuclear reactor decommissioning-related irradiation-and-cooldown scenarios. These sorted lists of the elements can guide engineers in selecting low-activation construction materials for new reactor facilities and guide decommissioning planners to know which irradiated materials will be highly problematic, less problematic and non-problematic.

6.4 Novel Contributions to the Field of Neutron Activation

In published literature, the concept of the non-linearity of neutron activation at high neutron fluence-rates appears to be wholly unknown. A “Google search” for the keywords “neutron activation, non-linear, high flux” leads to the conclusion that this phenomenon is either unknown or unpublished. A similar search under Google Scholar also fails to find any articles about this phenomenon.

Let us review an example in support of the above claim. The website

<https://www.ncnr.nist.gov/resources/activation/> hosts the *neutron activation and scattering calculator* of the *Center for Neutron Research (CNR)* at the *National Institute of Standards and Technology (NIST)* in the USA.

For the neutron activation of 100 grams of the element Cr in neutron fluence-rates of $\phi_{lo} = 1E8 \text{ cm}^{-2}\text{s}^{-1}$ and $\phi_{hi} = 1E15 \text{ cm}^{-2}\text{s}^{-1}$, with $T_{irr} = 1 \text{ yr}$ and $T_{cool} = 1 \text{ yr}$, the NIST’s *neutron activation calculator* reports the product-nuclides and activities listed in the LHS of Table 47. Next, the $\{N, A\}$ -matrix was quantified using the FISPACT-II models developed in this work, for identical neutron fluence-rates, irradiation time and cooling time; results are reported in the RHS of Table 47. From the latter table, it is evident that the phenomenon for which we have proposed the term *non-linear chain-breeding* is completely absent from the activation model on which the NIST’s *neutron activation calculator* functions.

Table 47: The NIST’s calculated results for the neutron activation of 100 grams of ^{nat}Cr in neutron fluence-rates of $\phi_{lo} = 1E8 \text{ cm}^{-2} \text{ s}^{-1}$ and $\phi_{hi} = 1E15 \text{ cm}^{-2} \text{ s}^{-1}$, for $T_{irr} = 1 \text{ yr}$ and $T_{cool} = 1 \text{ yr}$, compared with calculations using FISPACT-II models developed in this work, for identical exposures

NIST Calculator			FISPACT-II 3.00		
Product Isotope	$\phi = 1E8 \text{ cm}^{-2}\text{s}^{-1}$ Activity (Bq)	$\phi = 1E15 \text{ cm}^{-2}\text{s}^{-1}$ Activity (Bq)	Product Isotope	$\phi = 1E8 \text{ cm}^{-2}\text{s}^{-1}$ Activity (Bq)	$\phi = 1E15 \text{ cm}^{-2}\text{s}^{-1}$ Activity (Bq)
Cr-51	2.827E-01	1.680E+06	Co-60	-	1.617E+13
Total Activity	2.827E-01	1.680E+06	Fe-59	-	1.101E+11
			Ni-63	-	5.653E+10
			Fe55	-	4.404E+08
			Mn-54	-	1.460E+08
			H-3	5.462E-03	5.574E+07
			Zn-65	-	4.647E+07
			Co-60m	-	8.723E+06

Fe-60	-	8.723E+06
Cr-51	5.369E+03	2.974E+05
Co-58	-	8.709E+04
Ca-45	-	1.157E+03
Ni-59	-	3.338E+02
Sc-46	-	2.653E+02
V-49	2.447E+01	8.948E+00
Total Activity	5.393E+03	1.634E+13

From Table 47 it is evident that, compared to the FISPACT-II calculation model, the NIST *neutron activation calculator* (1) underpredicts the total activity achieved with ϕ_{lo} by a factor 1.9E4, and (2) also underpredicts the total activity achieved with ϕ_{hi} by a factor 9.7E6, i.e. almost 7 orders of magnitude. The NIST calculator is, clearly, incapable of correctly modelling the *non-linear chain-breeding* of the long-lived nuclide Co-60 — an effect that suddenly manifests at very high neutron fluence-rates such as is encountered in e.g. the structural material of MTR fuel-assemblies, especially so-called High-Flux Reactors (HFRs).

The phenomenon of the *non-linear ladder-activation* of e.g. Cs-137 from Cs-133, which suddenly manifests at high neutron fluence-rates, is also an unknown concept in all of published literature. This formation of the long-lived radionuclide Cs-137 is described in § 5.9.10 on page 177. The NIST's *neutron activation calculator* fails to account for the formation of any Cs-137 at high neutron fluence-rates, and predicts that only two radionuclides will be formed: Cs-134 and Cs-135.

Finally, published literature was unaware that the element barium (Ba) can activate to form the long-lived radionuclide Cs-137 (see § 5.8.2 on page 147).

6.5 Proposed Follow-Up Investigation(s)

Note by co-supervisor TJvR: The phenomena of (1) *non-linear chain-breeding* and (2) *non-linear ladder-breeding* of long-lived radionuclides via neutron activation at high neutron fluence-rates, have been uncovered and documented using only a single code — FISPACT-II

3.00. It is necessary to duplicate this discovery qualitatively and quantitatively using a second, independent neutron activation code²⁶.

It is expected that Oak Ridge National Laboratory (ORNL), Tennessee, USA, will release the code-system SCALE 6.3 by mid-2020. The code ORIGEN in SCALE 6.3 will be the ideal code to use in the required independent validation of the above non-linear phenomena in neutron activation. This new version of ORIGEN will be able to easily read high-fidelity neutron fluence-rate spectra $\phi(E)$ calculated by the code MCNP, and will furthermore include the latest US nuclear data release — ENDF/B-8.0 (Brown et al., 2018).

6.6 Proposed Publication of a Monograph

Note by co-supervisor TjvR: This dissertation contains valuable material of general interest to the wider reactor decommissioning community. It is proposed that an edited version of this dissertation, which should include the validation-step mentioned in § 6.5, be published (electronically) as a monograph dealing with the *neutron activation characterisation of the chemical elements in preparation for nuclear reactor decommissioning*.

²⁶ Note by co-supervisor TjvR: This is analogous to the *criterion of multiple, independent attestation* in e.g. the disciplines of hermeneutics and historiography.

ANNEXURE A: TECHNICAL DETAILS OF FISPACT-II CALCULATIONS

Discussion of a Representative FISPACT-II Calculation Model

Approximately 1600+ FISPACT-II calculation models were developed for the purposes of this study. Only one of these inputs will be displayed and discussed here.

Below is the FISPACT-II 3.00 (Sublet et al., 2015) calculation model for the activation of the element Fe (natural iron, i.e. ^{nat}Fe) by neutron irradiation. It is first shown in its entirety and then discussed section by section²⁷.

The FISPACT-II inputs and Windows batch-files were developed by the Co-Supervisor (TJvR), while Mr Lesego E. Moloko assisted greatly with overcoming difficult LINUX-related aspects of the initial installation of the code at Necsa's Radiation and Reactor Theory (RRT) Section, back in 2016.

```
CLOBBER
MONITOR      1
GETXS        0
GETDECAY     0
LIBVERSION   1
```

²⁷ Note by co-supervisor TJvR: The development of FISPACT began around 1995, and until circa 2012 its input data sets were restricted to the exclusive use of capital letters. Most scientists who cut their teeth on older code versions such as e.g. FISPACT-2007 are therefore still in the habit of writing inputs in capital letters. The inputs shown below continue the original input convention. This convention never applied to <<...>> style comment statements. In our FISPACT inputs, then, the chemical symbol for iron is written as FE and not as Fe, etc.

```

PROJECTILE 1
FISPACT
* 100 GRAMS OF 1 ELEMENT
<< Model Nuclear Fission >>
USEFISSION
FISYIELD +159
AC222M AC223 AC224 AC225 AC226 AC227 AC228 AC229 AC230 AC231
AM236 AM237 AM238 AM239 AM240 AM241 AM242 AM242M AM243 AM244 AM244M AM246M
BK241 BK242 BK243 BK244 BK245 BK246 BK247 BK248 BK248M BK249 BK250 BK251
CF243 CF244 CF245 CF246 CF247 CF248 CF249 CF250 CF251 CF252 CF253 CF254 CF255
CM241 CM242 CM243 CM244 CM245 CM246 CM247 CM248 CM249 CM250 CM251
ES250M ES254M ES256M
FM250M
FR217 FR218 FR219 FR220 FR221 FR222 FR223 FR224 FR225 FR226 FR227
NP230 NP231 NP232 NP233 NP234 NP235 NP236 NP236M NP237 NP238 NP239 NP240 NP240M NP241
NP242M
PA225 PA226 PA227 PA228 PA229 PA230 PA231 PA232 PA233 PA234 PA234M PA235 PA236 PA237
PU234 PU235 PU236 PU237 PU238 PU239 PU240 PU241 PU242 PU243
RA219 RA220 RA221 RA222 RA223 RA224 RA225 RA226 RA227 RA228 RA229
RN214 RN215 RN216 RN217 RN218 RN219 RN220 RN221 RN222 RN223 RN224 RN225
TH224 TH225 TH226 TH227 TH228 TH229 TH229M TH230 TH231 TH232 TH233 TH234
U229 U230 U231 U232 U233 U234 U235 U235M U236 U237 U238 U239
<< Convergence Parameters >>
LOOKAHEAD
PATHRESET 0
TOLERANCE 0 0.1 1.0E-08
TOLERANCE 1 0.1 1.0E-08
UNCERTAINTY 2
<< Target Material Spec >>
<< Total Mass in kg; Number of Elements in mtl>>
MASS 0.10 1
FE 100.0
<< GRAPH STUFF >>
GRAPH 2 0 1 1 2
<< Print HalfLife of each nuclide >>
HALF
<< Number of atoms considered irrelevant >>
MIND 1.0E-36
<< Dose-rate 1.0 m from a 1-gram point source >>

```

```
DOSE  2  1.0
HAZARDS
NOSTABLE
SPLIT  1
TIME  0  DAYS  ATOMS
<< Start: Irradiation >>
FLUX  1.00E12
TIME  60  YEARS  ATOMS
<< End: Irradiation >>
<< Start: Cooling >>
FLUX  0.0
ZERO
PULSE  50
      TIME  1  YEARS  ATOMS
ENDPULSE
<< End: Cooling >>
END
* END OF RUN
/*
```

The above calculation model is now discussed and explained section by section. The first part of the model input is as follows:

```
CLOBBER
MONITOR  1
GETXS  0
GETDECAY  0
LIBVERSION  1
PROJECTILE  1
FISPACT
* 100 GRAMS OF 1 ELEMENT
```

Note that FISPACT-II uses keyword-driven input. The code FISPACT is instructed to over-write (keyword: “CLOBBER”) existing output-files with new versions of these output-files, if necessary, without halting and flagging errors. FISPACT-II is also instructed to write messages to the

computer monitor (keyword: “MONITOR”) as the calculation progresses²⁸. The code is instructed that the problem-dependent 1-group binary-format cross-section library and the radionuclide decay, half-life, fission yield and gamma emission binary libraries were already created in previous steps (keyword: “GETXS 0” and keyword: “GETDECAY 0”). FISPACT will read cross-section libraries in ENDF format (keyword: “LIBVERSION 1”) and is instructed that the projectile is a neutron (keyword: “PROJECTILE 1”). It then writes the message “100 GRAMS OF 1 ELEMENT” in the output file, i.e. in the results file.

The next section of the calculation model is as follows:

```

<< Model Nuclear Fission >>
USEFISSION
FISYIELD +159
  AC222M AC223 AC224 AC225 AC226 AC227 AC228 AC229 AC230 AC231
  AM236 AM237 AM238 AM239 AM240 AM241 AM242 AM242M AM243 AM244 AM244M AM246M
  BK241 BK242 BK243 BK244 BK245 BK246 BK247 BK248 BK248M BK249 BK250 BK251
  CF243 CF244 CF245 CF246 CF247 CF248 CF249 CF250 CF251 CF252 CF253 CF254 CF255
  CM241 CM242 CM243 CM244 CM245 CM246 CM247 CM248 CM249 CM250 CM251
  ES250M ES254M ES256M
  FM250M
  FR217 FR218 FR219 FR220 FR221 FR222 FR223 FR224 FR225 FR226 FR227
  NP230 NP231 NP232 NP233 NP234 NP235 NP236 NP236M NP237 NP238 NP239 NP240 NP240M NP241
  NP242M
  PA225 PA226 PA227 PA228 PA229 PA230 PA231 PA232 PA233 PA234 PA234M PA235 PA236 PA237
  PU234 PU235 PU236 PU237 PU238 PU239 PU240 PU241 PU242 PU243
  RA219 RA220 RA221 RA222 RA223 RA224 RA225 RA226 RA227 RA228 RA229
  RN214 RN215 RN216 RN217 RN218 RN219 RN220 RN221 RN222 RN223 RN224 RN225
  TH224 TH225 TH226 TH227 TH228 TH229 TH229M TH230 TH231 TH232 TH233 TH234
  U229 U230 U231 U232 U233 U234 U235 U235M U236 U237 U238 U239

```

²⁸ Note by co-supervisor: The keyword “MONITOR” essentially commands the code FISPACT: “Thou shalt not be silent, but thou shalt speaketh to me”.

This input “switches on” the possibility of nuclear fission by 159 listed isotopes. The guiding principle is to switch on all possible physics options, even if these are not needed. For example, the irradiation of Fe or He or Mo by neutrons will not produce fission, but “fission physics” is nevertheless switched on, as a matter of principle.

The next section of the calculation model is:

```
<< Convergence Parameters >>
LOOKAHEAD
PATHRESET 0
TOLERANCE 0 0.1 1.0E-08
TOLERANCE 1 0.1 1.0E-08
UNCERTAINTY 2
```

In FISPACT-II, comment-statements begin with “<<” and end with “>>”. The keyword “LOOKAHEAD” instructs FISPACT to first follow the decay of radionuclides to the maximum specified time, in order “not to miss” i.e. “not to overlook” a nuclide that may be trivial at small values of the time t , but dominant after long decay times — this is necessary for UNCERTAINTY quantification and PATHWAY analysis. The two “TOLERANCE” keywords set very strict convergence criteria for the numerical solution of the system of rate-equations that is solved numerically, using an ordinary differential equation (ODE) solver. Finally, the “UNCERTAINTY 2” keyword and option instructs the code to perform a full pathway and uncertainty analysis. The PATHRESET keyword also instructs the code to include late-time dominant nuclides. The inclusion of the latter keyword leads to the calculation of pathways being repeated in the cooling phase and this causes the late-time dominant nuclides to be included in the uncertainty calculations. There are three values for the “showpathways” argument:

- -1 display pathways for a target nuclide for which pathways have not been displayed at earlier times.
- 0 do not display pathways but use the pathways in uncertainty estimates.
- 1 display pathways for all dominant nuclides at each “pathways reset”.

If the PATHRESET keyword is included in the initial conditions section of the input file, then pathways are recalculated at each step where there are new target nuclides, and all occurrences of the PATHRESET keyword in the inventory calculation phase are ignored. The recommended usage of this keyword is to use it where required in the cooling phase of the inventory calculation.

The next section of the calculation model is:

```
<< Target Material Spec >>  
<< Total Mass in kg; Number of Elements in mtl>>  
MASS 0.10 1  
FE 100.0
```

The irradiated material is 0.1 kg of 1 element, namely 100 % pure Fe.

The next part of the calculation model reads as follows:

```
<< GRAPH STUFF >>  
GRAPH 2 0 1 1 2  
<< Print HalfLife of each nuclide >>  
HALF  
<< Number of atoms considered irrelevant >>  
MIND 1.0E-36  
<< Dose-rate 1.0 m from a 1-gram point source >>  
DOSE 2 1.0  
HAZARDS  
NOSTABLE  
SPLIT 1
```

The keyword “GRAPH” requests that tabular data be written that can easily be used to construct graphs of e.g. activity vs. time, dose-rate vs. time and heat release rate vs. time. The keyword “HALF” requests that half-life data for all nuclides in the output file, be given in an extra column. The keyword “MIND” followed by the specification “1.0E-36” specifies a “minimum detectable” output concentration. Technically, it means that

a fraction 1E-36 of 1 atom will still be reported in the output, i.e. it specifies that the user wants to see all results, even trace-amounts. The keyword-driven specification “DOSE 2 1.0” states that photon dose-rates must be evaluated at a distance of 1 m from a point-source (“2”); this dose-rate data will be given in columnar format for the subsequent generation of graphs (with e.g. Matplotlib in Python). The keyword “HAZARDS” requests printout of biological hazard information per radionuclide and for all radionuclides together. The keyword “NOSTABLE” suppresses the printout of stable nuclides, i.e. only radionuclides will appear in the output file. Finally, “SPLIT 1” requests the display of an additional summary table at the end of the run. This summary table contains separate information on the heat production by beta and gamma radiation at each time interval and is output after the existing summary table. By default, this new summary table is not printed, but it can be displayed if the specification “SPLIT 1” is set. Note that if this additional summary table is required then the keyword “HAZARDS” must also be used to ensure that uncertainties are printed correctly.

The last part of the input is:

```
TIME 0 DAYS ATOMS
<< Start: Irradiation >>
FLUX 1.00E12
TIME 60 YEARS ATOMS
<< End: Irradiation >>
<< Start: Cooling >>
FLUX 0.0
ZERO
PULSE 50
    TIME 1 YEARS ATOMS
ENDPULSE
<< End: Cooling >>
END
```

The specification “TIME 0 DAYS ATOMS” simply requests a full printout of the isotopic content of the material at the onset, i.e. after zero elapsed time. The lines “FLUX 1.00E12” and “TIME 60 YEARS ATOMS” states that the material is irradiated non-stop for 60 years at an

integral neutron fluence-rate of $\phi = 10^{12} \text{ cm}^{-2} \text{ s}^{-1}$. Next, the integral neutron fluence-rate is allocated a new value of $\phi = 0 \text{ cm}^{-2} \text{ s}^{-1}$ when the cooldown phase begins and the time is reset to $t = 0$ at the beginning of the cooling phase by the keyword "ZERO". The numerical results of radioactive transitions are reported in 50 steps of 1 year per step; this allows data for use in graphs and tables, to be written at 50 points in time.

Before FISPACT-II can run, cross-section and radionuclide decay data must be written to binary library files. This is done in two steps. The first step executes the following keyword-driven instruction set:

```
<< -----collapse cross-section data----- >>
CLOBBER
MONITOR      1
LOGLEVEL     3
LIBVERSION   1
PROJECTILE   1
SAVELINES
SPEK
<< First collapse >>
GETXS        1 709
  << Condense decay data >>
GETDECAY     1
FISPACT
* TENDL-2017 709N
PRINTLIB     0
PRINTLIB     4
PRINTLIB     5
PRINTLIB     8
PRINTLIB     9
END
* END OF RUN
/*
```

All multigroup cross-sections are collapsed to 1-group effective cross-sections using the user-supplied 709-group neutron energy spectrum $\phi(E)$ and are written as a binary COLLAPX library file. A transport code such as MCNP is typically used to calculate the 709-group discrete approximation of the continuous function $\phi(E)$.

The second library-preparation step executes the following keyword-driven instruction set:

```
<< -----condense decay data----- >>
CLOBBER
MONITOR      1
LOGLEVEL     3
LIBVERSION   1
PROJECTILE   1
READSF
SAVELINES
SPEK
GETDECAY     1
FISPACT
* TENDL-2017 709Neutron
END
* END OF RUN
/*
```

All detail about neutron-induced fission, spontaneous fission (“READSF”), radiation emission (“SPEK”) and isotopic transition half-life and branching data (“GETDECAY 1”) is written to an ARRAYX binary library file.

The execution of FISPACT-II first runs the batch file **Get_Files_Fluxes.bat** (developed by the co-supervisor TjvR):

```
@ECHO OFF
VERIFY ON

rem SET TYPE="CENDL"
rem SET TYPE="JENDL"
```

```

rem SET TYPE="EAF2010"
rem SET TYPE="EAF2010_ENDF"
rem SET TYPE="ENDFB"
rem SET TYPE="JEFF"
    SET TYPE="TENDL"
rem SET TYPE="GROUPCONVERT"

set CENDL_path=C:\FISPACT-II\FP2_PROJECTS_WORKSPACE\FILES_REPOSITORY\CENDL31
set JENDL_path=C:\FISPACT-II\FP2_PROJECTS_WORKSPACE\FILES_REPOSITORY\JENDL4
set EAF2010_path=C:\FISPACT-II\FP2_PROJECTS_WORKSPACE\FILES_REPOSITORY\EAF2010
set EAF2010_ENDF_path=C:\FISPACT-II\FP2_PROJECTS_WORKSPACE\FILES_REPOSITORY\EAF2010_ENDF_FORMAT
set ENDFB_path=C:\FISPACT-II\FP2_PROJECTS_WORKSPACE\FILES_REPOSITORY\ENDFB71
set JEFF_path=C:\FISPACT-II\FP2_PROJECTS_WORKSPACE\FILES_REPOSITORY\JEFF32
set TENDL_path=C:\FISPACT-II\FP2_PROJECTS_WORKSPACE\FILES_REPOSITORY\TENDL2017
set GROUPCONVERT_path=C:\FISPACT-II\FP2_PROJECTS_WORKSPACE\FILES_REPOSITORY\CONVERT
rem
set Fluxes_path=C:\FISPACT-II\FP2_PROJECTS_WORKSPACE\FLUXES_REPOSITORY
rem
set Fluxes_709N=709N\01_SAF1_SiRollerRig_709N.FLX

IF %TYPE%=="CENDL"           GOTO :CENDL
IF %TYPE%=="JENDL"           GOTO :JENDL
IF %TYPE%=="EAF2010"         GOTO :EAF2010
IF %TYPE%=="EAF2010_ENDF"   GOTO :EAF2010_ENDF
IF %TYPE%=="ENDFB"          GOTO :ENDFB
IF %TYPE%=="JEFF"           GOTO :JEFF
IF %TYPE%=="TENDL"          GOTO :TENDL
IF %TYPE%=="GROUPCONVERT"   GOTO :GROUPCONVERT

rem CENDL cluster commands
:CENDL
copy %Fluxes_path%\%Fluxes_709N%           FLUXES
copy %CENDL_path%\01_arrayx_neutron.i      arrayx.i
copy %CENDL_path%\01_collapx_neutron.i     collapx.i
copy %CENDL_path%\01_printlib_neutron.i    printlib.i
copy %CENDL_path%\01_FILES_CENDL31_709N_294K FILES

```

```

rem copy %CENDL_path%01_FILES_CENDL31_709N_600K      FILES
rem copy %CENDL_path%01_FILES_CENDL31_709N_900K      FILES
PAUSE
GOTO :END

rem JENDL cluster commands
:JENDL
copy %Fluxes_path%\%Fluxes_709N%                     FLUXES
copy %JENDL_path%\01_arrayx_neutron.i                arrayx.i
copy %JENDL_path%\01_collapx_neutron.i               collapx.i
copy %JENDL_path%\01_printlib_neutron.i              printlib.i
copy %JENDL_path%\01_FILES_JENDL40_709N_294K        FILES
PAUSE
GOTO :END

rem EAF2010 cluster commands
:EAF2010
copy %Fluxes_path%\%Fluxes_172N%                     FLUXES
copy %EAF2010_path%\01_arrayx_neutron.i              arrayx.i
copy %EAF2010_path%\01_collapx_neutron.i            collapx.i
copy %EAF2010_path%\01_printlib_neutron.i           printlib.i
copy %EAF2010_path%\01_FILES_EAF2010_172N_294K      FILES
PAUSE
GOTO :END

rem EAF2010_ENDF cluster commands
:EAF2010_ENDF
copy %Fluxes_path%\%Fluxes_709N%                     FLUXES
copy %EAF2010_ENDF_path%\01_arrayx_neutron.i        arrayx.i
copy %EAF2010_ENDF_path%\01_collapx_neutron.i       collapx.i
copy %EAF2010_ENDF_path%\01_printlib_neutron.i      printlib.i
copy %EAF2010_ENDF_path%\01_FILES_EAF2010_ENDF_709N_294K  FILES
PAUSE
GOTO :END

```

```

rem ENDFB cluster commands
:ENDFB
copy %Fluxes_path%\%Fluxes_709N%           FLUXES
copy %ENDFB_path%\01_arrayx_neutron.i     arrayx.i
copy %ENDFB_path%\01_collapx_neutron.i    collapx.i
copy %ENDFB_path%\01_printlib_neutron.i   printlib.i
copy %ENDFB_path%\01_FILES_ENDFB71_709N_294K  FILES
PAUSE
GOTO :END

rem JEFF cluster commands
:JEFF
copy %Fluxes_path%\%Fluxes_709N%           FLUXES
copy %JEFF_path%\01_arrayx_neutron.i       arrayx.i
copy %JEFF_path%\01_collapx_neutron.i     collapx.i
copy %JEFF_path%\01_printlib_neutron.i    printlib.i
copy %JEFF_path%\01_FILES_JEFF32_709N_294K  FILES
PAUSE
GOTO :END

rem TENDL cluster commands
:TENDL
    copy %Fluxes_path%\%Fluxes_709N%           FLUXES
    copy %TENDL_path%\CollapX\01_CollapX_709N.i CollapX.i
    copy %TENDL_path%\arrayx\01_arrayx_neutron.i ArrayX.i
    copy %TENDL_path%\printlib\01_printlib_neutron.i PrintLib.i
    copy %TENDL_path%\files\01_FILES_TENDL2017_709N_294 FILES
rem copy %TENDL_path%\files\01_FILES_TENDL2017_709N_600 FILES
rem copy %TENDL_path%\files\01_FILES_TENDL2017_709N_900 FILES
rem copy %TENDL_path%\files\01_FILES_TENDL2017_709N_5K  FILES
rem copy %TENDL_path%\files\01_FILES_TENDL2015_709N_30K FILES
PAUSE
GOTO :END

rem CONVERT cluster commands
:GROUPCONVERT

```

```

copy %GROUPCONVERT_path%\FILES_GroupConvert          FILES
copy %GROUPCONVERT_path%\01_GroupConvert_172N_to_709N.i  GroupConvert.i
copy %GROUPCONVERT_path%\01_GroupConvert_Boundaries_Fluxes_eVolt_172N.FLX  ARB_FLUX
PAUSE
GOTO :END

:END

```

The energy-spectrum of the LWR neutron fluence-rate $\phi(E)$ is specified by the batch-file statement(s):

```

set Fluxes_path=C:\FISPACT-II\FP2_PROJECTS_WORKSPACE\FLUXES_REPOSITORY
set Fluxes_709N=709N\01_SAF1_SiRollerRig_709N.FLX

```

The specific neutron spectrum $\phi(E)$ that was used in this project, is displayed in Figure 6 on page 60.

Next, the following batch-file commands are executed:

```

@echo off
VERIFY ON

echo =====
echo FISPACT-II RUN - TITLE
echo =====

setlocal

set fispact=C:\FISPACT-II\bin\fispact.exe

rem Perform FISPACT-II Runs:
%fispact% CollapX
%fispact% ArrayX

```

```

%fspact% PrintLib
rem

%fspact% LWR_60yr_26_FE

endlocal

```

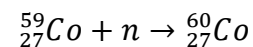
In the above `BAT` file, (1) the CollapX binary 1-group cross-section library is collapsed using the neutron fluence-rate function $\phi(E)$, (2) the ArrayX binary library is prepared, and then (3) the FISPACT-II calculation model input-file `LWR_60yr_26_FE.i` is read. The code FISPACT-II then executes to obtain the results for the exposure of ^{nat}Fe to an LWR neutron fluence-rate for 60 years.

The neutron spectrum inside long, thin Al-alloy rods in the water-pool surrounding the SAFARI-1 reactor (Figure 5 on page 59) was used to collapse reaction-cross-sections to 1-group values that are used by the activation code FISPACT-II to set up systems of rate-equations which are then solved numerically. Cross-section collapsing is performed by solving the integral in Eq. (8):

$$\sigma_{1g} = \frac{\int_0^{\infty} \phi(E) \sigma(E) dE}{\int_0^{\infty} \phi(E) dE} \quad (8)$$

The values of the collapsed 1-group reaction cross-sections are quite sensitive to the small differences between the weighting neutron spectra $\phi(E)$ used for the collapse-step.

Here follow some examples of the sensitivity of a 1-group collapsed reaction cross-section on the neutron spectrum used in the collapse-integral. Let us consider the neutron activation reaction



using ENDF/B-7.1 cross-section data, as supplied with JANIS-4 (Soppera et al., 2013). The continuous cross-section function $\sigma(E)$ for the above nuclear reaction is shown in Figure 52.

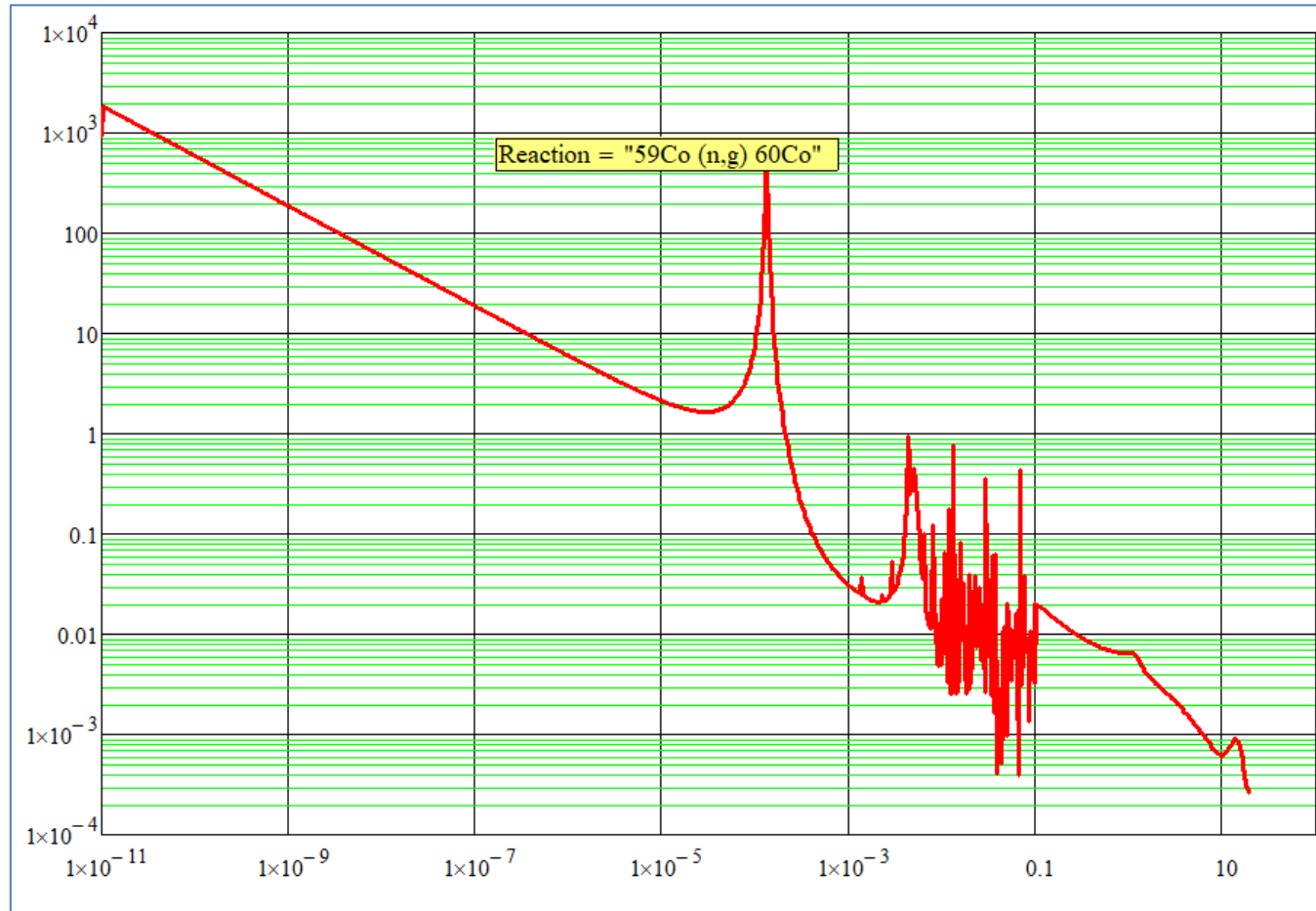


Figure 52: Reaction cross-section for the neutron activation reaction $\text{Co-59} + \text{n} \rightarrow \text{Co-60}$

The collapse-integral was evaluated²⁹ for several neutron spectra, and results vary between circa 9 barn and 24 barns for typical LWR spectra:

- For an unmoderated prompt fission neutron (PFN) spectrum³⁰, $\sigma_{1g} = 0.006$ barn.
- For the average neutron spectrum inside the “meat” of a target-plate irradiated in SAFARI-1, $\sigma_{1g} = 9.39$ barn.
- For the average neutron spectrum inside the cladding of a target-plate irradiated in SAFARI-1, $\sigma_{1g} = 11.13$ barn.
- For the average neutron spectrum inside the beryllium reflector (BER) elements of SAFARI-1, $\sigma_{1g} = 14.89$ barn.
- For the average neutron spectrum inside the Al-alloy of the SAFARI-1 core-box (CB) of SAFARI-1, $\sigma_{1g} = 16.37$ barn.
- For the average neutron spectrum inside in-core water in SAFARI-1, $\sigma_{1g} = 18.15$ barn.
- For the neutron spectrum in the ex-core pool water around SAFARI-1, $\sigma_{1g} = 24.40$ barn.
- For the neutron spectrum inside the grid-plate at SAFARI-1, $\sigma_{1g} = 20.73$ barn.
- For the idealised “text-book” neutron spectrum shown in Figure 7 (page 62), $\sigma_{1g} = 11.29$ barn.

From the above assessment, It is observed that the value of an effective, 1-group cross-section is markedly sensitive to the neutron spectrum used in the collapse-integral of Eq. (8). All LWR neutron spectra shown in Figure 7 on page 62 are clearly very similar. Despite the apparent similarity, we observe that neutron spectra that appear near-identical, yield σ_{1g} values that can have relative differences as large as a factor $\frac{24.4}{9.39} \approx 2.6$.

²⁹ Using a MathCAD-14 worksheet developed by the co-supervisor, TJvR.

³⁰ Note by co-supervisor TJvR: A Watt spectrum with coefficients determined by (Cranberg et al., 1956) — see (Van Rooyen and De Beer, 1993).

BIBLIOGRAPHY

Ackermann, T., 2017. *Methods for the Radiological Characterisation of the FiR-1 TRIGA Research Reactor Decommissioning Waste*. Stellenbosch University (SUN), South Africa, Stellenbosch, South Africa.

Alhajali, S., Kharita, M.H., Naoum, B., Yousef, S., and AlNassar, M., 2009. *Estimation of the activation of local reactor shielding concretes*. *Progress in Nuclear Energy* 51, 374–377.

Alhajali, S., Yousef, S., and Naoum, B., 2016. *Appropriate concrete for nuclear reactor shielding*. *Applied Radiation and Isotopes* 107, 29–32.

Audi, G., Kondev, F.G., Wang, M., Huang, W.J., and Naimi, S., 2017. *The NUBASE2016 evaluation of nuclear properties*. *Chinese Physics C* 41, 1–138. <https://doi.org/10.1088/1674-1137/41/3/030001>

Bingham, W.G., 1965. *Low activation shielding materials for nuclear reactor environmental test chambers*. *Nuclear Structural Engineering* 2, 243–247.

Brown, D.A., Chadwick, M.B., Capote, R., Kahler, A.C., Trkov, A., Herman, M.W., Sonzogni, A.A., Danon, Y., Carlson, A.D., and Dunn, M., 2018. *ENDF/B-VIII.0: The 8th Major Release of the Nuclear Reaction Data Library with CIELO-Project Cross Sections, New Standards and Thermal Scattering Data*. *Nuclear Data Sheets* 148, 1–142. <https://doi.org/10.1016/j.nds.2018.02.001>

Bylkin, B.K., Engovatov, I.A., Kozhevnikov, A.N., and Sinyushin, D.K., 2018. *On the Necessity and the Role of Descriptors of Neutron Activated Structural and Shielding Materials of Nuclear Installations for Future Decommissioning*. *Nuclear Energy and Technology* 4, 257–262. <https://doi.org/10.3897/nucet.4.31875>

CNSC, 2018. *Radionuclide Information Booklet*. Canadian Nuclear Safety Commission, Ottawa, Ontario K1P 5S9 CANADA.

Conlin, J.L., Haeck, W., Neudecker, D., Parsons, K.D., and White, M.C., 2018. *Release of ENDF/B-8.0-Based ACE Data Files for MCNP*. Report: LA-UR-18-24034. Nuclear Data Team, XCP-5, Los Alamos National Laboratory (LANL), Los Alamos, USA.

Cranberg, L., Frye, G., Nereson, N., and Rosen, L., 1956. *Fission neutron spectrum of U 235*. *Physical Review* 103, 662. <https://doi.org/10.1103/PhysRev.103.662>

Decommissioning a Nuclear Reactor, 2013.

Evans, J.C., Lepel, E.L., Sanders, R.W., Wilkerson, C.L., Silker, W., Thomas, C.W., Abel, K.H., and Robertson, D.R., 1984. *Long-Lived Activation Products in Reactor Materials*. <https://doi.org/10.2172/6776358>

Farrell, K., and King, R.T., 2009. *Tensile Properties of Neutron-Irradiated 6061 Aluminum Alloy in Annealed and Precipitation-Hardened Conditions*. *Effects of Radiation on Structural Materials* 440–440–10. <https://doi.org/10.1520/stp38180s>

Fetter, S., Cheng, E.T., and Mann, F.M., 1988. *Long-Term Radioactivity in Fusion Reactors*. *Fusion Engineering and Design* 6 (1988), 123–130.

Gallmeier, F., 2010. *Activation Calculations — Present and Future*. Presented at the SATIF-2010, Oak Ridge National Laboratories (ORNL), Oak Ridge, Tennessee, USA, p. 31.

Grünauer, F., 2005. *Design, Optimization and Implementation of the New Neutron Radiography Facility at FRM-II*.

Hasegawa, A., Kinno, M., Satou, M., Kakinuma, N., Abe, K., Kimura, K., Uematsu, M., Hayashi, K., Nakata, M., and Tanosaki, T., 2006. *Materials Selection and Activity Evaluation System to Reduce Radioactive Waste from Steel Reinforced Concrete of Nuclear Plants*, in: Pacific Basin Nuclear Conference 2006. Australian Nuclear Association, p. 918.

Hayashi, K., Nemezawa, S., Tanaka, M., Uematsu, M., Ogata, T., Nakata, M., Yamaguchi, K., Kinno, M., Kimura, K.I., and Tanosaki, T., 2009. *Development of Low-Activation Reinforced Concrete Design Methodology—II: Concrete Activation Analyses of BWR/PWR*. *Nuclear Technology* 168, 571–575. <https://doi.org/10.13182/NT09-A9245>

Holden, N.E., Coplen, T.B., Böhlke, J.K., Tarbox, L.V., Benefield, J., de Laeter John, J.R., Mahaffy, P.G., O'Connor, G., Roth, E., Tepper, D.H., Walczyk, T., Wieser, M.E., and Yoneda, S., 2018. *IUPAC Periodic Table of the Elements and Isotopes (IPTEI) for the Education Community (IUPAC Technical Report)*. *Pure and Applied Chemistry* 90, 1833. <https://doi.org/10.1515/pac-2015-0703>

Hou, X., 2005. *Radiochemical Determination of Ca-41 in Nuclear Reactor Concrete*. *Radiochimica Acta* 93, 611–617.

IAEA, 2019. *Methodologies for Assessing the Induced Activation Source Term for Use in Decommissioning Applications*, Safety Reports Series. International Atomic Energy Agency (IAEA), Vienna, Austria.

IAEA, 2007. *Characterization and Testing of Materials for Nuclear Reactors*. International Atomic Energy Agency (IAEA), Vienna, Austria.

IAEA, 2006. *Management of Problematic Waste and Material Generated During the Decommissioning of Nuclear Facilities*. International Atomic Energy Agency IAEA Technical reports series.

IAEA, 2005. *Research Reactor Utilization Safety Decommissioning Fuel and Waste Management.*, Proceedings of an International Conference Held in Santiago, Chile, 10–14 November 2003. International Atomic Energy Agency, Vienna, Austria.

IAEA, 2004. *Application of the Concepts of Exclusion, Exemption and Clearance*. Report: General Safety Guides RS-G-1.7, IAEA Safety Standards Series. IAEA, Vienna, Austria.

IAEA, 2002. *Safe Decommissioning for Nuclear Activities*, in: Proceedings of an International Conference on Safe Decommissioning for Nuclear Activities. Presented at the International Conference on Safe Decommissioning for Nuclear Activities Organized by the International Atomic Energy Agency (IAEA) and Hosted by the Government of Germany Through the Bundesamt für Strahlenschutz, and held in Berlin, 14–18 October 2002, IAEA, Berlin, Germany.

IAEA, 1998. *Radiological Characterization of Shut-Down Nuclear Reactors for Decommissioning Purposes*. Report: 389, Technical Report Series. International Atomic Energy Agency (IAEA), Vienna, Austria.

IAEA, 1996. *Clearance Levels for Radionuclides in Solid Materials*. Report: IAEA-TECDOC-855. International Atomic Energy Agency (IAEA), Vienna, Austria.

IAEA, 1988. *Decontamination and Demolition of Concrete and Metal Structures During the Decommissioning of Nuclear Facilities*. International Atomic Energy Agency (IAEA), Vienna, Austria.

ICRP, 2010. *Conversion Coefficients for Radiological Protection Quantities for External Radiation Exposures*. Report: ICRP-116. Elsevier.

ICRP, 2008. *Nuclear Decay Data for Dosimetric Calculations*. Report: ICRP Publication 107, Annals of the ICRP. Ottawa, Canada. <https://doi.org/10.1093/rpd/ncp259>

ICRU, 2011. *Fundamental Quantities and Units for Ionizing Radiation*. Report: Journal of the ICRU Vol 11 No 1 (2011) Report 85. International Commission on Radiation Units and Measurements, Bethesda, Maryland, USA. <https://doi.org/10.1093/jicru/nd>

ICRU, and ICRP, 2017. *Operational Quantities for External Radiation Exposure*. International Commission on Radiation Units and Measurements (ICRU) and International Commission on Radiological Protection (ICRP).

Ionescu, E., Gurau, D., Stanga, D., and Dului, O.G., 2012. *Decommissioning of the VVR-S Research Reactor — Radiological Characterization of the Reactor Block*. Romanian Reports in Physics 64, 387–398.

Israr, M., Shami, Q.D., and Pervez, S., 2003. *Experience with Partial Decommissioning of PARR-1 (5 MW) for Core-Conversion and Power Upgrade*, in: Proceedings of an International Conference on Research Reactor Utilization, Safety, Decommissioning, Fuel and Waste Management, Proceedings Series. IAEA, Santiago, Chile, pp. 583–586.

Kakinuma, N., Satou, M., Nogami, S., Hasegawa, A., Abe, K., Kinno, M., Tanosaki, T., and Yoshino, R., 2007. *Low-Activation Reinforced Concrete Design Methodology (5)–Low-Activation Material Development Support System*.

Kaliatka, A., 2016. *Lecture 14: Decommissioning Safety*.

Kapusta, B., Averty, X., Scibetta, M., Decroix, G.M., and Rommens, M., 2003. *Present Status on the Mechanical Characterization of Aluminum Alloys 5754-O and 6061-T6 Irradiated at High Neutron Fluences*. Presented at the Proceedings: 9th IGORR Conference, INIS-XA-C-030, Sydney, Australia, pp. 1–8.

Kimura, K.I., Hasegawa, A., Hayashi, K., Uematsu, M., Ogata, T., Tanosaki, T., Yoshino, R., Sato, M., Saito, M., and Kinno, M., 2009. *Development of Low-Activation Design Method for Reduction of Radioactive Waste Below Clearance Level*. Presented at the 16th International Conference on Nuclear Engineering, May 11–15, 2008, American Society of Mechanical Engineers (ASME), Digital Collection, Orlando, Florida, USA, pp. 617–626. <https://doi.org/10.1115/ICONE16-48484>

Kimura, K.I., Kinno, M., Nishida, H., Katayose, N., Nakata, M., Hayashi, K., Uematsu, M., and Hasegawa, A., 2007. *Low-activation Reinforced Concrete Design Methodology (8) Fundamental Investigation for Various Types of Low-activation Concrete*.

Kinno, M., Kimura, K., Fujukura, Y., Nishida, H., Katayose, N., Mori, T., Yoshino, R., Tanosaki, T., Ichitsubo, K., Nakata, M., Ogata, T., Uematsu, M., Hayashi, K., Sato, M., Sakakibara, M., et al., 2011. *Low-Activation Multilayer Shielding Structure of Light Water Reactor Using Various Types of Low-Activation Concrete*. Progress in Nuclear Science and Technology 1, 28–31. <https://doi.org/10.15669/pnst.1.28>

Kinno, M., Kimura, K., and Nakamura, T., 2002. *Raw Materials for Low-Activation Concrete Neutron Shields*. Journal of Nuclear Science and Technology 1275–1280. <https://doi.org/10/gf9tmf>

Kinno, M., Nishida, H., Kimura, K.I., Fujikura, Y., Katayose, N., Yoshino, R., Mori, T., and Hasegawa, A., 2007. *Low-Activation Reinforced Concrete Design Methodology (10) Low-Activation Concrete Based on Fused Alumina Aggregates and High Alumina Cement*. Proceeding, SMiRT 19.

Klein, M., Demeulemeester, Y., Moers, S., and Ponnet, M., 2001. *Management Routes for Materials Arising from the Decommissioning of a PWR Reactor*.

Klein, M., and Moers, S., 2000. *The free release of dismantled materials: The practical case of the BR3 reactor*. Applied Radiation and Isotopes 53, 323–329.

Kodama, K., Ozasa, K., and Okubo, T., 2012. *Radiation and cancer risk in atomic-bomb survivors*. Journal of Radiological Protection 32, N51. <https://doi.org/10.1088/0952-4746/32/1/N51>

Kolluri, M., n.d. *Neutron Irradiation Effects in 5xxx and 6xxx Series Aluminum Alloys: A Literature Review*.

LANL, 2018a. *RSICC Code Package CCC-850: MCNP6.2: Monte Carlo N–Particle Transport Code System Including MCNP6.2 and MCNPDATA Libraries*. RSICC, ORNL.

LANL, 2018b. *RSICC Code Package CCC-850: MCNP6.2: Monte Carlo N–Particle Transport Code System Including MCNP6.2 and MCNPDATA Libraries*. LANL, Los Alamos, USA.

Lee, K., Kim, J., and Kang, S., 2017. *Preliminary Evaluation of Decommissioning Wastes for the First Commercial Nuclear Power Reactor in South Korea*. International Journal of Nuclear and Quantum Engineering, World Academy of Science, Engineering and Technology 11.

Lentijo, J.C., 2002. *Release from Regulatory Control: The Spanish Experience*, in: Proceedings of an International Conference on Safe Decommissioning for Nuclear Activities, Berlin, Germany, 14–18 October 2002, Proceedings Series. Presented at the International Conference on Safe Decommissioning for Nuclear Activities, Berlin, Germany, 14–18 October 2002, International Atomic Energy Agency (IAEA), Vienna, Austria, pp. 451–473.

Leuraud, K., Richardson, D.B., Cardis, E., Daniels, R.D., Gillies, M., O’hagan, J.A., Hamra, G.B., Haylock, R., Laurier, D., and Moissonnier, M., 2015. *Ionising radiation and risk of death from leukaemia and lymphoma in radiation-monitored workers (INWORKS): an international cohort study*. The Lancet Haematology 2, e276–e281. [https://doi.org/10.1016/S2352-3026\(15\)00094-0](https://doi.org/10.1016/S2352-3026(15)00094-0)

- Lopes, E., and Pillette-Cousin, L., 2003. *Implementation of Stage 3 Decommissioning of the Triton Facility*, in: Proceedings of an International Conference on Research Reactor Utilization, Safety, Decommissioning, Fuel and Waste Management, Proceedings Series. Presented at the International Conference on Research Reactor Utilization, Safety, Decommissioning, Fuel and Waste Management, IAEA, Santiago, Chile.
- Ludwig, T.H., 2013. *Trace Elements in Al-Si Foundry Alloys*. PhD Thesis . Norwegian University of Science and Technology (NTNU), Trondheim, Norway.
- Lurchak, D., 2020. *200 – 400 Nuclear reactors to be decommissioned by 2040*. EnergyPost.eu. URL <https://energypost.eu/200-400-nuclear-reactors-to-be-decommissioned-by-2040/> (accessed 6.24.20).
- Luzginova, N.V., Nolles, H., Van den Berg, F., Van den Idsert, P., and Van der Schaaf, B., 2014. *Surveillance Program Results for the High Flux Reactor Vessel Material*. Effects of Radiation on Nuclear Materials: 26th Volume 30, 30–41. <https://doi.org/10.1520/stp157220130095>
- Meier, H.G., Brizuela, M., Maître, A.R.A., and Albornoz, F., 2017. *Activation Analysis of Decommissioning Operations for Research Reactors*. Rotterdam, Netherlands.
- Meija, J., Coplen, T.B., Berglund, M., Brand, W.A., De, B.P., Gröning, M., Holden, N.E., Irrgeher, J., Loss, R.D., Walczyk, T., and Prohaska, T., 2016. *Isotopic compositions of the elements 2013 (IUPAC Technical Report)*. Pure and Applied Chemistry 88, 293–306. <https://doi.org/10.1515/pac-2015-0503>
- Morioka, M., Sato, S., Ochiai, K., Kinno, M., Hori, J., Yamauchi, M., Nishitani, T., Matsukawa, M., and Tamai, H., 2004. *Neutron Irradiation Experiments of Boron-doped Low Activation Concrete*. JAERI-Review 2004-017.
- Mück, K., and Casta, J., 2000. *Planning for the Decommissioning of the ASTRA-Reactor*. Report: P-5-307. Austrian Research Center Seibersdorf, Seibersdorf, Austria.
- NEA, 2011. *Decontamination and Dismantling of Radioactive Concrete Structures*. Report: NEA/RWM/R(2011)1. Nuclear Energy Agency (NEA).
- NISDF, 2017. *The UK Nuclear Industry Guide To: Clearance and Radiological Sentencing: Principles, Process and Practices*. The Nuclear Institute (UK), Phoenix House, 18 King William Street, London EC4N 7BP.
- NNR, 2008. *Decommissioning of Nuclear Facilities*. Report: Regulatory Document RD-0026. National Nuclear Regulator (NNR), Centurion, South Africa.

Ogata, T., Muramatsu, T., Nagata, M., Hayashi, K., Kinno, M., Kimura, K.I., Yamaguchi, K., Hasegawa, A., Ito, S., and Tanosaki, T., 2007. *Low-Activation Reinforced Concrete Design Methodology (4) Classification System for Radioactive Waste Disposal*, in: 19th International Conference on Structural Mechanics in Reactor Technology, Toronto, Canada.

ORNL, and RSICC, 2018. *SCALE: A Comprehensive Modelling and Simulation Suite for Nuclear Safety Analysis and Design, Version 6.2.3*. Radiation Safety Information Computational Center (RSICC), Oak Ridge National Laboratory, USA.

Pampin, R., and Davis, A., 2008. *Novel Tools for Estimation of Activation Dose: Description, Preliminary Comparison and Nuclear Data Requirements*.

Pantelias Garces, M., 2013. *Activation Neutronics for the Swiss Nuclear Power Plants*. ETH Zurich, Zurich.

Parsons, D.K., 2018. *NJOY Processing of ENDF/B 8.0 Thermal Scattering Files*. Report: LA-UR-18-25096. Nuclear Data Team, XCP-5, Los Alamos National Laboratory (LANL), USA.

Portland General Electric Company, 2001. *Trojan Nuclear Plant Decommissioning Plan and License Termination Plan (PGE-1078) REV9*. Report: PGE-1061. Portland General Electric Company, USA.

Preston, D.L., Shimizu, Y., Pierce, D.A., Suyama, A., and Mabuchi, K., 2003. *Studies of mortality of atomic bomb survivors. Report 13: Solid cancer and noncancer disease mortality: 1950–1997*. Radiation Research 160, 381–407. <https://doi.org/10.1667/RR3049>

Public Health England, 2018. *Impact of Changes to Exemption and Clearance Values for Specific Radionuclides: Review and Industry Survey*. Report: PHE-CRCE-038. Public Health England, Chilton, Didcot, Oxfordshire, UK.

SAFARI-1, 2005. *SAFARI-1 Research Reactor Safety Analysis Report (SAR). Chapter 5: Description of the SAFARI-1 Reactor*. Necsa, Pelindaba, South Africa.

Schlömer, L., Phlippen, P.W., and Lukas, B., 2017. *Activation Calculation for the Dismantling and Decommissioning of a Light Water Reactor Using MCNP with ADVANTG and ORIGEN-S*. EPJ Web of Conferences 153, 05020. <https://doi.org/10/gf9tmc>

Shultis, J.K., and Faw, R.E., 2000. *Radiation Shielding*. American Nuclear Society (ANS), La Grange Park, IL.

Soppera, N., Bossant, M., Cabellos, O., Dupont, E., and Díez, C.J., 2013. *JANIS 4.0 JAVa-based Nuclear Information System*. OECD Nuclear Energy Agency (NEA), Paris, France. <https://doi.org/10.1051/epjconf/201714607006>

Stephens Jr, J.J., and Pohl, R.O., 1978. *Trace elements in reactor steels: implications for decommissioning*. Nuclear Engineering and Design 47, 125–134.

Strom, J.D., and Watson, C., 2002. *On being understood: Clarity and jargon in radiation protection*. Health physics 82, 373–386. <https://doi.org/10.1097/00004032-200203000-00010>

Sublet, J.-C., Eastwood, J.W., Morgan, J.G., Fleming, M., and Gilbert, M.R., 2015. *The FISPACT-II User Manual. Version 3.00*. UKAEA.

Tefelski, D.B., Piotrowski, T., Polański, A., Skubalski, J., and Blideanu, V., 2013. *Monte-Carlo Aided Design of Neutron Shielding Concretes*. Bulletin of the Polish Academy of Sciences: Technical Sciences 61, 161–171. <https://doi.org/10.2478/bpasts-2013-0015>

Uematsu, M., Hayashi, K., Nemezawa, S., Ogata, T., and Nakata, M., 2008. *Development of Low-Activation Design Method for Reduction of Radioactive Waste (2) Precise Neutron Flux and Activation Estimation of Nuclear Power Plants using MATXSLIB-J33T10*, in: Proceedings of the 16th Pacific Basin Nuclear Conference (PBNC). Presented at the 16th Pacific Basin Nuclear Conference (PBNC), Aomori, Japan, 13-18 Oct 2008, Atomic Energy Society of Japan, Tokyo (Japan), Aomori, Japan, pp. 13–18.

Van der Merwe, N.J., 2017. *System for the Classification and Demarcation of Radiological Areas*. Report: SHEQ-INS-8030. SHEQ Department, Necsa, Pelindaba, Pretoria, South Africa.

Van Niekerk, S.E., 2010. *Removal of Material from Radiological Areas*. Report: SHEQ-INS-8040. SHEQ Department, Necsa, Pelindaba, Pretoria, South Africa.

Van Rooyen, T.J., 2019. *Neutron-Induced Changes in the Elemental Composition of the Aluminium-Alloys of the Core-Box and Grid-Plate of the SAFARI-1 Reactor*. Report: RRT-SAFA-REP-19032. Radiation and Reactor Theory (RRT) Section, South African Nuclear Energy Corporation SOC Ltd. (Necsa), Pelindaba, Pretoria, South Africa.

Van Rooyen, T. J., 2017. *Calculation of Energy Deposition Rates and Dose-Rates for an Irradiated SAFARI-1 Fuel-Assembly in the Spent-Fuel Transport-Cask*. Report: RRT-SAFA-REP-17040. Radiation and Reactor Theory (RRT) Section, South African Nuclear Energy Corporation SOC Ltd. (Necsa), Pelindaba, Pretoria, South Africa.

Van Rooyen, T.J., 2017. *Photon and Electron Dose-Rate Calculations for the Silicone Roller Service Station (SRSS) for Silicon Roller Assemblies (SRA) at the SAFARI-1 Reactor*. Report: RRT-SHLD-REP-17002 REV 01. Radiation and Reactor Theory Section, Necsa, Pelindaba, South Africa., Radiation and Reactor Theory Section, Necsa, Pelindaba, South Africa.

Van Rooyen, T.J., 2016a. *Neutron-Induced Changes in the Elemental Composition of the Aluminium-Alloy of the Core-Box of the SAFARI-1 Reactor at Necsa*. Radiation and Reactor Theory Section, Necsa, Pelindaba, South Africa.

Van Rooyen, T.J., 2016b. *Shield Design Calculations for the New Neutron Radiography Facility at Necsa*. Report: RRT-SHLD-REP-15005. Radiation and Reactor Theory (RRT), South African Nuclear Energy Corporation (Necsa), Pelindaba, South Africa.

Van Rooyen, T.J., 2015. *Shield Design Calculations for the SRSS Service Station for the Silicon Roller Assembly (SRA) at the SAFARI-1 Reactor*. Report: RRT-SHLD-REP-15003 REV 04. Radiation and Reactor Theory Section, Necsa, Pelindaba, South Africa, Radiation and Reactor Theory Section, Necsa, Pelindaba, South Africa.

Van Rooyen, T.J., 2006. *The Science of Radiation Protection*. iThemba LABS, Somerset West, South Africa.

Van Rooyen, T.J., and De Beer, G.P., 1993. *A Burnup-Compensated Madland-Nix Prompt Fission Neutron Source Term for Multigroup Nuclear Reactor Shielding Calculations*. Nuclear Science and Engineering 114, 87–101. <https://doi.org/10.13182/NSE93-A24020>

Weeks, J.R., Czajkowski, C.J., and Tichler, P.R., 1990. *Effects of High Thermal and High Fast Neutron Fluences on the Mechanical Properties of Type 6061 Aluminum in the HFBR*, in: ASTM. Presented at the Effects of Radiation on Materials: 14th International Symposium, ASTM International, Philadelphia, PA, USA, pp. 441–452. <https://doi.org/10.1520/STP49465S>

Westall, W.A., and Tawton, B.L., 2012. *Radiological Characterisation Experience with Magnox Reactors*. Magnox Limited, Oldbury, Gloucestershire, UK.

Žagar, T., Božič, M., and Ravnik, M., 2004. *Long-lived activation products in TRIGA Mark II research reactor concrete shield: calculation and experiment*. Journal of nuclear materials 335, 379–386.

Žagar, T., and Ravnik, M., 2002. *Determination of long-lived neutron activation products in reactor shielding concrete samples*. Nuclear technology 140, 113–126. <https://doi.org/DOI:10.1080/18811248.2002.9715321>

Žagar, T., and Ravnik, M., 2000. *Measurement of Neutron Activation In Concrete Samples*. Presented at the International Conference on Nuclear Energy in Central Europe, 2000, Slovenia.

Žagar, T., Ravnik, M., and Božič, M., 2001. *Neutron Activation Measurements in Research Reactor Concrete Shield*. Presented at the International Conference on Nuclear Energy in Central Europe, 2001, Portorož, Slovenia.

Zamonsky, O.M., 2019a. *MCNP SAFARI-1 Calculation Model Description*. Report: RRT-SAFA-REP-13004 Rev 03. Radiation and Reactor Theory (RRT) Section, South African Nuclear Energy Corporation SOC Ltd. (Necsa), Pelindaba, Pretoria, South Africa.

Zamonsky, O.M., 2019b. *NNR Regulatory Guide RG-0016 Compliance of MCNP6.2 to Criticality and Shielding Calculations*. Report: RRT-SAFA-REP-18005. Radiation and Reactor Theory (RRT) Section, South African Nuclear Energy Corporation SOC Ltd. (Necsa), Pelindaba, Pretoria, South Africa.